THE DYNAMICS, INTERACTIONS AND PHENOTYPES ASSOCIATED WITH THE THREE MEMBERS OF THE 14-3-3 FAMILY IN *DROSOPHILA MELANOGASTER*

A Dissertation

by

SUMMER FONTAINE ACEVEDO

Submitted to the Office of Graduate Studies of
Texas A&M University
in partial fulfillment of the requirements for the degree of

DOCTOR OF PHILOSOPHY

August 2004

Major Subject: Genetics

THE DYNAMICS, INTERACTIONS AND PHENOTYPES ASSOCIATED WITH THE THREE MEMBERS OF THE 14-3-3 FAMILY IN *DROSOPHILA MELANOGASTER*

A Dissertation

by

SUMMER FONTAINE ACEVEDO

Submitted to the Texas A&M University
in partial fulfillment of the requirements
for the degree of

DOCTOR OF PHILOSOPHY

Approved as to style and content by:

Efthimios M. C. Skoulakis (Chair of Committee)	Sumana Datta (Member)
Linda A. Guarino (Member)	Craig J. Coates (Member)
Geoffrey M. Kapler (Chair of Genetics Faculty)	Vincent Cassone (Head of Department)

August 2004

Major Subject: Genetics

ABSTRACT

The Dynamics, Interactions and Phenotypes Associated with the Three Members of the 14-3-3 Family in *Drosophila melanogaster*.

(August 2004)

Summer Fontaine Acevedo, B.A., University of Northern Colorado

Chair of Advisory Committee: Dr. Efthimios M. C. Skoulakis

It has been proposed that the various 14-3-3 isotypes and isoforms present in all eukaryotes are largely functionally equivalent. However, this is not consistent with the conservation of multiple isoforms and isotypes, especially in vertebrates with seven 14-3-3 encoding genes and nine isotypes. The hypothesis tested in this thesis is that both isoform-specific and overlapping functions are likely mediated through tissue specific expression, colocalization and dimerization of 14-3-3 proteins occur in vivo. *Drosophila melanogaster* was selected because it offers a simple, but representative system to study these proteins functionally. This thesis focuses primarily on D14-3-3ε, although the expression pattern and phenotypes associated with all three *Drosophila* 14-3-3s were determined. I first determined the expression pattern of the three different 14-3-3 isotypes (*leoI*, *leoII* and *D14-3-3ε*) and described developmental phenotypes associated with mutations in 14-3-3 isotypes in *Drosophila*. I found that there is partial redundancy with respect to lethality. Both LEO and D14-3-3ε appear required for normal germ-line and somatic gonadal development. However, they do not appear to be functionally

equivalent with respect to this phenotype since LEO is unable to compensate for the loss of D14-3-3ε. I also determined that *D14-3-3ε* mutants have unique phenotypes including deficits in adult cross-vein formation and rapid habituation to olfactory and footshock stimuli. To further understand the unique role that D14-3-3ε plays in the adult CNS, I mapped the areas in the brain involved in olfactory and footshock habituation. I found that although the mushroom bodies (MBs) are necessary to inhibit premature habituation such as that exhibited by *D14-3-3ε* mutants, D14-3-3ε expression specifically in the MBs is not sufficient to rescue premature habituation. Although the loss of either LEO or D14-3-3ε appears to cause a deficit in olfactory associative learning, premature habituation is the cause of the deficit seen in D14-3-3ε mutants. As *leo* mutants do not exhibit a premature habituation phenotype, it appears that within the MBs LEO and D14-3-3ε are not functionally equivalent. Therefore, the data supports the hypothesis that 14-3-3s have functional specificity and redundancy likely to represent use of homo and heterodimers in different processes within the tissues of an organism.

ACKNOWLEDGEMENTS

There are several people I would like to say thanks to. I would not have succeeded in my goal of obtaining my Ph. D. without their support and advice. First, I would like to thank Dr. Efthimios M. C. Skoulakis for the many years of guidance, advice and support. The experience I have obtained will be forever valuable and will help me to succeed for many years to come. I would also truly like to thank Dr. Sumana Datta for her advice and patience, her friendship has helped guide my life in the right direction. To the other members of my committee: Dr. Linda A. Guarino and Craig J. Coates, thanks for your support and belief in my work. To all the members of the Skoulakis and Datta labs over the years, I thank you all for your assistance. I would also like to thank Sean and Jared of the Summers lab for their help with my confocal work and helpful advice. I would like to thank my family, my wonderful husband Christopher Acevedo, beautiful daughter Athena, my parents, sisters, grandparents and the Acevedo family for all their support and love.

TABLE OF CONTENTS

CHAPTER Page

LIST OF FIGURES

FIGURE Page

FIGURE Page

LIST OF TABLES

CHAPTER I

INTRODUCTION

14-3-3S

What are 14-3-3's?

The 14-3-3 proteins comprise a family of small acidic molecules with multiple and apparently diverse cellular functions (Skoulakis and Davis, 1998; Muslin and Xing, 2000; Fu et al., 2000; van Hemert et al., 2001; Berg et al., 2003). These small acidic proteins have molecular masses between 29-32 kD and isoelectric points of 4.5-5. While attempting to identify proteins unique to the nervous system, seven isoforms were purified from bovine brains in 1967. They were named, α, β, γ, δ, ε, ζ and η according to their order of elution from (DEAE)-cellulose chromatography columns and their position in starch electrophoresis gels (Moore and Perez, 1967). The initial seven, along with two additional proteins, σ and τ(θ) make up the nine family members of 14-3-3s in vertebrates. These nine proteins are products of seven distinct genes with the α and δ isoforms being the phosphorylated forms of β and ζ genes respectively (Aitken, 1995). Because of the complexity of the family, I will adapt the stringent nomenclature that 14-3-3 proteins derived from different genes will be called isotypes or family members.

This dissertation follows the style and format of Neuron.

In contrast, 14-3-3 proteins derived from the same gene by either alternative splicing or post-translational modification will be called isoforms.

The animal family members are divided into two groups based on protein sequence similarity. The typical group contains α/β, γ, η and ζ/δ. There is 92-75% sequence identity among members of the typical group (Figure 1). The ε, σ and τ(θ) species although most dissimilar with the typical isotypes are still 45-63% identical with each other (Figure 1) (Martin et al., 1993; Wang and Shakes, 1996). According to protein alignments there are three conserved regions shared by these proteins. Domain one is a possible protein kinase C phosophorylation site (62-69), domain two is a annexin-like sequence (139-154) and domain three occurs at the C-terminus affecting interactions with targets such as Raf and Bad (231-245) (Wang and Shakes, 1996; Aitkens et al., 2002). In contrast, the residues involved in dimerization at the amino terminus show some variation, which could affect 14-3-3 functional specificity by selective dimerization. Members of the 14-3-3 family have been found in all species examined including mammals, insects, nemotodes/frogs, plants and yeast (Aitken et al., 1992, Wang and Shakes, 1996; Muslin and Xing, 2000; Fu et al., 2000; Takahashi, 2003; Berg et al., 2003). Although every species has at least one isotype of 14-3-3, the number of isotypes/isoforms differs depending on the species. For instance, there are nine in *Homo sapiens* (and all vertebrates for which data is available), three in *Drosophila melanogaster*, two in the nemotode *Caenorhabditis elegans*, fourteen in the plant *Arabidopsis thaliana* and two in the yeasts *Schizosaccharomyces pombe* and *Saccharomyces cerevisiae* (Wang and Shakes, 1996; Yaffe and Elia, 2001; Ferl et al.,

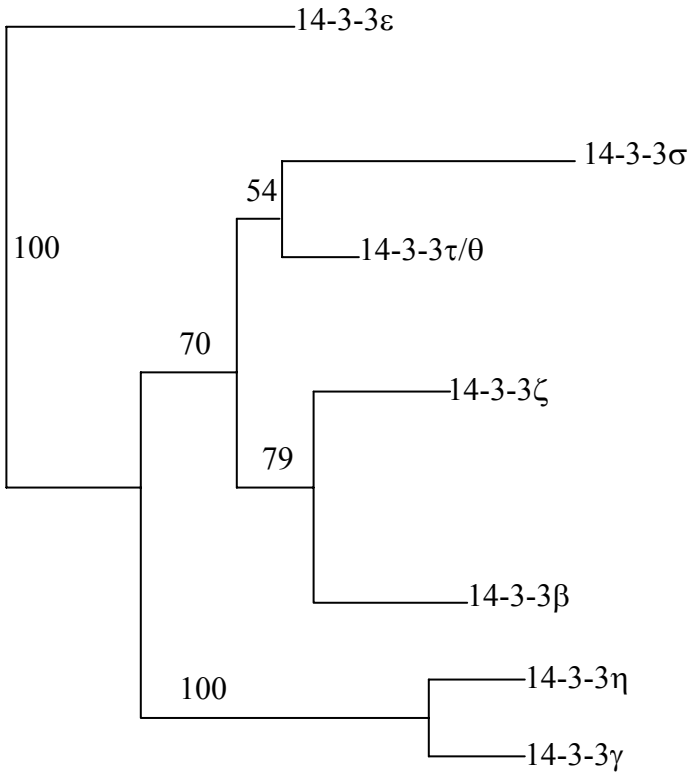

Figure 1. Phylogenetic tree of human 14-3-3s

Modified from Berg et al. 2003 with the length of the branches corresponds to the number of substitutions per site.

2002; van Hermert et al., 2001; Aitken et al., 2002). Sequence alignments between proteins from different species reveal that the ε protein in the animal lineage is more similar to yeast and plant isotypes (Wang and Shakes, 1996). This suggests ε may in fact be the oldest isotype, perhaps even ancestral to all animal 14-3-3s. Within the non-epsilon isotypes, the *Schizosaccharomyces pombe, Saccharomyces cerevisiae* and *Caenorhabditis elegans* proteins are more similar to each other than they are to proteins from any other species (Wang and Shakes, 1996), suggesting that these may represent primitive animal isotypes. The alignments also indicate that the non-epsilon *Caenorhabditis elegans* protein and one of the *Drosophila melanogaster* proteins (LEONARDO II) share particular amino acids in conserved domain that are divergent from the remaining isotypes suggesting that they potentially share a common ancestor in the early divergent β/ζ/τ group. The distribution, structural characteristics and functional attributes of 14-3-3s will be presented below.

14-3-3 Distribution

14-3-3s were initially identified as highly abundant proteins in vertebrate brains (up to 1% of soluble brain proteins), but they are also expressed at lower levels in most vertebrate tissues examined (Boston et al., 1982; Ichimura et al., 1991; Aitken et al., 1992; Aitken, 1995; Skoulakis and Davis, 1998; Takahashi, 2003; Berg et al., 2003). In vertebrates, they are highly enriched in the cerebellum, certain cerebral areas including the hippocampus, olfactory bulb and motor neurons in the brainstem and spinal cord (Table 1) (Boston et al., 1982; Ichimura et al., 1991; Watanabe et al., 1991; Watanabe et

al., 1993; Watanabe et al., 1994; Rosenboom et al., 1994; Toyooka et al., 2002; van der Brug et al., 2002; Baxter et al., 2002). With the exception of σ (epithelial cell specific) and τ(θ) (T−cell/Glia cell specific), all of the other vertebrate isotypes are primarily expressed in neurons (Skoulakis and Davis, 1998; Baxter et al., 2002). The overlapping expression of these proteins appears tightly regulated and highly patterned during development of the vertebrate central nervous system (CNS) (Watanabe et al., 1993; Baxter et al., 2002). Their abundance in the brain and recent evidence of up-regulation in various neurological disorders suggests they may play significant roles in neuronal functions. Some isotypes and particular isoforms have also been detected at lower levels in the ovaries, testes, retina, kidneys, spleen, thyroid, liver and lungs (Rosenboom et al., 1994; Aitken et al., 2002). Their widespread expression in tissues other than the CNS suggests that they may be involved in fundamental cellular activities as well as neuronal processes. In agreement with the importance of 14-3-3s for many fundamental cellular activities, the fourteen different isotypes in plants such as *Arabidopsis thaliana* are found in various tissues including stems, roots, leaves and flowers (Ferl et al., 2002). This research is focused on the characterization of metazoan isotypes, specifically those found in *Drosophila melanogaster*. Therefore, the focus of further discussion will be on animal isotypes with the exclusion of plants and yeast.

Table 1. Expression of 14-3-3s in vertebrate CNS

14-3-3 Isoform	Expression in vertebrate CNS
β/α	cerebellum (Purkinje cells), hippocampus (pyramidal cells), cerebral cortex, olfactory bulb, thalamus, hypothalamus
ζ/δ	cerebellum (Purkinje cells), hippocampus, cerebral cortex, caudate-putamen, neocortex, thalamus, brain stem, medulla, amygdale
η	cerebellum (Purkinje cells), hippocampus (pyramidal cells), olfactory bulb, thalamus, cerebral cortex, brain stem, spinal cord, medulla, hypothalamus
γ	cerebellum (Purkinje cells), hippocampus, cerebral cortex, olfactory bulb, medulla, thalamus, hypothalamus
τ(θ)	nueropil/glia cells - Cerebral cortex and hippocampus
ε	cerebellum, cerebral cortex, hypothalamus, retina

14-3-3 Structure and motifs

Conserved regions

14-3-3s contain three invariant regions, conserved in all species examined. The first region, residues 52-59 (Figure 2) at the amino-terminus contain a sequence highly homologous to a PKC phosphorylation site (pseudo substrate region) with the only difference seen in the τ and σ isotypes which lack it (Wang and Shakes, 1996; Aitken et al., 2002). Although here is no evidence yet that these residues are phosphorylated by PKC, Jones et al. (1995) showed that PKC can phosphorylate serine-63 which is also present in all 14-3-3 sequences (Figure 2). The second region is located towards the central portion of the protein and is homologous to a region in the calcium and phospholipid binding proteins annexin I and II at residues 139-154.

Research suggests that 14-3-3s ε, γ, β, η and ζ can directly bind phospholipids in a calcium independent manner allowing for aggregation of phospholipid vesicles (Roth et al., 1994). However, the actual function of this region (if any) remains unknown. The third region also named the C-terminal loop is comprised of mostly acidic amino-acids at the carboxy-terminus from residues 231 to 245 (Aitken, 1992; Aitken et al., 2002). Deletions of this C-terminal loop from 14-3-3ζ increase the binding affinity with target binding proteins Raf and Bad for reasons that are not apparent (Troung et al., 2002). Substitutions to residue 232 alter the conformation of 14-3-3s resulting in inhibition of phosphopeptide binding (Obsilova et al., 2003). Because this region is highly conserved among isotypes it suggests that all of them could potentially interact with similar target proteins. This data suggest that the C-terminal loop is a regulator of

```
                                                          *
MDKNELVQKA  KLAEQAERYD  DMAACMKSVT  EQGAELSNEE  RNLLSVAYKN   50
     *
VVGARRSSWR  VVSSIEQKTE  GAEKKQQMAR  EYREKIETEL  RDICNDVLSL  100
                            **
LEKFLIPNAS  QAESKVFYLK  MKGDYYRYLA  EVAAGDDKKG  IVDQSQQAYQ  150

ESFEISKKEM  QPTHPIRLGL  ALNFSVFYYE  ILNSPEKACS  LAKTAFDEAI  200

AELDTLSEES  YKDSTLIMQL  LRDNLTLWTS  DTQGDEAEAG  EGGEN       250
```

Figure 2. Vertebrate 14-3-3ζ phosphorylation sites and motifs

The amino acids in red 6 to 22 and 59 to 90 represents the regions involved in dimerization. The * above represents the amino acids involved in the binding site for phosphoserine target proteins. The blue represents potential phosphorylation sites.

14-3-3/ligand interactions. The combination of these regions is unique and characteristic of 14-3-3s among protein families.

Dimerization

The crystal structures of two typical mammalian isotypes, ζ and τ, demonstrate that these proteins are composed of nine anti-parallel α-helices that have the ability to form dimers (Liu et al., 1995; Xiao et al., 1995; Aitken, 1995; Fu et al., 2000; Yaffe and Elia, 2001; Obsil et al., 2001, Truong et al., 2002). The interaction occurs between residues 5-21 in helix 1 from one monomer and 58-89 in helices 3/4 from another monomer (Figure 2) (Aitken et al., 2002). Variations in these residues may affect the possible homo- and heterodimer combinations. This is consistent with studies in PC-12 cells that indicate that the γ isotype formed homodimers and heterodimerize with ε, whereas ε does not homodimerize and instead forms heterodimers with β, η, γ and ζ (Aitken et al., 2002). These variations could potentially influence which of the 14-3-3 interacting proteins can be brought together, hence altering functional specificity (Wang and Shakes, 1996). The 14-3-3 dimer forms a palisade around a central negatively charged amphipathic groove comprised mostly of invariant amino acids. From alignments of all known 14-3-3s, this groove with its cluster of polar residues from helices 3 and 5 and hydrophobic residues from helices 7 and 9 is over 70% conserved (Ferl et al., 2000). This groove provides a binding surface commonly, but not exclusively, for phosphoserine or phosphothreonine residues on target binding proteins (Figure 2) (Liu et al, 1995; Xiao et al., 1995; Fu et al., 2000; Aitken et al., 2002). The

fact that this region is highly conserved suggests that specificity for interacting proteins may by dictated by other less conserved regions.

Phosphorylation

In 14-3-3 proteins, there are four potential phosphorylation sites that could regulate potential dimer formation and target interaction. Serine-59 (Figure 2) can be phosphorylated by a novel sphingosine-dependent kinase or PKB/Akt (Megidish et al., 1998; Powell et al., 2002). Serine-63 (Figure 2) can be phosphorylated by PKC, but so far there is no evidence that this occurs in vivo (Toker et al., 1992; Jones et al., 1995; Aitken et al., 2002). There is evidence that the Bcr serine/threonine kinase can phosphorylate 14-3-3ζ, but the site of phosphorylation has not been determined yet (Reuther et al., 1994; Van Der Hoeven et al., 2000). In addition, a threonine (Thr-232) (Figure 2), conserved in all ζ isoforms and conservatively substituted with a serine in the τ isoforms is phosphorylated by casein kinase I and this modification appears to regulate interaction between 14-3-3ζ and c-Raf (Dubois et al., 1997). The motif SPEK (Figure 2) present in the ζ and β isoforms, is also a potential target for a proline directed kinase (Aitken et al., 2002). Although there is evidence that phosphorylation of various 14-3-3s occurs via several kinases (Jones et al., 1995; Van Der Hoeven et al., 2000; Reuther et al., 1994; Dubois et al., 1997; Megidish et al., 1998; Powell et al., 2002), there is no evidence that phosphorylation affects dimer formation or the role of 14-3-3s in basic cellular processes *in vivo.*

14-3-3 Functions

Binding motifs

The most common binding site for 14-3-3s is RSxSxP (where x = any amino acid), when the second serine in the motif is phosphorylated (Muslin et al., 1996). This motif is found in many 14-3-3 targets including Cdc25 phosphatase, Raf and two of the PKC isotypes (Muslin et al., 1996; Aitken et al., 2002). However, additional phosphorylated serine motifs have been identified making the consensus: R[S/Ar][+]pSXP or RX[Ar][+]pSXP, where Ar is an aromatic residue, + is a basic residue and pS is phosphoserine (Rittinger et al., 1999; Fu et al., 2000; Yaffe and Elia, 2001; Aitken et al., 2002). The binding site on the 14-3-3 monomer for the phosphoserine consists of a basic pocket composed of Lys-49, Arg-56, Arg-127 and Tyr-128 (Figure 2). Some of the kinases that appear to be involved in this serine/threonine phosphorylation include protein kinase B (Akt kinase), cAMP-dependent protein kinase, p21-activated protein kinase 1 (PAK), Ras-mitogen-activated protein kinase (RSK1 or MAPKAP-K1), MAP kinase-activated protein kinase-2 (MAPKAP-K2) and protein kinase C (PKC) (Fu et al., 1994; Michaud et al., 1995; Muslin et al., 1996, Aitken et al., 2002; Chen et al., 2003). One of these kinases has been investigated in *Drosophila*, the Akt kinase phosphorylates Ataxin-1 allowing its association with 14-3-3s (Chen et al., 2003). These experiments suggest that phosphorylation of target proteins is likely the primary mechanism to regulate 14-3-3 binding.

While many known target proteins appear to bind 14-3-3 via phosphoserine sequence motifs, additional modes of interaction are apparent (Aitken et al., 2002). The

crystal structure of 14-3-3s complexed with non-phosphorylated proteins suggests that the same negatively charged groove as that which binds phosphoserines is involved in these types of interactions (Fu et al., 2000). Evidence of this mode of interaction includes 14-3-3 binding to the cysteine-rich domain of Raf-1 (McPherson et al., 1999). Two unphosphorylated ligands that have been shown to bind with high affinity to14-3-3ζ are 5-phosphatase, which has a RSxSxP-like motif (RSESEE), and Exoenzyme S (ExoS) with a unique DALDL motif (Campbell et al., 1997; Masters et al., 1999; Aitken et al. 2002). Surface plasmon resonance spectroscopy between 14-3-3ζ and both glycoprotein I (GPI) bα (unphosphorylated GHSL motif) and GPIbβ (phosphorylation-dependent binding motif) indicate that the affinity for unphosphorylated ligands seems to be similar to that of phosphorylated ligands (Andrews et al., 1998; Aitken et al., 2002). The 14-3-3ζ binding to the WDLE motif of an unphosphorylated peptide derived from phage display library (R18, PHCVPRDLSWLDLEANMCLP) inhibits binding Raf-derived phosphopeptide (Petosa et al., 1998). The fact that these types of interactions can be inhibited by phosophoserine containing peptides is consistent with the hypothesis that both phosphorylated and unphosphorylated ligands use the same binding sites on 14-3-3's (Petosa et al., 1998; Masters et al., 1999). Binding of 14-3-3 to these types of proteins appears to alter their target binding, modify target localization, alter intrinsic catalytic activity, bringing proteins together and protecting proteins from modification (reviewed in Yaffe, 2002).

Enzyme activity modifiers

Tyrosine and tryptophan hydroxylase

14-3-3s were first identified as activators of tyrosine and tryptophan hydroxylases, the rate limiting enzymes in the biosynthesis of catecholamine and serotonin neurotransmitters (Ichimura et al., 1987; Ichimura et al., 1988; Makita et al., 1990). These studies assayed Ca2+/calmodulin-dependent protein kinase type II (kinase II)-dependent activation of tyrosine and tryptophan hydroxylases with and without the addition of excess 14-3-3 protein (Isobe et al., 1991). Their data suggested that kinase II phosphorylates the tyrosine and tryptophan hydroxylases creating a binding site for 14-3-3s leading to hydroxylase activation (Ichimura et al., 1988; Isobe et al., 1991). However, other research suggests that activation of tyrosine hydroxylase via phosphorylation is independent of 14-3-3 binding (Sutherland et al., 1993; Kumer and Vrana, 1996). They do agree that phosphorylations lead to the formation of a 14-3-3/hydroxylase complex (reviewed in Klein et al., 2003). Since this interaction has only been examined *in vitro* using brain extracts (Ichimura et al., 1988; Isobe et al., 1991; Furukawa et al., 1993; Sutherland et al., 1993; Kumer and Vrana, 1996; Banik et al., 1997), whether or not this complex truly activates tyrosine hydroxylase *in vivo* is still unknown.

Enzyme activity modulation

In addition to its interaction with tyrosine and tryptophan hydroxylases, 14-3-3s appear to interact with many other protein kinases including various isoforms of Raf,

protein kinase C (PKC), Kinase suppressor of Ras (KSR), Mitogen-activated protein kinase (MAPKs) and Bcr-Abl tyrosine kinase (reviewed in van Hermert et al., 2001). Although these studies indicated that 14-3-3 could interact with many different signal transduction molecules affecting the pathways in multiple steps, in most cases the function of the 14-3-3-protein association is still unclear. These interactions are presented below.

Enzyme activity modulation

Raf kinase

The most studied biological process involving 14-3-3s is the Ras/Raf pathway, where 14-3-3s have been shown to directly interact with various Raf's including Raf-1 and c-Raf (Jaumot and Hancock, 2001; Qui et al., 2000; Widen et al., 2000). The Ras/Raf signaling cascade is a major transduction pathway which links signals at the cell surface to changes in gene expression in the nucleus. The apparent primary role of 14-3-3 in the process is to directly bind Raf, recruiting it to the plasma membrane where it is protected from dephosphorylation (Figure 3) (Jaumot and Hancock, 2001; Widen et al., 2000; Morrison and Cutler, 1997; Fu et al., 2000; Chong et al., 2003). Raf is a mitogen-activated kinase (MAPK) kinase kinase that relays information by phosophorylation of MAPK kinase (MEK). Raf is composed of three conserved regions CR1 and CR2 that make up the regulatory domain and CR3 the catalytic kinase domain (reviewed in Chong et al., 2003). C1 contains the Ras binding domain (RBD) and cysteine rich domain (CRD) (residues 55-131) (Figure 3). The serine/threonine-rich CR2 appears to be where

phosphorylation dependent protein interactions occur that regulate localization and activity (Figure 3) (Dent et al., 1995; Roy et al. 1998; Chong et al., 2003).

At the plasma membrane, Raf interacts with the Ras-GTP complex through its CR1 domain at two sites RBD and CRD (Figure 3) (Morrison and Cutler, 1997; Roy et al., 1998; Fu et al., 2000; Chong et al., 2003). Raf also contains two phosphorylation dependent binding sites for14-3-3s including serine-259 in CR2 and serine-621 in CR3 and one phosphorylation independent site in the CRD of CR1 (Figure 3) (Morrison et al., 1993; Morrison and Cutler, 1997). The phosphorylation dependent sites and the ability of 14-3-3s to bind multiple sites on Raf may explain why some results indicate that 14-3-3s activate Raf and others imply that 14-3-3s suppress Raf activity (Morrison, 1994; Michaud et al. 1995; Morrison and Cutler, 1997). The current model is that the interaction between Ras and the CRD domain of Raf leads to activation of the kinase by displacement of 14-3-3 from the N-terminus (Morrison and Cutler, 1997; Roy et al., 1998). Evidence indicates that phosphatase 1 and 2A dephosphorylate serine-259 in the CR2 region, which allows the displacement of 14-3-3 from Raf (Figure 3) (Dent et al., 1995; Roy et al. 1998). Observations that Ras binding interferes with 14-3-3 interaction with the Raf N-terminal further support this model (Rommel et al., 1996; Morrison and Cutler, 1997). This displacement along with phosphorylation of serine-338 in the CR2 region completes the steps necessary for Raf association with the membrane and its activation (Roy et al., 1998; Jaumot and Hancock, 2001). This data is consistent with the CR2 region being necessary for localization and activation of Raf (Chong et al., 2003).

Raf displacement from the plasma membrane appears to occur when serine-259 is phosphorylated again (Figure 3) (Morrison and Cutler, 1997; Fu et al., 2000; Chong et al., 2003). This phosphorylation causes a conformational change that no longer allows Raf to bind the Ras-GTP complex (Figure 3) (Roy et al. 1998; Jaumont and Hancock, 2001). This model suggests that 14-3-3s have a dual role in modulating the catalytic activity of Raf, where binding to the CR1/CR2 region of Raf suppresses activation and binding to CR3 appears to be essential for Raf activity (Figure 3) (Light et al., 2002). The fact that more than one phosphorylation site is necessary for stable binding to Raf, suggests that 14-3-3s are likely to bind as dimers (Tzivion and Avruch, 2002). Evidence also suggests that any mutations in the amphipathic groove created by a 14-3-3 dimer disrupt binding to Raf (Wang et al., 1998). However, mutations that affect dimerization do not affect binding (Tzivion et al., 2001). This indicates that although 14-3-3s appear to form obligate dimers, they are capable of binding as monomers. It is unknown whether 14-3-3s interact with Raf as homo- or heterodimers, however, it is known that all isotypes are able to bind A-Raf, B-Raf and c-Raf-1 *in vitro* (Rittinger et al., 1999).

Active Raf

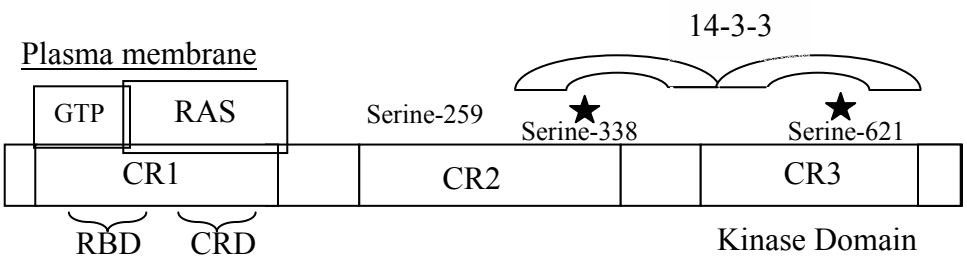

Inactive Raf

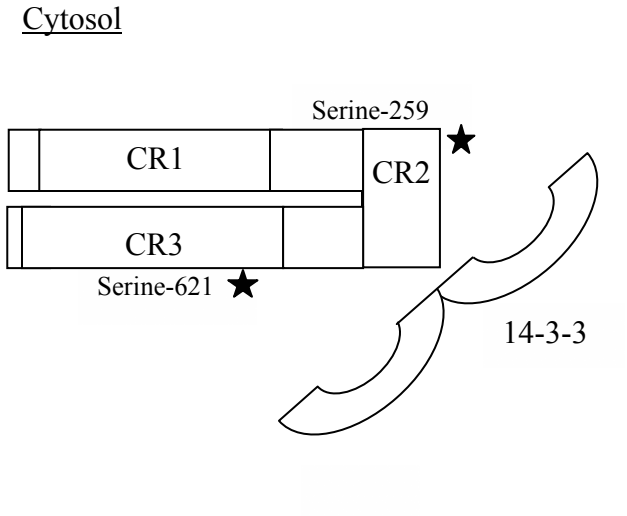

Figure 3. Map of Raf binding with 14-3-3 and Ras

(A) At the plasma membrane if the Ras-GTP complex is bound at the CR1 domain, serine-621 is phosphorylated (★) so a 14-3-3 dimer can bind and if serine-338 is phosphorylated, Raf is active. Ras binds to two sites, the Ras binding domain (RBD) and cysteine rich domain (CRD).
(B) If serine-259 is also phosphorylated the 14-3-3 dimer binds to Raf, creating a conformational change that no longer allows for Ras binding and shuttling Raf to the cytosol which causes Raf inactivation. Modified from Morrison and Cutler, 1997; Fu et al., 2000; Chong et al., 2003.

Protein kinase C (PKC)

To add to the dynamics of 14-3-3/Raf interactions, experimental evidence indicates that phosphorylation of 14-3-3 may regulate its ability to act as a scaffold between Protein kinase C (PKC) and Raf (Matto-Yelin et al., 1997; Van der Hoeven et al., 2000). Signal transduction mediated through PKC, is essential for basic cellular functions such as gene expression and proliferation (Nishizuka, 1988; Asaoka et al., 1992). The family of PKC isotypes share a conserved kinase core whose function is modulated by its regulatory domain (Figure 4). The three different types of PKC, the conventional (α, βI, βII, γ), novel (δ, ε, θ, η) and atypical (ζ, λ) groups, vary in their regulatory domain which dictates the cofactor dependence of the isotype (Figure 4). Unlike the conventional and novel PKCs that respond to diacylglcerol/phorbol esters, proteins of the atypical group do not respond to them, apparently because they lack the appropriate C1 domain (Figure 4). The conventional C2 domain binds phospholipid in a Ca^{2+} dependent manner, whereas the novel C2 domain binds neither Ca^{2+} nor membrane lipids. The regulatory domain is necessary for proper localization of the kinase and for regulation of kinase activity (Newton, 2003). PKC binds to 14-3-3 via a cysteine rich zinc-finger like region at its amino-terminal regulatory domain (Figure 4) (Aitken et al., 1992; Dai and Murakami, 2003). It is known that not all isotypes of 14-3-3 can bind to all isotypes of PKC (Van Der Hoeven et al., 2000). However if they do, the interaction occurs in the C1 not the C2 domain of PKC (Figure 4) (Matto-Yelin et al., 1997; Dai and Murakami, 2003). According to sequence data only PKC-γ, δ, ε, η, ζ, and λ contain the 14-3-3 phosphoserine consensus binding sequence. However, PKC-α and θ can also

complex with 14-3-3s, apparently in a phosphorylation independent manner by an unknown motif (Meller et al., 1996; Gannon-Murakami and Murakami, 2002).

The direct interaction between 14-3-3s and PKC appears to be both inhibitory and activating depending on the tissue examined (Toker et al., 1990; Toker et al., 1992; Isobe et al., 1992; Tanji et al., 1994; Matto-Yelin et al., 1997; Gannon-Murakami and Murakami, 2002). In *Dictyostelium discoideum*, PKC forms a complex with 14-3-3 in the cytosol in a cyclic AMP-dependent manner preventing PKC from attaching to the plasma membrane (Matto-Yelin et al., 1997). Only the membrane bound PKC is active; therefore, 14-3-3ζ's interaction with PKC in this case is inhibitory. This is consistent with evidence from PC-12 cells, where PKC-δ and ζ are bound by, and negatively regulated by 14-3-3ζ in differentiated cells (Meller et al., 1996; Matto-Yelin et al., 1997; Hausser et al., 1999; Gannon-Murakami and Murakami, 2002; Dai and Murkami, 2003). However, bound 14-3-3ζ allows constitutive PKC-ε activation in mouse brains (Dai and Murakami, 2003). This suggests that activation or inhibition may vary depending on the isotypes of PKC and/or isotypes of 14-3-3 present within any given tissue.

Apparently due to their interaction with PKC, 14-3-3s appear to play a role in exocytosis in cultured PC-12 cells. This process requires Ca^{2+}, is stimulated by PKC activation (at least in the system used) and seems to be augmented by the addition of 14-3-3s leading to an increase in catecholamine secretion (Morgan and Burgoyne, 1992a; Morgan and Burgoyne, 1992b; Chamberlain et al., 1995; Gannon-Murakami and Murakami, 2002). Anti-14-3-3 antibodies are able to block stimulation of this type of

Protein Kinase C

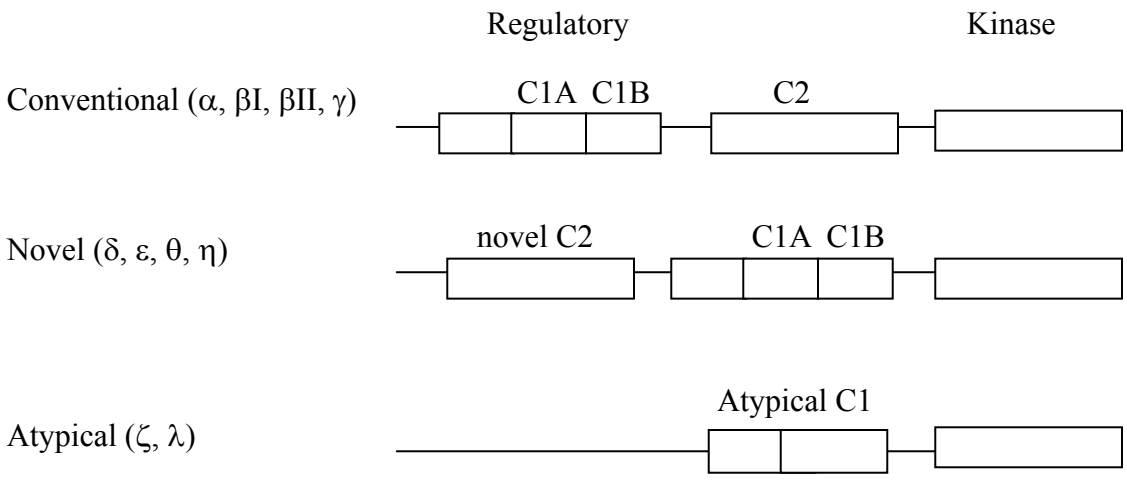

Figure 4. Domain maps of PKC isotypes

There are several isotypes of protein kinase C. The conventional group (α, βI, βII, γ) and novel (δ, ε, θ, η) have a regulatory domain composed of C1A/C1B, which are tandem repeats that function as a diacylglycerol sensor. In the atypical group the C1 domain does not respond to diacylglcerol/phorbol esters. The conventional C2 domain serves as a Ca^{2+}-regulated phospholipid-binding module; whereas the novel C2 domain binds neither Ca^{2+} nor membrane lipids. (Modified from Newton, 2003).

exocytosis (Wu et al., 1992). Furthermore, stimulation of exocytosis by 14-3-3 is blocked by excess of an oligopeptide identical to the centrally located invariant domain of the protein partially homologous to a domain in the synaptosomal protein annexin II (Roth et al., 1993). Interestingly, in independent experiments an oligopeptide largely identical to this domain was shown to block binding of activated PKC to annexin I, a membrane bound receptor protein for activated PKC (Mochly-Rosen, 1991). However, the interaction between 14-3-3 and annexin is not essential for exocytosis (Roth et al., 1993; Roth et al., 1999). It is likely then, that 14-3-3 interacts directly or indirectly with PKC in a way that regulates the effect of the kinase on exocytosis. In addition, 14-3-3s appears to increase PKC mediated exocytosis by reorganizing the cortical actin barrier allowing for the release of secretory vesicles (Roth and Burgoyne, 1995; Misonou et al., 1998; Roth et al., 1999)

Other enzymes

Another kinase that associates with 14-3-3s is the kinase suppressor of Ras (KSR), which typically appears to form a complex with Raf (Xing et al., 1997). Isolated in Ras suppressor screens, evidence suggests that KSR does not have kinase activity. It still plays an important role as a scaffold protein that has its location and function regulated by phosphorylation (Dhillion and Kolch, 2002). KSR can bind Raf, mitogen-activated protein kinases (MEKs) and extracellular signal-regulated kinases (ERKs) stimulating MEK activation at the plasma membrane (Figure 5) (Roy et al., 2002). Mitogen induced phosphorylation of serine-392 creates a 14-3-3 binding site and KSR is

sequestered into the cytosol (Muller et al., 2001; Dhillion and Kolch, 2002; Ory et al., 2003). Once protein phosphatase 2A dephosphorylates KSR at serine-392, it releases 14-3-3 allowing the translocation of KSR back to the membrane where it again interacts with Raf (Muller et al., 2001; Ory et al., 2003). Therefore, it appears that the interaction between KSR/14-3-3 is another step in regulating the Ras/Raf pathway (Figure 5).

14-3-3s also bind to mitogen-activated kinase kinase (MEK) (Figure 5) (Fanger et al., 1998; van Hermert et al., 2001). The binding between 14-3-3 and MEK has been mapped to the terminal 393 residues outside the kinase domain. In *S. cerevisiae*, 14-3-3 homologs (BMH1 and BMH2) bind multiple MEKs as well as the upstream activator ST20 similar to KSR. When a cell receives an extra-cellular signal to induce apoptosis, the MEK regulatory domain can be selectively cleaved by caspase-3 thereby removing the 14-3-3 binding site and inducing apoptosis (Fanger et al., 1997; Fanger et al., 1998). In fibroblasts, expression of the cleaved or activated form of MEK inhibited clonal expansion of transfected cells causing DNA fragmentation, cytoplasmic shrinkage and nuclear condensation, all characteristics of apoptosis (Johnson et al., 1996). Mutations in the cleavage site suppress adherence-induced apoptosis (Fanger et al. 1998). The interaction between 14-3-3s and MEK does not appear to influence activity or the caspase-mediated cleavage, but simply scaffold the kinase to other endogenous proteins (Fanger et al., 1998; van Hermert et al., 2001). From this data it appears that 14-3-3s allow selective organization and localization of signaling complexes.

Bcr is a multi-domain kinase which complexes with Raf via 14-3-3. However, its unique regions suggest it is involved in a different intracellular signaling pathway

from that of the typical Ras-Raf-MAPK signaling (Reuther et al., 1994; Braselmann and McCormick, 1995; van Hermert et al., 2001). The N-terminus of the *bcr* gene encodes a novel serine/theonine kinase domain where 14-3-3s appear to bind (Pendergast et al., 1991). It is known that Bcr does not bind directly to Raf. However, in the presence of 14-3-3β, a complex can be formed (Braselmann and McCormick, 1995). First discovered as the cause of Ph1-positive leukemias, the *bcr* gene had fused to the c-abl proto-oncogene forming the Bcr-Abl chimeric protein (reviewed in Reuther et al., 1994). 14-3-3 can also bind to the Bcr-Abl chimeric proteins. This protein is activated by the first exon of Bcr mediating the transformation of normal cells into leukemia positive cells (Reuther et al., 1994). Although there is no evidence that Bcr-Abl and Bcr are simultaneously bound to 14-3-3s, the fact that both have the ability to bind suggests that 14-3-3s may facilitate their interaction and/or simply allow them to complex with other signaling proteins such as Raf (Reuther et al., 1994; van Hermert et al., 2001).

14-3-3 also interacts with an acetyl transferase, Arylalkylamine N-acetyltransferase (AANAT). 14-3-3ζ and 14-3-3ε dimers bind a single AANAT in a phospho-dependent manner (Obsil et al., 2001). AANAT is necessary for regulating the daily rhythm of melatonin synthesis (Osbil et al., 2001). The interaction between 14-3-3s and AANAT appears to affect access to the N-terminal of AANAT preventing dephosphorylation (Ganguly et al., 2001; Obsil et al., 2001). Crystallographic analysis suggests that 14-3-3s have a role in modulating AANAT activity by stabilizing its substrate binding region (Obsil et al., 2001). However, it is unknown whether this interaction alters melatonin synthesis.

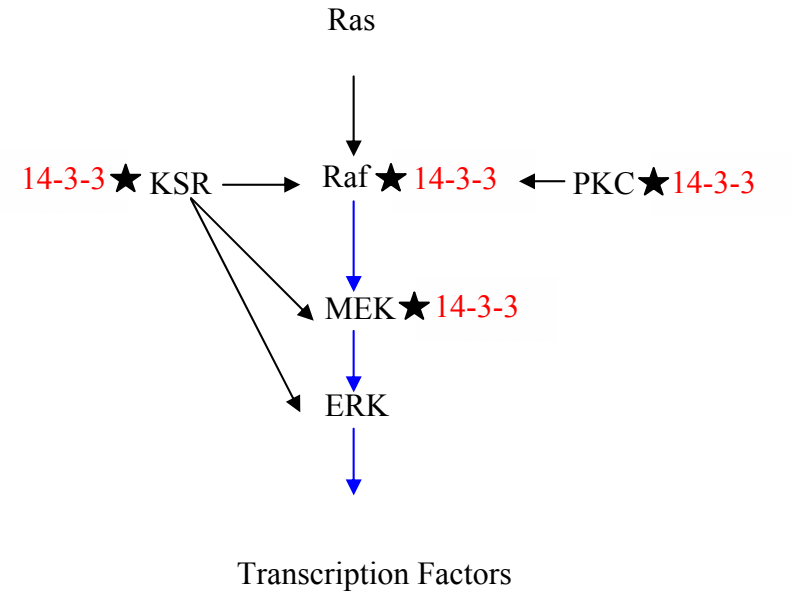

Figure 5. The role of 14-3-3s in the Ras-Raf-MAPK signaling pathway

14-3-3s can bind Raf (mitogen–activated protein kinase (MAPK) kinase kinase), protein kinase C (PKC) and Kinase suppressor of Ras (KSR) and MAPK kinase (MEK) potentially regulating their localization and subsequent kinase activity. In this pathway, Raf phosphorylates MEK, which phosphorylates extracellular signal-regulated kinase (ERK) leading to the activation of transcription factors.

Cell cycle

Another process that 14-3-3 proteins are essential for in vertebrates is regulating the cell cycle (Fu et al., 2000; Muslin and Xing, 2000; van Hemert et al., 2001). The four stages of the cell cycle include G1 (gap mitosis and before DNA synthesis), S (synthesis of DNA) phase, G2 (gap after DNA synthesis and before mitosis), and M (Mitosis). The transition between stages is highly regulated by the cyclin-dependent protein kinase (Cdks) such as Wee1/Mik1/Myt1, which are activated by their association with cyclin subunits and by phosphorylation of tyrosine and threonine residues (reviewed in Donzelli and Draetta, 2003). These complexes are inactivated by specific phosphatases that dephosphorylate phosphotyrosines and phosphothreonines such as Cdc25 (cell division cycle 25). In the mammalian system, there are three Cdc25's that have specific roles in cell-cycle regulation. The Cdc25A regulates the G1/S transition, S phase and G2/M transition, whereas Cdc25B and Cdc25C have a role in only the G2/M transition (van Hermert et al., 2001; Donzelli and Draetta, 2003). The localization of these proteins varies, with Cdc25A in the nucleus, Cdc25B in the cytosol and Cdc25C found in both nucleus and cytosol (Gabrielli et al., 1996; Donzelli and Draetta, 2003). This suggests that their localization may be linked to their roles in regulating cell cycle transitions.

One of the primary roles for 14-3-3s in the cell cycle is to regulate the cytoplasmic localization of Cdc25B and Cdc25C phosphatases, which affect the G2 to M transition (Forrest and Gabrielli, 2001). In yeast, 14-3-3's have been shown to have a role in G2 checkpoint regulation (Forrest and Gabrielli, 2001). The mechanism appears

to involve a direct interaction between 14-3-3σ and a phosphorylated Serine-(216) on Cdc25C or Cdc25B during the G2 interphase. The binding leads to cytoplasmic sequestering of Cdc25C or Cdc25B (Figure 6A) (Forrest and Gabrielli, 2001; van Hermert et al., 2001; Fu et al., 2000). Mutations in Serine-216 eliminate the ability of Cdc25C to bind 14-3-3σ compromising the G2/M transition (Graves et al., 2001). Nuclear localization of Cdc25C at the end of G2 is necessary for dephosphorylation of Cdc2, which allows the cell to enter mitosis (Figure 6A) (Su et al., 1998; Fu et al., 2000; van Hermert et al., 2001; Graves et al., 2001). Over-activation of Cdc2 has been shown to induce apoptosis in proliferating cells (Shi et al., 1994, Yu et al., 1998). In Hela cells in particular, loss of this type of Cdc25 regulation by 14-3-3's leads to a high proportion of abnormal mitotic phenotypes including DNA fragmentation, one of the characteristics of apoptosis (Forrest and Gabrielli, 2001). This is consistent with data from over-expression of 14-3-3σ in cell culture resulting in G2 arrest (Hermeking et al., 1997).

Apparently different 14-3-3s regulate the various transitions of the cell cycle by interacting with different enzymes. In mammalian tissue culture, 14-3-3σ specifically interacts with Cdc25B or Cdc25C to regulate the G2 to M transition (Hermeking et al., 1997; Forrest and Gabrielli, 2001; van Hermert et al., 2001; Donzelli and Draetta, 2003), whereas, 14-3-3ε interacts with Cdc25A regulating both the G1 to S and the G2 to M transitions (Chen et al. 2003). The mouse isoforms of 14-3-3ζ and β bind to Wee1 in a phospho-dependent manner increasing protein stability and activity which affects the G2 to M transition (Wang et al. 2000; van Hermert et al., 2001). 14-3-3ζ and ε interactions with Cdc25 appear to affect the DNA damage checkpoint that occurs during the G2 to M

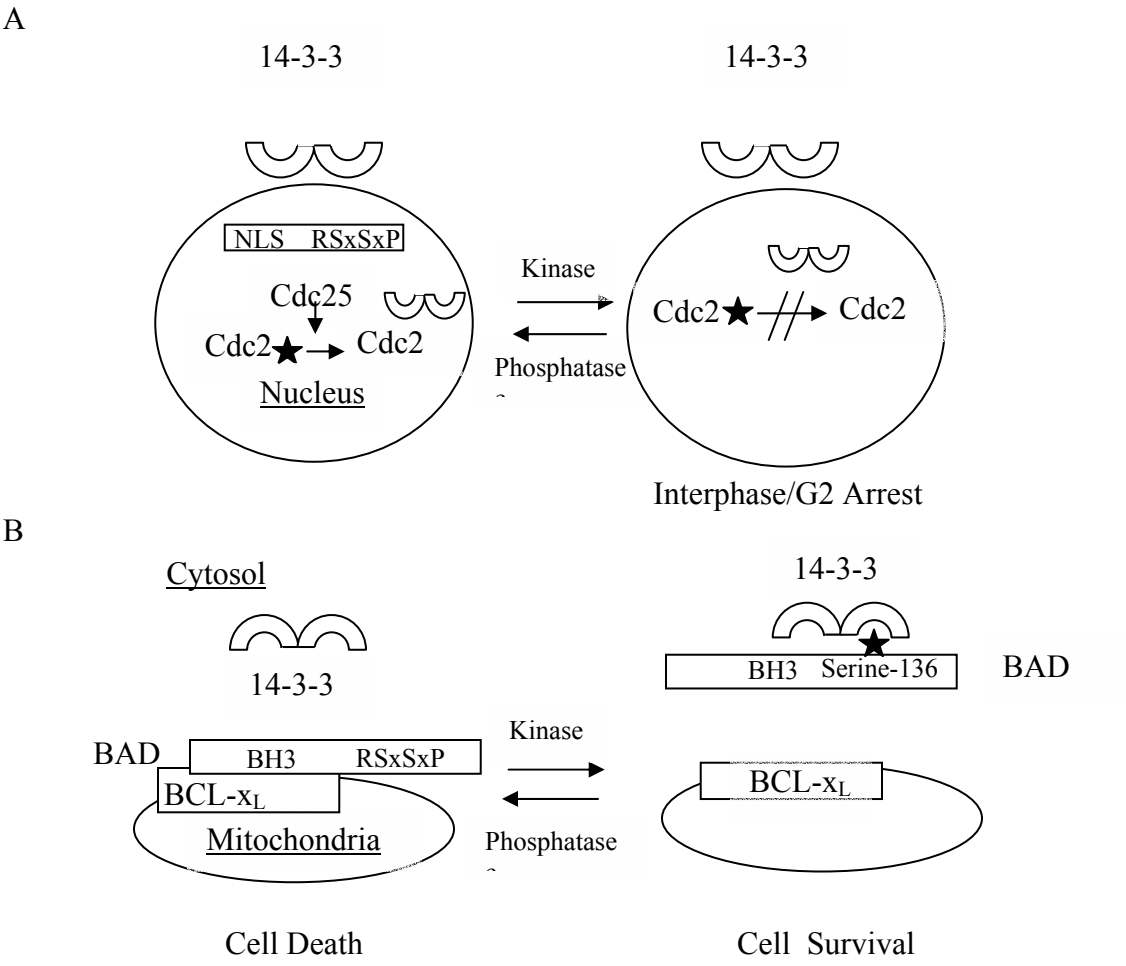

Figure 6. Role of 14-3-3 in the cell cycle and cell apoptosis

(A) During M-phase Cdc25 is in the nucleus dephosphorylating Cdc2 thus inactivating. At the end of G2, Cdc25 phosphorylation (★) at serine-216 leads to the cytoplasmic localization of Cdc25 and blockage of the nuclear localization signal (NLS) on Cdc25. Modified from Fu et al., 2000 and Muslin et al., 2000.
(B) Cell death occurs when BAD interacts with BCL-x_L in the mitochondria. If BAD is phosphorylated at serine-136, it interacts with 14-3-3 leading to blockage of the BH3 domain thus allowing for cell survival.

transition. When a cell has damaged DNA, there is a cell cycle arrest while the cell repairs it before mitosis continues. In *Drosophila*, mutations that do not allow Cdc25 to bind to 14-3-3ζ and ε cause embryos to prematurely proceed into mitosis (Su et al., 2001). In colorectal cancer cells, ionized radiation causes increased levels 14-3-3σ proteins, which results in arrest at both the G1 to S and G2 to M transitions (reviewed in van Hermert et al., 2001). The G1 to S transition is arrested when the p53 transcription factor is dephosphorylated allowing 14-3-3 to bind (Waterman et al., 1998; van Hermert et al., 2001). This interaction increases the DNA sequence-specific binding activity of p53 leading to transcriptional activation of genes that induce cell cycle arrest (p21 and GADD25) or apoptosis (Bax) (Levine, 2003; van Hermert et al., 2001). In all of these cases, 14-3-3s have an inhibitory effect on the progression of the cell cycle by inactivation via nuclear export and cytoplasmic sequestering or activation of different cell cycle regulators.

Apoptosis

Results from Konishi et al. (2002) suggest a direct link between components of the cell cycle and cell death that involves 14-3-3 proteins. Cell survival requires continuous cues from the extracellular environment. These cues include a series of cytokines that signal through tyrosine receptor kinases (TRKs) and insulin growth factor receptors (IGFR) (Zha et al., 1996). Conversely there are ligands that trigger apoptosis, such as FasL that signal through tumor necrosis factor (TNF) receptors (FAS and TNFR-55) (Zha et al., 1996). Within cells, there are proteins that promote survival (Bcl-2, Bcl-

xL, Mcl-1 and A1) or apoptosis (Bas, Bak, Bcl-xS and BAD) that dictate whether any given cell will respond to the extracellular signal (Zha et al, 1996; Adachi et al., 2003). These proteins function as apoptosis/survival heterodimers (BAD/Bcl-2), suggesting they act to counter each other with the extracellular signals tipping the scale in one direction or the other (Datta et al., 2000). The pro-apoptotic proteins all contain a BH3 domain to allow interaction with the survival factors. BAD is unique among BH3 containing proteins because it is regulated by a series of serine phosphorylations (Zha et al., 1996; Adachi et al., 2003).

When a cell receives a survival factor, BAD is phosphorylated at serine-155 and serine-136, where a binding site for a 14-3-3 is created (Datta et al., 2000). Binding of 14-3-3 to BAD induces a conformational change that inhibits BAD from associating with BCL-x_L, resulting in the cytoplasmic localization of BAD, which allows cell survival (Figure 6B) (Datta et al., 2000; Muslin et al. 2000; van Hermert et al., 2001). When BAD is dephosphorylated it binds to Bcl-x_L at its BH3 domain, which localizes BAD to the mitochondrial membrane leading to apoptosis (Muslin et al., 2000; van Hermert et al., 2001). However, if Cdc2 phosphorylates serine-128 on BAD, it inhibits the ability of 14-3-3s to bind, leading to apoptosis (Figure 6B) (Konishi et al., 2002). This research supports earlier work done by Xing et al. (2000) in cultured cells and cardiac tissue that concluded the primary function of mammalian 14-3-3s is to inhibit apoptosis. They suggested the role of 14-3-3s in apoptosis involves sequestering phosphorylated BAD to the cytosol, thereby preventing its interaction with Bcl (Springer et al., 2000). It is unknown whether in these tissues this interaction is affected by Cdc2,

only that when an apoptotic stimulus is present BAD is dephosphorylated allowing dissociation from 14-3-3.

Modifiers of receptors and channels

Localization

Recently 14-3-3 proteins have been found to play a role in controlling the function and localization of different receptors and ion channels (Couve et al., 2001; Ganguly et al., 2001; Kagan et al., 2002; Berg et al., 2003). In rat brains, 14-3-3ζ associates with γ-Amino-butyric acid GABA type B receptor ($GABA_BR1$) to regulate aspects of its trafficking and targeting of $GABA_B$ to the plasma membrane (Couve et al., 2001). The glycoprotein Ib-IX complex (GP Ib-IX) is a platelet receptor that plays a role in platelet adhesion and aggregation during injured vascular walls (van Hermert et al., 2001). 14-3-3ζ has the ability to interact with several proteins in this complex including GP Ibz, GP Ibb and GP-V (Andrews et al., 1998). When injury occurs, the platelets are stimulated and 14-3-3ζ the GP Ib-IX complex and phosphoinositide 3-kinase (PI3-Kinase) are all translocated to the cytoskeleton (Munday et al., 2000). This suggests that 14-3-3ζ functions as a link between the GP Ib-IX complex and PI3-Kinase that may be involved in this translocation (Andrews et al., 1998; Munday et al., 2000; van Hermert et al., 2001). Another example of the potential role of 14-3-3s in translocation of a receptor occurs when 14-3-3η binds to glucocorticoid receptor (GR) leading to its translocation into the nucleus (Wakui et al., 1997). This data is consistent with the model that 14-3-3s modulate the activity of the receptors by altering their

location and/or ability to bind other target proteins (Kagan et al., 2002; Ganguly et al., 2001; Obsil et al., 2001).

Functional modulation

In human tissue, ether-a-go-go related protein HERG, a rectifier potassium channel, binds directly with 14-3-3ε accelerating and enhancing HERG activation which regulates membrane potential (Kagan et al., 2002). In rats, 14-3-3ζ and 14-3-3ε bind with chloride intracellular channel proteins (CLIC4) and DYNAMIN I to influence membrane trafficking (Sugita et al., 2001). In *Drosophila,* there is evidence that 14-3-3ζ complexes with the calcium dependent potassium channel Slowpoke via Slowpoke binding protein (Slob) regulating voltage sensitivity of the membrane at pre-synaptic nerve terminals (Zhou et al., 1999; Zhou et al., 2001). This interaction is dependent on the phosphorylation of Slob and can occur in the absence of 14-3-3 dimerization, suggesting that 14-3-3 monomers can regulate channel activity (Zhou et al., 2003). These experiments indicate that 14-3-3s may regulate channel activity by mediating phosphorylation of the receptor/channel or coupling them with other proteins or signaling complexes (Sugita et al., 2001; Zhou et al., 1999; Zhou et al., 2003). However, the effect of these interactions on development or information processing in the nervous system is still unknown.

Adapters/Chaperones

In vertebrates, 14-3-3s appear to participate in many diverse cellular processes where they bring two different proteins together in an adapter like manner. Their ability to dimerize allows them to simultaneously bind two proteins facilitating the formation of signaling complexes. 14-3-3s interact with signaling proteins typically in a serine/threonine phosphorylation dependent manner to regulate their localization, activity, and ability to bind other proteins or be modified. 14-3-3s bring various enzymes together such as Raf and KSR or Raf and PKC or MEK and KSR all of which may play a role in regulating the Ras-Raf-MAPK signaling pathway (Figure 5) (reviewed in van Hermert et al., 2001). Although considered to be part of another signaling pathway, 14-3-3β also facilitates interaction between Bcr/Raf and c-Bcr/Bcr-Abl in regulation of cell proliferation (Reuther et al., 1994; Braselmann and McCormick, 1995). Furthermore, 14-3-3s have the ability to bring together different receptors with their associated proteins, for example insulin-like growth factor I receptor (IGFIR) with the insulin receptor substrate I (IRS-1), in regulation of cellular growth and differentiation (Craparo et al., 1997). Another example, is the binding of 14-3-3ζ to chloride intracellular channel proteins (CLIC4) and DYNAMIN I creating a complex that regulates membrane trafficking (Suginta et al., 2001). 14-3-3s bind together GP Ib-IX complex and PI3-Kinase to regulate the activity of the kinase (Andrews et al., 1998; Munday et al., 2000; van Hermert et al., 2001). In many of these cases, 14-3-3s have the ability to activate or inhibit enzymes allowing them to regulate multiple steps in several signaling pathways.

Table 2. Proteins with 14-3-3-dependent alternate cellular location

Interacting protein	Unbound location	Bound location
Calmodulin	cytosol	Centrosome/spindle apparatus
Raf	plasma membrane	Cytosol (Serine-259)
PKC	plasma membrane	Cytosol
KSR	plasma membrane	Cytosol
BAD	mitochondria	Cytosol
Cdc25	nucleus	Cytosol
Histone deacetylase	nucleus	Cytosol
$GABA_BR1$	cytosol	plasma membrane
GP Iβ-IX / PI3-Kinase	cytosol	Cytoskeleton
GR	cytosol	Nucleus

Raf(mitogen-activated kinase kinase kinase)
KSR (Kinase suppressor of Ras)
PKC (Protein kinase C)
Cdc25 (cell division cycle 25)
$GABA_BR1$ (α-Amino-butyric acid GABA type B receptor)
GP (glycoproteins)
GR (glucocortcoid receptor)

Although there are several examples of 14-3-3s functioning as adapters, their predominant role appears to be as chaperones. 14-3-3s modulate the localization of target proteins such as calmodulin from the cytosol to the centrosome and spindle apparatus (Table 2) (Chan et al., 2000). Other proteins that interact with 14-3-3 appear to be directed or sequestered to the cytosol including Raf (Jaumot and Hancock, 2001; Widen et al., 2000), PKC (Matto-Yelin et al., 1997), KSR (Ory et al., 2003), Cdc25 (McGonrangle et al., 2001), BAD (Zha et al., 1996), and histone deacetylase (Grozinger and Schreiber, 2000) (Table 2). The signaling mechanism that allows 14-3-3s to bind and translocate proteins to their appropriate location appears to be phosphorylation dependent in all of these cases. Moreover, 14-3-3s control localization of different receptors $GABA_BR1$ (Couve et al., 2001), GP Iβ-IX/PI3 Kinase (Munday et al., 2000) and GR (Wakui et al., 1997) from the cytosol to their appropriate locations (Table 2). It is unknown whether or not these interactions are phosphorylation dependent. In addition, this unique family of adapter/chaperones has the ability to bind non-phosophorylated motifs, increasing the number of potential target proteins. Regardless of their mode of action, it is clear that 14-3-3s are essential in several basic cellular processes.

14-3-3 implications in disease

14-3-3s and neurodegenerative disease

Recent studies indicate that the distribution of 14-3-3 proteins changes in multiple human neuro-degenerative diseases including spongiform encephalitis or

Creutzfeldt-Jakob disease (CJD) (reviewed in Berg et al., 2003). The human transmissible spongiform encepalopathy or prion disease was first characterized by Hans Gerhard Cretzfeldt and Alfons Jakob in the1920's (Creutfeldt, 1920; Jakob, 1921). New clinical diagnostics indicate that there are two forms of transmittable CJD, sporadic CJD and variant CJD (Zerr and Poser, 2002). Sporadic CJD occurs in patients in their seventies and is characterized by rapid dementia that lasts 6 to 14 months resulting in death (Zerr and Poser, 2002). In contrast, variant CJD occurs in patients from 14 to 74 years of age and has a slower progression that may last years (Zerr and Poser, 2002). To characterize this and other neurodegenerative diseases, researchers are looking for changes in the protein levels in cerebral spinal fluid (CSF) or in disease specific lesions within the brain.

Clinical studies have described increases in different 14-3-3s (β, ε, γ, τ and ζ) in the cerebrospinal fluid from patients with Creutzfeldt-Jakob disease (CJD) (Table 3) (Takahashi et al., 1999; Sanchez-Valle et al., 2002). The anti-14-3-3β antibody appears to be both sensitive and specific for sporadic CJD in suspected patients (Zerr et al., 1998; Zerr et al., 2000; Takahashi et al., 1999; Wiltfang et al., 1999; Wakabayashi et al., 2001; Giraud et al., 2002). On the other hand, increased levels of 14-3-3γ and 14-3-3ε were present in the CSF of patients with CJD, Alzheimer's disease and Down Syndrome (Table 3), suggesting they may be more general markers for neurodegeneration (Fountoulakis et al., 1999; Tschampa et al., 2001). Research indicates that 14-3-3β is also elevated in the CSF of multiple sclerosis patients who have severe inflammation-induced extensive damage of the central nervous system (Sanchez-Valle et al., 2002;

Table 3. Changes in 14-3-3 expression in diseases

Disease	CSF/Tissue	Isotypes up-regulated	Isotypes down-regulated
Creutzfeldt-Jakob disease (Sporadic)	CSF	β, ε, γ, τ, ζ	
Alzheimer's disease	CSF	ε, γ	
Down Syndrome	CSF	ε, γ	
Multiple sclerosis	CSF	β	
Scrapie	Hippocampus Thalamus		β, γ, η, ζ
Herpetic encephalitis	CSF	β	
Small Cell Lung Cancer	Cells	ζ, β, ε, τ/θ	σ
Breast Cancer	Cells		σ
Mammary carcinoma	Cells		σ
Anaplastic carcinomas	Cells	σ	
Papillary carcinomas	Cells	σ	

CSF(CerebralSpinalFluid)

Satoh et al, 2003). The levels of the different 14-3-3s in the CSF appear to correlate with the particular areas of the brain that are damaged and how rapidly neurodegeneration occurs (Zerr and Poser, 2002; Huang et al., 2003). In the hippocampus and the thalamus of scrapie-infected mice there appears to be preferential loss of 14-3-3β, γ, η and ζ proteins in areas of severe degeneration (Table 3) (Baxter et al., 2002; Berg et al., 2003). In some cases, such as herpetic encephalitis 14-3-3s may be present in the CSF initially (Table 3), but not later on. In addition, in dementia caused by Lewy bodies, 14-3-3s may not start to appear until later stages of dementia (Huang et al., 2003). Therefore, examining the level of 14-3-3 proteins in the CSF is not sufficient for a full diagnosis of any of these diseases, but rather in conjunction with clinical data may help with the diagnosis and characterization of different neurodegenerative diseases (Zerr et al, 2000; Zerr and Poser, 2002).

14-3-3s are highly abundant in the central nervous system (Table 1), but whether the presence of 14-3-3s is a cause or effect of neurodegeneration remains unclear. However, there is evidence that 14-3-3ζ appears to affects the stability of microtubule associated protein, τ (Hashiquchi et al., 2001). The tight association appears to lead to abnormal phosphorylation of τ via protein kinase A (PKA). This abnormal phosphorylation τ is a key event the development of Alzheimer's disease pathology (Wang et al., 1995; Hashiquchi et al.,2000). In Spinocerebellar ataxia type 1 (SCA1), a polyglutamine disease, neurological disorders are caused by expansion of ataxin-1 protein (Chen et al., 2003). 14-3-3s have the ability to interact with both the wild type and mutant ataxin-1 and when 14-3-3ε is co-over-expressed it enhances neurotoxicity by

stabilizing the mutant ataxin-1 (Chen et al., 2003; Berg et al., 2003). In Parkinson's disease, there is an accumulation of α-synuclein that results in formation of Lewy bodies leading to neurodegeneration (Kawamoto et al, 2002). 14-3-3s complexes with α-synuclein mediate dopamine dependent neurotoxicity (Xu et al., 2002; Berg et al., 2003). All of these studies suggest that 14-3-3 proteins may in fact promote neurodegeneration by stabilizing neurotoxic proteins (Hashiquichi et al., 2001; Xu et al., 2002; Chen et al., 2003)

It is unclear why in the adult central nervous system (CNS) 14-3-3 proteins are necessary to regulate neurodegeneration. One explanation for why they are necessary relates to their potential involvement in regulating neuronal regeneration (Berg et al., 2003). Research in rats indicates that 14-3-3ζ and τ/θ are upregulated in injured motor neurons (Namikama et al., 1998). Their model suggest that when 14-3-3s are upregulated it facilitates the Ras-Raf-MAPK signaling pathway (Figure 5) that is known to alter gene expression during neuron regeneration (Kiryu et al., 1998; Namikama et al, 1998). In this case, 14-3-3s appear to activate Raf-1 in response to nerve injury stimulating the expression of growth factors necessary for peripheral nerve regeneration (Kiryu et al., 1995; Tanabe et al., 1998; Kiryu et al., 1998). This activation along with down regulation of PKA, which inhibits Raf-1 leads to stimulation of the Ras-Raf-MAPK signaling pathway (Kiryu et al., 1995). The up-regulation of 14-3-3 may also promote cell survival through its interaction with BAD, a protein that promotes cell death. Therefore, 14-3-3s may be necessary for maintaining neuronal integrity by promoting both survival and nerve regeneration (Berg et al., 2003).

14-3-3s and cancer

Due to their ability to regulate the cell cycle, 14-3-3s have been studied for their potential role in tumorigenesis. 14-3-3σ regulates the G2 cell cycle check point by sequestering Cdc2-cyclinB into the cytoplasm (Chan et al., 1999). In lung and breast cancers, there is a frequent loss of 14-3-3σ expression (Table 3) (Ferguson et al., 2000; Osada et al., 2001). This inactivation appears to be linked to hypermethylation that silences 14-3-3σ gene expression in the most aggressive type of lung cancer, small cell lung cancers (Osada et al., 2001). 14-3-3σ is also down-regulated in transformed mammary carcinoma cells (Table 3) (Yang et al., 2003). It was found that the link between 14-3-3σ and the tumor-suppressor p53 is important for transcriptional activity, which regulates cell cycle transitions (Laronga et al., 2000; van Hermert et al., 2001; Yang et al., 2003). This data is consistent with over expression of 14-3-3σ inhibiting cell proliferation and preventing growth of breast cancer cells (Laronga et al., 2000). In contrast, 14-3-3ζ, β, ε and τ/θ appear to be highly expressed in lung cancers (Table 3), suggesting that likely there are differential roles for 14-3-3s in cell cycle regulation (Qi and Martinez, 2003).

A further understanding of how 14-3-3's affect the cell cycle may provide evidence for potential treatment options for these types of cancers. The level of 14-3-3s appears to vary depending on the type of cancer cells (Yang et al., 2003; Ito et al., 2003; Qi and Martinez et al., 2003). For example, 14-3-3σ is expressed at a higher level in anaplastic carcinomas than papillary carcinomas and is down-regulated in breast and lung cancers (Table 3) (Ito et al., 2003; Yang et al., 2003). Therefore, changes in the

level of 14-3-3 proteins may be a useful diagnostic tool for cancer detection and characterization.

Are 14-3-3s functionally redundant?

The dynamic roles of 14-3-3s in signaling processes raise the question of whether all 14-3-3 isotypes exhibit similar activities toward all potential substrates, or have functional specificity. All 14-3-3 proteins are capable of dimer formation mediated by the amino-terminal helix (Jones et al., 1995; Luo et al., 1995). The crystal structure indicates a compact, globular molecule. The properties of the dimer interface or temporal and spatial distribution of 14-3-3 isotypes may play the primary role in which homo- or heterodimers can be formed (Aitkens, 1995; Jones et al., 1995; Aitkens et al., 2002). However, data suggest that the variability in the dimerization region may actually limit the possible heterodimers (Aitkens, 1995; Aitkens et al., 2002). For example, in PC12-cells, 14-3-3γ formed homodimers and heterodimers with ε (Aitkens et al., 2002). In contrast, ε formed heterodimers with all the 14-3-3 isotypes tested (β,η,γ and ζ), but apparently no homodimers, suggesting that the differences in the dimer interface correlate to dimer preference and not the sub-cellular localization of an isotype (Aitken et al., 2002). It is known that α and δ are phosphorylated forms, a modification that could change dimerization preferences among isoforms (Aitkens, 1995). Phosphorylation could limit dimer formation and the selectivity, or specificity of dimers towards their targets. The ability of 14-3-3 to be modified by phosphorylation increases the probability of differential target interactions and does not appear to inhibit their

ability to bind phosophoserine target proteins (Woodcock et al., 2003). It is likely however that dimer interface, modifications and subcellular localization contribute to homo and heterodimer formation depending on the particular isotypes under consideration. In addition, as yet unknown proteins may mediate dimer formation by promoting particular combinations of isotypes to form homo and heterodimers and/or preventing others from forming. These putative processes could result in selective and regulated dimer formation even within a particular cell.

Different combinations of 14-3-3s could potentially form distinct populations of dimers that each recognize unique ligand binding motifs or have different binding affinities (Yaffe, 2002). The interaction may be dependent on the target binding motif. Rittinger et al. (1999) demonstrated that all 14-3-3 isotypes were able to bind A-Raf, B-Raf, c-Raf-1 and BAD *in vitro*. All of these proteins share the same optimal consensus motif RSxpSxP (Rittinger et al., 1999; Fu et al., 2000; Aitkens et al., 2002). Experiments using this RSxpSxP peptide as the target protein indicated that 14-3-3s interact with the same specificity (Wang et al., 1998; Andrews et al., 1998; Yaffe et al. 1997). However, Rosenquist et al. (2000) postulated that 14-3-3 specificity may be similar for this optimized motif, but more selective towards more diverse motifs. This is supported by evidence that 14-3-3σ specifically interacts with Cdc25B or Cdc25C whereas, 14-3-3ε interacts with Cdc25A (Hermeking et al., 1997; Forrest and Gabrielli, 2001; van Hermert et al., 2001; Donzelli and Draetta, 2003). Preferential interactions between PKC-θ and 14-3-3τ (Meller et al., 1996), the IGF1 receptor and 14-3-3ε (Craparo et al., 1997) and the glucocorticoid receptor and 14-3-3η (Wakui et al., 1997;

Yaffe et al., 1997) have been documented. Due to the high homology within the inner binding surface, the functional specificity among isotypes is likely the result of variability in the outer surface of the 14-3-3 dimers caused by the particular isotype combination of each dimer (Yaffe et al., 1997; Fu et al., 2000; Aitkens et al., 2002).

Studies suggest that 14-3-3 monomers are thermodynamically unstable; therefore, 14-3-3s form obligate dimers (Aitken et al., 2002). However, mutations that affect dimerization do not inhibit the ability to bind target proteins or modulate target activity, suggesting that 14-3-3s may function both as dimers and monomers (Tzivion et al., 2001; Zhou et al., 2003). In fact, Woodcook et al., (2003) have been able to detect 14-3-3 monomers *in vivo*. It appears that both 14-3-3 monomers and dimers are able to interact with targets *in vivo*, for example Raf (Shen et al., 2003). However, only the interaction between the 14-3-3 dimer and Raf appears to be phosphorylation dependent and the dimer has reduced susceptibility to phosphorylation (Shen et al., 2003). This suggests that phosphorylation may both regulate the interaction between 14-3-3s and target binding proteins. 14-3-3ζ monomers and dimers are both able complex with Slob (channel binding protein) and the *Drosophila* calcium-dependent potassium channel (dSlo) (Zhou et al., 2003). In this case, the dimer is not necessary for modulation of the dSlo channel (Zhou et al., 2003). The suggests that 14-3-3 interactions with target proteins is independent of dimerization (Tzivion et al., 1998; Shen et al., 2003; Zhou et al., 2003).

EXPERIMENTAL MODEL

The *Drosophila melanogaster* or fruit fly model system is useful for genetic dissection of developmental and anatomical traits (Nusslein-Volhard et al., 1987; Sokolowski, 2001). These insects have a relatively short generation time of approximately 9 days, allowing for rapid production of specimens for experimental purposes. Their life cycle is divided in the following stages: embryonic (0-16 hours after egg lay (AEL)), 1st instar larval (16-48 hours AEL), 2nd instar larval (48-72 hours AEL), 3rd instar larval (72-120 hours AEL), pupariation (120-200 hours AEL) and the adult stage that can last up to 90 days depending on the genetic background (Ashburner, 1989). Each stage can be easily identified by morphological differences, which allow the examination of specific traits throughout development and in the adult.

This research project examines the role of 14-3-3s in basic cellular process and in information processing using an integrated molecular, genetic, histological and behavioral approach. *Drosophila* provides a simple model system for studying isotype/isoform specific function and regulation with at least one member of each major 14-3-3 isotype groups. This allows the systematic investigation of 14-3-3 functions *in vivo*. In *Drosophila*, the distribution of 14-3-3s is similar to that of vertebrates, where 14-3-3s are enriched in the nervous system, as well as expressed at lower levels throughout other tissues (Skoulakis and Davis, 1996; Broadie et al., 1997; Philip et al., 2001). Since, *Drosophila* are amenable to behavioral manipulation and are capable of both associative and non–associative learning and memory (Davis, 1996; Roman and Davis, 2001, Heisenberg, 2003), by combining sophisticated molecular and classical

genetics with behavioral manipulation, the role of 14-3-3 can be examined in development as well as in information processing in the adult central nervous system (CNS).

In *Drosophila*, temporal and spatial specific gene expression can be regulated with a wide variety of transgenic constructs including heat shock inducible transgenes and the UAS/GAL4 system. This system is especially suited for the study of genes with multiple temporally and tissue distinct roles like *leo*, because it allows their temporal and tissue specific dissociation allowing for the study of multiple phenotypes individually. The availability of several different GAL4 lines that express specifically in different tissues and stages of development provides a system to dissect each phenotype individually and identify the tissue affected by mutations in the gene in different temporally distinct (developmental or not) phases. There are several different available mutants of the two 14-3-3 isotypes in *Drosophila* including P-element insertions, deletions and point mutations. Each was used to accurately map phenotypes and help us to further understand the role of each isotype throughout early development and adult neuronal processes.

Learning and memory in *Drosophila*

Drosophila are capable of learning in a variety of positively or negatively reinforced associative or non-associative tasks utilizing olfactory, visual and tactile stimuli. *Drosophila* share all the same basic elementary characteristics of learning and memory with mammalian species, including humans and are capable of learning and

remembering what they are taught for significant portion of their lives (Cheng et al., 2001; Sokolowski, 2001). The *Drosophila* genome also contains genes for neuronal signaling proteins including neuronal cell adhesion receptors, ion channels, neurotransmitter receptors, synapse-organizing proteins and synaptic vesicle-trafficking proteins that share homology in mammals (reviewed in Yoshihara et al., 2001). There are also high number of fly homologs of human neurological disease loci (Yoshihara et al., 2001). Therefore, understanding of genes that have roles in learning and memory and neuronal physiology in *Drosophila* will enable comprehension of these processes in humans and other vertebrates.

Associative learning in *Drosophila* involves experience dependent encoding of temporal and spatial relationships that exist between stimuli. This type of Pavlovian or classical conditioning (Pavlov, 1927), involves pairing a neutral stimulus (the conditioned stimulus (CS)) with a biologically meaningful event (the unconditioned stimulus (US)). The fly learns to respond differently to a CS that was paired with a US (the CS+) and a stimulus that was not paired to a US (the CS-). This type of conditioning has been demonstrated in several species, suggesting that the basic biological processes involved are likely evolutionarily conserved. There are also different types of non-associative learning that can produce a differential response to the CS+. These include habituation, desensitization and sensory fatigue or adaptation. Repeated or prolonged exposure to a stimulus can cause desensitization, sensory fatigue or adaptation, which involve physiological changes that decrease the sensitivity to a stimulus (Dalton, 2000). Habituation is also a gradual diminution of response to a

repetitive stimulus, but it does not appear to involve changes in sensitivity and the response will return after the presentation of a noxious novel stimulus (dishabituation).

In *Drosophila*, it appears that associative learning involves the integration of information within the mushroom bodies (reviewed in Heisenberg, 2001). However, where non-associative learning occurs is unknown. To further understand the flow, processing and integration of associative and non-associative information in the adult CNS the following questions need to be addressed. What structures or neurons are necessary for learning and memory? What physiological or biochemical changes occur in those cells and how does information get in and around specific neurons (Davis, 2001)? The variety of genetic mutants in *Drosophila* have been great tools in understanding the CNS structures and neurons involved in various associative learning and memory tasks and some of the physiological or biochemical changes that may be occurring, although the flow of information within the CNS is less clear.

There are different behavioral paradigms that can be used to address the previous questions including assays based on an all-or-nothing response or choice assays. Assays based on all-or-nothing response include the proboscis extension reflex and the chemosensory jump. These assays involve a simple response to a single stimulus, although it is sometimes difficult to determine whether the lack of response is due to inability to detect the stimulus or its incorrect identification. For the choice assay, most commonly used to study olfactory learning and memory, attraction and avoidance are measured by the response of the flies when presented with two similar stimuli (Devaud

et al., 2003). The following is a summary of *Drosophila* behavioral paradigms, anatomical structures and genetic methods that are relevant to this analysis.

Sensory stimuli

Olfaction

The system primarily studied in *Drosophila* is the pathway of information flow necessary for olfactory learning. The perception of odors is essential in *Drosophila* for the identification of food sources and suitable sites for egg laying among other functions (Vosshall, 2000). 60 odorant receptors (ORs) located on sensilla on the surface of the maxillary palp (bulbous protrusion at the anterior proboscis) and aristas (hair like protrusions extending from the 3rd antennal segment or funiculus) receive olfactory information (Stocker, 1994; Vosshall, 2000). The sharp-tipped trichoid sensilla, the club-shaped basiconic sensilla, and tiny coeloconic sensilla can all be found on the surface of the funiculus but, the maxillary palps contain only basiconic sensilla (reviewed in Stocker, 2001). The information is then relayed by the 1500 olfactory receptor neurons (ORNs) to glomeruli in the antennal lobe (Figure 7) (Stocker, 1994; de Bruyne et al., 2001). The glomeruli are the sites of synaptic integration between terminal branches of ORNs and the dendritic arborizations of interneurons (Laissue et al., 1999). There are 43 morphologically distinct glomeruli in the antennal lobes that process the information from the ORNs (Laissue et al., 1999; Vosshall, 2000). Blocking neurotransmission from any individual glomerulus selectively affects odorant perception (Devaud et al., 2003). Local interneurons that connect various glomeruli and projection

interneurons relay the information from the antennal lobe to higher order brain centers (Stocker, 1994; Laissue et al., 1999; Stocker, 2001). Extra-cellular electrophysiological recordings were able to map the olfactory response to a spectrum of odors within the *Drosophila* antennal lobes (de Bruyne et al., 2001). This allowed the classification of groups of ORNs that respond to specific odors (de Bruyne et al., 2001; Stocker, 2001). Using this type of assay, de Bruyne et al., (2001) determined that the mechanism for olfactory encoding depends on the odor identity, odor concentration and length of odor presentation. Exposure to a strong odor can also reduce the response to, or salience of subsequent odors (Preat, 1998). Studies of a single ORN suggest that an odorant has the potential to bind multiple ORs and activate or inhibit any of several different ORNs (Laurent et al., 1996; Vosshall, 2000).

Olfactory information from the antennal lobe is then relayed via the projection neurons to the mushroom bodies and the lateral horn (Figure 7 and 8) (Stocker, 1994; Heisenberg, 2003). Since the *Drosophila* olfactory system appears to be similar to, but a lot simpler than that of mammals, it is a powerful model system to studying odor processing (Stocker, 2001). The mushroom bodies apparently process olfactory information, but are not essential for odor recognition and elementary responses such as avoidance of aversive odors and attraction to appetitive odors (osmotaxis). However, recent evidence (Wang et al. 2003), suggests that blocking neurotransmission to mushroom bodies selectively impairs responses to attractive but not aversive odors. This information contrasts with previous studies (de Belle and Heisenberg, 1994; McQuire et al., 2001) and our own evidence

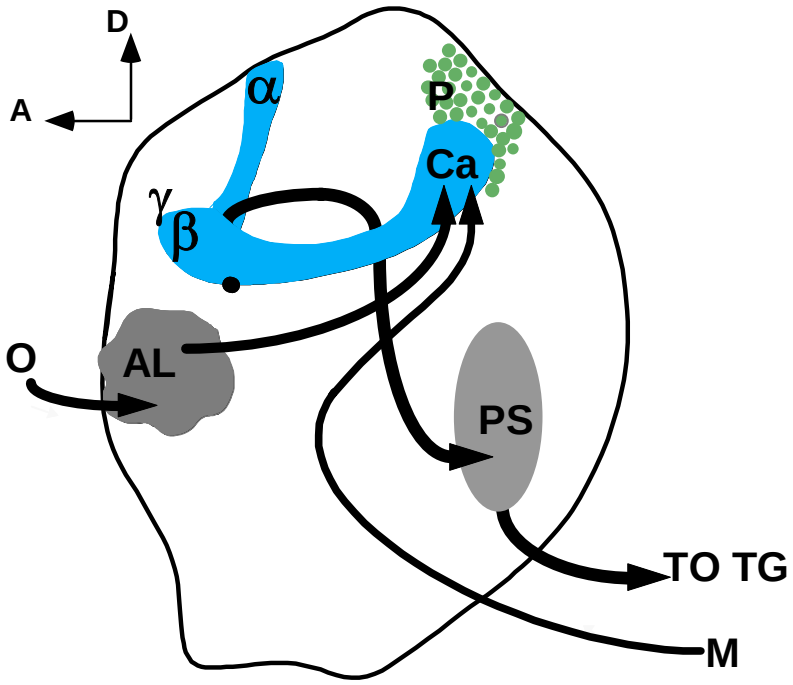

Figure 7. Pathway of information in the *Drosophila* CNS

Olfactory information initiated by the odor (o) is received by the antennal lobe (AL), then passes through the middle/inner antennal cerebral tracts to the mushroom body dendrite or calyx (Ca). Mechanosensory information arrives at the calyces via an unknown route but likely through the lateral horn and becomes integrated with olfactory information in the calyces and probably the pedunculus and lobes. The information is then past to the posterior slope (PS) to the thoracic ganglia (TG) where motor neurons are stimulated. The arrow indicates the direction of the dorsal (D) and anterior (A) portions of the adult head (Modified from Nighorn et al 1992).

provided below. Olfactory information flows to the lateral horn from the antennal lobes either directly via the middle Antennal Cerebral Track (mACT) and inner Antennal Cerebral Track (iACT) or indirectly through the mushroom bodies, which receive inputs from these tracks as well. Therefore, mushroom body-lateral horn interactions are likely to be important for the evaluation and response to olfactory information. This is consistent with evidence that flies without mushroom bodies can categorize aversive and attractive odors (Guo and Gotz, 1997; Strauss et al., 2001; Heisenberg, 2003).

Footshock information

The pathway of electric shock information flow to the brain differs from that of olfactory information in that the major apparent target is the lateral horn (Ito et al., 1998). Electric shock stimulates nerves in the legs that relay the information to the thoracic ganglia. The thoracic nervous system is connected to the suboesophageal ganglion in the adult brain. The information is then relayed to its major target in the lateral horn (Ito et al., 1998). Little is known about the pathway or the mechanisms for processing this type of information. However there is apparent convergence with olfactory information within the mushroom bodies during associative olfactory learning (Ito et al., 1998; Waddell and Quinn., 2001a; Sokolowski, 2001; Heisenberg, 2003). It is also unknown whether the electric shock information can be relayed directly from the suboesophageal ganglion to the mushroom bodies or if it always feeds back through the lateral horn.

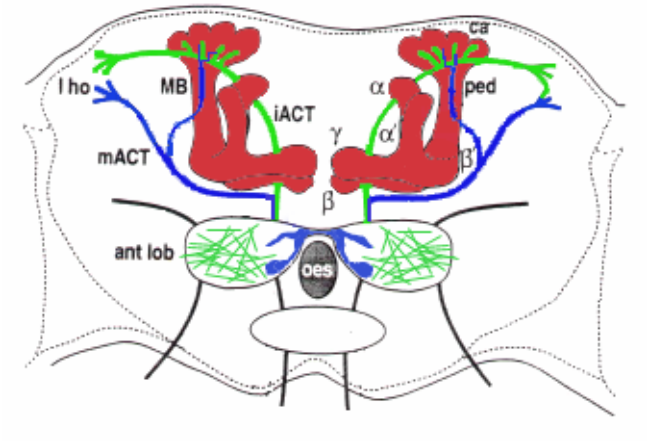

Figure 8. Expression of GAL4 drivers

The red structures represent the expression pattern of the 247-GAL4 driver with expression in the entire the mushroom bodies (MB) including the calyx (ca), peduncle (ped), lobes (α, α', β, β', γ). The blue represents expression of the GH146-GAL4 line that expresses in the middle antennal cerebral tract (mACT), leading to the lateral horn (l ho) and mushroom body calyces from interneurons located in the antennal lobe (ant lob). The green represents the expression pattern of the OK72-GAL4 driver that expresses in the inner antennal cerebral tract (iACT), which leads to the lateral horn and mushroom body calyces from four glomeruli in the antennal lobes. (Modified from Ito et al., 1998 and Heisenberg, 2003)

There is information on a mechanosensory response pathway in *Drosophila* involving the giant fiber interneurons. This pathway mediates a jump-and-flight escape response to visual stimuli (Trimarchi and Schneiderman, 1995; Engel and Wu, 1996; Engel and Wu, 1998). Visual information is passed through the central nervous system to the bilateral cervical giant fibers that extend into the thorax. However, the particular neurons that are necessary for the flow of information in the central nervous system are unknown. The visual or mechanical stimulation to the cervical giant fiber leads to a jump-and-flight response, which can be measured by the spike pattern in the tergotrochanteral "jump" and dorsal longitudinal "flight" muscles (Engel and Wu, 1998). However, olfactory stimulation activates a non-giant fiber pathway, suggesting there are different mechanosensory response pathways for different stimulus modalities (Trimarchi and Schneiderman, 1995).

There is a second mechanosensory response pathway in *Drosophila* known to involve sensory neurons controlling the femoral-tibial joint reflex (leg positioning reflex) (Reddy et al., 1997; Jin et al., 1998). In this simple reflex paradigm, decapitated flies are immobilized with only their mesothoracic leg free to move (Jin et al., 1998). Stimulation is then applied to the femoral chorodotonal organ leading to the excitation of two motor neurons innervating the tibial extensor muscle that ultimately leads to the reflex of the femoral-tibial joint (Reddy et al., 1997; Jin et al., 1998). Any anatomical disruption of the femoral chorodotonal organ axons (Reddy et al., 1997) or blockage of neurotransmission (Sweeney et al., 1995) corresponds to disruption of the leg positioning reflex. This suggests that these neurons are necessary for normal reflex

function (Reddy et al., 1997; Jin et al., 1998). Because this paradigm uses decapitated flies, any potential involvement from the central brain is unknown (Reddy et al., 1997; Jin et al., 1998).

Associative learning

Associative learning involves the acquisition of information about the environment and results in an alteration of the organism's behavior (Davis, 1996). Associative learning requires the CS+ to be paired to the US and causes a behavioral change or conditioned response (CR) to the CS+ but no CR to the CS-, which is not paired to US. The CS+/US temporal contiguity is a critical factor affecting the magnitude of the CR, therefore the presentation of the US or CS alone should not evoke the CR. Conditioning is dependent on the training schedule defined by the duration of the CS and US, the number of pairings and the interval between pairings (Joynes and Grau, 1996). In *Drosophila*, there are several different instrumental conditioning paradigms to study associative learning including courtship conditioning, heat avoidance with visual stimuli, proboscis extension reflex, motor learning, and spatial learning in a heating chamber (Wolf et al., 1998). There are also classical conditioning paradigms such color choice, intensity contrast, heat avoidance with stationary patterns and the paradigm used in this research, the conditioned olfactory avoidance assay.

In the conditioned avoidance assay, used to study olfactory learning and memory, the CS+ (odor) paired to US (shock) causes a CR to the CS+ but no CR to the CS- (Tully and Quinn, 1985). This is a classical conditioning paradigm also termed Pavlovian

conditioning because the response is dependent on the training schedule and not initiated by the fly itself as in instrumental conditioning. The following is a summary of the three different conditioned olfactory avoidance assay-training protocols used to study olfactory associative learning and memory in *Drosophila*.

During olfactory learning training, 50-70 flies are presented with the shock-associated odor (CS+) concomitant with the US, 12, 1.25-second 90V electric shocks followed by the control odor (CS-) in the absence of the US. Two groups of animals of the same genotype are trained in parallel, so that each odorant serves as a CS+ and the complementary odorant as the respective control. We term this training schedule the LONG PROGRAM because it requires 12 CS/US pairings. The animals are tested immediately after training in a T-maze, where they choose between the two converging odors. Memory is tested tens of minutes or hours after training. The fraction of flies that avoid the shock-associated odor reflects learning of the conditioning stimuli and is quantified as a performance index ranging from a maximum of 100 to 0.

Though the protocol described above is sufficient to generate good learning, Short Term Memory and Middle Term Memory scores up to 6 hrs post-training, a second more rigorous training regime is necessary to induce true Long Term Memory generating reliable scores 24 hrs to 7 days post training. In this modification (SPACED TRAINING) the 12 pairing LONG PROGRAM is repeated 8-10 times with an interval of 15 minutes between each 12 CS/US pairing episode. This regime produces learning scores slightly higher than one set of 12 US/CS pairings, but produces memories of the association that last at least 7 days. The interval between pairing episodes is essential

for Long Term Memory formation because if the 10 CS/US pairing episodes are given sequentially without rest (MASSED TRAINING) it generates normal learning and memory up to 6 hrs but no 7-day Long Term Memory (Yin et al., 1994; Yin et al., 1995).

There is also a modification of the training protocol (SHORT PROGRAM) that differs only in the number of US/CS pairings (Beck et al., 2000; Roman and Davis, 2001). Animals are trained with a single 10-second pulse of odorant (CS+ and CS-), and a single 1.25-second shock (US) delivered 6-7 seconds into the CS+ presentation. This results in performance indices that are lower than for the LONG paradigm, but consistently reproducible. Using the SHORT PROGRAM training with a rest interval (ITI) of 15 minutes also allows a study of acquisition of information (Beck et al., 2000).

Although the LONG PROGRAM is quicker and more convenient for screening mutants for potential learning and memory deficits, the 12 pairings could induce a ceiling level of performance after only one training session (Beck et al., 2000). This type of massed training with a high number of shock pulses is also thought to produce a stressful situation that could potentially alter the salience of odors. Roman and Davis (2001) also suggest that the LONG PROGRAM may reflect a combination of extinction (when presentation of the CS alone diminishes the CR), odor desensitization (repeated exposure to CS diminishes effectiveness of the CS to induce a CR), stress, and potentially other types of adaptive processes. The SHORT PROGRAM produces only modest performance after a single training and makes it possible to compare the memory formed after one, two or three training sessions to measure the rate of memory formation or acquisition of information (Beck et al., 2000). The SHORT PROGRAM is less

stressful on the flies and in addition it allows study of mutants involved in memory formation. The shortened odor presentation reduces the possibility of altered response to the odors themselves and possible complications due to repeated shock presentations (Roman and Davis, 2001). Both of these training protocols have provided significant insights into the mechanisms of learning and memory in *Drosophila*.

A number of learning and/or memory mutants have been isolated in the past 25 years. Associative learning mutants are subdivided into three classes: those with defects in sensory processing, disruptions in CNS development and those with altered biochemistry and physiology of the relevant cells or conditioning mutants (Davis, 1996). Only those mutants with normal sensory processing and CNS development are considered true learning and memory mutants. Some of the first genes identified to play a role in learning and memory through the isolation of mutants were the cAMP-dependent phosphodiesterase *dunce,* the adenylyl cyclase *rutabaga*, the cAMP-dependent kinase (PKA) catalytic subunit *DCO*, and *amnesiac* the homolog to the mammalian pituitary adenylyl cyclase-activating peptide all effecting cAMP signaling (Nighorn et al., 1991; Han et al., 1992; Skoulakis et al., 1993; Davis, 1996; Waddell and Quinn, 2001). The *amn* gene codes for a protein with features of a preproneuropeptide and sequence similarity to pituitary-adenylyl cyclase-activating peptide (PACAP) (Feany and Quinn, 1995; Moore et al., 1998).

Through the study of these mutants, models have emerged that suggest a significant role of the cAMP pathway in *Drosophila* associative olfactory learning and memory. The US and CS pathways must somehow converge in the mushroom bodies

activating adenylyl cyclase (*rutabaga*), thereby increasing cAMP synthesis (reviewed in Heisenberg, 2003). The level of cAMP can also be increased by neuropeptides such as that encoded by the *amnesiac* gene expressed in the dorsal paired medial neurons (DPM) that project into the mushroom bodies (Figure 9) (Feany and Quinn, 1995; Waddell et al., 2000). The increase in cAMP activates cAMP-dependent kinase (PKA), phosphorylating targets such as potassium channels at the synapse potentially involved in short-term memory (STM) (Figure 9) (Waddell and Quinn, 2001b; Sokolowski, 2001; Schwaerzef et al., 2002; Heisenberg, 2003). PKA (the *DCO* gene encodes the catalytic subunit) phosphorylates CREB, which mediates the transcription of new genes necessary for long-term memory (LTM) formation (Figure 9) (Yin et al., 1994; Bourtshouladze et al., 1994; Bartsch et al., 1995; DeZazzo and Tully, 1995; Roman and Davis, 2001). The cAMP is degraded by a phosphodiesterase (*dunce*) (Figure 9) and loss of proper degradation leads to cAMP elevation and is manifested as an olfactory learning defect (Dudai et al., 1976, Davis and Kieger, 1981; Davis and Davidson, 1986; Zhong et al., 1991; Waddell and Quinn, 2001b). All of these mutants affect the level of PKA activation either by reducing it as in the case of *rut* and *DCO* mutants, or increasing it in the case of *dnc*, thereby inhibiting learning and the formation of memory (Waddell and Quinn, 2001a; Sokolowski, 2001; Heisenberg, 2003)

There are four distinct memory phases in *Drosophila*. Short-term memory (STM) that decays in less than an hour (reviewed in Heisenberg, 2003). Middle-term memory (MTM) lasts from one to three hours and requires new protein synthesis from pre-existing messages. There are two types of long term memory, one independent of

protein synthesis (anesthesia-resistant memory, ARM) and the other requiring protein synthesis (long-term memory, LTM) (reviewed in Heisenberg, 2003). The different phases of memory were determined using pharmacological assays and analysis of genetic mutations. In *Drosophila*, ARM appears to be insensitive to cycloheximide, which blocks transcription, but LTM is cycloheximide-sensitive (DeZazzo and Tully, 1995). MTM can be disrupted by diethylthiocarbomate, which inhibits synthesis of noradrenaline (DeZazzo and Tully, 1995). In *Aplysia*, STM is unaffected by an inhibitor of transcription (actinomycin) and an inhibitor of translation (anisomycin) (Mueller and Carew, 1998). In contrast, MTM and LTM are both disrupted by anisomycin and LTM is also disrupted by actinomycin (Mueller and Carew, 1998). In either model system, experiments have lead to the same conclusion that STM is independent of translation and transcription, MTM is dependent on translation and LTM is dependent on both translation and transcription (DeZazzo and Tully, 1995; Mueller and Carew, 1998).

Genetic mutations in *Drosophila* have added invaluable *in vivo* information in further understanding the mechanism of memory formation as well as neurons involved in storage. For example, LTM requires repeated training that includes rest intervals (spaced training) and the cAMP response-element binding protein (CREB) transcription factor (Yin et al., 1994; Tully et al., 1994; Waddell and Quinn, 2001a). The role of CREB in LTM formation appears to be evolutionarily conserved (Yin et al., 1994). In addition, the *radish* (*rsh*) mutation eliminates ARM without effecting LTM (Figure 9)

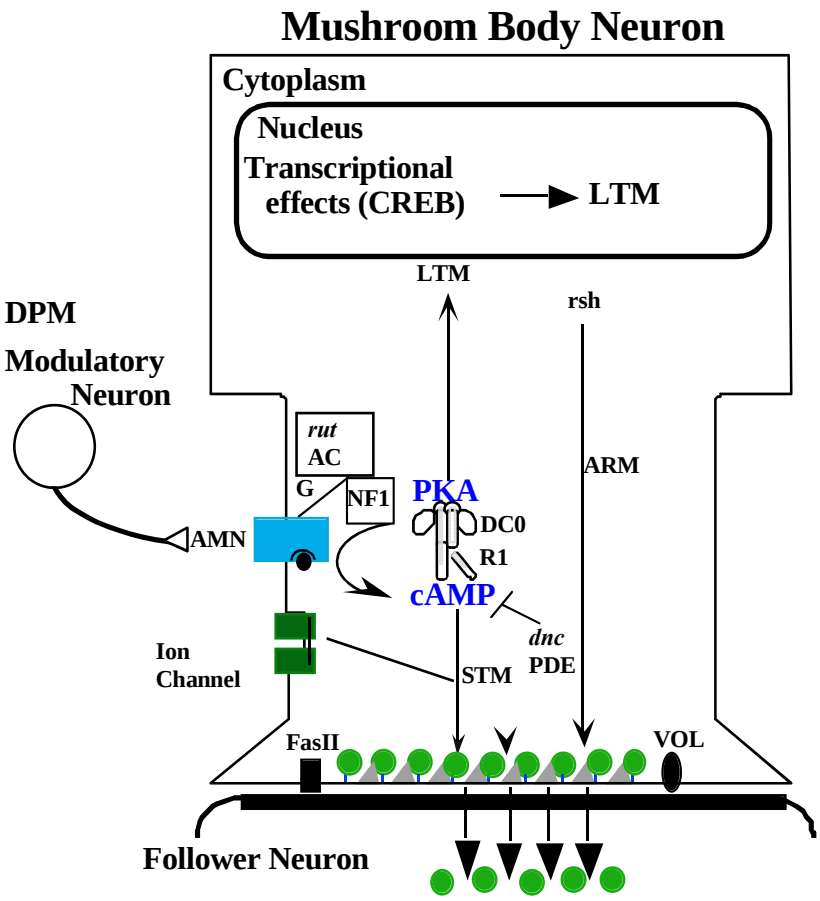

Figure 9. Mediating learning and memory in the *Drosophila* mushroom bodies

The *Drosophila* mushroom bodies receive olfactory information through the antennocerebral tract from the antennal lobe glomeruli and electric-shock input from an unknown source. The dorsal paired medial (DPM) neurons potentially modulate that information with the release of the AMN neuropeptides leading to up-regulation of cAMP. The electroshock stimulation increases the level of cAMP by activation of RUT adenylyl cyclase (*rut*-AC) through a G-protein coupled receptor (G), which may also interact with neurofibromin (NF1) regulating short term memory (STM). The protein kinase A (PKA) catalytic subunits (DCO) and regulatory subunit R1 also affect the level of cAMP within the neuron. cAMP is then deactivated by a phosphodiesterase encoded by the *dnc* gene. When the mushroom bodies receive repeated olfactory and electroshock input simultaneously, PKA phosphorylates cAMP response-element binding protein (CREB) leading to transcriptional activation and long term memory (LTM). Mutations in the *radish (rsh)* gene lead to loss of anesthesia-resistant memory (ARM). The neuronal cell adhesion protein fasciclinII (FasII) and an α-intregrin volado (VOL) can also alter the release of neurotransmitters. (Modified from Waddell and Quinn, 2001a)

(Folkers et al., 1993; Tully et al., 1994; Waddell and Quinn, 2001a) and the α-lobe absent (*ala*) mutation lacking the mushroom body α lobe on both sides, have normal STM and ARM, but lack LTM (Pascual and Preat, 2001; Heisenberg, 2003).

It appears that all memory phases except ARM, for which the mechanism is relatively unknown, are affected by PKA activation (DeZazzo and Tully, 1995; Roman and Davis, 2001). In addition, there are other factors that do not appear to affect PKA that alter learning and memory processes (Groteweil et al., 1998). For example, the *vol* gene encodes an α-integrin subunit thought to alter necessary cell adhesion during short-term memory formation when mutated, leading to deficits in this process (Figure 9). Mutations in *fasII* cause a deficit in a different neuronal cell adhesion molecule (NCAM) apparently altering olfactory learning (Figure 9) (Cheng et al., 2001). There are also mutants that block the initial phase of learning including *NF1*, a GTPase-activating protein for *Ras* and *Ddc* an aromatic-amino-acid-decarboxylase necessary in the making monoamine neurotransmitters such as serotonin and dopamine (Figure 9) (reviewed in Waddell and Quinn, 2001b). This information has led to the current model of how learning and memory formation may occur within the mushroom bodies (Figure 9) (Waddell and Quinn, 2001a; Roman and Davis, 2001; Sokolowski, 2003). With the discovery of new mutants the mechanism of olfactory learning and memory in *Drosophila* is unfolding and will hopefully lead to further understanding of higher order brain functions.

Non-associative behaviors

Non-associative learning could occur when an organism habituates, or is sensitized to a stimulus, whereas associative learning occurs when an organism learns relationships among stimuli (Dudai, 1988; Devaud et al., 2003). In order to understand olfactory learning and memory, appropriate controls must be performed to ascertain that any defects in learning and memory are due to altered physiology or biochemistry that affect integration of information not stimulus perception. In this case, proper responses to olfactory and electric shock stimuli are the necessary task relevant controls. These controls are used to identify sensory deficits that potentially interfere with stimulus input or processing necessary for olfactory learning. However, additional essential controls are needed to investigate the effect of the US (shock) on CS+ and CS- (odor) perception and processing, and CS+ pre-exposure to subsequent CS- perception and processing. Tully and Quinn (1985) suggested that pre-exposure to odor or shock then subsequent testing of proper response to the CS+, CS- and US should also be included as task relevant controls. Presenting only one odor during the training period resulted in a response decrement to the same odor, but not to a novel odor (Tully and Quinn, 1985). Therefore, these controls need to be performed in order to determine whether a proposed associative olfactory learning mutant has non-associative or sensory deficits, which could account for the "mutant" phenotype. Using attractive odors in olfactory assays may also be necessary because of data suggesting that *dnc* mutants have a learning deficit when conditioned with negative stimuli, but are normal when conditioned to positive CS (Temple et al., 1983). In fact, experiments indicate that mutants such as

amnesiac (*amn*), *rutabaga* (rut^1) and *dunce* (dnc^1) exhibited deficits in olfactory avoidance when pre-exposed to an odor paired with shock (Preat, 1998). Is then the deficit due to odor pre-exposure alone and what structures are necessary for proper response to an odor after such pre-exposure? The olfactory avoidance deficit in the *amn* mutant also occurs when they are pre-exposed to shock alone. This effect of shock pre-exposure on odor avoidance did not recover for 24 hours.

In addition, examining non-associative behaviors offers some understanding of the pathway of the CS and US information flow through the adult CNS. To understand the effect of possible pre-exposure dependent non-associative deficits, it is important to examine if they require the mushroom bodies or other tissues. In the case of *amn*, the protein accumulates in dorsal paired medial neurons, which project axons medially that innervate the ipsilateral mushroom body lobes (Feany and Quinn, 1995; Waddell and Quinn, 2001a). AMN is not found in mushroom bodies, antennal lobe or lateral horn. Suggesting, the deficit may be due to perturbation in mushroom body function because AMN is required in modulatory neurons. Experiments with vertebrate PACAP in *Drosophila* neuromuscular junctions (NMJ's), indicate that application of synthetic PACAP increased voltage-dependent potassium channel activity (Zhong, 1995), thereby altering the potential of the neuron to respond to subsequent stimuli.

Mutants in genes encoding channel proteins such as in the gene *Transient receptor potential* (*Trp*)-Ca^{2+} channel also have been shown to have non-associative behavioral defects (Stortkuhl et al., 1999). They responded to a dilute odor after pre-exposure to the same strong odor, whereas wild type strains showed no avoidance. The

researchers proposed that this deficit resulted from loss of olfactory "adaptation", which is odor concentration and exposure duration dependent. These experiments used only aversive odors, octanol and isoamyl alcohol, resulting in an effect that could last anywhere from one minute to several hours (Dalton, 2000). It is uncertain whether this experiment was indeed a measure of adaptation, but it was consistent with the definition of adaptation: the repeated or prolonged exposure of a stimulus leads to a specific decrease in sensitivity to that stimulus (Dalton, 2000). More experiments are necessary to understand how and where this type of deficit occurs and if it is truly adaptation or possibly some form of non-associative learning.

In addition to the various types of non-associative learning, it is essential to not only explore where associative learning occurs within the CNS, but also the neurons essential for non-associative learning in order to accurately couple or uncouple the two processes. For example, in Aplysia, studies indicated that the site of habituation is within the CNS rather than the thoracic portion of the giant fiber pathway (Marcus et al., 1988), however it is unknown where in the central nervous system habituation occurs. It is also unknown whether associative learning and habituation are dependent or independent processes. During associative training, habituation or desensitization to the CS could potentially inhibit proper CS/US association that leads to CS+ vs. CS- discrimination (Joynes and Grau, 1996). The non-associative effects attributed to habituation, desensitization or sensory fatigue are all manifested as diminished or eliminated responses to stimuli after pre-exposure to the same type of stimulus and spontaneously recover in a time dependent manner. Only for habituation can the

response be recovered by dishabituation with a novel stimulus. Furthermore, it is unknown whether any of these non-associative defects share similar biochemical mechanisms with associative olfactory learning.

Habituation and desensitization are necessary processes that likely allow *Drosophila* to reduce their behavioral response to a stimulus with no reinforcement and focus on more relevant stimuli (Devaud et al., 2003). Many different assays have been used to study non-associative behaviors in *Drosophila*, including the cleaning reflex (Corfas and Dudai, 1990), the proboscis extension reflex (Duerr and Quinn, 1982), the landing response (Asztalos et al., 1993), the visual escape jump (Engel and Wu, 1996), the leg position reflex (Jin et al., 1998) and the jump-and-flight escape response (Engel et al., 2000). With the exception of the proboscis extension reflex, these assays involve the study of simple proprioceptive reflexes within the thoracic sensory neurons of the peripheral nervous system (PNS) (Jin et al., 1998). Apparently the cAMP mutants *rutabaga* (*rut*) and *dunce* (*dnc*), which have deficits in associative olfactory learning could habituate and dishabituate in these paradigms. However, habituation occurred more quickly and was short lived for the *rut* and *dnc* mutants (Corfas and Dudai, 1989; Duerr and Quinn, 1982; Engel and Wu, 1996). Habituation could also be eliminated by targeted expression of calcium independent CaMKII in the thoracic sensory neurons, which also has a function in learning (Mayford et al., 1996; Jin et al., 1998). The *Su-var(3)6*^{01} mutants that lack protein phosphatase 1 that habituated faster are also severely impaired in olfactory learning (Asztalos et al., 1993). The fact that these mutants affect both habituation and associative olfactory learning suggests the two might be linked

biochemically and/or associated with the same region of the brain (Corfas and Dudai, 1989; Duerr and Quinn, 1982; Asztalos et al., 1993; Engel and Wu, 1996; Jin et al., 1998).

Mushroom body mediated behaviors

Olfactory learning and memory

In *Drosophila*, most of the genes important for olfactory learning and memory are expressed preferentially in mushroom body neurons (reviewed in Waddell and Quinn, 2001; Sokolowski, 2001; Heisenberg, 2003). However, olfactory learning mutants that disrupt mushroom body function such as *mushroom body deranged* (*mbd*) are capable of associative visual learning (Heisenberg et al., 1985). This suggests that the mushroom bodies may be essential for olfactory learning, but are dispensable for some other types of associative learning (Wolf et al., 1998; Heisenberg, 2003). The mushroom bodies are clusters of about 2500 neurons, situated bilaterally in the dorsal and posterior cortex of the *Drosophila* brain (Figure 7). Evidence suggests that olfactory information received by the olfactory receptors is transmitted from antennal lobe glomeruli through the antenno-cerebral tracts to the mushroom bodies (Stocker et al., 1990; Ito et al., 1998; Heisenberg, 1998; Heisenberg, 2003). There are two main ascending tracks, the inner antenno-cerebral tract (iACT) and the middle antenno-cerebral tract (mACT). These two tracks also feed directly into the lateral horn and as demonstrated by Ito et al., (1998) there are bi-directional connections between specific anatomical regions of the mushroom bodies and the lateral horn. This suggests that

responses to olfactory information could be mediated by both the mushroom bodies and lateral horn independently or by both. Marin et al., (2002) suggests that the lateral horn is necessary for olfactory discrimination and the mushroom bodies are necessary for associative olfactory learning. The information from the antenno-cerebral tracts arrives at the mushroom body calyces, which are composed of dendrites comprising a neuropil just ventral to the cell bodies (Figure 7). In contrast, the axons of mushroom body neurons fasciculate to form the peduncle that projects to the anterior of the brain. There, the axons bifurcate, with some processes extending medially and others projecting dorsally to comprise the lobes (Figure 7) (Strausfeld et al., 1976; Crittenden et al., 1998; Ito et al., 1998; Heisenberg, 2003). There are five major axonal projections that comprise the lobes of the mushroom bodies: the dorsally projecting α and α' along with the three medially projecting β, β' and γ (Critttenden et al., 1998; Heisenberg, 2003). Developmentally, these structures arise from differentiation of four mushroom body neuroblasts to create a tripartite structure of projections with α and β branches, α' and β' branches and the unbranched axon projection to the heel and γ lobe (Crittenden et al., 1998).

The different neuronal types that comprise the lobes exhibit different mushroom body specific and preferential gene expression patterns indicating possible functional differences between lobes (Crittenden et al., 1998). Evidence suggests that the γ lobes are responsible for associative olfactory learning (Zars et al., 2000) and α lobes responsible for storage of long term memory (Pascual and Preat, 2001). However, little

is known about whether non-associative learning is processed in the mushroom bodies and if it is lobe specific.

Visual learning and memory

Apparently mushroom bodies are dispensable for some types of learning paradigms that involve visual stimuli including color choice, arena test, heat avoidance, avoidance of turbulence and spatial learning in a heating chamber (reviewed in Wolf et al., 1998). However, the mushroom bodies are necessary for context generalization in visual learning that is performed in a flight simulator (Zars, 2000). Context generalization involves learning the relationship between discrete stimuli in a particular environmental setup (context) and then being able to remember that relationship in a different context (Bouton et al., 1999). In this paradigm, flies learn to anticipate a future event based on a past experience as a consequence of their own response. This type of conditioning is called operant or instrumental (Thorndike, 1911).

In the flight simulator, a fly is tethered to a string and placed in an arena with T-shaped patterns as landmarks while its movements are measured by a torque meter (Wolf and Heisenberg, 1991; Zars, 2000). The fly is negatively conditioned when heading towards one of the patterns with the presence of heat. After the training phase, the fly's memory is measured by testing for its preference of orientation with respect to the landmarks (Wolf and Heisenberg, 1991; Zars, 2000). Mushroom body defective flies are normal for this type of learning (Wolf et al., 1998). However, when the background color of the arena is changed from white to green or blue (a different context) between

the training and testing phases, these flies failed to remember the training situation (Liu, et al., 1999; Zars et al., 2000). This suggests that the mushroom bodies are necessary for the integration and generalization of visual information with respect to context changes.

Courtship and courtship conditioning

The conditioned courtship suppression paradigm is based on natural sexual behavior involving only natural stimulation and can be performed with relatively few animals (Kamyshev et al., 1999). In *Drosophila*, courtship involves the processing of visual, chemosensory and auditory information between the two sexes (reviewed by Hall, 1994). Females produce a courtship-stimulating pheromone (cuticular hydrocarbon) that the male perceives by contact (gustation) (Ferveur, 1997). Virgin females stimulate males to court more vigorously than do fertilized females due to reduced levels of cuticular hydrocarbons in the latter (Siegel and Hall, 1979; Kamyshev et al., 1999). However, mated females still induce courtship, but once mated they are no longer receptive to copulation. This change in mated female behavior leads to extrusion of female ovipositor in response to male courtship blocking copulation attempts (Connolly and Cook, 1973; Kamyshev et al., 1999). Males exposed to mated females and rejected, tend not to court subsequent virgin females for 2-3 hours, or fertilized females for one day (Siegel and Hall, 1979; Kamyshev et al., 1999). Male flies with mutations in genes that affect learning (*dunce, rutabaga* and *amnesiac*) show their failure to learn in this paradigm as continued courtship regardless of previous

experiences courting fertilized females (Siegel et al., 1984; Siwicki and Ladewski, 2003; Sokolowski, 2003).

A single one-hour pairing of a male fly with a mated female leads to 2-3 hour conditioned courtship suppression or short term memory (STM) formation, whereas three one-hour pairings or one five hour pairing leads to 9 day conditioned courtship suppression or long term memory (LTM) (McBride et al., 1999). In this paradigm immediate recall tested zero minutes after training is no considered to require consolidation of information. Whereas, STM tested 30-60 minutes after training and LTM tested 9 days after training do require some type of consolidation of information (McBride et al., 1999). Blocking neurotransmission within the projection neurons from the antennal lobe to the lateral horn and mushroom bodies leads to deficit in odor detection and all stages of male courtship (Joiner and Griffith, 1999; Heimbeck et al., 2001; Siwicki and Ladeski, 2003). However, if only mushroom bodies are missing, male flies are able to learn and recall courtship conditioning immediately, but are unable to form STM or LTM (Ito et al., 1998; McBride et al., 1999; Heimbeck et al., 2001). This data is consistent with the lateral horn being necessary for processing chemosensory information and the mushroom bodies necessary for associative memory formation, however the precise neural systems responsible for learning in the courtship paradigm have not been identified yet.

Locomotion control

In *Drosophila*, the mushroom bodies appear to influence locomotor activity (de Belle and Heisenberg, 1996; Martin et al., 1998; Wolf et al., 1998; Helfrich-Forster et al., 2002; Putz and Heisenberg, 2002). Locomotor activity is a measure of a fly's continuous walking in a tube from one end to the other and back for a period of time (Martin et al., 1998; Helfrich-Forster et al., 2002). Flies with non-functional mushroom bodies have more frequent initiation of spontaneous walking activity than normal flies, suggesting that the mushroom bodies normally suppress locomotor activity (Martin et al., 1998; Helfrich-Forster et al., 2002). This is consistent with the interpretation that mushroom bodies do not affect maintenance of general motor activity rhythms, but rather their ablation induced hyperactivity under continuous darkness (free running activity) (Helfrich-Forster et al., 2002). The Helfrich-Forster et al., (2002) studies imply that the mushroom bodies are not involved in circadian activity rhythms (cycles of stereotypical behaviors driven by autonomous gene expression), but do affect initiation of general locomotor activity.

Alcohol addiction

In *Drosophila*, genes expressed in the mushroom bodies involved in olfactory learning also appear to influence acute and chronic response to ethanol (Bellen, 1998; Heberlein, 2000; Cheng et al., 2001; Guarnieri and Heberlein, 2002). Though it is presently unclear why, it may be related to the fact that genes involved in cAMP signaling are preferentially expressed there and mediate olfactory learning and memory.

In cell culture, acute exposure to ethanol apparently potentiated receptor activated cAMP synthesis leading to CREB activation (Diamond and Gordon, 1997). Whereas, chronic exposure decreased cAMP production (Bellen, 1998). To investigate the behavior of a fly upon ethanol exposure, the animals are presented with ethanol vapor within a specialized devise called an inebriometer (Cohan and Graf, 1985). This devise measures ethanol resistance by the time it takes a fly to roll down a series of baffles as it becomes more uncoordinated due to the ethanol vapor (Cohan and Graf, 1985; Bellen, 1998).

Flies with mutations in the *amnesiac* (*amn*), *rutabaga* (*rut*) and *DCO* genes leading to decreased levels of cAMP exhibit increased sensitivity to alcohol (Lane and Kalderon, 1993; Moore et al., 1998; Bellen, 1998). Flies lacking DUNCE which precipitates an increase in cAMP appear to be desensitized to up-regulation of cAMP during acute exposure therefore showing sensitivity similar to controls (Bellen, 1998). These experiments support the model that the cAMP pathway regulates the response to ethanol. However, as for learning, the ethanol response is likely more complex as suggested by evidence that mutations in the *fasciclinII* (*fasII*) gene, encoding a cell adhesion receptor also cause heightened sensitivity to ethanol vapors (Cheng et al., 2001). The fact that several genes that affect mushroom body- dependent olfactory learning also affect response to ethanol (Bellen, 1998; Heberlein, 2000; Cheng et al., 2001; Guarnieri and Heberlein, 2002), suggests that these two behaviors may share biochemistries and a common anatomical structure, the mushroom bodies.

Tools to study behavior

Mapping of non-associative and associative behaviors in the brain of *Drosophila* can be accomplished using biochemical and genetic manipulations. Hydroxyurea ablations stop the four mushroom bodies and one antennal lobe neuroblast from dividing during development. In *Drosophila*, these five neuroblasts are the only proliferating cells from 0 through 8 hours after hatching (Ito and Hotta, 1992). Therefore, if newly hatched larvae are fed the cell cycle inhibitor hydroxyurea those five neuroblasts fail to proliferate deleting the mushroom body and specific antennal lobe lineages (de Belle and Heisenberg, 1994). This manipulation has been reported to lead to defective associative learning (de Belle and Heisenberg, 1994). However, the results are difficult to interpret since the treatment affects not only the mushroom bodies, but there is also loss of 2/3 of the inner antenno-cerebral tract and most of the lateral relay interneurons (Heimbeck et al., 2001; Stocker et al., 2001). Therefore, to truly understand the contribution and roles of the structures in the pathway of olfactory information, blockage of the information flow in each specific structure involved is necessary.

A very useful tool for such studies was offered by adapting the yeast UAS/GAL4 system for use in *Drosophila*. An enhancer-less construct bearing the GAL4 gene was inserted randomly into multiple independent genomic locations, where its expression is driven by different resident enhancers (Brand and Perrimon, 1993). Because the GAL4 protein is a transcription factor, it can activate target transgenes attached to its binding sequence, the Upstream Activating Sequence (UAS). This target gene is silent in the absence of GAL4. To express any UAS bearing transgene, flies carrying this transgene

are crossed to flies expressing the GAL4 in the desired tissue or temporally restricted pattern (Enhancer Trap GAL4). In the progeny of this cross, the UAS-gene is activated in cells or tissues where GAL4 is expressed and the effects of this restricted or ubiquitous expression can be studied (Brand and Perrimon, 1993). There are also UAS-bearing transgenic strains available that allow direct visualization of the expression pattern (such as UASGFP and UASlacZ etc).

Using various CNS specific GAL4 lines to express neurotransmission-blocker transgenes under UAS, the function of specific neurons and brain areas can be permanently or conditionally inhibited allowing study of its effects on olfactory and mechanosensory behaviors. There are two types of such transgenes available to date. First, transgenes based on the *Shibire*^{ts} mutation. *Shibire*^{ts} is a temperature sensitive allele of the dynamin GTPase protein that functions during the clathrin-mediated endocytosis necessary for neurotransmitter re-uptake in synapses. At the non-permissive temperature (>32^{o}C) and in competition with the normal resident dynamin protein, SHI^{ts} prevents neurotransmitter re-uptake and subsequent release due to a conformational change (Kitamoto, 2001). Dynamin mutants have been found to block endocytosis without affecting protein trafficking along the exocytic pathway or the morphology of the nerve terminal (vanderBliek et al., 1993). This conditional system allows separation between the direct physiological consequences of perturbing neuronal subsets with a conditional neurotransmission blockade and potential developmental effects that may arise by a permanent blockade. A simple temperature shift from 25ºC to the non-permissive temperature can induce rapid perturbation of neuronal activities allowing

study of its acute behavioral consequences. Importantly, the effects of SHI^{ts} are fully reversible after a 15 minute rest period at the permissive temperature (25ºC) (Kitamoto, 2001).

The second system utilizes the tetanus toxin light chain protein. The Tetanus toxin light chain (TeTxLC or TNT) gene, produces part of a neurotoxin protein from *Clostridium tetani* (Schiavo et al., 2000). This particular neurotoxin is a metalloprotease capable of cleaving the synaptic vesicle-associated membrane protein, synaptobrevin (Schiavo et al., 1992; Martin et al., 2001). Synaptobrevin is necessary for regulating exocytosis by interacting with various presynaptic proteins such as SNAP-25 and syntaxin (Schiavo et al., 2000). Disruption of this association completely blocks evoked exocytosis (Schiavo et al., 1992; Martin et al., 2001). In *Drosophila*, only a neuronally expressed form of synaptobrevin (dn-syn) is sensitive to the tetanus toxin light chain (Sweeney et al., 1995; Martin et al., 2001). Although the effects of tetanus toxin are irreversible, there is no retrograde transport, no morphological defects and no known targets outside the nervous system (Martin et al., 2001). This makes TNT expression a powerful tool to understand the structures in the central nervous system necessary for specific behaviors in *Drosophila*. In fact, previous studies using UAS driven tetanus toxin indicate that it is capable of blocking neural activity affecting a particular behavioral response (Keller et al., 2002; Martin et al., 2002).

These powerful techniques will allow the identification of deficits that are mushroom body specific and deficits outside the mushroom bodies, but still within the central olfactory information pathway. There are a few GAL4 driver lines (Enhancer

Trap GAL4s) that label different structures in the olfactory information-processing pathway. 247-GAL4, is expressed in most mushroom body neuronal types which allows specific neurotransmission blockage into and out of the mushroom bodies (Figure 8) (Zars, 2000). There are several other mushroom body GAL4 lines that vary in temporal and spatial expression, however many have sensory defects (Zars et al., 2000; McQuire et al., 2001). 247-GAL4 expresses late in development without causing any apparent sensory defects (McQuire et al., 2001). This allows use of this line to block neurotransmission specifically in these neurons of the adult fly. In fact, McGuire et al. (2001) have shown that expression of the *shibire*^{ts} mutation with the 247-GAL4 driver at the non-permissive temperature (37ºC) affects memory retrieval, but not acquisition or consolidation.

In addition, a mutant isolated by de Belle and Heisenberg (1996) which exhibits a severe mushroom body structural defect known as *mushroom body miniature* (*mbm*^{1}), will also be used to investigate mushroom body specific functions. The *mbm* gene apparently supports the maintenance of mushroom body cells during third instar larva and metamorphosis (de Belle and Heisenberg, 1996). The reduction in mushroom body cells impairs olfactory learning, without reduction in odor avoidance, shock reactivity or locomotor behavior (de Belle and Heisenberg, 1996).

GH146-GAL4 is expressed in the antennal lobe interneurons, $\pm$ 100 relay interneurons and 2/3 of inner antennocerebral tract leading to the calyx and lateral horn (Figure 8). Using this driver allows neurotransmission blockage from the inner projection neurons to both the calyx and lateral horn (Stocker et al., 1997; Heimbeck et

al., 2001). Previous behavioral analysis performed on GH146 transgenic flies that were crossed to UAS-TNT indicated that expression of tetanus toxin in those neurons affects responses to dilute odors and abolishes male courtship (Heimbeck et al, 2001; Martin et al., 2002).

OK72-GAL4 is expressed in the middle antennocerebral tract leading to the calyx and lateral horn and glomeruli VM1, VM4 and DL1, allowing blockage of neurotransmission from the middle projection neurons to both the calyx and lateral horn (Figure 8) (Acebes and Ferrus, 2001; Devaud et al., 2003). OK72-GAL4 crossed to UAS-TNT appears to affect olfactory perception of benzaldehyde, but not butanol (Devaud et al., 2003). This suggests that there is specificity with respect to odor coding among the different GAL4 drivers. Unfortunately, none of the known GAL4 expression lines are specific to the lateral horn or the entire iACT and/or mACT.

14-3-3's in *Drosophila melanogaster*

All 14-3-3 proteins were named after their mammalian counterparts based on their degree of similarity. In *Drosophila melanogaster,* there are two isoforms of ζ from the typical protein group, LEO I and LEO II, which arise by alternative splicing of the *14-3-3ζ* (*leonardo)* transcript, with only a five amino acid difference between the two isoforms (Figure 10). In contrast, *Drosophila* contains only one member of the atypical group, D14-3-3ε. The *Drosophila* homologs are highly conserved, sharing 88% and 82% identity with the human 14-3-3ζ and 14-3-3ε respectively (Table 4) (Skoulakis and

Table 4. Percent identity between *Drosophila* and vertebrate 14-3-3s

Drosophila Isotype	% Identity	Vertebrate Isotype
Dζ (LEO)	81	ζ
	78	β
	77	τ
	75	γ
	73	η
	68	ε
61%	65	σ
	83	ε
	67	ζ
Dε	65	β
	65	τ
	63	γ

Davis, 1998), verified by completion of the respective genome projects (Table 4). Therefore, results obtained by this study in *Drosophila* will contribute significantly to our understanding of human 14-3-3s.

In adult flies, the LEO proteins are found enriched in the mushroom bodies and ellipsoid body and at lower levels throughout the entire body (Skoulakis and Davis, 1998; Philip et al., 2001). *D14-3-3ε* is present in all stages of development and in all tissues examined (Figure 11) (Philip et al., 2001). Due to the high isotype homology, understanding the role of these 14-3-3s in the *Drosophila* central nervous system is likely to contribute to understanding the role of these proteins in the normal function and neuro-degenerative diseases in the human brain. The following is a summary of what is already known about the functions of 14-3-3s in *Drosophila melanogaster*.

14-3-3ζ

The *leonardo* gene is contained within 26 kb of genomic DNA encoding three RNA populations of 2.9, 1.9 and 1.0 kb, with the 2.9 kb specific to the adult head (Skoulakis and Davis, 1996). Those RNAs populations contain five species of mRNAs that differ by the alternative use of the non-coding exons 1 or 1' and the coding exons 6 or 6'. In addition one of three different poly(A) addition sites can be used with the 2.9 kb transcript always using the furthest one (Figure 11) (Kockel et al., 1997). These mRNAs produce two different LEO isoforms with LEO I containing exon 6 and LEO II containing exon 6' (Kockel et al., 1997). The fact that the 2.9 kb head specific RNA

A

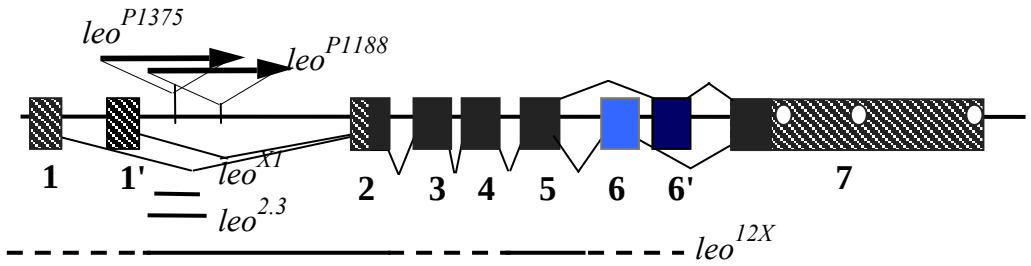

B

```
MSTVDKEELV QKAKLAEQSE RYDDMAQAMK SVTETGVELS NEERNLLSVA      50

YKNVVGARRS SWRVISSIEQ KTEASARKQQ LAREYRERVE KELREICYEV     100

LGLMDKYLIP KASNPESKVF YLKMKGDYYR YLAEVATGDA RNTVVDDSQT     150
                                                      KN
AYQDAFDISK GKMQPTHPIR LGLALNFSVF YYEILNSPDK ACQLAKQAFD     200
   E    A  T
DAIAELDTLN EDSYKDSTLI MQLLRDNLTL WTSDTQGDEA EPQEGGDN      250
```

Figure 10. Map of *leonardo* transcripts and mutations

41 The genomic region, structure and mutations of the *D14-3-3ζ* gene. Boxes represent exons, whereas lines represent introns and surrounding non-transcribed regions. The stippled boxes indicate untranslated portions of exons. LEO I includes the splice variation with exon 6 and LEO II contains the splice variation with exon 6'. The white circles in exon 7 represent polyadenylation sites. The arrows indicate the P-element insertions in the introns. The solid black bar indicates the extent of the *leo12X* deletion, whereas the hatched bars indicate a region of uncertainty at the ends. (Adapted Skoulakis and Davis, 1996, Philip et al., 2001).
(B) PROTEIN sequence of LEO I exon 6 underlined and the differences in exon 6' that produce LEO II underneath.

encodes a LEO I specific cDNA suggested that there might be differences in the temporal and spatial expression of the two isoforms (Kockel et al., 1997). However, two-dimensional westerns indicated that only one protein can be detected from heads or bodies (Skoulakis and Davis, 1996). This was likely due to the fact that the two LEO isoforms differ only by five amino acids and the differences are mostly conservative in size and charge (Figure 10) (Kockel et al., 1997; Philip et al., 2001). The amino acids encoded by exon 6 are the least conserved throughout the 14-3-3 protein family suggesting that the differences between the exons might affect target specificity (Figure 10) (Skoulakis and Davis, 1998; Philip et al., 2001).

Due to the high homology among isoforms, RT-PCR was required to determine possible differences in the temporal and spatial pattern of the two isoforms. *leoI* RNA was found to be expressed in early embryos, late embryos, all larval stages, and in adult heads (Figure 11). In 12-14 hour embryos, when the nervous system is developing, *leoI* is absent (Figure 11) (Philip et al., 2001). In contrast, *leoII* appeared to be adult mushroom body specific and found in all embryonic stages including 12-14 hour embryos and larval stages. Using mushroom body ablated adult flies, *leoI* was found to be present throughout the head and apparently enriched in ellipsoid body (Figure 11) (de Belle and Heisenberg 1994, Philip et al., 2001). *leoII* appeared to be adult mushroom body specific as well as expressed in the thorax, abdomen, and adult heads outside the mushroom bodies like *leoI* (Figure 11) (Philip et al., 2001). This evidence suggested

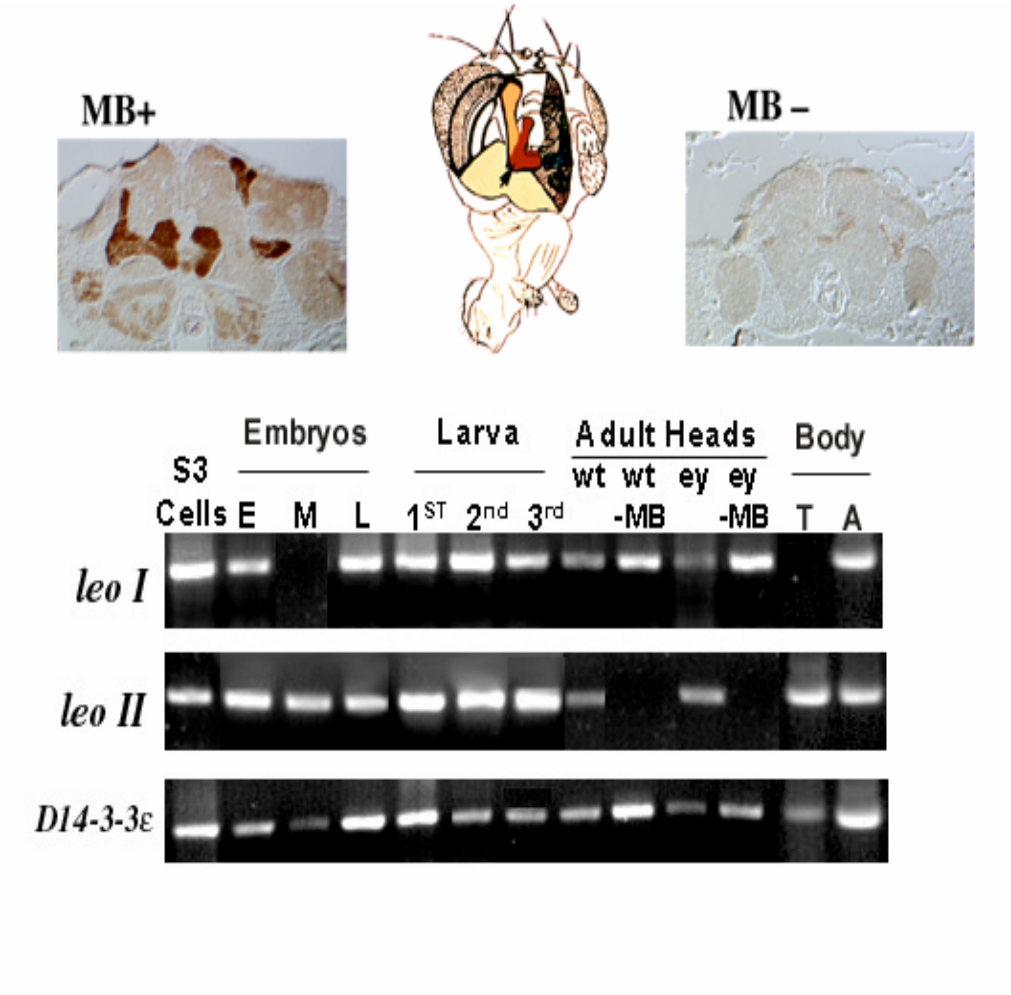

Figure 11. Expression of *leo* and *D14-3-3ε* mRNA

(A) Wild type adult fly head sections stained with anti-LEO without (MB+) and with hydroxyurea treatment (MB-).
(B) mRNA was isolated from 0-2 hr (E), 12-14 hr (M) and 18-20 hr (L) embryos, first, second and third instar larvae, adult heads control (wt), eyes-absent (eya) and control hydroxyurea mushroom ablated (MB-) and eyes-absent animals, and from wt thoraces and abdomens (Adapted from Philip et al, 2001).

that there is differential expression of *leo I* and *leo II* throughout development, although it is unknown whether each may have unique developmental roles. It is possible that the two LEO isoforms are functionally distinct, perhaps in analogy to the two ζ phospho-isoforms (the ζ/δ pair) in vertebrates (Aitkens et al., 1995), since LEO proteins apparently are not phosphorylated (Skoulakis and Davis, 1998)

An enhancer detector screen for genes that express preferentially in the mushroom bodies produced several *leo* mutant alleles including a semi-lethal P-element insertion leo^{P1375}, a lethal P-element insertion leo^{P1188} and a lethal imprecise deletion leo^{12X} (Figure 10) (Skoulakis and Davis, 1996). Small imprecise excisions (leo^{X1} and $leo^{2.3}$) that apparently removed the mushroom body enhancer and therefore are homozygous viable with reduced staining in the adult mushroom bodies were also isolated (Skoulakis and Davis, 1996). These mutants allowed investigation of the role of LEO in eye, embryonic and oocyte development as well as synaptic activity and olfactory learning and memory (Chang and Rubin, 1996; Skoulakis and Davis, 1996; Broadie et al., 1997; Kockel et al., 1997; Li et al., 1997; Skoulakis and Davis, 1998; Philip et al., 2001; Benton et al., 2002). The following is a summary of the known functions of the *Drosophila 14-3-3ζ* (*D14-3-3ζ*) or *leonardo (leo)* gene.

Embryonic development

Homozygous leo^{P1375} and leo^{P1188} embryos die as apparently normal fully formed larvae and leo^{P1188} embryos exhibit a large deficit in neurotransmission, which is the likely cause of their failure to hatch (Skoulakis and Davis, 1996; Broadie et al., 1997).

This finding is consistent with the lethal phenotypes of homozygous LEO loss of function mutants derived from heterozygous mothers (Skoulakis and Davis, 1996, Broadie et al., 1997, Kockel et al., 1997, Li et al., 1997). Although the mechanism by which neurotransmission may be affected in these mutant embryos is unknown, this was the first evidence of 14-3-3s having a role in neuronal physiology/ neurotransmission. An explanation of the phenotype may lie in evidence from bovine adrenal chromaffin cells that 14-3-3ζ affects exocytosis (Roth and Burgoyne, 1995; Wu et al., 1992). 14-3-3ζ affects exocytosis apparently by participating in cortical actin disassembly and secretory vesicle release (Roth and Burgoyne, 1995) (see section III.B.2.b.). The *leo* mutant lethality however could not be rescued by expression of a single LEO isoform suggesting that more than one of the LEO proteins is necessary for viability (Kockel et al., 1997). However, both *leoI* and *leoII* transgenes can support development to adulthood of the weakest P-element insertion leo^{P1375} in agreement with the observations that there is leaky expression from the *leo* gene in this mutant.

LEO has been shown to interact with the *Drosophila* homolog of Raf, D-RAF (Li et al., 1997; Rommel et al., 1997; Jones et al., 1995a). Although its exact role in Raf activation is still not fully understood, LEO plays an essential role in the Torso (Tor) receptor tyrosine kinase (RTK) pathway, which activates the Ras-Raf-MAPK signaling controlling *tailless* (*tll*) expression in syncytial blastoderm embryos (Li et al., 1997). It appears that in the absence of Tor, over-expression of *leo* is able to activate *tll* expression. Li et al., (1997) also concluded that the interaction between LEO and Raf is

necessary, but not sufficient for activation of Raf and over-expression of LEO still requires Ras1 to activate D-Raf.

Although, the *leonardo* gene is required for viability there is a strong maternal contribution that allows embryos to proceed through the initial stages of embryogenesis without any abnormalities (Skoulakis and Davis, 1996). Therefore, genetic mosaics in the germ-line of heterozygous *leo* mutant females were created to study its potential effects on early cell cycle progression (Su et al., 2001). In syncytial embryos prior to stage 13 of embryogenesis, LEO is dispersed during interphase and found in the proximity of the chromosomes during metaphase, anaphase and telophase (Su et al., 2001). D14-3-3ζ-deficient embryos contained defects such as DNA bridges between chromosomes, pronounced asynchrony in divisions, free microtubule-organizing centers not associated to nuclei and larger than normal DNA masses (Su et al., 2001). These observations suggested that these embryos retained spindle function, but lacked proper chromosomal segregation (Su et al., 2001). Therefore, D14-3-3ζ appears to be required for normal chromosome separation during syncytial mitoses.

Eye development

In *Drosophila*, photoreceptor development depends on two different receptor tyrosine kinases (RTK) that activate and lie upstream of the Ras-Raf signaling pathway (Simon, 1994; Zipursky and Rubin, 1994). The R1-R6 photoreceptors require signaling from *Drosophila* EGF receptor (DER), whereas the R7 photoreceptor requires signaling from the Sevenless receptor (Simon, 1994; Wasserman et al., 1995). Mitotic clones that

reduce LEO, or expression of anti-sense LEO cause defects in photoreceptor differentiation (Kockel et al., 1997). The mutant ommatidia appeared to have lost the outer and R7 photoreceptor cells, but the outer cells seemed more sensitive to loss of LEO than the Sevenless-requiring R7 cells. In addition, D14-3-3ζ mutants were unable to modify the abnormal rough eye phenotype produced by constitutively active Ras (Chang and Rubin, 1997). Therefore, LEO appears to be essential in photoreceptor differentiation and Ras-independent cell proliferation (Kockel et al., 1997; Chang and Rubin, 1997).

Oocyte development

LEO is expressed in nurse cells and maturing oocytes of female flies, suggesting it may play a role in their development (Skoulakis and Davis, 1996). Results from a yeast two hybrid screen, indicated that LEO associates with the kinase domain of partitioning defective (PAR-1), which contains a phosphorylation dependent conserved motif (Fu et al., 2000; Benton et al., 2002). In epithelia, the apical domain is defined by a complex containing Bazooka (BAZ), PAR-6 and a protein kinase C (aPKC) (Petronczki and Knoblich, 2001). PAR-1 phosphorylates BAZ/PAR-3 to generate a 14-3-3 binding site that inhibits the formation of the BAZ/PAR-6/aPKC complex in the lateral region of the epithelia between the apical and basal regions (Rose and Kemphues, 1998). Follicle cell clones homozygous for the *leo* null allele leo^{12X} show severe defects in apical-basal polarity (Benton and St Johnston, 2003). Earlier follicle cell clones homozygous for the leo^{P1188} allele displayed defects in tissue organization that fail to

encapsulate germ-line cysts, a phenotype that can be partially rescued by components of the BAZ/PAR-6/aPKC complex (Benton and St Johnston, 2003). This suggests that *leo* is necessary for apical-basal polarity in the epithelia of developing oocytes.

Nervous system functions

Since investigation of synaptic physiology is not currently possible in the *Drosophila* central nervous system, neuromuscular junctions (NMJs), have been used as a model in determining the role of many molecules in synaptic physiology and plasticity (Zhong and Wu, 1991; Zhong et al., 1992; Davis, 1996; Featherstone and Broadie, 2000). Since severe *leo* mutations are lethal, electrophysiological investigation was performed in the mature embryonic NMJ, where LEO is enriched in pre-synaptic neurons (Broadie et al., 1997). Synaptogenesis and basic synaptic function is normal, but synaptic transmission, amplitude and fidelity, as well as long-term facilitation and post-tetanic potentiation were impaired in the mutant embryos. This did not appear to be the result of synaptic vesicle deficits, or defective vesicle release, but rather a failure to recruit them properly in the synapses (Broadie et al., 1997). These defects in synaptic plasticity may underlie all, or part of the behavioral deficits of *leo* mutants. Further research is needed to determine whether loss of one or both LEO isoforms is responsible for this deficit.

At the synaptic boutons of neuromuscular junctions, LEO can be found along with the *Drosophila* Slowpoke (dSlo) calcium dependent potassium (K_{Ca}) channel and Slowpoke-binding protein (Slob) (Broadie et al., 1997; Zhou et al., 1999). LEO is

capable of interacting with Slob in a phosphorylation dependent manner to create a 14-3-3/Slob/dSlo complex (Zhou et al., 1999). Electrophysiological recordings of transfected tsA201 cells indicated that the presence of D14-3-3ζ and wild type Slob changed dSlo voltage sensitivity and channel activity which was not evoked with 14-3-3 alone (Zhou et al., 1999). This effect appeared to be independent of D14-3-3ζ dimerization (Zhou et al., 2003). Although, D14-3-3ζ appeared to interact and modify dSlo via Slob, it is unknown what effect this may have on neurotransmission at the neuromuscular junction or behavioral defects associated with *D14-3-3ζ* mutants.

In viable *leo* mutants, there is a 30-35% learning and 90 minute memory decrement using the LONG training paradigm, consistent with the lack of LEO in the mushroom bodies of the leo^{X1} and $leo^{2.3}$ mutants (Figure 10) (Skoulakis and Davis, 1996; Philip et al., 2001). However, the mutants did not exhibit any morphological defects in the central nervous system or stimulus perception deficits (Skoulakis and Davis, 1996). In addition, the mutants exhibited a highly significant 50% reduction in performance upon single stimulus pairing (SHORT PROGRAM). However, the performance of the mutant animals improved significantly after a second training episode to the level of singly trained controls. This is consistent with the interpretation that the mutants do not harbor developmental defects, which inhibit them to acquire and process information, but rather, they learn and remember inefficiently.

The decrement in learning and memory using the LONG PROGRAM seen in viable mutants can be restored with acute induction of LI or LII transgenes in the *Drosophila* mushroom bodies (Philip et al., 2001). This suggests that both LEO

isoforms are capable of rescuing the learning and memory deficit. Moreover, lethal homozygotes and heteroallelic mutants rescued to adulthood by conditional induction of LI or LI/LII transgenes are learning and memory impaired. These adult animals contain only 10% of normal LEO throughout their bodies. Conditional induction of LI, LII or LI/LII transgenes in the rescued lethal homozygotes restores their defective learning and memory (Philip et al., 2001). However, the decrement returns when the transgenically supplied LEO is allowed to decay, suggesting that LEO is acutely necessary for learning. This is further evidence that LEO is not necessary for neuronal development, but instead necessary for information processing in the adult mushroom bodies.

This data along with the apparent ability of LEO to interact with PKC and Raf suggests an additional model for how learning and memory formation may occur within the mushroom bodies (Figure 12) (Philip et al., 2001; Dubnau et al., 2003). In contrast to the current model (Figure 9) (Waddell and Quinn, et al., 2001; Roman and Davis, 2001; Sokolowski, 2003), this model proposes that in addition to PKA-dependent processes known to play essential roles, long-term memory (LTM) formation involves phosphorylation of CREB by MAPK, a member of the Ras-Raf-MAPK pathway, or by PKC (Dudnau et al., 2003) (Figure 12). In agreement with this proposal, in the courtship paradigm also mediated by the mushroom bodies, disrupting PKC function suppress associative learning and memory (Kane et al., 1997). Similar to the current model (Figure 9), short-term memory (STM) involves the acute release of neurotransmitter (Figure 12) (Waddell and Quinn, 2001b; Roman and Davis, 2001; Sokolowski, 2003), mediated by PKC and the ability 14-3-3s to promote exocytosis (see Section IV.B.2.b),

in addition to the standard mechanisms (Figure 12) (Morgan, 1992a; Morgan, 1992b; Chamberlain et al., 1995; Gannon-Murakami and Murakami, 2002; Drier et al., 2002; Dudnau et al., 2003). The release may also be mediated by 14-3-3 directly as suggested by their role in neurotransmitter release at the NMJ (Broadie et al., 1997). This new model (Figure 12) added to what is already known about learning and memory formation in *Drosophila* mushrooms bodies (Figure 9), helps to further explain the biochemical complexities that translate synaptic plasticity into experience-dependent behavioral responses.

14-3-3ε

The D14-3-3ε isotype is the most similar in sequence and length to the ancient plant and yeast 14-3-3 proteins (Roseboom et al., 1994; Wang and Shakes, 1996). At the onset of this study, the available *D14-3-3ε* alleles were a P-element insertion (*D14-3-3ε*$^{l(3)j2B10}$ and three mis-sense mutations (*D14-3-3ε*^{E183K}, *D14-3-3ε*^{F199Y} and *D14-3-3ε*^{Y214F}) (Figure 13) isolated in a screen for modifiers of a RAS1 dominant allele that caused a rough eye phenotype (Chang and Rubin, 1997). Due to the fact that the only available insertion allele may not be a null, we obtained and characterized three novel alleles generated by mobilization of the transposon in *D14-3-3ε*$^{l(3)j2B10}$ (Chang and Rubin, 1997), *D14-3-3ε*^{ex5}, *D14-3-3ε*^{ex4}, *D14-3-3ε*^{ex24} generated by H. C. Chang (Chang and Rubin, unpublished). The following is a summary of the known functions of the *Drosophila D14-3-3ε* gene.

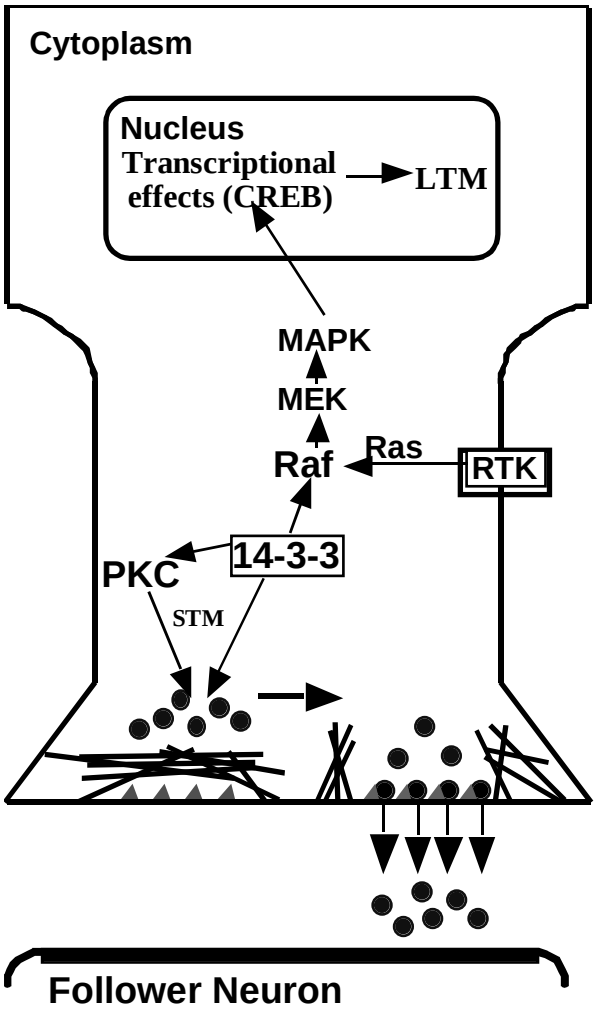

Figure 12. LEO is involved in mediating learning and memory in the *Drosophila* mushroom bodies

A stimulus activates receptor tryosine kinase (RTK) activating Ras and Raf (mitogen–activated protein kinase (MAPK) kinase kinase) which is bound to a14-3-3 dimer. The Raf then phosphorylate MAPK kinase (MEK) which phosphorylates MAPK which then phosphorylates CREB allowing for transcriptional activation, thereby long term memory (LTM) formation. Protein kinase C (PKC) via 14-3-3s or 14-3-3 directly regulate the acute release of neurotransmitters leading to short term memory (STM).

A

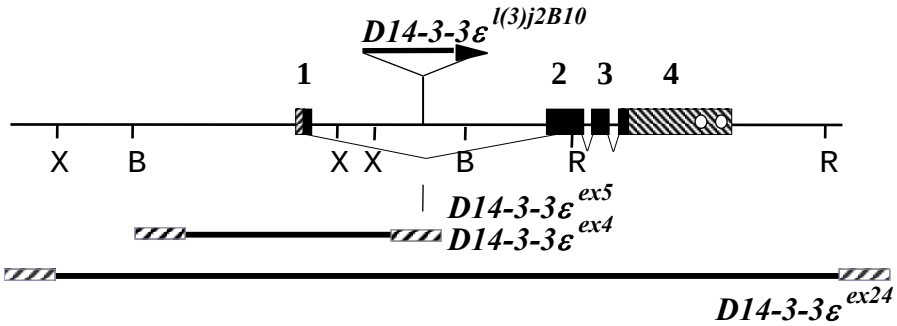


```
MTERENNVYK AKLAEQAERY DEMVEAMKKV ASMDVELTVE ERNLLSVAYK  50

NVIGARRASW RIITSIEQKE ENKGAEEKLE MIKTYRGQVE KELRDICSDI  100

KNVLEKHLIP CATSGESKVF YYKMKGDYHR YLAEFATGSD RKDAAENSLI  150
                                   *(E183K)          * (F199Y)
AYKAASDIAM NHLPPTHPIR LGLALNFSVF YYEILNSPDR ACRLAKAAFD  200
              *(Y214F)              K                   Y
DAIAELDTLS EESYKDSTLI MQLLRDNLTL WTSDMQAEDP NAGDGEPKEQ  250
              F
IQDVEDQDVS                                              260
```

Figure 13. Map of *D14-3-3ε* mutations

A. The genomic region, structure and mutations of the *D14-3-3ε* gene. Boxes represent exons, whereas lines represent introns and surrounding non-transcribed regions. The stippled boxes indicate untranslated portions of exons. The white circles in exon V represent polyadenylation sites. Restriction endonuclease sites are indicated by capital letters (X: Xba I, B: BamHI, R: EcoRI). The location of the P-element insertion in intron I is indicated by the arrow. The extension of the deficiencies for $D14\text{-}3\text{-}3\varepsilon^{ex4}$ and $D14\text{-}3\text{-}3\varepsilon^{ex24}$ are indicated by the black bars, whereas the regions of uncertainty are indicated by the hatched bars. (Adapted from Chang and Rubin 1997).
(B) $D14\text{-}3\text{-}3\varepsilon^{E183K}$ at position 183 is a glutamic acid changed to a lysine $D14\text{-}3\text{-}3\varepsilon^{F199Y}$ at position 199 has a phenylalanine changed to a tyrosine and $D14\text{-}3\text{-}3\varepsilon^{Y214F}$ at position 214 has a tyrosine change to a phenylalanine (Adapted from Chang and Rubin, 1997).

Embryonic development

Drosophila D14-3-3ε is ubiquitously expressed in all tissues, and stages of development examined (Figure 11) (Philip et al., 2001). D14-3-3ε appears to be expressed in cells during embryonic development immediately prior to MAPK activation (Tien et al., 1999), suggestive of its importance in Ras-Raf-MAPK signaling. The crystal structure of *D14-3-3ε* is unknown, but the apparently highly conserved quaternary structure of all 14-3-3s (Xiao et al., 1995) suggests that the point mutants available likely map to the middle of the dimer pocket, the proposed site of ligand binding (Li et al, 1997). Using *in vitro* analysis Rittinger et al. (1999) established that 14-3-3's with the E183K mutation no longer bind to A-Raf, B-Raf, C-Raf-1 or BAD. In addition to being capable of binding D-Raf, the E183K mutation dominantly enhanced lethality in a partial loss of function D-Raf background (Chang and Rubin, 1997). These data led to the conclusion that D14-3-3ε is necessary for the Ras1-dependent process required for viability (Chang and Rubin, 1997).

Consistent with vertebrate studies, 14-3-3ε appears to be required for timing of mitosis and regulation of the cell cycle in *Drosophila* (Su et al., 2001). During the first 13 synchronous nuclear divisions of embryogenesis, D14-3-3ε appeared dispersed in interphase and nuclear prior to mitosis (Su et al., 2001). D14-3-3ε was found in various locations during the mitotic cycle including proximal to the chromosome during anaphase/telophase (Su et al., 2001). Nuclear localization for D14-3-3ε continued when the embryo became cellularized (Su et al., 2001). This localization of D14-3-3ε to the chromosomes was apparently coupled to the cycles of Cdk1 activation and inactivation

that occur when entering and exiting mitosis (Su et al., 2001). In agreement with this hypothesis, lack of D14-3-3ε allowed premature entry into and out of mitosis, advancing the entire schedule without disrupting its relative order (Su et al., 2001). There was a similar effect after embryos were irradiated. Instead of a delay in the cell cycle to allow for DNA repair, embryos that lack D14-3-3ε advanced their schedule and entered mitosis (Su et al., 2001). This suggests that D14-3-3ε is necessary for the timing of mitosis during post-blastoderm cell cycles and after irradiation.

Eye development

D14-3-3ε mutants were first identified as effectors of Ras/Raf signaling in photoreceptor differentiation (Chang and Rubin, 1997). In photoreceptors, *D14-3-3ε* mutants appeared to increase the efficiency of Ras1 signaling (Wasserman and Therrien, 1997; Chang and Rubin, 1997). There was not a dominant interaction with either *yan* or *sev-phyl,* two downstream targets of the SEV/Ras1 signaling cascade, suggesting that *D14-3-3ε* acts downstream of *Ras* and upstream of these two nuclear factors (Chang and Rubin, 1997; Therrien et al., 2000). The mutations were also capable of suppressing rough eye deficits caused by constitutively activated Raf, suggesting *D14-3-3ε* acts downstream or parallel to Raf (Chang and Rubin, 1997). This suggests that *D14-3-3ε* is necessary for photoreceptor differentiation via the Ras/Raf signaling pathway.

Oocyte development

The P-element insertion *l(3)j2B10* located in the first intron of *D14-3-3ε* isolated in this suppressor screen, appeared not to be essential for viability, but necessary for fertility. With regard to fertility, there were still eggs laid by *D14-3-3ε* homozygotes (Chang and Rubin, 1997; Benton et al., 2002). Recent studies indicate these eggs do not develop because D14-3-3ε plays a role in oocyte determination and the polarization in the A-P axis (Benton et al., 2002). Apparently, unlike LEO, D14-3-3ε interacts with PAR-1 via a novel non-phosphorylation dependent interface on the external surface of the 14-3-3 molecule (Benton et al., 2002). This association is abolished by the Y214F and F199Y point mutations located outside the phosphoserine binding pocket in a hydrophobic region, but not the E183K point mutation that lies within the pocket (Chang and Rubin, 1997; Rittinger et al., 1999).

Using germ-line clones, Benton et al., (2002) determined that like PAR-1, D14-3-3ε is required for oocyte differentiation, which depends on microtubule (MT) dependent transport of specific factors (Benton et al., 2002). Both *par-1* null mutants and *D14-3-3ε* mutants failed to form the microtubule cytoskeleton (MTOC) in the oocyte, suggesting that they function in parallel in this step of oocyte differentiation. Similarities between *par-1* and *D14-3-3ε* mutants can also be seen in their altered localization of *osk* mRNA, *bcd* mRNA and STAU, which play a role in oocyte anterior-posterior (A-P) polarity (Benton et al., 2002). The mis-localization of osk mRNA and STAU affect the proper microtubule anterior to posterior gradient, a phenotype which is

unique to *par-1* and *D14-3-3ε* mutants. This suggests that *D14-3-3ε* has a predominant function in A-P polarity in the oocytes.

Nervous system functions

14-3-3ε appears particularly abundant in the CNS (Rosenboom et al., 1994). *Drosophila* is the only metazoan model system with genetic mutations available to study the role of this particular isotype in cell signaling, in the developing and the adult CNS. D14-3-3ε is expressed in the adult head (Philip et al., 2001), although it's potential role in associative and non associative processes is unknown.

Link between 14-3-3's and Neurodegeneration in *Drosophila*

In *Drosophila*, the Akt kinase phosphorylates wild type and mutant Ataxin-1 allowing its association with 14-3-3s (Chen et al., 2003). Both D14-3-3ζ and D14-3-3ε appear to have higher binding affinity to the mutant form of Ataxin-1, which has the additional CAG repeats and produces a long polyglutamine tract (Chen et al., 2003). This expansion of the polyglutamine tract is similar to other inherited neurodegenerative diseases such as Huntington's. Using D14-3-3ε UAS constructs that I generated, Chen et al. (2003) investigated the interaction between mutant Ataxin-1 and 14-3-3ε. This interaction appears to stabilize Ataxin-1 leading to its accumulation and formation of spinocellular ataxia type 1 like aggregates that can cause neurodegeneration. The over-expression of D14-3-3ε in *ataxin-1* mutant ($SCA1^{30Q}$) backgrounds enhanced neurotoxicity, which led to the conclusion that higher levels of certain 14-3-3 isoforms

may contribute to neuronal vulnerability (Chen et al., 2003). This is the first evidence that any 14-3-3 protein has an active role in the pathogenesis of neuronal degeneration.

Are *Drosophila* 14-3-3's functionally redundant?

There is a 66% sequence identity among LEO and D14-3-3ε isotypes (Table 4), but are they functionally redundant? It appears that in the case of embryonic development, the reduction to one copy of *leo* in the $D14\text{-}3\text{-}3\varepsilon^{l(3)j2B10}$ homozygous flies, which are partially viable results in complete lethality (Chang and Rubin, 1997). With respect to eye development, although only *14-3-3ε* mutants modified constitutively activated Ras, the phenotype of homozygous *14-3-3ε* mutants is weaker than those of other components of the SEV/Ras1 pathway and appears to become stronger by reduction of LEO (Chang and Rubin, 1997). This data led to the conclusion that the 14-3-3 proteins were at least partially redundant in viability and photoreceptor development (Chang and Rubin, 1997).

D14-3-3ε and LEO share a common cycle of perichromosomal localization during syncytial mitosis, suggesting that both play a role in mitotic progression during embryogenesis (Su et al., 2001). Although the two 14-3-3 isotypes co-localize, they have very different functions with respect to cell cycle progression. D14-3-3ε is required for the timing of mitosis during post-blastoderm cell cycles and after irradiation, whereas, LEO is required for normal chromosome separation during syncytial mitoses (Su et al., 2001). This is evidence that in *Drosophila* the two 14-3-3s

are not functionally redundant, they in fact have specific functions even when they are present within the same cells.

Analysis using germ-line clones determined that D14-3-3ε is required for oocyte differentiation, whereas clones of strong lethal alleles of *leo* had no effect (Benton et al., 2002). *D14-3-3ε* mutants also appeared to affect the proper localization of *osk* mRNA, *bcd* mRNA and STAU necessary for anterior-posterior polarity, whereas the oocytes homozygous for leo^{P1188} had no polarity defects (Benton et al., 2002). However, the D14-3-3ε phenotypes were incompletely penetrant and could be enhanced with reduction in *leo* copy number, suggesting LEO can partially compensate for the absence of D14-3-3ε in oocytes (Benton et al., 2002). The oocyte epithelia of *leo* mutants appeared to have defects in apical-basal polarity, whereas *D14-3-3ε* mutants showed no obvious defects (Benton and St Johnston, 2003). However, reduction of *D14-3-3ε* worsened the phenotype associated with *leo* mutants, suggesting that D14-3-3ε can partially compensate for the absence of LEO in the epithelia (Benton and St Johnston, 2003). In the case of oocyte determination, A-P polarity and epithelial apical-basal polarity, the two 14-3-3 isotypes appeared to partially compensate for one another, although the evidence also argued for functional specificity among isotypes (Benton et al., 2002; Benton and St Johnston, 2003).

Both 14-3-3 isotypes are capable of binding the PAR-1 kinase that regulates oocyte differentiation, A-P polarity and apical-basal polarity in the epithelia (Benton et al., 2002; Benton and St Johnston, 2003). D14-3-3ε is highly expressed in the dividing germ-line cell in the germarium and co-localizes with PAR-1 at the ring canals (Lin et

al., 1997; Benton et al., 2002). LEO also co-localizes with PAR-1 at the ring canals, but is expressed at very low levels in the germarium (Benton et al., 2002). Apparently, the LEO-PAR1 interaction occurs within the phosphoserine pocket and the interaction with D14-3-3ε occurs on the external surface of the dimer (Benton et al., 2002). The differences in target specificity with PAR-1 and spatial expression may account for the phenotypic differences between the two isotypes.

Overall, despite the high homology among the 14-3-3 isotypes in *Drosophila* the data suggest that the isotypes may be at least partially functionally redundant in certain biological processes but not in others. This appears to be the case for viability and photoreceptor differentiation (Chang and Rubin, 1997; Kockel et al., 1997; Philip et al., 2001). Differences in temporal and spatial expression may account for 14-3-3 isotype specificity in oocyte determination, A-P polarity and epithelial apical-basal polarity (Benton et al., 2002; Benton and St Johnston, 2003). However, with respect to cell cycle progression D14-3-3ε and LEO co-localize, but apparently have different functions (Su et al., 2001). This suggests that whether the two can functionally compensate for one another is likely to depend on the particular 14-3-3 targets involved in each particular process under study. Therefore, it is very likely that D14-3-3ε and LEO can be both functionally redundant in some cases and thus the two be able to functionally compensate each other, but in addition there are distinct isoform specific functions.

A possible explanation for the apparent functional redundancy between the two *Drosophila* 14-3-3 isotypes (LEO and D14-3-3ε) is that they work together as heterodimers at least in some cases. The fact that both are capable of binding signaling

molecules such as Raf and are both expressed in embryos and the eye supports the idea that LEO and D14-3-3ε may work together as heterodimers to regulate signaling in these tissues. In the adult head, LEO is expressed preferentially in the mushroom bodies, whereas D14-3-3ε is ubiquitous through the adult head, suggesting the potential for unique function. However, behavioral research needs to be done to understand the function of D14-3-3ε in the adult CNS. Research aimed at confirming the presence of heterodimers within the specific tissues and developmental stages where 14-3-3 mutants display phenotypes. The following experiments will provide evidence for whether 14-3-3s have redundant functions or that in *Drosophila*, the different 14-3-3s have unique functions.

CHAPTER II

14-3-3 FUNCTIONAL SPECIFICITY AND HOMEOSTASIS IN *DROSOPHILA MELANOGASTER*

INTRODUCTION

The 14-3-3 proteins comprise a highly conserved family of small 28-32 kD acidic molecules present in all eukaryotes. 14-3-3s appear to share a common structure composed of nine anti-parallel α-helices forming a U-shaped palisade around a central negatively charged groove of largely invariant amino acids (Aitken, 1995; Fu et al., 2000; Tzivion and Avruch, 2002). All 14-3-3s form homo- and heterodimers by interaction of hydrophobic residues in helix 1 of one monomer with similar residues in helixes 3 and 4 of another (Fu et al., 2000; Liu et al., 1995; Tzivion and Avruch, 2002; Xiao et al., 1995). A phosphoprotein binding surface formed by conserved amino acids in the negatively charged groove interacts with target proteins that contain the motifs RSxpS/TxP, or RxxxpS/TxP (where x=any amino acid, pS/T=phosphoserine or phosphothreonine). Target proteins bind dimeric 14-3-3s preferentially, but instances where monomers are able to bind such sequences are known (Muslin et al., 1996; Muslin and Xing, 2000; Tzivion and Avruch, 2002).

14-3-3 binding on a target protein may protect it from dephosphorylation or proteolysis, modulate its activity, alter its ability to interact with other partners, or

modify its cytoplasmic/nuclear partition (Tzivion and Avruch, 2002). Therefore, it is not unusual that 14-3-3 proteins have been implicated in a diverse number of processes and biochemical pathways (Fu et al., 2000; Skoulakis and Davis, 1998; Van Hemert et al., 2001). 14-3-3s are involved in regulation of multiple members of signaling cascades in response to growth factors, cytokines, or environmental stress (Fu et al., 2000; Morrison, 1994; Skoulakis and Davis, 1998; Van Hemert et al., 2001). These signaling cascades occur through a series of phosphorylations that activate the Mitogen-activated protein kinases (MAPKs) which in turn translocate to the nucleus where they activate transcription factors that modulate gene expression in response to the stimuli. The phosphorylation cascade is initiated by activation of MAPK kinase kinases (MAPKKs), which activate MAPK kinases that in turn activate MAPKs. These series of phosohorylations generate 14-3-3 binding sites, which are thought to modulate the activity or cellular location of the kinases (Kyriakis and Avruch, 2001; Tzivion and Avruch, 2002).

An extraordinary feature of this protein family is the high sequence conservation among related isotypes from diverse species. This clearly reflects their evolutionary age, which apparently precedes the separation of plants and animals since they are ubiquitous in both (Rosenquist et al., 2000; Wang and Shakes, 1996). Vertebrates contain seven distinct 14-3-3 genes (β, ζ, γ, η, σ, τ(θ), and ε) that yield nine structurally distinct protein isotypes (with α and δ being the phosphorylated forms of β and ζ, respectively) classed into two conservation groups (Rosenquist et al., 2000; Skoulakis and Davis, 1998; Wang and Shakes, 1996). Of these, the epsilon (ε) isoforms are unique because

they are more similar to yeast and plant than other animal isotypes. This suggests that they may be closer to the ancestral 14-3-3 protein(s) and form their own unique branch among eukaryotic 14-3-3s (Rosenquist et al., 2000; Wang and Shakes, 1996). In vertebrate brains where these proteins are highly abundant, there is some specificity in isotype distribution, but generally 14-3-3s are expressed in complex overlapping patterns (Baxter et al., 2002). This suggests that multiple heterodimers are possible in tissues that contain more than one isotype and some of these have been detected *in vitro* and *in vivo* (Jones et al., 1995). It is unknown whether the possible heterodimers and homodimers are functionally divergent *in vivo*, or as suggested by *in vitro* studies, all isotypes can act equivalently in the diverse processes 14-3-3s have been implicated (Muslin et al., 1996; Yaffe et al., 1997). In addition, it is unknown whether homodimers or heterodimers exhibit the same temporal or tissue specificity *in vivo.*

Drosophila melanogaster contains two 14-3-3 genes. Alternative splicing of the *leonardo* gene encodes two nearly identical protein isoforms (LEOI and LEOII) of the typical 14-3-3 conservation group with 88% identity to mammalian ζ, (Philip et al., 2001; Skoulakis and Davis, 1996). There are differences in the temporal and spatial distribution of the two *leo* isoforms, although it is unknown what controls expression. According to RT-PCR, *leoI* is present in early and late embryos, all larva stages, the adult head and abdomen; whereas, *leoII* is present in all embryo stages, larva stages and adult tissues. Although, *leoII* appears to be specific to the mushroom bodies and thorax (Philip et al., 2001), it is unknown if each isoform has unique functions. The *D14-3-3ε* gene encodes a single protein 82% identical to the mammalian ε isoform (Chang and

Rubin, 1997). As in vertebrates, the LEO proteins are found enriched in adult brain and in low levels throughout the body, as well as embryos, larvae and pupae. Whereas, D14-3-3ε is present in all developmental stages and in all tissues examined with only slight enrichment in the adult brain (Philip et al., 2001). Therefore, *Drosophila* provides a simple genetically tractable model system to study 14-3-3 isotype specific functions and interactions *in vivo.*

Total lack of LEO results in lethality likely due to its involvement in activation of the MAPKK RAF-1 required for early embryonic developmental decisions (LI *et al.* 1997). However, *leo* loss of function mutants exhibit additional late developmental phenotypes and functional impairments of their nervous system (Broadie et al., 1997), but whether these result from a requirement for LEO in additional signaling pathways is not known. In addition, LEO functions during photoreceptor development, another process that involves signaling through RAF-1 kinase (Kockel et al., 1997). LEO is acutely required in adult brain neurons, the mushroom bodies, for processes underlying learning and memory (Philip et al., 2001; Skoulakis and Davis, 1996), but the signaling pathways they involve remain unknown. The *D14-3-3ε* gene was identified in genetic screens for factors essential for signaling through RAF-1 in photoreceptor development in the eye (Karim et al., 1996; Therrien et al., 2000) and embryonic development (Li et al., 2000). D14-3-3ε and LEO appeared partially redundant for photoreceptor development and viability (Chang and Rubin, 1997), but the observed redundancy may reflect heterodimerizarion of the two proteins. Furthermore, *D14-3-3ε* mutants exhibited additional phenotypes suggestive of participation of the protein in additional processes.

In accord with this hypothesis, unique roles for each 14-3-3 protein in regulating entry to mitosis in embryos were recently described (Su et al., 2001). These results may underlie multiple tissue and temporal requirements for D14-3-3ε activity.

To investigate involvement of D14-3-3ε in temporal and tissue specific processes and potential 14-3-3 isotype-specific functions, I systematically examined its role by mutant analysis. Since roles of this protein in photoreceptor development and embryonic mitotic decisions have been established (Chang and Rubin, 1997; Su et al., 2001), I focused on novel phenotypes. To avoid potential complications due to allele-specific phenotypes, in addition to the described alleles, I utilized novel loss of function alleles in a normalized genetic background. In addition, I addressed the question of redundancy with LEO by analysis of *leo* loss of function phenotypes and investigation of heterodimerization of the two isotypes. The results indicate involvement of D14-3-3ε in multiple processes, reveal D14-3-3ε specific mutant phenotypes and suggest a dynamic temporal and spatial interaction of the two 14-3-3 isotypes.

RESULTS

Morphological characterization of D14-3-3ε mutants

At the onset of this study the available *D14-3-3ε* alleles were a P-element insertion (*D14-3-3ε* $^{l(3)j2B10}$. We obtained three novel alleles generated by mobilization of the transposon in *D14-3-3ε* $^{l(3)j2B10}$ (Chang and Rubin, 1997), generated by H. C. Chang (Chang and Rubin, unpublished). Southern analysis (not shown) demonstrated that the

D14-3-3ε genomic region in *D14-3-3ε*^{ex5} appeared identical to the *w*^{1118} and *ry*^{506} isogenic strains consistent with precise excision of the transposon in *D14-3-3ε*$^{l(3)j2B10}$. In contrast, alleles *D14-3-3ε*^{ex4} and *D14-3-3ε*^{ex24} harbored molecular lesions in this region. In *D14-3-3ε*^{ex24}, a large deletion (>10 kb) extending beyond the entire *D14-3-3ε* coding region and likely encompasses neighboring transcription units on either side. *D14-3-3ε*^{ex4} harbors a smaller deletion removing exon 1 of the gene. Therefore, both *D14-3-3ε*^{ex4} and *D14-3-3ε*^{ex24} alleles remove all, or part of the *D14-3-3ε* coding region and are likely null alleles. As predicted from these results, whereas there is normal D14-3-3ε protein accumulation in *D14-3-3ε*^{ex5} homozygotes, the *D14-3-3ε*$^{l(3)j2B10}$, *D14-3-3ε*^{ex4} and *D14-3-3ε*^{ex24} alleles do not yield detectable protein (see below and Figure 15). Although these mutants contain no detectable D14-3-3ε and appear smaller than controls *D14-3-3ε*^{ex5}, the homozygous embryos are morphologically normal (Figure 14). Thus, these alleles permit a systematic investigation of the role of this gene in the complex phenotypes suggested by a prior (Chang and Rubin, 1997).

Morphological characterization of *D14-3-3ε* mutants

Since a significant fraction of *D14-3-3ε*^{ex4} and *D14-3-3ε*$^{l(3)j2B10}$ homozygotes die prior to adulthood, I determined the lethal phase of these null mutations. I did not include the *D14-3-3ε*^{ex24} homozygotes because the deficiency harbored in this allele is likely to encompass neighboring genes, thus complicating the analysis. In agreement

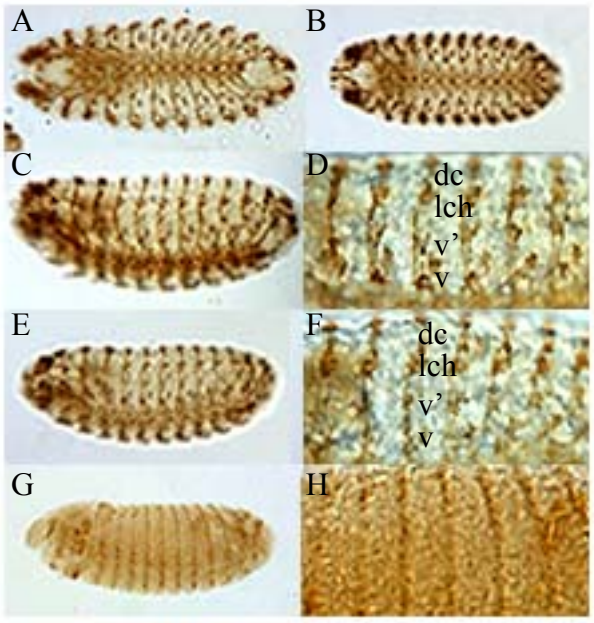

Figure 14. Morphology of *D14-3-3ε* mutant embryos

Anterior is to the left for the 16-18 hour embryos. Photographs 20X magnification (A) ventral view of control *D14-3-3ε*^{ex5} homozygotes, (B) ventral view of mutant *D14-3-3ε*^{ex4} homozygotes, (C) lateral view of *D14-3-3ε*^{ex5} homozygotes and (D) lateral view of *D14-3-3ε*^{ex4} homozygotes were stained with mAb22c10 indicate PNS is morphologically normal. Photographs 40X magnification (I) lateral view of *D14-3-3ε*^{ex5} homozygotes, and (J) lateral view of *D14-3-3ε*^{ex4} homozygotes indicates the CNS are morphological normal. Magnification of the lateral side of embryos focused on the PNS neuronal clusters. Abbreviations: (dc) dorsal cluster; (hy) hypophysis; (lch) lateral chordotonals; (v and v') ventral cell clusters. Lateral views of (G) *D14-3-3ε*^{ex5} homozygotes and (H) *D14-3-3ε*^{ex4} homozygotes stained with anti-engrailed staining indicate that striping is normal and there are a proper number of segments. All embryos were photographed at the same magnification (200X) to illustrate the smaller size of *D14-3-3ε*^{ex5} homozygotes. According to staining and observations of *D14-3-3ε*^{ex4} homozygotes, death occurs at hatching and the embryos do not have any developmental defects.

with data on Table 5, a fraction of null embryos of either genotype die prior to hatching (data not shown). However, apparently all null embryos that hatch successfully proceed to adulthood. If manually removed from the egg, larvae that failed to hatch were able to move around and feed, albeit slowly. Furthermore, embryos that failed to hatch remained alive within the egg for an additional 24 hrs, indicated by their occasional peristaltic movements.

To determine whether null embryos that fail to hatch exhibit developmental defects, we subjected them to immunohistochemical analysis. Morphological examination and immunohistochemical results with a number of antigenic markers did not reveal gross developmental defects except homozygous embryos were smaller in size (Figure 14). I focused on the nervous system because I hypothesized that the inability to hatch was likely a reflection of neuro-developmental deficits since both D14-3-3ε and LEO are abundant in this tissue in late embryos (Skoulakis and Davis, 1996; Tien et al., 1999). The results of mAb22c10 immunohistochemistry indicated that the central nervous system (CNS) and peripheral nervous system (PNS) were largely normal, except for a slight reduction in the density of the ventral nerve cord in $D14\text{-}3\text{-}3\varepsilon^{ex4}$ homozygotes (Figure 15). Identical results were obtained with $D14\text{-}3\text{-}3\varepsilon^{l(3)j2B10}$ homozygotes (not shown). Therefore, lack of D14-3-3ε did not precipitate gross anomalies of the embryonic nervous system and the embryos died as apparently fully formed larvae. However, our results did not eliminate the possibility that the failure to hatch was due to functional deficits of the nervous system, which do not facilitate this process properly. Similarly, homozygous leo^{P1188} embryos die as fully formed larvae and exhibit a large

Table 5. Complementation for viability of *D14-3-3ε* mutants

Genotype	% Lethality (Observed/Expected)	n[a]
$D14\text{-}3\text{-}3\varepsilon^{ex5}/D14\text{-}3\text{-}3\varepsilon^{ex5}$	0	550
$D14\text{-}3\text{-}3\varepsilon^{ex5}/D14\text{-}3\text{-}3\varepsilon^{l(3)j2B10}$	0	413
$D14\text{-}3\text{-}3\varepsilon^{ex5}/D14\text{-}3\text{-}3\varepsilon^{ex4}$	0	546
$D14\text{-}3\text{-}3\varepsilon^{ex5}/D14\text{-}3\text{-}3\varepsilon^{ex24}$	0	660
$D14\text{-}3\text{-}3\varepsilon^{l(3)j2B10}/D14\text{-}3\text{-}3\varepsilon^{l(3)j2B10}$	25	645
$D14\text{-}3\text{-}3\varepsilon^{l(3)j2B10}/D14\text{-}3\text{-}3\varepsilon^{ex4}$	22	510
$D14\text{-}3\text{-}3\varepsilon^{l(3)j2B10}/D14\text{-}3\text{-}3\varepsilon^{ex24}$	39	510
$D14\text{-}3\text{-}3\varepsilon^{ex4}/D14\text{-}3\text{-}3\varepsilon^{ex4}$	58	495
$D14\text{-}3\text{-}3\varepsilon^{ex4}/D14\text{-}3\text{-}3\varepsilon^{ex24}$	61	684
$D14\text{-}3\text{-}3\varepsilon^{ex24}/D14\text{-}3\text{-}3\varepsilon^{ex24}$	100	650

a : number of total flies scored per cross.

deficit in neurotransmission, which is the likely cause of the failure to hatch (Broadie et al., 1997).

D14-3-3ε mutations affect viability

Because we observed a small number of homozygotes for the $D14\text{-}3\text{-}3\varepsilon^{l(3)j2B10}$ and $D14\text{-}3\text{-}3\varepsilon^{ex4}$ mutations, but none for $D14\text{-}3\text{-}3\varepsilon^{ex24}$, an undergraduate in the lab performed complementation tests, which I continued to determine whether all mutations map to the *D14-3-3ε* gene and whether the gene is essential for viability. The results in Table 5 indicate that all tested mutations are alleles of the *D14-3-3ε* gene. Homozygotes for the transposon insertion ($D14\text{-}3\text{-}3\varepsilon^{l(3)j2B10}$) and the null excision allele $D14\text{-}3\text{-}3\varepsilon^{ex4}$ were recessive sub-viable. Whereas 75% $D14\text{-}3\text{-}3\varepsilon^{l(3)j2B10}$ homozygotes were recovered, only 42% of expected $D14\text{-}3\text{-}3\varepsilon^{ex4}$ homozygotes were observed, indicating that the former is a hypomorphic mutation. In contrast, both EMS induced alleles and the $D14\text{-}3\text{-}3\varepsilon^{ex24}$ deletion were recessive lethal. Congruent with the molecular analysis, $D14\text{-}3\text{-}3\varepsilon^{ex24}$/ $D14\text{-}3\text{-}3\varepsilon^{ex4}$ and $D14\text{-}3\text{-}3\varepsilon^{ex24}$/ $D14\text{-}3\text{-}3\varepsilon^{l(3)j2B10}$ heteroallelics were recovered as readily as $D14\text{-}3\text{-}3\varepsilon^{ex4}$ and $D14\text{-}3\text{-}3\varepsilon^{l(3)j2B10}$ homozygotes, indicating that the full lethality associated with the $D14\text{-}3\text{-}3\varepsilon^{ex24}$ allele is likely the result of disruption of neighboring gene(s) in addition to *D14-3-3ε*.

14-3-3 homeostasis in embryonic development

In homozygous null embryos, there was a highly significant ($p<0.001$) increase in the amount of LEO compared to that in heterozygotes, or control animals (Figure 15A and Table 6A). Because we cannot distinguish which of the embryos utilized in this assay would survive to hatching, we cannot determine whether this increase occurs in all embryos, or only in potential survivors. In the latter case, our measurement is an underestimate of the actual level of LEO in embryos that survive. Nevertheless, it is likely that this near doubling in the amount of LEO functionally compensates for the absence of D14-3-3ε and allows survival to hatching for a fraction of homozygotes. To examine when in embryogenesis this elevation occurs, the exact time of hatching was examined in null embryos and controls and a two-hour delay in hatching of null embryos was uncovered. It was apparently during this delay when the embryos up-regulated the level of LEO protein (Figure 15B and Table 6B). This large increase in the amount of protein, may be due to increased LEO accumulation stability, increased translation, increased transcription or combination of thereof.

LEO up regulation in *D14-3-3ε* mutants

Due to the similarity between the two *leo* isoforms, the only way to determine which isoform is up regulated is using quantitative RT-PCR techniques. Three independent RT-PCR experiments utilizing the comparative Ct method indicated no change in the level of *leo I,* but a significant accumulation of of *leoII* transcripts (Figure 16). This type of transcriptional up-regulation, whose mechanism is currently unknown,

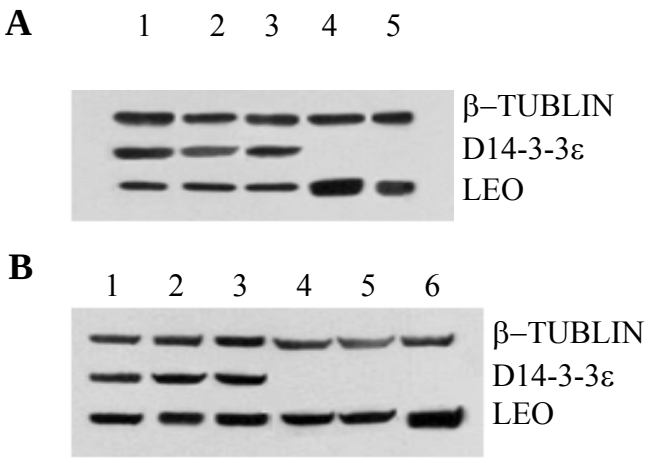

Figure 15. Western blot analysis from *D14-3-3ε* mutant and control lysates

i. A representative blot from embryonic lysates used in acquisition of the data on Table 6a. Genotypes: (1) $D14\text{-}3\text{-}3\varepsilon^{ex5}$ homozygotes, (2) $D14\text{-}3\text{-}3\varepsilon^{ex5}/\ D14\text{-}3\text{-}3\varepsilon^{l(3)j2B10}$, (3) $D14\text{-}3\text{-}3\varepsilon^{ex5}/\ D14\text{-}3\text{-}3\varepsilon^{ex4}$, (4) $D14\text{-}3\text{-}3\varepsilon^{l(3)j2B10}\ D14\text{-}3\text{-}3\varepsilon^{l(3)j2B10}$ and (5) $D14\text{-}3\text{-}3\varepsilon^{ex4}/\ D14\text{-}3\text{-}3\varepsilon^{ex4}$. There is a significant increase in the amount of LEO that accumulates in homozygous null embryos compared to heterozygotes and controls.
ii. A time course of pre-hatching embryonic lysates used in acquisition of the data on Table 6b. Genotypes: (1-3) $D14\text{-}3\text{-}3\varepsilon^{ex5}$ homozygotes and (4-6) $D14\text{-}3\text{-}3\varepsilon^{ex4}$ homozygotes. In addition to a two-hour delay in hatching of $D14\text{-}3\text{-}3\varepsilon^{ex4}$ homozygotes, there is a significant increase in the amount of LEO during those extra two hours compared to controls.

Table 6. D14-3-3ε and LEO levels in embryo lysates

A	Genotype	D14-3-3ε/β-TUB	LEO/β-TUB
1	*D14-3-3ε^{ex5}/D14-3-3ε^{ex5}*	1	1
2	*D14-3-3ε$^{l(3)j2B10}$/TM3SerGFP*	1.1863 ± 0.0495	1.1077 ± 0.1147
3	*D14-3-3ε^{ex4}/TM3SerGFP*	0.9972 ± 0.1260	1.2871 ± 0.1358
4	*D14-3-3ε$^{l(3)j2B10}$/D14-3-3ε$^{l(3)j2B10}$*	0	3.1404 ± 0.2281
5	*D14-3-3ε^{ex4}/D14-3-3ε^{ex4}*	0	2.8778 ± 0.0623

B	Genotype	Hour of embryogenesis	D14-3-3ε/β-TUB	LEO/β-TUB
1	*D14-3-3ε^{ex5}*	1-3	1	1
2	*D14-3-3ε^{ex5}*	20	.9503 ± 0.1734	1.0762 ± 0.1759
3	*D14-3-3ε^{ex5}*	22	.9912 ± 0.1273	1.0318 ± 0.1030
4	*D14-3-3ε^{ex4}*	1-3	0	1.0535 ± 0.0987
5	*D14-3-3ε^{ex4}*	22	0	1.4515 ± 0.0887
6	*D14-3-3ε^{ex4}*	24	0	2.7356 ± 0.0748

Mean ± SEM is shown for three independent experiments. Numbers 1-5 correspond to the respective genotypes in the representative western blot in Figure 15 A. Numbers 1-6 correspond to the respective genotypes in the representative western blot in Figure 15 B.

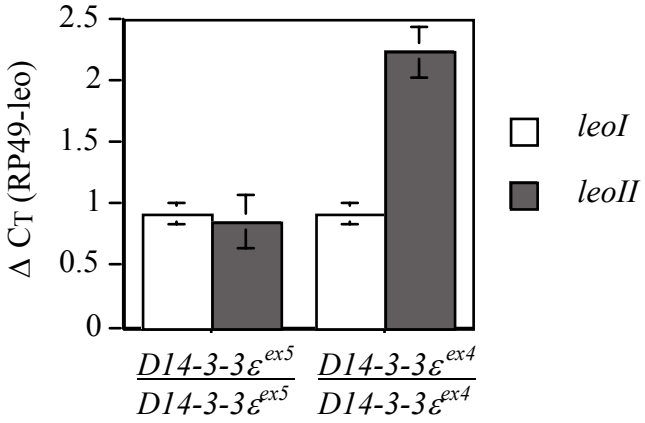

Figure 16. Quantitative RT-PCR of *leo* in D14-3-3ε mutant and control lysates

The change in Ct between internal control RP49 and *leoI* or *leoII* for three different RNA concentrations using three independent embryo lysates was calculated for *D14-3-3ε ex5* heterozygotes and *D14-3-3ε ex5* homozygotes. Results indicate that there is an increase in *leoII* transcript in the *D14-3-3ε ex5* homozygotes and no change is the level of *leoI*.

is unique in *D14-3-3ε* null embryos, suggesting that with respect to developmental processes LEOII is at least partially redundant with D14-3-3ε as previously proposed (Chang and Rubin, 1997). Compensation of D14-3-3ε loss by elevation of *leoII* transcripts and therefore LEOII protein explains the observed accumulation of LEO protein in pre-hatching *D14-3-3ε* null embryos. It is possible that LEO II homodimers functionally compensate for LEO II/D14-3-3ε potential heterodimers for processes essential for embryonic development. In fact, as reported by Chang and Rubin (1997) removal of a single copy of *leo* completely abolishes recovery of either $D14\text{-}3\text{-}3\varepsilon^{ex4}$ or $D14\text{-}3\text{-}3\varepsilon^{l(3)j2B10}$ homozygous adults (not shown).

Rescue of D*14-3-3ε* lethality with D14-3-3ε

To verify if the heat shock *D14-3-3ε* transgenes are able to rescue *D14-3-3ε* mutant lethality, single pair matings were performed and allowed to develop at 18°C, room temperature (RT) and under 3 daily heat shocks of 32°C (HS) (Table 7). The variability in the rescue by the heat shock transgenes is likely due to the expression level of the transgenes (Figure 17). The rescuing transgenic strains were labeled low and high

based on D14-3-3ε protein expression determined by westerns (Figure 17). *hsD14-3-3ε* could completely rescue the P-element mutation *l(3)j2B10* and partially rescue the *ex4* deletion (83%) (Table 7). In addition, UAS*mycD14-3-3ε* containing flies were crossed to various GAL4 expression lines to determine were D14-3-3ε needs to be

Table 7. Rescue of *D14-3-3ε* mutant lethality with D14-3-3ε

D14-3-3ε Allele	hs / UAS	GAL4	% Lethality (Observed/Expected)	n[a]	% Rescue[b,c]
$D14\text{-}3\text{-}3\varepsilon^{l(3)j2B10}$	---	---	25	645	NA
$D14\text{-}3\text{-}3\varepsilon^{l(3)j2B10}$	$hsD14\text{-}3\text{-}3\varepsilon^{L}$ (18)	---	25	505	0[b]
$D14\text{-}3\text{-}3\varepsilon^{l(3)j2B10}$	$hsD14\text{-}3\text{-}3\varepsilon^{L}$ (RT)	---	22	518	12[b]
$D14\text{-}3\text{-}3\varepsilon^{l(3)j2B10}$	$hsD14\text{-}3\text{-}3\varepsilon^{L}$ (HS)	---	12	501	52[b]
$D14\text{-}3\text{-}3\varepsilon^{l(3)j2B10}$	$hsD14\text{-}3\text{-}3\varepsilon^{H}$ (18)	---	25	499	0[b]
$D14\text{-}3\text{-}3\varepsilon^{l(3)j2B10}$	$hsD14\text{-}3\text{-}3\varepsilon^{H}$ (RT)	---	15	610	40[b]
$D14\text{-}3\text{-}3\varepsilon^{l(3)j2B10}$	$hsD14\text{-}3\text{-}3\varepsilon^{H}$ (HS)	---	0	440	100[b]
$D14\text{-}3\text{-}3\varepsilon^{ex4}$	---	---	58	495	NA
$D14\text{-}3\text{-}3\varepsilon^{ex4}$	$hsD14\text{-}3\text{-}3\varepsilon^{L}$ (18)	---	57	582	2[c]
$D14\text{-}3\text{-}3\varepsilon^{ex4}$	$hsD14\text{-}3\text{-}3\varepsilon^{L}$ (RT)	---	39	577	33[c]
$D14\text{-}3\text{-}3\varepsilon^{ex4}$	$hsD14\text{-}3\text{-}3\varepsilon^{L}$ (HS)	---	39	427	33[c]
$D14\text{-}3\text{-}3\varepsilon^{ex4}$	$hsD14\text{-}3\text{-}3\varepsilon^{H}$ (18)	---	57	552	2[c]
$D14\text{-}3\text{-}3\varepsilon^{ex4}$	$hsD14\text{-}3\text{-}3\varepsilon^{H}$ (RT)	---	44	416	28[c]
$D14\text{-}3\text{-}3\varepsilon^{ex4}$	$hsD14\text{-}3\text{-}3\varepsilon^{H}$ (HS)	---	10	458	83[c]
$D14\text{-}3\text{-}3\varepsilon^{ex4}$	*UAS mycD14-3-3ε*^{L}	*TUB*	0	441	100[c]
$D14\text{-}3\text{-}3\varepsilon^{ex4}$	*UAS mycD14-3-3ε*^{H}	*TUB*	12	478	79[c]
$D14\text{-}3\text{-}3\varepsilon^{ex4}$	*UAS mycD14-3-3ε*^{L}	*Act5C*	7	502	88[c]
$D14\text{-}3\text{-}3\varepsilon^{ex4}$	*UAS mycD14-3-3ε*^{H}	*Act5C*	7	562	88[c]
$D14\text{-}3\text{-}3\varepsilon^{ex4}$	*UAS mycD14-3-3ε*^{L}	*C155*	0	680	100[c]
$D14\text{-}3\text{-}3\varepsilon^{ex4}$	*UAS mycD14-3-3ε*^{H}	*C155*	0	701	100[c]

HS: Three daily 20-minute heat shocks at 32°C through development to adulthood.
RT: Constant 20-22°C. 18: Constant 18°C. NA = not applicable.
a : number of total flies scored per cross.
b: 100 minus %Lethality divided by % lethality for $D14\text{-}3\text{-}3\varepsilon^{l(3)j2B10}/D14\text{-}3\text{-}3\varepsilon^{l(3)j2B10}$ (25%)
c: 100 minus %Lethality divided by % lethality for $D14\text{-}3\text{-}3\varepsilon^{ex4}/D14\text{-}3\text{-}3\varepsilon^{ex4}$ (58%)

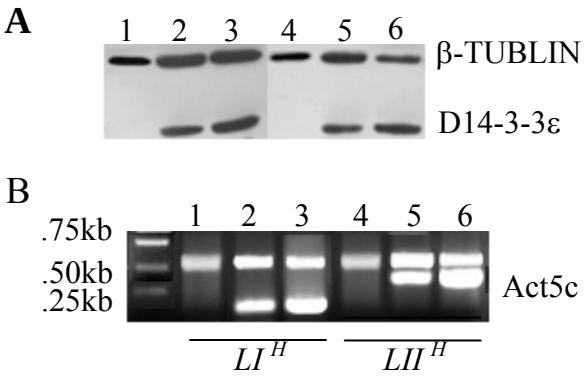

Figure 17. Western blot/RT-PCR analysis of level of D14-3-3ε or LEO expression with heat shock drivers

(A) To verify the level of D14-3-3ε produced by the *D14-3-3ε*^{L} and *D14-3-3ε*^{H} lysates prepared from *D14-3-3ε*^{ex4} homozygous adult flies, raised at 18°C (1,4), room temperature (RT) 22-23°C (2,5) or 25C with three daily 37°C heat shocks (3,6) were run on gels, blotted and probed with anti-tublin and anti-D14-3-3ε. Results indicate varying levels of expression that increase with heat shock induction.
(B) RT-PCR was used to verify the expression levels of LI or LII transgenes at 18°C (1,4), room temperature (RT) 22-23°C (2,5) or 25°C with three daily 37°C heat shocks (3,6) using Act5C as a loading control. Results indicate varying levels of expression that increase with heat shock induction.

expressed in order to rescue lethality (Table 7). Ubiquitous expression using a tubulin driver (TUB), or nervous system specific driver (elav-GAL4, C155) were both able to completely rescue D14-3-3ε mutant lethality (Table 7). However, expression of the UAS*mycD14-3-3ε* via an actin5C driver (ACT5C) was only able to partially rescue *D14-3-3ε* mutant lethality (Table 7). This consistent with the possibility that *D14-3-3ε* mutant lethality is due to functional deficits in the nervous system.

Rescue of D*14-3-3ε* lethality with LEO

To more closely examine whether and which of the two *leo* isoforms could rescue *D14-3-3ε* mutant lethality, the *leo*-bearing heat shock transgenes were raised at the different temperatures mentioned above (Table 8). The expression levels of *leoI (LI)* and *leoII (LII)* transgenes were examined using RT-PCR (Figure 17). It appears that low levels of LII expression were able to completely rescue, whereas high LI expression could only partially rescue the lethality of *D14-3-3ε* homozygotes (Figure 17 and Table 8). This suggests that the two LEO isoforms are not equivalent in their ability to compensate for the lack of D14-3-3ε. This data is consistent with LEO being partially redundant with D14-3-3ε in vital functions in the embryo and is consistent with the observed *leoII* up-regulation in *D14-3-3ε* mutants embryos. This compensation by LEOII may allow survival of some of the *D14-3-3ε* mutant homozygotes (Figure 16).

D14-3-3ε plays a role in wing cross-vein formation

Adult *D14-3-3ε*^{ex4} and *D14-3-3ε*$^{l(3)j2B10}$ homozygotes have smaller wings. Cell counts along the longitudinal veins of homozygous and heteroallelic adults indicated a 10% proportional reduction in length compared to control *D14-3-3ε*^{ex5} homozygotes. This may be the result of the overall reduction in size observed in null homozygous and heteroallelic embryos (Figure 14), larvae and adults (not shown). Lack of LEO in adult tissues (Philip et al., 2001) does not result in any wing malformation (Figure 18A and Table 8), however homozygous and heteroallelic *D14-3-3ε* mutant adults exhibit wing venation aberrations. The majority of adult *D14-3-3ε*^{ex4} and *D14-3-3ε*$^{l(3)j2B10}$ homozygotes exhibited a conspicuous lack, of the dorsal posterior cross-vein (>75%) and with lesser penetrance, malformation of the ventral anterior cross-vein (Figure 18A and Table 9).

Rescue of the *D14-3-3ε* mutant wing cross-vein aberrations

The defect maps to *D14-3-3ε* as all null alleles and heteroallelics with the *D14-3-3ε*^{ex24} deletion exhibit the phenotype despite its variable penetrance (Table 9). This phenotype can be rescued when heat shock transgenes expressing D14-3-3ε are placed in a homozygous null background (Figure 18B and Table 9). To examine if LEO may be able to partially compensate for the D14-3-3ε requirement in wing venation, LI and LII heat shock constructs were placde in the homozygous null D14-3-3ε mutant background. Constructs that express only high levels of LI were able to completely rescue the

Table 8. Rescue of *D14-3-3ε* mutant lethality with LEO

D14-3-3ε Allele	hs construct (Temperature)	% Lethality (Observed/Expected)	n[a]	% Rescue[b,c]
$D14\text{-}3\text{-}3\varepsilon^{l(3)j2B10}$	(18)	25	645	NA
$D14\text{-}3\text{-}3\varepsilon^{l(3)j2B10}$	(RT)	22	501	12[b]
$D14\text{-}3\text{-}3\varepsilon^{l(3)j2B10}$	(HS)	18	485	38[b]
$D14\text{-}3\text{-}3\varepsilon^{l(3)j2B10}$	LI^{L} (18)	24	462	4[b]
$D14\text{-}3\text{-}3\varepsilon^{l(3)j2B10}$	LI^{L} (RT)	16	455	46[b]
$D14\text{-}3\text{-}3\varepsilon^{l(3)j2B10}$	LI^{L} (HS)	12	524	52[b]
$D14\text{-}3\text{-}3\varepsilon^{l(3)j2B10}$	LII^{L} (18)	20	412	20[b]
$D14\text{-}3\text{-}3\varepsilon^{l(3)j2B10}$	LII^{L} (RT)	0	479	100[b]
$D14\text{-}3\text{-}3\varepsilon^{l(3)j2B10}$	LII^{L} (HS)	0	425	100[b]
$D14\text{-}3\text{-}3\varepsilon^{ex4}$	(18)	58	495	NA
$D14\text{-}3\text{-}3\varepsilon^{ex4}$	(RT)	51	470	13[c]
$D14\text{-}3\text{-}3\varepsilon^{ex4}$	(HS)	46	433	21[c]
$D14\text{-}3\text{-}3\varepsilon^{ex4}$	LI^{L} (18)	51	481	13[c]
$D14\text{-}3\text{-}3\varepsilon^{ex4}$	LI^{L} (RT)	44	440	24[c]
$D14\text{-}3\text{-}3\varepsilon^{ex4}$	LI^{L} (HS)	13	493	77[c]
$D14\text{-}3\text{-}3\varepsilon^{ex4}$	LI^{H} (18)	49	415	16[c]
$D14\text{-}3\text{-}3\varepsilon^{ex4}$	LI^{H} (RT)	39	429	33[c]
$D14\text{-}3\text{-}3\varepsilon^{ex4}$	LI^{H} (HS)	23	440	60[c]
$D14\text{-}3\text{-}3\varepsilon^{ex4}$	LII^{L} (18)	51	496	13[c]
$D14\text{-}3\text{-}3\varepsilon^{ex4}$	LII^{L} (RT)	24	481	59[c]
$D14\text{-}3\text{-}3\varepsilon^{ex4}$	LII^{L} (HS)	0	555	100[c]
$D14\text{-}3\text{-}3\varepsilon^{ex4}$	LII^{H} (18)	34	477	42[c]
$D14\text{-}3\text{-}3\varepsilon^{ex4}$	LII^{H} (RT)	0	464	100[c]
$D14\text{-}3\text{-}3\varepsilon^{ex4}$	LII^{H} (HS)	0	485	100[c]

HS: Three daily 20-minute heat shocks at 32°C through development to adulthood.
RT: Constant 20-22°C. 18: Constant 18°C.
a : number of total flies scored per cross. NA = not applicable.
b: 100 minus %Lethality divided by % lethality for $D14\text{-}3\text{-}3\varepsilon^{l(3)j2B10}/D14\text{-}3\text{-}3\varepsilon^{l(3)j2B10}$ (25%)
c: 100 minus %Lethality divided by % lethality for $D14\text{-}3\text{-}3\varepsilon^{ex4}/D14\text{-}3\text{-}3\varepsilon^{ex4}$ (58%)

malformations of the anterior cross-veins (Figure 18B and Table 9). Neither isoform of LEO was able to rescue the posterior cross-vein malformation, suggesting that these two isotypes are not redundant with respect to this cross-vein formation. In agreement with this result, in control wing disks, RT-PCR indicated that *leoI* is the only isoform present (Figure 19B). We used different GAL4 lines that expressed specifically in the developing wing disk to examine where D14-3-3ε expression was necessary for normal development. *wg-GAL4* was able to partially rescue the anterior cross-vein deficit, while *dpp-GAL4* was able to completely rescue when crossed to the strongly expressing *UAS mycD14-3-3ε*^{D} (Table 9 and Figure 18B). Therefore, it appears that D14-3-3ε is necessary in the *dpp* pattern of expression during the developing wing disk for proper anterior cross-vein formation. The fact that expression using the *dpp*-GAL4 driver can rescue the anterior cross-vein deficit and not posterior cross-vein deficit (Table 9), suggests there may be two different mechanisms for posterior and anterior cross-vein formation.

D14-3-3ε mutant wing disk

To investigate whether the malformations of the adult wings were detectable in the larval wing disk, *D14-3-3ε* ^{ex5} and *D14-3-3ε* ^{ex4} homozygous wing disks were challenged with the anti-LEO and anti-D14-3-3ε antibodies (Figure 19A). There is a high level of co-localization and with LEO which appeared ubiquitously in the developing wing disk, although *leo* null homozygous have no apparent wing defects. This suggested that co-localization is not the only requirement for LEO/D14-3-3ε

Table 9. Deficits of adult wing cross-veins in *D14-3-3ε* mutants

	14-3-3 Allele	hs / UAS	GAL4	Anterior cross-vein		Posterior cross-vein	
				% Malformed	% Rescue[a]	% Malformed	% Rescue[a]
1	$D14\text{-}3\text{-}3\varepsilon^{ex5}$	---	---	0	NA	0	NA
	leo^{P1188} (R)[b]	---	---	0	NA	0	NA
2	leo^{12X} (R) [c]	---	---	0	NA	0	NA
	$\frac{D14\text{-}3\text{-}3\varepsilon^{ex5}}{D14\text{-}3\text{-}3\varepsilon^{l(3)j2B10}}$	---	---	0	NA	0	NA
3	$D14\text{-}3\text{-}3\varepsilon^{l(3)j2B10}$	---	---	25	NA	75	NA
4	$\frac{D14\text{-}3\text{-}3\varepsilon^{l(3)j2B10}}{D14\text{-}3\text{-}3\varepsilon^{ex4}}$	---	---	26.7	NA	86.7	NA
	$\frac{D14\text{-}3\text{-}3\varepsilon^{l(3)j2B10}}{D14\text{-}3\text{-}3\varepsilon^{ex24}}$	---	---	25	NA	80	NA
	$\frac{D14\text{-}3\text{-}3\varepsilon^{ex5}}{D14\text{-}3\text{-}3\varepsilon^{ex24}}$	---	---	0	NA	0	NA
5	$D14\text{-}3\text{-}3\varepsilon^{ex4}$	---	---	42.9	NA	80.9	NA
6	$\frac{D14\text{-}3\text{-}3\varepsilon^{ex4}}{D14\text{-}3\text{-}3\varepsilon^{ex24}}$	---	---	64.3	NA	78.6	NA
	$D14\text{-}3\text{-}3\varepsilon^{ex4}$	$hsD14\text{-}3\text{-}3\varepsilon^{L}$	---	9.3	78.3	14	83
7	$D14\text{-}3\text{-}3\varepsilon^{ex4}$	$hsD14\text{-}3\text{-}3\varepsilon^{H}$	---	0	100	3.6	95.6
	$D14\text{-}3\text{-}3\varepsilon^{ex4}$	LI^{L}	---	29	32.4	72	11
8	$D14\text{-}3\text{-}3\varepsilon^{ex4}$	LI^{H}	---	0	100	60	25.8
	$D14\text{-}3\text{-}3\varepsilon^{ex4}$	LII^{L}	---	40	6.8	78.3	3.2
9	$D14\text{-}3\text{-}3\varepsilon^{ex4}$	LII^{H}	---	33	23	73	9.8
10	$D14\text{-}3\text{-}3\varepsilon^{ex4}$	$UAS\ mycD14\text{-}3\text{-}3\varepsilon^{L}$	*TUB*	3	93	1.5	98
	$D14\text{-}3\text{-}3\varepsilon^{ex4}$	$UAS\ mycD14\text{-}3\text{-}3\varepsilon^{H}$	*TUB*	1.4	96.7	4.3	95.7
11	$D14\text{-}3\text{-}3\varepsilon^{ex4}$	$UAS\ mycD14\text{-}3\text{-}3\varepsilon^{L}$	*Act5C*	4.7	89	11	86.4
	$D14\text{-}3\text{-}3\varepsilon^{ex4}$	$UAS\ mycD14\text{-}3\text{-}3\varepsilon^{H}$	*Act5C*	17.6	60	34	58
12	$D14\text{-}3\text{-}3\varepsilon^{ex4}$	$UAS\ mycD14\text{-}3\text{-}3\varepsilon^{L}$	*wg*	17	60.4	72	11
	$D14\text{-}3\text{-}3\varepsilon^{ex4}$	$UAS\ mycD14\text{-}3\text{-}3\varepsilon^{H}$	*wg*	33	23	100	0
13	$D14\text{-}3\text{-}3\varepsilon^{ex4}$	$UAS\ mycD14\text{-}3\text{-}3\varepsilon^{L}$	*dpp*	0	100	63	22
	$D14\text{-}3\text{-}3\varepsilon^{ex4}$	$UAS\ mycD14\text{-}3\text{-}3\varepsilon^{H}$	*dpp*	3.7	91.4	63	22

Numbers on the left correspond to genotypes in Figure 19. (n>40 wings) NA = not applicable.
a: 100 minus % malformed/missing divide by %malformed/missing for $D14\text{-}3\text{-}3\varepsilon^{ex4}/D14\text{-}3\text{-}3\varepsilon^{ex4}$
b, c: homozygotes rescued (R) from lethality

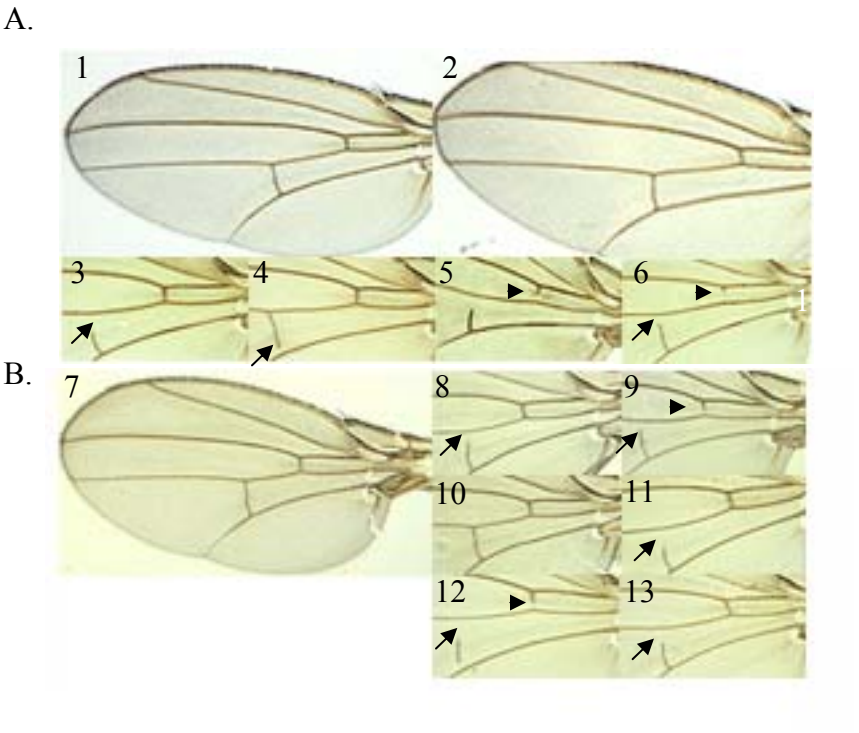

Figure 18. Abnormal cross-vein formation in *D14-3-3ε* mutant wings

3. Adult cross-vein phenotypes define three classes of aberrations in mutants compared to (1) *D14-3-3ε*^{ex5} homozygous controls and (2) homozygous null *leo*^{12X} adults rescued from lethality. Arrowheads indicate anterior cross-veins, while arrows indicate posterior cross-veins. The aberrations are characterized by missing or malformed anterior and posterior cross-veins are represented by (3) *D14-3-3ε*$^{l(3)j2B10}$ homozygotes, (4) *D14-3-3ε*^{ex4}/*D14-3-3ε*$^{l(3)j2B10}$, (5) *D14-3-3ε*^{ex4} homozygotes and (6) *D14-3-3ε*^{ex4}/*D14-3-3ε*^{ex24}. The adult wing aberrations are unique to *14-3-3ε* mutants and vary in penetrance.

4. Rescue of *D14-3-3ε*^{ex4} homozygotes missing or malformed cross-veins with three daily heat shocks of (7) *hsD14-3-3ε* ^{H} is able to completely rescue, whereas (8) *LI* ^{H} can only rescue anterior cross-vein deficit and (9) *LII* ^{H} is unable to rescue either deficit. General GAL4 transgenic lines (10) *tubP-GAL4* and (11) *act5C-GAL4* were able to rescue when crossed to *UAS mycD14-3-3ε*^{D}. GAL4 lines that expressed specifically in the developing wing disk *wg-GAL4* was only able to partially rescue the anterior cross-vein deficit, while *dpp-GAL4* was able to completely rescue when crossed to *UAS mycD14-3-3ε*^{D}. It appears that 14-3-3ε is necessary in the dpp pattern of expression during the developing wing disk for proper anterior cross-vein formation.

heterodimerization. Another potential explanation is that the proteins involved in this signaling pathway interact only with the D14-3-3ε homodimer, since neither LEO isoform can rescue the posterior cross-vein deficit the D14-3-3ε protein was present throughout the wing disks, but was particularly abundant along the distal edge of the disk (Figure 19A).

Although mutant disks did not exhibit gross anomalies, the characteristic folding pattern in the medial region was malformed, the folds were ill defined and appeared fused in the *D14-3-3ε*^{ex4} disks (Figure 19A). These wing disk folds are likely the tissues that give rise to the cross-veins which are malformed in the mutants. These results suggest that normal D14-3-3ε activity is required for proper cross-vein formation. In support of this conclusion, the transcription factor OMB is expressed in a pattern similar to that of D14-3-3ε, especially in these wing disk folds. Perturbation of this expression pattern results in complete absence or cross-vein malformation (Adachi-Yamada et al., 1999).

The results of this study expand the established functions of D14-3-3ε in photoreceptor development and timing of mitosis in post-blastoderm embryos (Chang and Rubin, 1997; Su et al., 2001). Roles in hatching and wing cross-vein formation have been elucidated by this analysis. Since both 14-3-3 proteins are maternally supplied in early embryos (Skoulakis and Davis, 1996; Broadie et al., 1997; Li et al., 1997; Tien et al., 1999; Philip et al., 2001; Su et al., 2001), I focused our analysis on late stage embryos and adults. In addition, our results revealed a novel compensatory over-accumulation of LEO upon loss of D14-3-3ε.

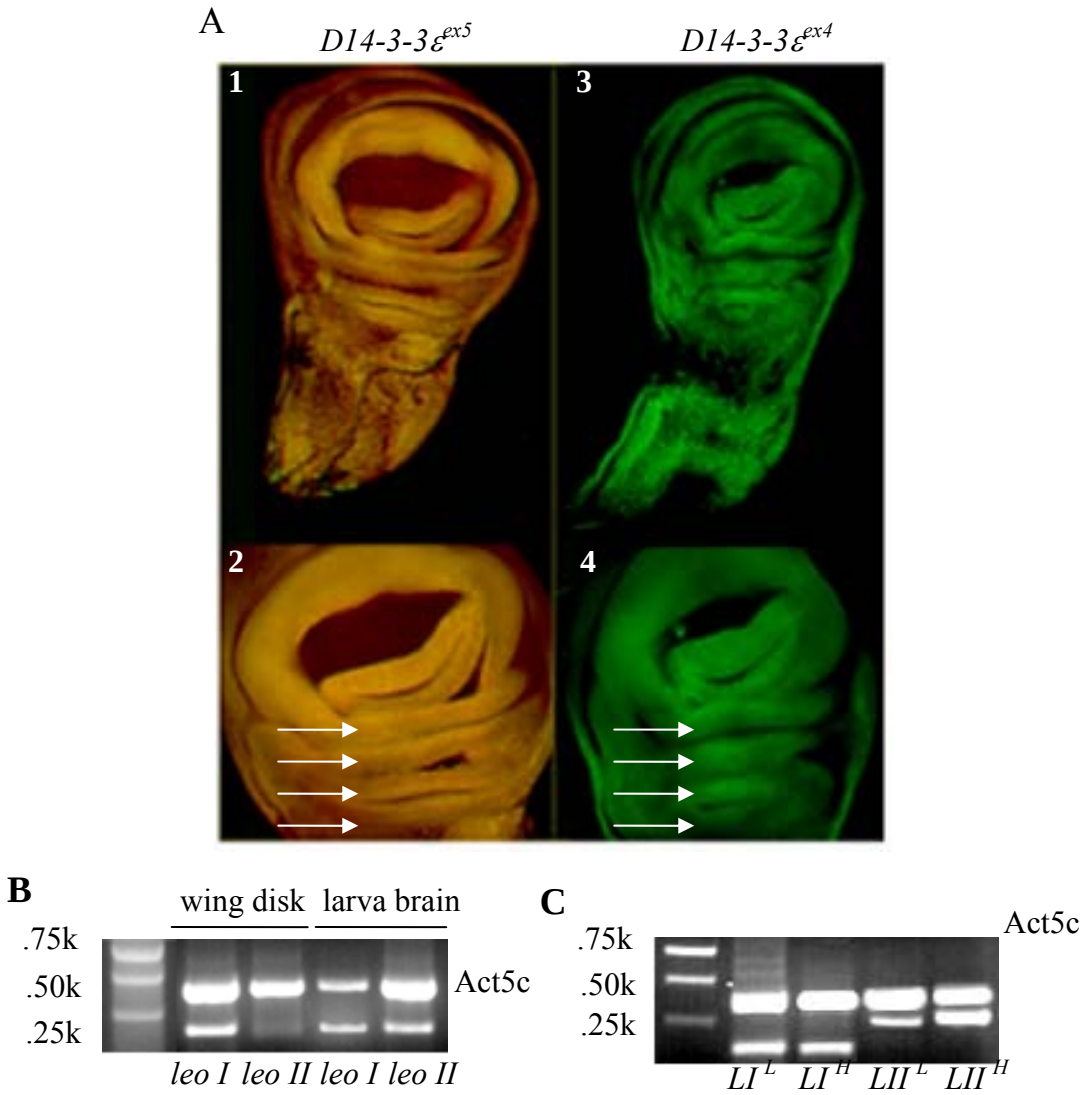

Figure 19. Expression pattern and malformations in wing disk in *D14-3-3ε* mutants

(A) Co-localization of LEO (green Alexa 488) and D14-3-3ε (red Alexa 594) in third instar larva wing disk. (1) Co-localization of LEO/D14-3-3ε in third instar larva wing disk, the arrows in 2 indicate the normal arrangement of the central folds and primary folds in control *D14-3-3ε*^{ex5} homozygotes. (2) Co-localization of LEO/D14-3-3ε in *D14-3-3ε*^{ex4} homozygotes, the arrows in 4 indicate the malformation in the central folds.
(B) RT-PCR to examine which *leo* isoform is normally present in third instar wing disk or larva brain. Using Act5C as a loading control, results indicate that only *leoI* is present in wing disk, whereas both *leoI* and *leoII* are present in the larva brain.
(C) RT-PCR to verify that hsleo transgene are being expressed in the wing during development. Using Act5C as loading control results indicate that both *LI* and *LII* transgenes are expressed in the wing disk.

DISCUSSION

The new excision alleles were instrumental in understanding the role of D14-3-3ε. Complementation data indicate that while *D14-3-3ε*^{ex4} and *D14-3-3ε*^{ex24} are null alleles, the *D14-3-3ε*$^{l(3)j2B10}$ appears a strong hypomorphic mutation despite the apparent lack of protein in our western analyses. This suggests occasional successful removal of the transposon in intron 1 by splicing and protein production, albeit below the detection limits of our western assays. Recovery of 75% of homozygous embryos as adults, suggested that the gene is dispensable for viability (Chang and Rubin, 1997). However, only about 40% of null homozygotes and heteroallelics yielded adults. In addition, recovery of these mutant homozygotes is likely due to the observed over-accumulation of LEO indicating that the gene is essential for viability.

The mechanism of over-accumulation of LEO in *D14-3-3ε* null embryos is unknown. I propose that this may be a manifestation of the known function of 14-3-3s in nuclear/cytoplasmic partition of transcription factors among other proteins (Muslin and Xing, 2000; Rittinger et al., 1999; Tzivion and Avruch, 2002). In this model, wild type D14-3-3ε modulates the level of *leoII* mRNA either by exclusion of transcription factors from the nucleus, or by keeping factors in an inactive conformation that are necessary for its transcription. The up-regulation of *leoII* compared to *leoI* may be due to the fact that one of the *leoII* transcripts has a unique promoter (Kockel et al., 1997). In either case, loss of D14-3-3ε in null embryos allows elevated transcription of *leoII* specifically. Therefore, LEO appears partially redundant with D14-3-3ε only when

expressed at high levels, and even then it is only LEOII that can compensate for the loss of D14-3-3ε. This is further supported by the observation that removal of one copy of *leo* eliminated recovery of *D14-3-3ε* null homozygotes (E. M. C. Skoulakis, unpublished observations and (Chang and Rubin, 1997)). Finally, despite its reported abundance (Skoulakis and Davis, 1996; Skoulakis and Davis, 1998), LEO does not appear in excess relative to its potential binding sites, because a large increase was necessary for *D14-3-3ε* null embryos to survive.

The over-accumulation of LEO if *D14-3-3ε* null embryos may be the reason they progress normally through development. However, a significant number of null mutant embryos die, likely due to neuronal or musculature deficits that do not allow hatching. This is consistent with the preferential distribution of the protein in the CNS and PNS of late embryos (Tien et al., 1999) and suggests a requirement for D14-3-3ε in nervous system function. Interestingly, post-embryonic developmental processes did not appear to require D14-3-3ε, as successfully hatched null embryos yielded phenotypically normal adults except for the wing-vein aberrations and their smaller size. These adults did not harbor elevated levels of LEO in the head or other tissues.

This analysis established novel roles for D14-3-3ε in wing cross-vein development. Clearly, D14-3-3ε homodimers, or monomers are required for wing cross-vein formation since the process is not disrupted in *leo* mutants and all *D14-3-3ε* null combinations exhibit the defect. These mutations are consistent with the loss of wing veins upon inhibition of Ras signaling in the wing disk (Prober and Edgar, 2000) for three reasons. First, *D14-3-3ε* mutants were isolated as dominant suppressors of

activated Ras (Karim et al., 1996) and secondly, they are known to regulate Ras signaling through their interactions with Raf (Morrison, 1994; Michaud et al. 1995; Morrison and Cutler, 1997). The third reason is that if mutant activated Ras1 is expressed using *dpp*-GAL4, it specifically affects anterior cross-vein formation producing similar aberrations to that seen in *D14-3-3ε* mutants. Interestingly these are aberrations that can be completely rescued by expressing UAS *mycD14-3-3ε* transgenes with the *dpp*-GAL4 driver.

Patterning of the wing blade largely depends on DPP signaling (Martin-Blanco, 2000; Raftery and Sutherland, 1999) and it is likely to involve the *Drosophila* homolog of the p38 MAPK (Adachi-Yamada et al.,1999). Given the positive regulation of the TGFβ type I receptor by 14-3-3ε in human cells (McGonigle et al., 2001; McGonigle et al., 2002), it is possible that the *Drosophila* protein plays a similar role in wing blade patterning. Interestingly despite the elevated accumulation of D14-3-3ε in the posterior distal wing disk, no additional malformations were observed. This indicates either that despite its accumulation D14-3-3ε activity is not required there, or a redundant activity compensates for it in the morphogenesis of this tissue.

LEO accumulates ubiquitously in the developing wing disk, although *leo* null homozygotes have no apparent wing defects. However, only *leoI* is present in wild type wing disks; therefore, maybe its is the only *leo* isoform capable interacting with target proteins that recognize D14-3-3ε within the wing disk. In agreement, only the *LI* transgenes were able to functionally compensate for the loss of D14-3-3ε in anterior cross-vein formation. The fact that only the anterior cross-vein deficit can be rescued is

consistent with the conclusion that there are two different mechanisms for anterior and posterior cross-vein formation.

In summary, our results indicate that there are 14-3-3 isotype-specific functions and the dynamic interactions among them are necessary in multiple tissues and processes necessary for normal development in *Drosophila*. This analysis demonstrated that co-localization is not the only requirement for hetero-dimerization. Since LEO has two isoforms that differ by only six amino acids it may not be surprising that they exhibit such specific temporal and tissue distributions (Philip et al., 2001). It is surprising that they exhibit such differential ability to functional compensate for D14-3-3ε mutations, suggesting specificity not only in hetero-dimerization with D14-3-3ε, but potentially in target binding specificity as well.

EXPERIMENTAL PROCEDURES

Drosophila culture and strains

The *Drosophila* were cultured in standard cornmeal sugar food supplemented with soy flour and $CaCl_2$ at 20-22^{o}C. The $D14\text{-}3\text{-}3\varepsilon^{l(3)j2B10}$ mutant allele has been described previously [Chang, 1997 #278]. Alleles $D14\text{-}3\text{-}3\varepsilon^{ex5}$, $D14\text{-}3\text{-}3\varepsilon^{ex4}$ and $D14\text{-}3\text{-}3\varepsilon^{ex24}$ generated by mobilization of the transposon in $D14\text{-}3\text{-}3\varepsilon^{l(3)j2B10}$ were a kind gift of Dr. Henry Chang. The genetic background of these alleles was normalized to that of Cantonized w^{1118} using balancer chromosomes in a Cantonized w^{1118} background. Allelism was assessed by complementation tests. Homozygotes for the lethal null leo^{12X}

and *leo*^{P1188} alleles Broadie et al., 1997) were obtained by heat shock induction of a *leo* transgene as described by Philip et al (2001) (Philip et al., 2001). Briefly, *leo*^{12X} /CyO; hsLEOI and *leo*^{P1188} /CyO; hsLEOI virgin females raised under three daily induction's of the transgene were mated with their brothers and progeny was allowed to develop at 22-23^{0}C. This protocol yields adults harboring less than 10% of normal LEONARDO protein (Philip et al., 2001). Complementation tests for viability were performed by crossing parents of the appropriate genotypes *en masse* and scoring the progeny of multiple such crosses per genotype. Complementation for the wing vein phenotype was assessed similarly. Sterility of homozygous, or heteroallelic mutants was assessed by placing single mutant males or females with a minimum of three *w*^{1118} individuals of the opposite sex. For a 2-week period the food vials were investigated for the presence of larvae. Presence of a single larva signified a fertile subject. To determine the lethal phase of null homozygotes, embryos were collected from *D14-3-3ε*$^{l(3)j2B10}$*/TM3SerGFP* and *D14-3-3ε*^{ex4}*/TM3SerGFP* flies and manually separated into GFP fluorescence-negative (homozygous mutant) and GFP fluorescence-positive. After hatching, they were monitored in separate food vials until emergence of adult flies at which time their genotype was verified again based on adult visible markers.

Immunohistochemistry

Embryos were collected on apple juice plates. To obtain homozygous embryos, 12-16 hr GFP fluorescence-negative embryos were hand selected from eggs laid by *D14-3-3ε*$^{l(3)j2B10}$*/TM3SerGFP* and *D14-3-3ε*$^{l(3)j2B10}$*/TM3SerGFP* parents. Sibling GFP

fluorescence-positive embryos or larva were selected as controls based on their less intense fluorescence and apparent normal appearance in contrast to the abnormal appearance and intense fluorescence of *TM3SerGFP* homozygotes. Embryos were dechorionated and fixed in 43.2 mM Hepes, 0.96 mM MgSO4, 0.48 mM EGTA, pH 6.9, 1.6% formaldehyde in 59% heptane, followed by rinses in methanol, 5% EGTA. The embryos were rehydrated to BBT (140 mM NaCl, 2.7 mM KCl, 4.3 mM Na_2HPO_4, 1.4 mM KH_2PO_4, pH 7.3, 0.1% Tween-20, 1%, Bovine Serum Albumin) and blocked for 1 hr in BBT-250 (BBT, 250 mM NaCl), 10% normal goat serum. Incubation with primary antibodies in 5% normal goat serum BBT-250 was as follows: chicken anti-D14-3-3ε (1:3,000), mouse mAb-22c10 (1:2,000) (Developmental Hybridoma Studies Bank, University of Iowa, Iowa City, IA), mouse anti-engrailed (1:5 Developmental Hybridoma Studies Bank, University of Iowa, Iowa City, IA), mouse anti-HRP (1:500 Developmental Hybridoma Studies Bank, University of Iowa, Iowa City, IA). Secondary antibodies anti-mouse HRP (1:2,000). Images were captured on a Ziess Axiovert 35 microscope using a 20X objective lens. Third instar larval wing disks were dissected in PBS (150 mM NaCl, 2.7 mM KCl, 4.3 mM Na_2HPO_4, 1.4 mM KH_2PO_4, pH 7.3), fixed with 1% gluderaldehyde (Sigma, St. Louis, MO), washed with PBST (PBS with 0.1% Triton X-100) and blocked with 10% normal donkey serum. Anti-LEO (1:50,000) and anti-D14-3-3ε (1:30,000) in 5% normal donkey serum in PBST was followed with Alexa anti-rabbit 488 (1:2,000) and Alexa anti-chicken 594 then mounted in Dako anti-fluorescent medium (Carpinteria, CA). Images were captured on a Ziess

Axiovert 135 microscope with an Atto Carv confocal module (Nipkow spinning disk) using a 25X objective lens.

Western blot analysis

To obtain extracts from homozygous embryos, 12-16 hr GFP fluorescence-negative embryos were hand selected from eggs laid by *D14-3-3ε$^{l(3)j2B10}$/TM3SerGFP* and *D14-3-3ε$^{l(3)j2B10}$/TM3SerGFP* parents. Sibling GFP fluorescence-positive embryos were selected as controls based on their less intense fluorescence and apparent normal appearance in contrast to the abnormal appearance and intense fluorescence of *TM3SerGFP* homozygotes. The fidelity of the embryonic genotype based on the above criteria was verified on similarly selected embryos by immunohistochemistry. Single whole flies or embryo equivalent to three fly heads per lane from control and mutant animals were homogenized in 10μl of modified radioimmunoprecipitation assay (RIPA) buffer as previously described (Philip et al., 2001). Extracts were then run on 18% acrylamide gels. Blots were probed at room temperature for 1 hour with rabbit anti-LEONARDO (1:40,000), or for 4 hours with chicken anti-D14-3-3ε (1:5000) or mouse anti-Cmyc (1:200 Developmental Hybridoma Studies Bank, University of Iowa, Iowa City, IA) and a 1:300 dilution of mouse anti-tublin (Developmental Hybridoma Studies Bank, University of Iowa, Iowa City, IA). Secondary antibodies were used 1:15,000 for anti-rabbit HRP, 1:5,000 for anti-chicken HRP, 1:5000 for anti-mouse HRP and the results were visualized with enhanced chemiluminescense (Pierce). The results of three

independent experiments utilizing different extract preparations were quantified densitometrically and analyzed statistically.

RT-PCR analysis

Twenty head equivalents of hand selected embryo's or larva wing disk samples were prepared and RT-PCR reactions conditions with *leoI, leo II* and *D14-3-3ε* primers were performed as previously described (Philips et al., 2001). As an internal control primers *Act5C* forward (GATGACCCAGATCATGTTCG) and *Act5C* reverse (GGTGATCTCCTTGTGCATAC) were used to quantify the relative amount of RNA in each sample. To identify *hsleo I (LI)*, the *leo I* forward primer was used with *SV40* specific reverse primer and for *hsleo II (LII)*, the *leo II* forward primer was used with a *Hsp70* specific reverse primer.

Quantitative PCR

To perform the one-step RT-PCR reaction described by Applied Biosystems, 25 µl of SYBR green PCR master mix, 0.25 µl Taqman reverse transcriptase, 0.50 µl RNAse inhibitor, 120nm of each primer were used in each 50µl reaction. 1ng, 0.40ng and 0.10ng of each type of RNA was used to establish a standard curve. Specific *leoI* and *leoII* forward primers were combined with a common *leo* reverse primer. As the comparative control, *RP49* forward (GATCGTGAAGAAGCGCAC) and *RP49* reverse (CGCTCGACAATCTCCTGG) primers were used. Samples were run on ABI Prism 7700 Sequence Detection system (Applied Biosystems), the thermal cycling conditions

were 48° for 30min, 95° for 10min, 40 cycles of 95° 15sec and 58° for 1min. A melting curve was analyzed for each sample to verify specificity. The comparative Ct method described by Applied Biosystems was used to analysis the results of three independent experiments.

Wing mounting

Adult flies were dissected in 95% ethanol. Wings were placed in Xylene for 10 minutes, washed twice with ethanol and mounted in Canada balsam (C-1795, Sigma, St. Louis, MO). Images were captured on a Ziess Axiovert 35 microscope using a 20X objective lens.

Statistical analysis

Untransformed data from densitometric quantification of protein amounts and the results of all cell counting experiments, complementation tests and Q-PCR results were analyzed using the JMP3.1 statistical software package (SAS Institute, Cary, NC). Following initial ANOVA, the data were analyzed by planned comparisons to a control (Dunnett's test) or Tukey–Kramer tests.

CHAPTER III

14-3-3 PROTEINS ARE ESSENTIAL FOR POLE CELL SURVIVAL IN *DROSOPHILA MELANOGASTER*

INTRODUCTION

To date, 14-3-3 proteins have been identified in all eukaryotes examined and comprise a highly conserved family of small 28-32kD acidic molecules. 14-3-3s share a common structure composed of nine anti-parallel α-helices that form a U-shaped palisade around a central negatively charged groove of largely invariant amino acids. Apparently all 14-3-3s are capable of homo- and hetero-dimer formation by interaction of hydrophobic residues in helix 1 of one monomer with similar residues in helixes 3 and 4 of another (Skoulakis and Davis, 1998; Fu et al., 2000; Tzivion and Avruch, 2002). A phosphoprotein binding surface formed by conserved amino acids in the negatively charged groove interacts with target proteins that contain the motifs RSxpS/TxP, or RxxxpS/TxP (where x=any amino acid, pS/T=phosphoserine or phosphothreonine) (Muslin and Xing, 2000; Tzivion and Avruch, 2002).

The effects of 14-3-3 binding on target proteins can be classified in three main categories: 1) modulation of enzymatic activities, 2) phosphoserine binding adapter molecules mediating protein-protein interactions, 3) regulators of the subcellular localization of proteins (Skoulakis and Davis, 1998; Fu et al., 2000; Muslin and Xing,

2000; van Hemert et al., 2001). In accord with their apparent multi-functionality, though highly abundant in vertebrate brains (up to 1% of soluble brain proteins), these proteins are present, albeit at lower levels in most vertebrate tissues examined (Aitken, 1995). One of the major questions in relation to these diverse roles is whether homo-dimers of the various isotypes and hetero-dimers with other co-expressed 14-3-3s are functionally unique or redundant. The widespread tissue and temporal distribution of 14-3-3s and their extensive co-expression in complex overlapping patterns (Skoulakis and Davis, 1998; Baxter et al., 2002) is consistent with both hypotheses. To approach this question then, the contribution of each isotype in a particular function has to be investigated.

Unlike vertebrates that harbor seven 14-3-3 genes with largely overlapping expression profiles, *Drosophila* have only two, *leonardo* encoding two 14-3-3ζ isoforms (81% identity with the vertebrate isoform) and *D14-3-3ε (*83% identity with the vertebrate cognate) (Skoulakis and Davis, 1998; Fu et al., 2000; Philip et al., 2001). Despite the simplicity of *Drosophila*, multiple *in vivo* roles for 14-3-3s have been described through the isolation and characterization of mutants in the two 14-3-3 genes. The two *Drosophila* isotypes are involved in embryonic development (Chang and Rubin, 1997; Li et al., 1997; Su et al., 2001), eye neuronal specification (Chang and Rubin, 1997; Kockel et al., 1997; Rommel et al., 1997), behavioral and physiological neuroplasticity (Skoulakis and Davis, 1996; Broadie et al., 1997; Philip et al., 2001) and recently in oocyte determination and A-P polarization (Benton et al., 2001). Both 14-3-3 proteins appear to regulate activity of the kinase Raf in embryonic development and eye neuronal determination (Chang and Rubin, 1997; Kockel et al., 1997; Skoulakis and

Davis, 1998) and their roles may be redundant. However, during early syncytial embryonic divisions, the two proteins appear to have unique roles (Su et al., 2001). Partial functional redundancy of the two 14-3-3 isotypes was observed in their interaction with the PAR-5 kinase in oocyte determination and polarization (Benton et al., 2001). In order to understand the functional specificity of 14-3-3 proteins that may underlie these differences, it is necessary to establish the different tissue and temporal roles of each isotype.

Development of the germ line in *Drosophila* starts with the precocious cellularization of 8-10 nuclei at the posterior of the otherwise syncytial embryo. Some of these cells do not divide further, while others undergo 1-2 rounds non-synchronous divisions to yield 35-40 pole cells by stage 5 (Sonnenblick, 1950; Williamson and Lehman, 1996). At this stage pole cells become mitotically arrested in cell cycle phase G_2 (Su et al., 1998). Pole cells migrate into the posterior midgut pocket at the completion of germ band extension on stage 10 of embryogenesis and then transit this epithelium and become incorporated in the developing gonad by stage 15 (Williamson and Lehman, 1996). Cells that remain outside the gonad at this stage die, suggesting that mechanisms regulating germ cell survival must exist (Sonnenblick, 1950; Williamson and Lehman, 1996; Coffman et al., 2002). In addition, only about 50% of the early pole cells survive to complete migration, suggesting that programmed cell death mechanisms must be present within them (Sonnenblick, 1950; Williamson and Lehman, 1996). However, the mechanisms that regulate pole cell migration and survival are largely

unknown, since only a couple of genes specifically affecting these processes were identified recently (Coffman et al., 2002).

Since we are interested in the roles and functional specificity of 14-3-3s in *Drosophila*, we investigated the causes of male and female sterility of *D14-3-3ε* and *leonardo* mutant animals. Since such females lay very few eggs, we focused on the germ-line in these mutants. Our results demonstrate that both 14-3-3 proteins are present in pole cells and appear to play essential roles in their survival, but not in their divisions or migration.

RESULTS AND DISCUSSION

D14-3-3ε alleles utilized

To avoid potential complications due to allele-specific phenotypes of the known point mutations (Chang and Rubin, 1997), we characterized three novel alleles generated by mobilization of the transposon in P-element insertion allele D14-3-3ε $^{l(3)j2B10}$ in a normalized genetic background. Southern analysis (not shown) demonstrated that the D14-3-3ε genomic region in D14-3-3ε^{ex5} appeared identical to the w^{1118} and ry^{506} isogenic strains consistent with precise excision of the transposon in D14-3-3ε $^{l(3)j2B10}$ (Figure 20A). In contrast, allele D14-3-3ε^{ex24} harbors a large deletion (>10 kb) that encompasses the entire D14-3-3ε coding region and likely neighboring transcription units (Figure 20A). D14-3-3ε^{ex4} is a smaller deletion confined within the BamHI

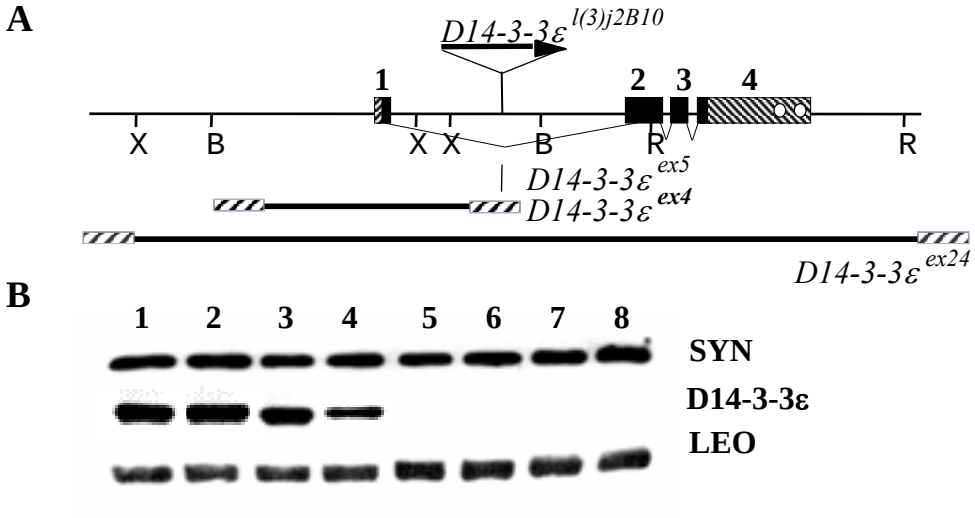

Figure 20. Mutations in the *D14-3-3ε* gene and their effects on protein accumulation

(A) The genomic region and mutations of the *D14-3-3ε* gene. Exons are represented by boxes, introns and surrounding non-transcribed regions by lines. The untranslated portions of exons are indicated by the striped boxes with the open circles in exon 4 representing the polyadenylation sites. The P-element insertion in intron 1 is indicated by the arrow, deleted DNA in $D14\text{-}3\text{-}3\varepsilon^{ex4}$ and $D14\text{-}3\text{-}3\varepsilon^{ex24}$ is indicated by the black bars. The hatched bars represent regions of uncertainty at the ends of the deficiencies. A perpendicular line indicates the precise excision of the 1(3)j2B10 in the reverent allele $D14\text{-}3\text{-}3\varepsilon^{ex5}$. X: Xba I, B: BamHI, R: EcoRI. (Adapted from Chang and Rubin, 1997).
(B) Mutant homozygotes and heteroallelic combinations yield adult animals lacking D14-3-3ε protein. Semi-quantitative western blot analysis of whole animal lysates of the following genotypes: (1) $D14\text{-}3\text{-}3\varepsilon^{ex5}$ homozygotes, (2) $D14\text{-}3\text{-}3\varepsilon^{ex5}/\ D14\text{-}3\text{-}3\varepsilon^{l(3)j2B10}$, (3) $D14\text{-}3\text{-}3\varepsilon^{ex5}/\ D14\text{-}3\text{-}3\varepsilon^{ex4}$, (4) $D14\text{-}3\text{-}3\varepsilon^{ex5}/\ D14\text{-}3\text{-}3\varepsilon^{ex24}$, (5) $D14\text{-}3\text{-}3\varepsilon^{l(3)j2B10}\ D14\text{-}3\text{-}3\varepsilon^{l(3)j2B10}$, (6) $D14\text{-}3\text{-}3\varepsilon^{l(3)j2B10}/\ D14\text{-}3\text{-}3\varepsilon^{ex4}$, (7) $D14\text{-}3\text{-}3\varepsilon^{ex4}/\ D14\text{-}3\text{-}3\varepsilon^{ex4}$ and (8) $D14\text{-}3\text{-}3\varepsilon/\ D14\text{-}3\text{-}3\varepsilon^{ex24}$.

fragment flanking the j2B10 transposon, which removes exon 1 of the gene. Therefore, both *D14-3-3ε^{ex4}* and *D14-3-3ε^{ex24}* alleles are predicted to be null and in fact, whereas there is normal D14-3-3ε protein accumulation in D14-3-3ε ^{ex5} homozygotes, the D14-3-3ε ^{ex4} and D14-3-3ε ^{ex24}alleles do not yield detectable protein (Figure 20B). Since allele D14-3-3ε^{ex24} extends beyond the D14-3-3ε gene, we did not include it in any subsequent analyses. Significantly, the D14-3-3ε $^{l(3)j2B10}$ allele appeared to be a protein null despite its modest phenotypes.

D14-3-3ζ alleles utilised

leo alleles utilised in this analysis have been described previously and are shown schematically in Figure 21A. *leo^{P1188}* and *leo^{P1375}* are a strong and weak respectively lethal transposon insertion alleles (Skoulakis and Davis, 1996; Li et al., 1997). The complex deletion/rearrangement allele *leo^{12X}* is a protein null (Broadie et al., 1997). Furthermore, two different methods (protocols A and B), have been described that yield viable homozygotes for lethal *leo* mutations by transgenic rescue (Philip et al., 2001). Newly eclosed rescued animals and homozygous escapers for the weak *leo^{P1375}* allele harbour drastically reduced levels of LEO protein (Figure 21B). In fact, *leo^{P1375}/leo^{12X}*; *hsleoI* rescued adults were nearly devoid of LEO, whereas homozygous escapers for the weak insertion allele *leo^{P1375}* harboured ≤ 10% of the protein previously reported for rescued *leo^{P1188}/leo^{P1188}*; *hsleoI* homozygotes (Figure 21B and Philip et al., 2001). Therefore, animals that lack D14-3-3ε, or are nearly devoid of LEO can be obtained and they were used in the analyses below. Doubly mutant adults lacking both D14-3-3ε and

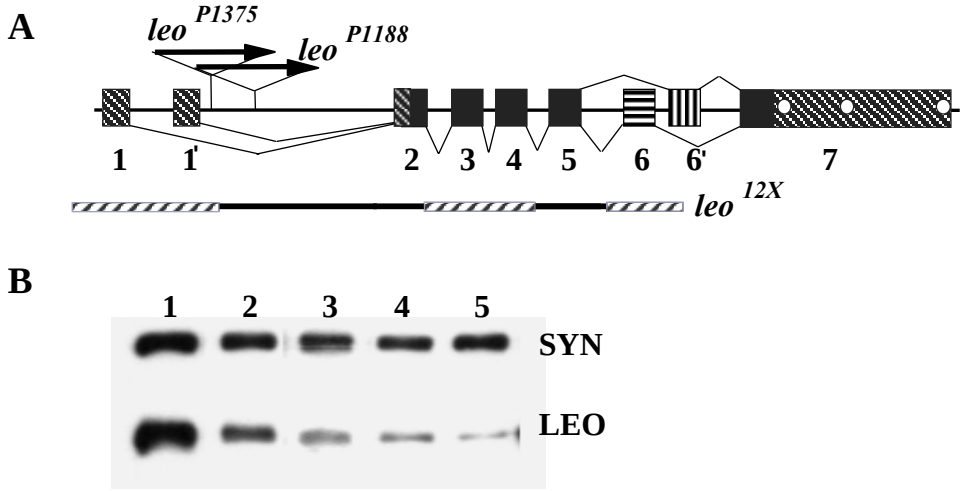

Figure 21. Mutations in the *D14-3-3ζ* gene and their effects on protein accumulation

(A) Structure and mutations of the *D14-3-3ζ* (*leonardo*) gene. Boxes represent exons, lines represent introns and surrounding non-transcribed regions and stippled boxes indicate untranslated portions of exons. The alternatively spliced exons 6 and 6' giving rise to *leoI* and *leoII* mRNAs respectively (Philip et al., 2001), are indicated by the striped boxes. The white circles in exon 7 represent polyadenylation sites. The arrows indicate the P-element insertions in intron 2. The complex deletion/re-arrangement allele leo^{12X} is indicated by the black bar and includes internal and terminal regions of uncertainty (hatched bars). (Adapted from Skoulakis and Davis,, 1996, Philip et al., 2001).

(B) Semi-quantitative Western blot analysis of whole animal lysates of the following genotypes: (1) w^{1118}, (2) leo^{P1375}/leo^{P1375}; *hsleoI* (*LI*) adults rescued from lethality with protocol B (R^B), (3) leo^{P1188}/leo^{P1188}; *LI* (R^B), (4) leo^{P1375}/leo^{P1375} homozygous escapers and (5) leo^{P1375}/leo^{12X}; *LI* adults (R^B).

LEO cannot be obtained, as they are lethal in early embryonic stages (Chang and Rubin, 1997; Skoulakis, unpublished observations).

D14-3-3s are essential for fertility

In agreement with a prior report (Chang and Rubin, 1997), homozygous loss of function *D14-3-3ε* mutant adults exhibited recessive male and female sterility. Few eggs were laid by homozygous mutant females and these failed to hatch likely due to the described defects in oocyte determination (Benton et al., 2001). Similar sterility was observed for *leo* mutant homozygotes and allelic combinations that harbour less than 10% of normal LEO protein (Philip and Skoulakis, unpublished observations). To determine whether these deficits map to the *D14-3-3ε* and *leo* genes, we performed complementation analysis. Male and female individuals harbouring the $D14\text{-}3\text{-}3\varepsilon^{ex5}$ revertant allele were indistinguishable from the w^{1118} control strains and exhibited 100% fertility. In contrast, all mutant homozygotes and heteroallelics were fully sterile (Table 10). The effect is recessive, since all animals heterozygous for the mutant alleles were fertile.

Similarly, the rare escapers homozygous or heteroallelic with the weak leo^{P1375} lethal allele were sterile (Table 10). leo^{P1188} homozygotes or $leo^{P1375}/\ leo^{12X}$ heteroallelics rescued from lethality by maternal *leoI* transgene expression (see experimental procedures and (Philip et al., 2001) were similarly sterile. Partial sterility was observed with rescued leo^{P1375} homozygotes (Table 10) likely because this is not a null allele (Skoulakis and Davis, 1996) and the observed perdurance of the transgenic

Table 10. Sterility of homozygous and heteroallelic *D14-3-3ε* and *leonardo* mutants

Genotype	Female		Male	
	n	% Fertile[a]	n	% Fertile[a]
$D14\text{-}3\text{-}3\varepsilon^{ex5}/D14\text{-}3\text{-}3\varepsilon^{ex5}$	20	100	20	100
$D14\text{-}3\text{-}3\varepsilon^{l(3)j2B10}/D14\text{-}3\text{-}3\varepsilon^{ex5}$	20	100	20	100
$D14\text{-}3\text{-}3\varepsilon^{l(3)j2B10}/D14\text{-}3\text{-}3\varepsilon^{l(3)j2B10}$	30	0	27	0
$D14\text{-}3\text{-}3\varepsilon^{l(3)j2B10}/D14\text{-}3\text{-}3\varepsilon^{ex4}$	30	0	25	0
$D14\text{-}3\text{-}3\varepsilon^{l(3)j2B10}/D14\text{-}3\text{-}3\varepsilon^{ex24}$	23	0	21	0
$D14\text{-}3\text{-}3\varepsilon^{ex4}/D14\text{-}3\text{-}3\varepsilon^{ex5}$	18	100	18	100
$D14\text{-}3\text{-}3\varepsilon^{ex4}/D14\text{-}3\text{-}3\varepsilon^{ex4}$	25	0	26	0
$D14\text{-}3\text{-}3\varepsilon^{ex4}/D14\text{-}3\text{-}3\varepsilon^{ex24}$	21	0	18	0
w^{1118}	25	100	25	100
leo^{P1375}/leo^{P1375}	58	0	38	0
leo^{P1375}/leo^{P1188}	31	0	8	0
leo^{P1375}/leo^{12X}; *hsleoI* (R^B)	26	0	28	0
leo^{P1375}/leo^{P1375}; *hsleoI* (R^B)	46	13	35	17
leo^{P1188}/leo^{P1188}; *hsleoI* (R^B)	38	0	28	0

[a] The number of single crosses that yielded larvae over the total number of animals crossed per genotype. Strains used as controls ($D14\text{-}3\text{-}3\varepsilon^{ex5}$ for *D14-3-3ε* mutants and w^{1118} for *leo*) have the same genetic background as the mutants.

n = number single pair matings

R^B: Lethal homozygotes rescued from lethality with protocol B as indicated in experimental procedures.

protein (Philip et al., 2001). This is reflected in the higher level of LEO in these animals in relation to that in *leo*^{P1188} rescued animals or *leo*^{P1375} escapers (Figure 21B). It appears then that adults lacking *D14-3-3ε*, or harbouring less than 10% LEO are sterile. These mutant animals were observed mating and devoid of gross morphological aberrations of their genitalia. Since all mutations reside in normalised genetic backgrounds, the observed sterility likely maps genetically to the 14-3-3 genes and not to other associated mutations that cause sterility. Therefore, the results suggest roles for both 14-3-3 proteins in physiological or developmental processes requisite for fertility. It should be noted that since fertility or levels of 14-3-3s are not different between *D14-3-3ε*^{ex5} and *w*^{1118}, with which all mutants tested herein share genetic backgrounds, the former strain was used as control in all subsequent experiments.

Transgenic rescue of sterility in *14-3-3* mutants

To unequivocally demonstrate that the observed sterility is indeed associated with mutations in the two *14-3-3* genes, we attempted transgenic rescue of the phenotype. Transgenic lines that carried either inducible, heat shock-driven (hs) *D14-3-3ε* or myc-tagged UAS-*D14-3-3ε* transgenes were introduced into *D14-3-3ε* mutant backgrounds. Similarly, the *hsleoI* (*LI*) transgenes introduced into *leo* mutant backgrounds were employed under different induction protocols as reported before (Philip et al., 2001) and detailed in experimental procedures. The *hsleoII* (*LII*) transgenic lines were excluded from this analysis though tested in preliminary tests,

because they did not rescue lethality. This is consistent with previous results suggesting that LEOII is apparently not involved in developmental processes (Philip et al., 2001). Highly expressed *D14-3-3ε* transgenes rescued conditionally the sterility of $D14\text{-}3\text{-}3\varepsilon^{ex4}$ homozygotes, while the apparent basal rescue (no HS) was likely due to position effect-dependent "leakiness" of the heat shock promoter (Table 11). Partial rescue was obtained with transgenes of apparently lower expression level ($hsD14\text{-}3\text{-}3\varepsilon^{L}$). In congruence, basal rescue was not observed with these transgenes. Similarly, complete rescue was obtained with UAS-*D14-3-3ε* transgenes driven with GAL4 (Brand and Perrimon 1993) under the direction of the beta tubulin promoter (*tub-GAL4)*, but not the cytoplasmic actin 5C promoter (*act5C-GAL4*). Again, complete rescue was obtained with highly expressed transgenes ($UAS\text{-}mycD14\text{-}3\text{-}3\varepsilon^{D}$). Identical rescue results were obtained with $D14\text{-}3\text{-}3\varepsilon^{j2B10}$ homozygotes (data not shown).

Both *tub* and *act5C* GAL4 drivers were able to direct equivalent transgene expression (Figure 22A), indicating that the reason for the failure to rescue under *act5C-GAL4* was not the result of decreased expression. In addition, this experiment confirmed that the $UAS\text{-}mycD14\text{-}3\text{-}3\varepsilon^{L}$ transgenes express at lower levels as suggested by the data in Table 11. To investigate whether both *tub-GAL4* and *act5C-GAL4* can drive expression in pole cells, we crossed these driver lines to *UAS-GFP* transgenic animals and stained the progeny with both anti-GFP and the pole cell-specific anti-VASA antibody (Hay et al., 1988). Figure 22B demonstrates that whereas *tub-GAL4* can drive GFP expression (and thus *UAS-mycD14-3-3ε*) in pole cells, the *act5C-GAL4* driver does

Table 11. Rescue of sterility of *D14-3-3ε* mutants with D14-3-3ε transgenes

14-3-3 Allele	hs / UAS	GAL4	Female		Male	
			n	% Fertile [a]	n	% Fertile [a]
$D14\text{-}3\text{-}3\varepsilon^{l(3)j2B10}$	---	---	30	0	25	0
$D14\text{-}3\text{-}3\varepsilon^{l(3)j2B10}$	$hsD14\text{-}3\text{-}3\varepsilon^{L}$ (18)	---	22	0	24	0
$D14\text{-}3\text{-}3\varepsilon^{l(3)j2B10}$	$hsD14\text{-}3\text{-}3\varepsilon^{L}$ (RT)	---	27	0	24	0
$D14\text{-}3\text{-}3\varepsilon^{l(3)j2B10}$	$hsD14\text{-}3\text{-}3\varepsilon^{L}$ (HS)	---	24	100	26	100
$D14\text{-}3\text{-}3\varepsilon^{l(3)j2B10}$	$hsD14\text{-}3\text{-}3\varepsilon^{H}$ (18)	---	25	0	23	0
$D14\text{-}3\text{-}3\varepsilon^{l(3)j2B10}$	$hsD14\text{-}3\text{-}3\varepsilon^{H}$ (RT)	---	25	20	24	25
$D14\text{-}3\text{-}3\varepsilon^{l(3)j2B10}$	$hsD14\text{-}3\text{-}3\varepsilon^{H}$ (HS)	---	25	100	25	100
$D14\text{-}3\text{-}3\varepsilon^{ex4}$	---	---	25	0	25	0
$D14\text{-}3\text{-}3\varepsilon^{ex4}$	$hsD14\text{-}3\text{-}3\varepsilon^{L}$ (18)	---	23	0	25	0
$D14\text{-}3\text{-}3\varepsilon^{ex4}$	$hsD14\text{-}3\text{-}3\varepsilon^{L}$ (RT)	---	25	0	25	0
$D14\text{-}3\text{-}3\varepsilon^{ex4}$	$hsD14\text{-}3\text{-}3\varepsilon^{L}$ (HS)	---	28	66	22	50
$D14\text{-}3\text{-}3\varepsilon^{ex4}$	$hsD14\text{-}3\text{-}3\varepsilon^{H}$ (18)	---	25	0	24	0
$D14\text{-}3\text{-}3\varepsilon^{ex4}$	$hsD14\text{-}3\text{-}3\varepsilon^{H}$ (RT)	---	25	8	27	7
$D14\text{-}3\text{-}3\varepsilon^{ex4}$	$hsD14\text{-}3\text{-}3\varepsilon^{H}$ (HS)	---	24	100	25	100
$D14\text{-}3\text{-}3\varepsilon^{ex4}$	*UAS mycD14-3-3*ε^{L}	*TUB*	28	100	23	100
$D14\text{-}3\text{-}3\varepsilon^{ex4}$	*UAS mycD14-3-3*ε^{H}	*TUB*	24	50	18	50
$D14\text{-}3\text{-}3\varepsilon^{ex4}$	*UAS mycD14-3-3*ε^{L}	*Act5C*	21	0	16	0
$D14\text{-}3\text{-}3\varepsilon^{ex4}$	*UAS mycD14-3-3*ε^{H}	*Act5C*	24	0	18	0

[a] The number of single crosses that yielded larvae over the total number of animals crossed per genotype. n = number of single pair matings.

HS: Three daily 20-minute heat shocks at 32°C through development to adulthood.

RT: Constant 20-22°C. 18: Constant 18°C.

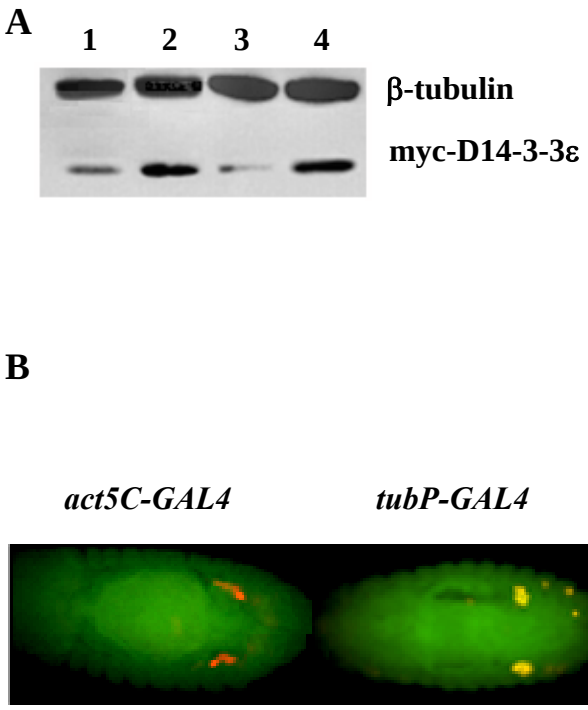

Figure 22. Differential activity of GAL4 drivers in pole cells

(A) Western blot analysis of stage 11 embryos of the genotypes: (1) *act5C-GAL4/+; UAS-mycD14-3-3ε^{L}, D14-3-3ε^{ex4}/+*, (2) *act5C-GAL4/+; UAS-mycD14-3-3ε^{H}, D14-3-3ε^{ex4}/+*, (3) *tub-GAL4/ UAS-myc D14-3-3ε^{l}, D14-3-3ε^{ex4}*, (4) *tub-GAL4 / UAS-mycD14-3-3ε^{H}, D14-3-3ε^{ex4}*. The blots were probed simultaneously with anti-myc and anti-β tubulin, which served as loading control. Expression levels of the *mycD14-3-3ε* transgenes were found equivalent under both GAL4 drivers.
(B) Stage 11 of embryogenesis in *act5C-GAL4/ UAS-GFP* and *UAS-GFP/+* ; *tub-GAL4/+* embryos. Merged confocal images of female embryos stained with anti-GFP (green) and anti-VASA (red). The *act5C-GAL4* driver does not direct expression in pole cells. Identical results were obtained with male embryos.

not. Therefore, rescue from sterility requires transgene expression in the germ-line. The complete rescue obtained under the heat-shock promoter indicates that these transgenes were expressed in the pole cells as well. In addition, the data demonstrate that the observed homozygous sterility was indeed precipitated by mutations in the *D14-3-3ε* gene.

To rescue the sterility associated with *leo* mutations, homozygotes (leo^{P1188}) and heteroallelics (leo^{P1188}/ leo^{12X}) of strong *leo* mutant alleles harbouring the *hsleoI* transgene were raised under conditions of continuous heat shocks through development until adult emergence (protocol A, see Experimental procedures and (Philip et al., 2001)). Adult animals obtained under these conditions were fully fertile, whereas animals raised under conditions that yielded low levels of LEO upon emergence (protocol B, see Experimental procedures and (Philip et al., 2001) remained sterile (Table 11).

Since induced heat shock-driven transgenes rescued *D14-3-3ε* mutations, the results suggest that these transgenes were indeed expressed in the germ-line (Table 11). However, similarly expressed *hsleo* transgenes could not rescue the *D14-3-3ε* mutations (Table 12), suggesting that with respect to pole cell development LEO cannot functionally compensate for the loss of D14-3-3ε. Both D14-3-3ε and LEO appear essential for fertility, in agreement with the reported role of 14-3-3s in *Drosophila* oocyte determination and polarization (Benton et al., 2001), which addressed the inability of eggs laid by mothers mutant in either of the 14-3-3s to hatch. However, the cause for the severe reduction in the number of laid eggs remained unknown.

Table 12. Rescue of sterility of *D14-3-3ε* mutants with LEO transgenes

14-3-3 Allele	hs / UAS	GAL4	Female		Male	
			n	% Fertile [a]	n	% Fertile [a]
D14-3-3ε$^{l(3)j2B10}$	*LI*^{L} (18)	---	25	0	25	0
D14-3-3ε$^{l(3)j2B10}$	*LI*^{L} (RT)	---	25	66	24	50
D14-3-3ε$^{l(3)j2B10}$	*LI*^{L} (HS)	---	24	100	25	100
D14-3-3ε$^{l(3)j2B10}$	*LII*^{L} (18)	---	25	0	25	0
D14-3-3ε$^{l(3)j2B10}$	*LII*^{L} (RT)	---	22	0	25	0
D14-3-3ε$^{l(3)j2B10}$	*LII*^{L} (HS)	---	25	8	24	8
D14-3-3ε^{ex4}	*LI*^{L} (HS)	---	25	0	23	0
D14-3-3ε^{ex4}	*LI*^{H} (HS)	---	21	0	19	0
D14-3-3ε^{ex4}	*LII*^{L} (HS)	---	22	0	21	0
D14-3-3ε^{ex4}	*LII*^{H} (HS)	---	18	0	17	0

[a] The number of single crosses that yielded larvae over the total number of animals crossed per genotype. n = number of single pair matings.
HS: Three daily 20-minute heat shocks at 32°C through development to adulthood.
RT: Constant 20-22°C. 18: Constant 18°C.

Severe reduction of the germ line in *14-3-3* mutants

To investigate the causes of reduced fecundity in 14-3-3 mutants, sagittal sections of adult male and female abdomens were examined histologically. While 16-20 ovarioles were found in each ovary of control females (Figure 23A), on average a single ovariole with one cell cyst per ovary were found in $D14\text{-}3\text{-}3\varepsilon^{ex4}$ homozygotes (Figure 23B). In leo^{P1188} homozygous females rescued from lethality by induction of the *hsleoI* transgene, the number of ovarioles was severely reduced with few cell cysts per ovariole (data not shown). There also seem to be an affect on somatic gonadal development, since the follicle cells in $D14\text{-}3\text{-}3\varepsilon^{ex4}$ homozygous (Figure 23D) derived from somatic gonadal tissues appear disorganized and reduced in cellular mass. The role of D14-3-3ε in somatic gonadal tissue development is unknown. $D14\text{-}3\text{-}3\varepsilon^{ex5}$ homozygotes males contain abundance of groups of 64 mature sperm (Figure 23G) derived from germ-line stem cells. However, testes do not appear to contain as many groups of mature sperm (Figure 23F and 23H) in $D14\text{-}3\text{-}3\varepsilon^{ex4}$ homozygotes. Defects in somatic gonadal tissues in males were not observed. Identical results were obtained with $D14\text{-}3\text{-}3\varepsilon^{l(3)j2B10}$ homozygotes and all $D14\text{-}3\text{-}3\varepsilon$ and *leo* mutant and heteroallelic combinations (data not shown). Therefore, the lack of either 14-3-3 protein appears to affect both the germ-line and somatic gonadal development. The atrophied germaria and small number of germ-line cysts in females resembled those of *vasa* mutant homozygotes (Styhler et al., 1998), suggesting that fewer germ cells were present in the mutants.

To determine whether lack of mature ovarioles and sperm was due to deficits or reduction in the number of pole cells, homozygous mutant embryos were stained with

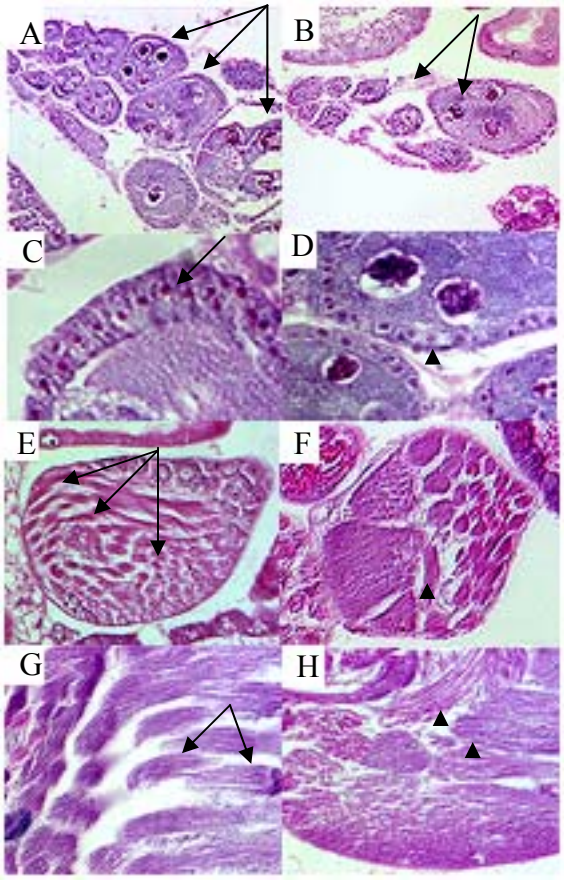

Figure 23. Loss of ovariole and groups of mature sperm in *D14-3-3ε* mutants

Severe reduction in adult germ line. Representative sagittal sections through the abdomen of control 20X females ovaries (A), 100X single maturing oocyte (B), 20X males testis (E) and 100X male testis (F) $D14\text{-}3\text{-}3\varepsilon^{ex5}$ homozygotes, 20X female ovaries (B), 100X single maturing oocyte (D) and males testis (F) and 100X male testis (H) $D14\text{-}3\text{-}3\varepsilon^{ex4}$ homozygotes. Mutant females (B) have fewer ovarioles per ovary, fewer cell cysts per ovariole and fewer nurse cells per cell cyst (arrows). The follicle cells in $D14\text{-}3\text{-}3\varepsilon^{ex4}$ homozygous (D) derived from somatic gonadal tissues appear disorganized and reduced in cellular mass (arrowhead) when compared to controls (C). $D14\text{-}3\text{-}3\varepsilon^{ex5}$ homozygotes males contain abundance of groups of 64 mature sperm (E,G,arrow); however testes do not appear to contain as many groups of mature sperm (F,H, arrowhead) in $D14\text{-}3\text{-}3\varepsilon^{ex4}$ homozygotes.

anti-VASA, a protein specific to and necessary for germ cell specification (Hay et al., 1988; Lasko and Ashburner, 1990). We used stage 14 embryos because by that stage pole cells have gone through their typical divisions to yield the final number of 35-40 pole cells and have finished their migration and encapsulation by the mesoderm to form gonads (Williamson and Lehman, 1996). Moreover, VASA expression is an appropriate marker for cells of the germ-line since it is present in all stages of their development (Hay et al., 1988; Lasko and Ashburner, 1990), and is essential for oocyte differentiation, anterior-posterior egg patterning and dorsal-ventral follicle patterning (Styhler et al., 1998).

As indicated in Figure 24A and 24D, D14-3-3ε and LEO appear present within pole cells since they co-localize with VASA. Furthermore, both *D14-3-3ε*$^{l(3)j2B10}$ and *D14-3-3ε*^{ex4} homozygous mutant embryos appeared to have normal VASA-positive cells. However, whereas controls and mutant heterozygotes had 35-37 pole cells, homozygous mutant embryos contained on average 8-10 (Table 13). The pole cells that are produced except for 8 to 10 fail to migrate properly and are lost leading to reduced ovariole and sperm production. Similar results were obtained with homozygotes for the independently isolated *D14-3-3ε*^{E183K} point mutation (Chang and Rubin, 1997) (data not shown). In stage 14 *leo*^{P1188} homozygotes (Figure 24E), pole cells appeared to form and migrate normally, except their number was significantly lower (22-24 cells, Table 13) than in controls. Since *leo*^{12X} homozygotes exhibit deficits in dorsal closure (Broadie et al., 1997), they harbour severe deficits in the dorsal mesoderm tissue where pole cells migrate and become encapsulated. This is the likely reason for the apparent defects in

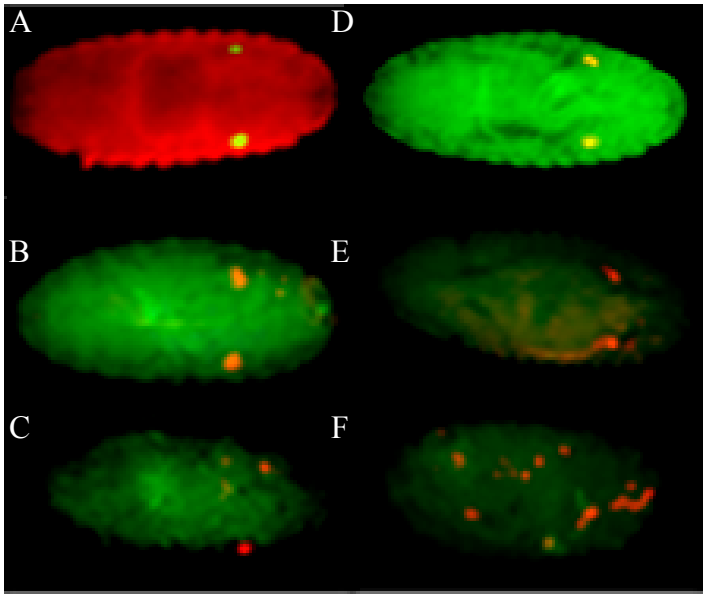

Figure 24. Loss of germ cells in *D14-3-3ε* and *leonardo* mutants

Distribution of pole cells in control and mutant female embryos. (1, 4) Merged confocal images of stage 14 female *D14-3-3ε* $^{l(3)j2B10}$*/TM3GFP* and *leo*^{P1188}*/CyOGFP* heterozygotes stained with (A) anti-D14-3-3ε (red) and anti-VASA (green) and (D) anti-LEO (green) and anti-VASA (red). Heterozygotes were hand selected due to their GFP fluorescence. (B, C) Stage 14 *D14-3-3ε* homozygous mutant embryos stained with anti-GFP (green) to differentiate homozygotes and heterozygotes and anti-VASA (red). Genotypes: (B) *D14-3-3ε* $^{l(3)j2B10}$ homozygote, (C) *D14-3-3ε* ^{ex4} homozygote. (E) Stage 14 *leo*^{P1188} homozygous mutant embryos and (F) stage 11 *leo*^{12X} homozygote stained as for 2 and 3. The green background fluorescence in C, D, E and F has been enhanced for better visibility of the embryos. Mutant embryos have fewer pole cells than wild type controls. Identical results were obtained with male embryos.

Table 13. Quantification of vasa positive cells

	Genotype	# vasa positive cells
	D14-3-3ε^{ex5}/ D14-3-3ε^{ex5}	34.25 ± 0.44
A	*D14-3-3ε$^{l(3)j2B10}$/TM3SerGFP*	35.00 ± 1.00
B	*D14-3-3ε$^{l(3)j2B10}$/ D14-3-3ε$^{l(3)j2B10}$*	8.00 ± 2.00
	D14-3-3ε^{ex4}/TM3SerGFP	34.50 ± 0.50
C	*D14-3-3ε^{ex4}/ D14-3-3ε^{ex4}*	9.00 ± 1.00
D	*leo^{P1188}/ CyO GFP*	34.50 ± 0.50
E	*leo^{P1188}/ leo^{P1188}*	22.87 ± 0.69
F	*leo^{12X}/ leo^{12X}*	22.00 ± 1.05

Letters A-F correspond to the respective genotypes of the embryos in Figure 24.
n =8.

pole cell migration evident as VASA positive cells present throughout the embryos. In addition, the number of pole cells in *leo*^{12X} homozygotes was significantly less than controls, but not different than that in *leo*^{P1188}.

Collectively, the results are consistent with a blockade, or inability of cells to divide in the absence of 14-3-3 proteins. In *D14-3-3ε* mutants, pole cells do not appear to be able to divide beyond the initial eight. In *leo* mutants initial divisions appeared normal since pole cell numbers indicated at least one successful division (Table 13), perhaps due to perdurance of maternal LEO in homozygous embryos (Philip et al., 2001). This is consistent with known essential roles for 14-3-3s in vertebrate cell cycle regulation (Fu et al., 2000; Muslin and Xing, 2000; van Hemert et al., 2001) and recent results suggesting similar roles for the *Drosophila* isotypes during early embryonic divisions (Su et al., 2001). Alternatively, pole cells may divide properly, but be unable to survive, or maintain pole cell identity when they lack 14-3-3s.

The number of pole cells decreases through development in *14-3-3* mutant embryos

To differentiate among these alternative hypotheses, we initially examined the levels of maternal and zygotic D14-3-3ε and LEO proteins in relation to the number of pole cells during embryogenesis. In control embryos, the levels of both D14-3-3ε and LEO appeared to remain relatively constant throughout the developmental periods tested (Figure 25A). As in control animals, there was abundant D14-3-3ε in stage 5 *leo*^{12X} and

D14-3-3ε^{ex4} homozygotes suggesting that the protein represents perduring maternal contribution (Figure 25A). Whereas the level of D14-3-3ε remained relatively constant through stage 11 in *leo*^{12X} homozygotes, it was not detectable by stage 8 in *D14-3-3ε*^{ex4} homozygotes (Figure 25A and Table 14). In contrast, maternally contributed LEO perdured through stage 8 in *leo*^{12X} homozygotes, but by stage 11 was barely detectable, whereas D14-3-3ε remained relatively unchanged (Figure 25A and Table 14).

There was a dramatic change in the number of pole cells among control and mutant embryos through these stages of embryogenesis. The number of pole cells remained at 35-37 in control embryos through stage 11 (Figure 25B and 25C) and stage 14 (Figure 24C). The number of pole cells in stage 5 *D14-3-3ε*^{ex4} homozygotes was consistently lower (27-28) than controls and their number actually decreased through stage 8 and 11 to 8-10 by stage 14 (Figure 24B and 24C, Figure 25C). In *leo*^{12X} homozygous embryos, pole cell number was identical to that of controls in stage 5, but as in *D14-3-3ε*^{ex4} homozygotes, their numbers declined through stage 8 and 11 to 22-23 (Figure 25B and 25C). These results suggested that pole cell survival declined concomitantly with the level of either 14-3-3 protein in mutant homozygotes. Consistent with this interpretation, in *leo*^{12X} homozygotes, longer perdurance of LEO may be the reason these embryos, have a larger number of pole cells than *D14-3-3ε*^{ex4} homozygotes

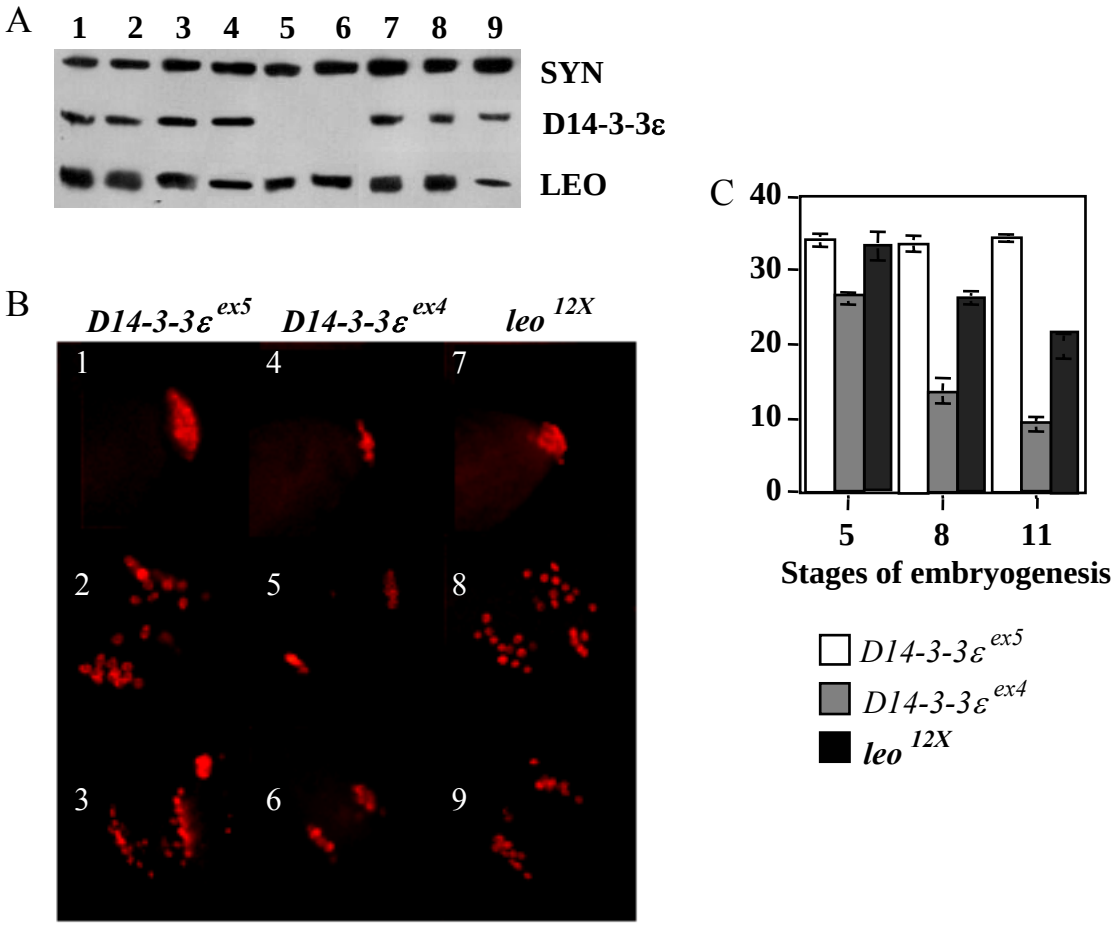

Figure 25. Decrease in D14-3-3ε and LEO levels and in pole cell numbers in mutant embryos

(A) Semi-quantitative Western blot analysis of lysates from 10 *D14-3-3ε*^{ex5} (1-3), *D14-3-3ε*^{ex4}(4-6) and *leo*^{12X} (7-9) homozygous embryos at stage 5 (1,4,7), stage 8 (2,5,8) and stage 11 (3,6,9) of embryogenesis. Blots were simultaneously probed for the presence of LEO, D14-3-3ε and SYNTAXIN.
(B) Pole cell number and location in female control *D14-3-3ε*^{ex5} (1-3), *D14-3-3ε*^{ex4} (4-6), and *leo*^{12X} homozygotes (7-9). Embryos stained with anti-VASA are shown in stage 5 (1,4,7), stage 8 (2,5,8) and stage 11(3,6,9) of embryogenesis. Identical results were obtained with male embryos.
(C) Quantification of the number of VASA labelled cells at stage 5, 8, and 11 of embryogenesis for control and *D14-3-3ε*^{ex4} and *leo*^{12X} homozygous mutants (n>8).

Table 14. Quantification of D14-3-3ε and LEO levels in staged embryo lysates

	Genotype	Stages of embryogenesis	D14-3-3ε/SYN Ratio	LEO/SYN ratio
1	*D14-3-3ε^{ex4}*	5	1	1
2	*D14-3-3ε^{ex4}*	8	0	1.1567 ± 0.1235
3	*D14-3-3ε^{ex4}*	11	0	0.9687 ± 0.0568
4	*leo^{12X}*	5	1	1
5	*leo^{12X}*	8	0.9625 ± 0.1038	1.2579 ± 0.1001
6	*leo^{12X}*	11	1.0388 ± 0.0887	0.1578 ± 0.0326

[a] In carefully staged embryo collections, *D14-3-3ε^{ex4}* homozygotes were separated from *D14-3-3ε^{ex4} /TM3GFP* heterozygotes and *leo^{12X}* homozygotes from *leo^{12X}/CyOGFP* based on GFP fluorescence. Western blots of lysates from 10 such embryos were simultaneously probed for the presence of LEO, D14-3-3ε and SYNTAXIN, which was used to normalise the blots and obtain quantitative data. The mean ± SEM is shown for three independent experiments. Numbers 1-6 correspond to the respective genotypes in the representative western blot in Figure 25A.

in stage 14. Similar results were obtained with leo^{P1188} homozygotes (data not shown). The fewer initial pole cells observed in stage 5, $D14\text{-}3\text{-}3\varepsilon^{ex4}$ homozygotes may reflect a contribution of D14-3-3ε in early pole cell divisions. In fact, a role in timing entry into somatic cell mitoses in *Drosophila* embryos has been suggested by Su *et al.* (Su et al., 2001). Alternatively, fewer pole cells may be a reflection of the observed overall smaller size of *D14-3-3ε* homozygous mutant embryos. Therefore, it appears that mutations that limit or eliminate 14-3-3 proteins during embryogenesis affect pole cell survival or maintenance of their fate, with a possible minor role of *D14-3-3ε* on early pole cell divisions.

Increased pole cell death in *14-3-3* mutants

The hypothesis that pole cells do not survive in the absence of 14-3-3 proteins was addressed by acridine orange staining to investigate increased cell death would be observed in areas occupied by pole cells in hand selected homozygous mutant embryos and controls. The pattern of cell death in stage 5, 8 and 11 for $D14\text{-}3\text{-}3\varepsilon^{ex5}$ control embryos was similar to that described previously (Abrams et al., 1993). However, in stage 8 and 11 of $D14\text{-}3\text{-}3\varepsilon^{ex4}$ and leo^{12X} homozygotes, intense acridine orange staining was observed where pole cells were expected to be located. The number of acridine orange-positive cells and their location appeared higher in leo^{12X} homozygotes and this may reflect their described dorsal closure deficits and possibly additional unknown defects. Interestingly, in $D14\text{-}3\text{-}3\varepsilon^{ex4}$ embryos, aberrant acridine orange staining was

largely confined to areas likely occupied by pole cells. This indicated that in contrast to *leo*^{12X}, apoptosis was largely limited to these cells in *D14-3-3ε*^{ex4} homozygotes.

The role of 14-3-3s in pole cells

Programmed cell death in the germ line is normally used to reduce pole cell numbers, likely ones with damaged DNA (Sonnenblick, 1950; Coffman et al., 2002). Moreover, the mechanism for apoptotic death has been proposed to be present within pole cells and to be an active and highly regulated process (Starz-Gaiano and Lehmann, 2001; Coffman, et al., 2002). 14-3-3 proteins are known to inhibit apoptosis by binding and sequestering in the cytoplasm phosphorylated BAD, thus preventing it from interacting with and inactivating members of the anti-apoptotic Bcl-2 family. Similarly, 14-3-3 proteins bind and retain in the cytoplasm Forkhead-family transcription factors, thus preventing them from transcribing cell death genes (van Hemert et al., 2001). It is possible then that loss of 14-3-3s in mutant embryos results in activation of pole cell apoptotic pathways they normally help keep inactive. The observed loss of pole cells concomitantly with the loss of 14-3-3s, early in *D14-3-3ε* mutant embryos and later in *leo* homozygotes due to LEO perdurance, is consistent with this interpretation. Similar strong anti-apoptotic roles for 14-3-3s have been described before for mammalian cells (Xing et al., 2000; Datta et al., 2001; van Hemert et al., 2001). Additional genes apparently involved in regulation of programmed cell death in pole cells have been identified recently (Coffman, et al., 2002).

Alternatively, death of pole cells may be the result of ectopic activation of their cell cycle, in the regulation of which the role of 14-3-3s is well established (reviewed in van Hemert et al., 2001). Following stage 7 of embryogenesis, pole cells enter quiescence through G_2 cell cycle arrest mediated apparently by phosphorylation-dependent inhibition of Cdc2 (Su et al., 1998). Activation of Cdc2 requires removal of the inhibitory phosphates by $Cdc25^{stg}$ (Edgar et al., 1994; Edgar and Lehner, 1996). In yeast and mammalian systems, cytoplasmic sequestering of Cdc25, necessary for proper Cdc2 inhibition and G_2 arrest is known to be mediated by 14-3-3 proteins (Forrest and Gabrielli, 2001; van Hemert et al., 2001). Similarly in *Drosophila* pole cells, proper localization of Cdc25 is necessary for Cdc2 inhibition and G_2 arrest (Su et al., 1998). In addition, pole cells appear unable to enter mitosis and S phase and proceed directly to G_1 upon temporally miss-regulated activation of Cdc2 (Su et al., 1998), which may lead to apoptosis. In Hela cells, abrogation of 14-3-3 binding and cytoplasmic localization of Cdc25 precipitated a high proportion of abnormal mitotic phenotypes including apoptosis (Forrest and Gabrielli, 2001), consistent with the reported apoptotic phenotypes upon Cdc2 over-activation (Shi et al., 1994; Yu et al., 1998) and the anti-apoptotic functions of 14-3-3s (Xing et al., 2000). Moreover, both 14-3-3 proteins play specific roles in cell cycle regulation of syncytial mitoses in early embryos (Su et al., 2001). Given these observations, loss of pole cells in 14-3-3 mutant embryos may be the result of the decline in maternally loaded 14-3-3s, which results in gradual $Cdc25^{stg}$ relocation in pole cells, precipitating Cdc2 activation and apoptotic cell death. The

observation that the number of pole cells declines as the levels of maternal 14-3-3s decline during development in homozygous mutant embryos lends support to this notion.

The similarity in the *D14-3-3ε* and *leo* mutant phenotypes and co-localization of the two proteins in pole cells suggests that both are involved in preventing cell death, or maintaining G_2 arrest, likely by heterodimer formation. The importance of 14-3-3 heterodimers instead of homodimers is consistent with the fact that the two 14-3-3s are not functionally redundant, suggesting roles for both 14-3-3s in maintenance of pole cells. This is supported by the dramatic loss of pole cells in *D14-3-3ε* mutant homozygotes despite the presence of abundant LEO homodimers, which did not appear to functionally compensate for the proposed D14-3-3ε LEO heterodimers. In fact, it appears that considering the perdurance of LEO, the reduction in pole cells occurs as soon as D14-3-3ε disappears (Fig 25). Similarly, loss of LEO was not compensated by D14-3-3ε in *leo* mutants. The two proteins are capable of heterodimerization *in vivo*. Therefore, with respect to pole cell survival loss of either 14-3-3 protein appears rate limiting, consistent with the proposed obligate heterodimers. This is in contrast to the reported partial compensation of D14-3-3ε by LEO in oocyte determination and polarization of the A-P axis (Benton et al., 2001). An alternative interpretation is that in pole cells, the two 14-3-3 proteins regulate different, but closely related aspects either of G_2 arrest or apoptosis prevention. In fact, in syncytial mitosis regulation, the two proteins appear to have distinct roles, as D14-3-3ε is apparently required to time the mitoses and LEO appears to be required for normal chromosome separation (Su et al., 2001).

Our data extend the requirement for 14-3-3 proteins in oocyte determination and polarization of the A-P axis (Benton et al., 2001), which is the likely explanation of why the few eggs laid by the *D14-3-3ε* and *leo* mutant females do not hatch. The earlier requirement for both 14-3-3 proteins in pole cell survival is the likely explanation of the observed small number of eggs laid by these mutant females and the sterility of mutant males (Chang and Rubin, 1997; Coffman, et al., 2002; and this paper). It is interesting that in oocyte determination and polarization, the two 14-3-3 isotypes can be partially functionally redundant, but in the earlier processes of pole cell survival they do not appear to be. It is currently unknown whether this pattern of 14-3-3 isotype involvement in distinct steps of a process, unique properties of heterodimers versus homodimers and partial or complete functional compensation will be characteristic of each of the growing number of roles for 14-3-3 proteins *in vivo.*

EXPERIMENTAL PROCEDURES

Drosophila culture and strains

Drosophila were cultured in standard cornmeal sugar food supplemented with soy flour and $CaCl_2$ at 20-22^{o}C. The $D14\text{-}3\text{-}3\varepsilon^{l(3)j2B10}$ mutant allele has been described previously (Chang and Rubin, 1997). Alleles $D14\text{-}3\text{-}3\varepsilon^{ex5}$, $D14\text{-}3\text{-}3\varepsilon^{ex4}$ and $D14\text{-}3\text{-}3\varepsilon^{ex24}$ generated by mobilisation of the transposon in $D14\text{-}3\text{-}3\varepsilon^{l(3)j2B10}$ were a gift of Dr. Henry Chang. The genetic background of these alleles was normalised to that of Cantonized

w^{1118} using balancer chromosomes in a Cantonized w^{1118} background. Allelism was assessed by complementation tests.

D14-3-3ε transgenic strains were generated by sub-cloning wild type *D14-3-3ε*, and myc-tagged *D14-3-3ε* cDNAs provided by Chang and Rubin, (data not published), into pUAST (Brand and Perrimon, 1993) or pCaSpeR-hs and injecting w^{1118} embryos. Multiple independent transformant lines were obtained and the ones with the darkest w^{+} eye color were used for this analysis. The *hsleoI* (*LI*) transgenic strains have been described elsewhere (Philip et al., 2001). The Gal4 "driver" strains containing the transgenes *tubP-GAL4* (BL#5138) and *act5C-GAL4* (BL#3957) were provided by the Bloomington Stock center.

Southern blot analysis

Genomic samples were prepared as previously described (Skoulakis and Davis, 1996), blots were obtained using the Turboblotter rapid downward neutral transfer system (Schleicher & Schuell, Keene, NH) and probed with *D14-3-3ε* cDNA and genomic DNA fragments.

Generation of anti-D14-3-3ε antibodies

The *D14-3-3ε* pRSET expression vector was a kind gift of Dr. Chien (Tien et al., 1999). Recombinant D14-3-3 protein was purified from bacterial cultures by virtue of the hexahistidine tag and injected into hens (Charles River laboratories). IgY was purified from eggs using standard protocols (Charles River laboratories). The specificity

of the anti-D14-3-3ε antibodies was tested with recombinant D14-3-3ε and LEO proteins and fly head lysates by western blots (see below).

Western blot analysis

Two whole flies from control and mutant animals were homogenized in 10 μl of modified radioimmunoprecipitation assay (RIPA) buffer as previously described (Philip et al., 2001). Extracts, equivalent to one fly per lane were run on 18% acrylamide gels. Blots were probed at room temperature with rabbit anti-LEO (1:40,000), or chicken anti-D14-3-3ε (1:5000) and a 1:200 dilution of mouse anti-SYNTAXIN (9E10, Developmental Hybridoma Studies Bank, University of Iowa, Iowa City, IA). The blots anti-tubulin (E7 Developmental Hybridoma Studies Bank, University of Iowa, Iowa City, IA) was used at 1:500 dilution. Secondary antibodies were used at 1:15,000 for anti-rabbit, 1:5,000 for anti-chicken and 1:4000 for anti-mouse and the results were visualised with enhanced chemiluminescense (Pierce).

To obtain homozygous mutant embryos for Western analysis, timed egg collections from *D14-3-3ε^{ex4}/TM3GFP* and *leo^{12X}/CyOGFP* stocks were obtained. Homozygotes were hand-selected due to their lack of GFP fluorescence and an equal number of GFP-positive morphologically normal heterozygotes were homogenized in RIPA buffer and processed for Western blot analysis. Unless specified otherwise, 20 embryos from a tight 1-hour collection were homogenized in RIPA buffer, 10 μl Laemli buffer was added and 10 μl of the homogenate were run per lane. Quantification of the results was obtained by densitometry and the ratios of LEO/SYNTAXIN and D14-3-

3ε/SYNTAXIN were determined for each sample in minimally three independent experiments.

Fertility assays

To test fertility, single mutant male or female flies were paired with three tester w^{1118} females or males accordingly and the vials were tested for the presence of larvae for 7 days. Presence of even a single larva within a vial was scored to denote fertility for the tested animal. Vials that did not contain offspring were scored as sterile only when at the least the female parent was still alive at the end of the 7-day period.

Homozygotes for the lethal null leo^{12X} and leo^{P1188} alleles (Skoulakis and Davis, 1996; Broadie et al., 1997) were obtained by heat shock induction of a *leo* transgene as described (Philip et al., 2001). Briefly, leo^{12X} /CyO; *hsleoI (LI)* and leo^{P1188} /CyO; *LI* virgin females raised under three daily induction's of the transgene were mated either with their brothers, or leo^{P1375} /CyO; *LI* males and progeny was allowed to develop at 22-23^{0}C. This protocol (protocol B) yields adults harbouring less than 10% of normal LEO protein (Philip et al., 2001), which along with the rare leo^{P1375} homozygous and leo^{P1375}/ leo^{P1188} heteroallelic escapers were tested for fertility. Alternatively (protocol A) leo^{12X} /CyO; *LI* and leo^{P1188} /CyO; *hsleoI* animals were allowed to develop to adulthood under 3 daily 20 minute heat shocks, collected and fertility tested at 22-23^{0}C. To rescue sterility of *D14-3-3ε* mutants, *hsD14-3-3ε*, $D14\text{-}3\text{-}3\varepsilon^{ex4}$homozygotes were collected, paired to appropriate tester w^{1118} individuals and given three daily 20-minute heat shocks. In addition, *UAS-mycD14-3-3ε*$D14\text{-}3\text{-}3\varepsilon^{ex4}$/TM3Sb transgenic lines were mated

either to *tubP-GAL4, D14-3-3ε ^{ex4}*/TM3Sb, or *act5C-GAL4*/CyO*; UAS-mycD14-3-3ε D14-3-3ε ^{ex4}*/TM3Sb and the progeny were tested for fertility as described above. For the *leo* transgenics, *leo^{12X}* / *leo^{P1375}*or *leo^{P1188}* homozygous virgin females rescued from lethality as outlined above, were paired to appropriate tester *w^{1118}* individuals, given three daily 20-minute heat shocks and their fertility was assessed.

Immunohistochemistry

To obtain homozygous embryos for immunohistochemistry, GFP fluorescence-negative embryos were hand selected from eggs laid by *D14-3-3ε ^{ex4}/TM3SerGFP* and *leo^{12X}/CyOGFP* parents. Sibling GFP fluorescence-positive embryos were selected as controls based on their less intense fluorescence and apparent normal appearance in contrast to the abnormal appearance and intense fluorescence of balancer homozygotes.

Embryos were collected on apple juice plates, dechorionated and fixed in 43.2 mM Hepes, 0.96 mM MgSO4, 0.48 mM EGTA, pH 6.9, 1.6% formaldehyde in 59% heptane, followed by rinses in methanol, 5% EGTA. The embryos were rehydrated to BBT (140 mM NaCl, 2.7 mM KCl, 4.3 mM Na_2HPO_4, 1.4 mM KH_2PO_4, pH 7.3, 0.1% Tween-20, 1%, Bovine Serum Albumin) and blocked for 1 hr in BBT-250 (BBT, 250 mM NaCl), 10% normal goat serum. Incubation with primary antibodies in 5% normal goat serum BBT-250 was as follows: rabbit anti-LEO (1:4000), chicken anti-D14-3-3ε (1:3,000), mouse anti-GFP (1:30,000) and rat anti-VASA (1:2,000) (Provided by Dr. T. Lasko). Fluorescent secondary antibodies diluted 1:2,000 were Alexa 594 anti-chicken, Alexa 488 anti-mouse and Alexa 488 or 594 anti-rabbit. Images were captured on a

Zeiss Axiovert 135 microscope with an Atto Carv confocal module (Nipkow spinning disk) using a 25X objective lens.

Statistical analysis

The results of all cell-counting experiments were analyzed using the JMP3.1 statistical software package (SAS Institute, Cary, NC). Following initial ANOVA, the data were analyzed by planned comparisons to a control (Dunnett's test) or Tukey–Kramer tests.

CHAPTER IV

PROTECTION FROM PREMATURE HABITUATION REQUIRES FUNCTIONAL MUSHROOM BODIES IN *DROSOPHILA*

INTRODUCTION

Selection of an appropriate behavioral response depends on the ability of an organism to discriminate between novel and pre-experienced environmental stimuli. Sensory information that elicits a particular response maybe enhanced or suppressed by additional novel or pre-experienced sensory inputs. Therefore, filtering less significant events, such as a non-reinforced prolonged or repetitive stimulus is likely essential in avoiding inappropriate behavioral responses. Habituation is a major mechanism to decrease responsiveness to repetitive or prolonged non-reinforced stimuli (Thomson and Spencer, 1966; Rankin, 2000; Rose and Rankin, 2001). Equally important, since habituation may be the foundation of selective attention, inappropriate or premature habituation to a stimulus would not permit discrimination between novel and pre-experienced stimuli essential in mediating appropriate responses (Mackintosh, 1974). In humans, defective habituation has been associated with schizophrenia (Freedman et al., 1991; Adler et al., 1999; Meincke et al., 2004), learning disabilities (Gillberg, 2003; Slaats-Willemse et al., 2003) and migraines (Siniatchkin et al., 2003) among other conditions.

In addition to stimulus gating, habituation as a form of non-associative learning has been studied in a variety of models (Thomson and Spencer, 1966; Hawkins, 1988; Rose and Rankin, 2001). In *Drosophila*, a number of different assays have been developed to study habituation focused mainly on the effects of known associative learning mutations on habituation (Duerr and Quinn, 1982; Corfas and Dudai, 1989; Asztalos et al., 1993; Engel and Wu, 1996; Jin et al., 1998; Engel et al., 2000). Moreover, with the exception of the proboscis extension reflex (Duerr and Quinn, 1982), most assays focused on habituation of Peripheral Nervous System sensory neurons. Little has been done in *Drosophila* to investigate habituation mediated by the Central Nervous System (CNS), and in particular to stimuli used for associative conditioning. Since this could provide a direct comparison of associative and non-associative processes we investigated habituation to the olfactory and footshock stimuli used in negatively reinforced olfactory associative conditioning in *Drosophila* (Tully and Quinn, 1985).

Two main neural centers in the *Drosophila* CNS have been implicated in processing of olfactory and footshock information processing, the Mushroom Bodies (MBs) and the Lateral Horn (LH) (Heisenberg, 2003; Tanaka et al., 2004). The MBs, essential for olfactory associative learning and memory, but not olfaction *per se*, are bilateral neuronal clusters in the dorsal posterior cortex of each *Drosophila* brain lobe (Roman and Davis, 2001; Heisenberg, 2003). The dendrites (calyces) lie ventrally to the somata, while their axons fasciculate to form the peduncles, which projects to the anterior of the brain. There, it bifurcates with processes extending medially (β, β′ and

γ lobes) and others projecting dorsally to comprise the α and α′ lobes (Crittenden et al., 1998). The LH which has been suggested to mediate direct responses to olfactory stimuli (Marin et al., 2002; Tanaka et al., 2004) lies lateral to the MB calyces and the two neuropils appear to interact bi-directionally (Ito et al., 1998). Olfactory information arrives at the MBs and the LH from the antennal lobe via two ascending tracks of projection neurons, the medial (mACT) and inner (iACT) antenocerebral tracks (Marin et al., 2002; Heisenberg, 2003). The iACT connects the antennal lobes to the posterior brain where it bifurcates into one branch of axons projecting to the MB calyces, while the other projects to the lateral horn (LH) of the protocerebrum (Stocker et al., 1997; Heimbeck et al., 2001). The mACT leads primarily to the LH and a minor track branches to the MB calyces (Acebes and Ferrus, 2001).

To investigate CNS mediated habituation and the anatomical sites that participate in the response, we focused on olfactory and footshock responses. Avoidance of aversive and attraction to appetitive odors (osmotactic responses) constitute essential behaviors in *Drosophila* and have been used to investigate the organization and function of the olfactory system in this insect (de Bruyne et al., 2001; Stocker, 2001; Devaud, 2003). We aimed to capitalize on the robustness of these responses and their use in conditioning paradigms (Tully and Quinn, 1985; Davis and Han, 1996; Roman and Davis, 2001; Waddell and Quinn, 2001; Heisenberg, 2003), and the extensive information regarding the organization and function of the olfactory system in *Drosophila* (Vosshall, 2000; Stocker, 2001). We report on the establishment of two

novel habituation paradigms and the role of the MBs and potentially the lateral horn in protecting from premature habituation to the stimuli.

RESULTS

An experience-dependent odor specific decrement in osmotaxis

Because the decrease in response characteristic of habituation depends on repeated stimulation (Thomson and Spencer, 1966) which is difficult to deliver discretely and with high frequency with airborne odorants, we used continuous exposure to odors adjusted such as to elicit relatively mild responses. We exposed flies (w^{1118} and ex^{5}) to aversive and attractive odors for different lengths of time (pre-exposure) and tested their subsequent performance when confronted with a choice of the same odor and air. Naïve animals exhibited mild osmotactic responses (Avoidance Indices of about 50) in avoidance of octanol (OCT) and benzaldehyde (BNZ) and attraction to ethyl acetate (ETA) (Figure 26A and 26.II, naïve, and Table 15). After 3 minutes of pre-exposure to OCT, a highly significant 60% reduction in subsequent avoidance of this odor was observed (Figure 26A). However, OCT avoidance did not change if the flies were pre-exposed to equally aversive BNZ (Figure 26A), indicating odor specificity in the pre-exposure dependent osmotactic decrement and argued against generalized olfactory fatigue or sensory adaptation both predicted to have poor odor specificity (Thomson and Spencer, 1966; Devaud, 2003). Pre-exposure to BNZ precipitated a similar decline in subsequent avoidance of this odor with respect to pre-exposure time required, magnitude

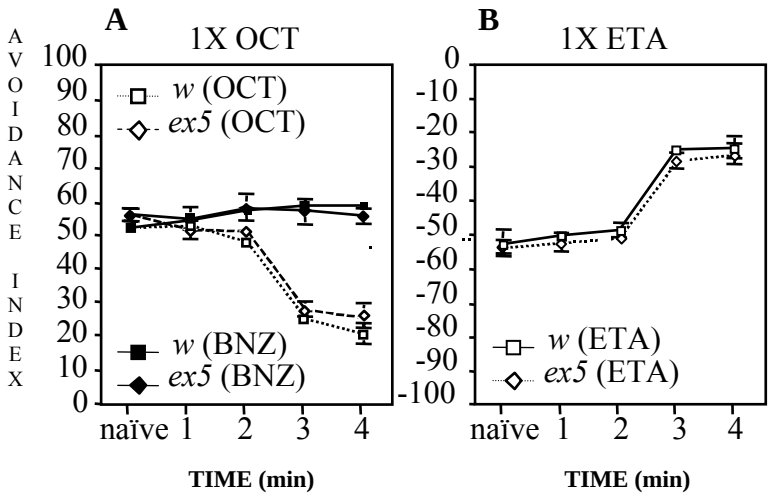

Figure 26. Odor pre-exposure-dependent osmotactic decline

The mean index (AI) for odor avoidance (I) or attraction (II) are shown ± SEM after pre-exposure for 0 (naïve) to 4 minutes to the odors indicated. After pre-exposure, avoidance of aversive odors was tested for 90 seconds and attraction for 180 seconds. SD: significant differences, NSD: non significant differences

(I) Octanol (OCT) avoidance after pre-exposure for the indicated times to OCT (open symbols), or benzaldehyde (BNZ, filled symbols). ANOVA indicated significant differences ($F_{(9,82)}$=49.46 $p<0.0001$, SD) among the AIs. Subsequent planned comparisons between naïve and pre-exposed *w* and *ex5* demonstrated significant reductions in OCT avoidance ($p<0.0001$) after 3 and 4 minutes pre-exposure to this odor. Shorter pre-exposure did not have any effects. In contrast, no significant differences in OCT avoidance (ANOVA ($F_{(9,83)}$=0.73 $p<0.6826$, NSD) were observed after pre-exposure to BNZ. OCT avoidance declined after 2 minutes of pre-exposure to this odor. ($n\geq 8$ for all measurements).

(II) Attraction to ethyl acetate (ETA) by control flies after pre-exposure for the indicated times to the same odor. Note the negative AI scores indicating attraction. ANOVA indicated significant differences ($F_{(9,84)}$=32.65 $p<0.0001$). Subsequent planned comparisons revealed significant differences ($p<0.0001$) in attraction to ETA only between naïve and flies pre-exposed to the odor for 3 and 4 minutes. Attraction declined after 2 minutes of pre-exposure to ETA ($n\geq 8$ for all measurements).

Table 15. Odor acuity and shock avoidance

I.	Genotype	0.1X OCT	0.1X ETA	1X BNZ
	w1118	51.79 ± 4.08	-43.75 ± 5.52	56.24 ± 1.67
	w1118 HU	48.50 ± 2.94	-39.80 ± 2.43	48.35 ± 2.25
	ex5/ex5	48.32 ± 1.92	-37.02 ± 1.79	54.58 ± 2.41
	ex5/ex5 HU	52.55 ± 1.91	-46.65 ± 2.89	56.52 ± 2.15

II.	Genotype	45V	90V
	w1118	72.59 ± 1.12	79.82 ± 2.04
	w1118 HU	73.63 ± 2.50	84.24 ± 1.58
	ex5/ex5	70.85 ± 1.20	84.37 ± 1.50
	ex5/ex5 HU	72.50 ± 1.07	85.23 ± 2.16
	Berlin	75.34 + 4.43	82.30 ± 1.00
	mbm^{1}	78.59 + 3.10	80.29 ± 0.96
	w; UAS-TNT	74.38 ± 1.16	84.38 ± 1.16
	UAS-TNT / 247	74.93 ± 1.43	84.93 ± 1.43
	UAS-TNT / GH146	78.41 + 0.81	84.77 ± 0.84
D	w; UAS-*shi*^{5ts}	74.56 ± 1.02	84.56 ± 1.02
	UAS-*shi*^{5ts} / 247	71.39 ± 1.33	81.39 ± 1.33
	UAS-*shi*^{5ts} / GH146	72.77 + 1.23	82.29 ± 1.24
	UAS-*shi*^{5ts} / OK72	73.66 + 0.88	82.85 ± 1.28
	w; UAS-*shi*^{10ts}	74.38 ± 1.29	84.38 ± 1.29
	UAS-*shi*^{10ts} / 247	73.72 ± 1.52	83.72 ± 1.52
	UAS-*shi*^{10ts} / GH146	72.01 + 2.06	84.88 ± 1.36
	UAS-*shi*^{10ts} / OK72	74.33 + 1.52	83.40 ± 1.80

(I) The PI for olfactory acuity are shown ± SEM. Positive values indicate avoidance and negative values indicate attraction to odors. ANOVA's for olfactory acuity indicate no significant differences (NSD) for 0.1X OCT ($F_{(3,35)}$=2.14 P<0.1139 NSD), 0.1X ETA ($F_{(3,32)}$=1.18 P<0.3347 NSD) and BNZ avoidance ($F_{(3,31)}$=3.18 P<0.0391). (n≥8 for all measurements)
(II) The following ANOVA's for shock avoidance indicated no significant difference: (n>8)
A) 45V ($F_{(3,39)}$=3.26 P<0.0324) and 90V ($F_{(3,32)}$=1.90 P<0.1569).
B) 45V ($F_{(1,16)}$=3.09 P<0.1024) and 90V ($F_{(1,16)}$=3.09 P<0.1024).
C) 45V ($F_{(2,24)}$=3.68 P<0.0772) and 90V ($F_{(2,25)}$=0.21 P<0.8109).
D) 45V ($F_{(3,35)}$=0.11 P<0.7417) and 90V ($F_{(3,32)}$=0.88 P<0.4643).
E) 45V ($F_{(3,55)}$=0.13 P<0.7231) and 90V ($F_{(3,33)}$=0.30 P<0.8279).

of the decline and odor specificity (not shown). Furthermore, a similar decline in ETA attraction was observed after 3 minutes of pre-exposure to this odor (Figure 26B) and identical results were obtained with additional attractive odors such as butanedione (not shown).

Interestingly, in all experiments we observed a refractory period when animals appeared to respond to the pre-exposed odor as if they were naïve. In the experiments shown in Figure 26 the refractory period was about 120 seconds, but this time varied depending on stimulus strength. Strong stimulation increased the refractory period (Figure 27B.II and data not shown), consistent with predictions for habituation and in contrast to olfactory fatigue or desensitization predicted to have the opposite effect (Thomson and Spencer, 1966). Failure to move away from, or towards the test stimulus could not be attributed to odor-induced impairments in locomotion for three reasons. First, flies pre-exposed to one aversive odor and tested against another avoided the latter normally (Figure 26A). Second, the vast majority of animals moved away from the central compartment of the maze during the testing phase of the experiment. Third, in the absence of test odors, both naïve and pre-exposed animals distributed equally in the two arms of the maze within 30-35 seconds, a time 3 times faster than the 90-second period allotted for testing (not shown).

The osmotactic response decrement conforms to habituation parameters

Because the pre-exposure dependent osmotactic decline was stimulus specific, we investigated whether it conforms to additional classically defined habituation

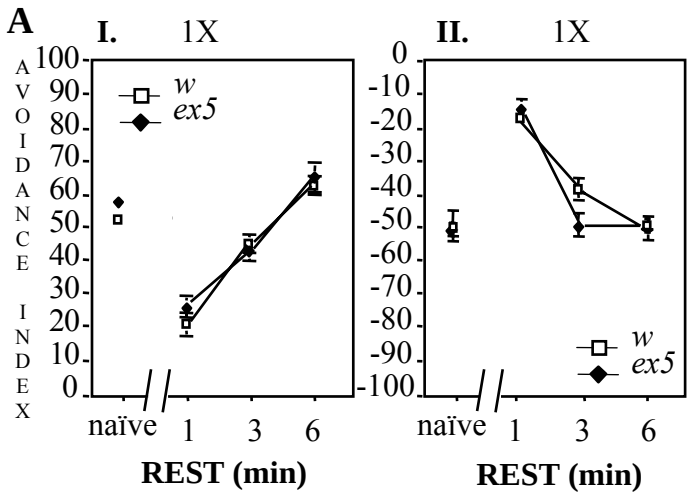

Figure 27. Parameters of olfactory habituation

The mean AI for odor avoidance (positive scales) or attraction (negative scales) ± SEM are shown in all panels. SD: significant differences. NSD: non significant differences
(A) Spontaneous recovery of the pre-exposure-dependent reduction in osmotaxis within 3 minutes.
(I) Recovery of OCT avoidance to naïve levels by *w* (open symbols) and *ex5* (filled symbols) animals after the indicated rest period following 4 minutes of OCT pre-exposure. ANOVA ($F_{(7,66)}$=33.34 $p<0.0001$, SD) and planned comparisons indicated a performance deficit of pre-exposed animals in comparison to naïve, after 1 minute of rest ($p<0.0001$), but not for other rest periods. Therefore recovery occurred after 3 minutes of rest post pre-exposure ($n\geq8$ for all measurements).
(II) Recovery of attraction to ETA by *w* (open symbols) and *ex5* (filled symbols) after the indicated rest period following 4 minutes of ETA pre-exposure. ANOVA ($F_{(7,66)}$=21.43, $p<0.0001$ SD) and subsequent planned comparisons indicated that differences in attraction between ETA pre-exposed and naïve animals were significant only after 1 minute of rest ($p<0.0001$) but not after 3 or 6 minutes. Therefore recovery occurred after 3 minutes of rest post pre-exposure ($n\geq8$ for all measurements).

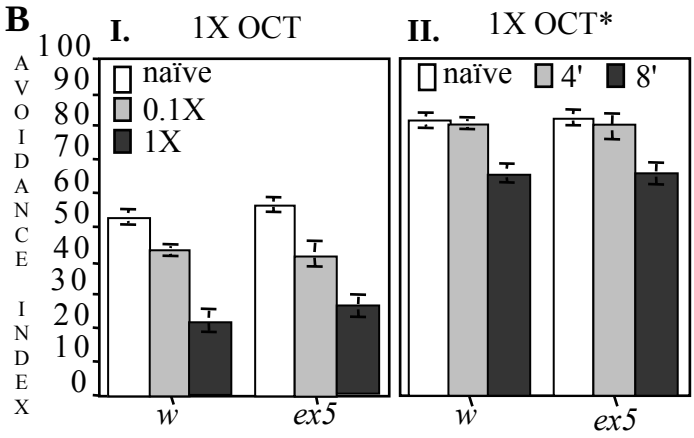

Figure 27. (continued)

(B) Dependence of the pre-exposure-dependent reduction in osmotaxis on stimulus strength.
(I) Avoidance of 1X OCT after pre-exposure to 1X or 0.1X OCT compared to avoidance of naïve animals. ANOVA ($F_{(5,50)}$=30.58 $p<0.0001$ SD). The differences between naïve and pre-exposed animals were significant ($p<0.0001$) regardless of the amount of odorant (Dunnett's tests). In addition, the differences in avoidance of animals pre-exposed to 1X OCT and 0.1X OCT were significant ($p<0.0001$). A decrease in the pre-exposed odorant (0.1X) resulted in a smaller pre-exposure-dependent reduction in avoidance of full strength odor ($n\geq 8$ for all measurements).
(II) Avoidance of 1X OCT delivered at increased (600 ml/min) flow rate (1X OCT*) after 4 minute and 8 minute pre-exposure to the same conditions (1X OCT*). ANOVA ($F_{(5,64)}$= 13.27 $p<0.0001$ SD). Subsequent planned comparisons (Dunnett's test) indicated significant differences only between animals pre-exposed for 8 minutes ($p<0.0001$) and naïve controls but not for naïve and animals pre-exposed for 4 minutes. Increased stimulus strength decreased habituation ($n\geq 8$ for all measurements).

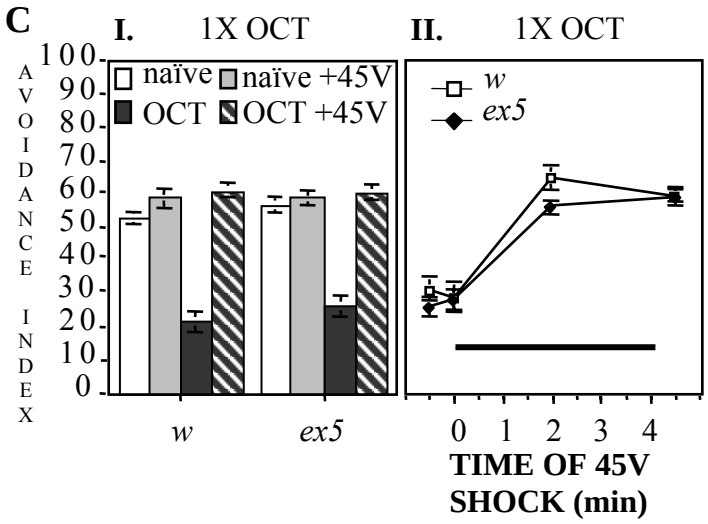

Figure 27. (continued)

(C) Dishabituation of the pre-exposure-dependent reduction in osmotaxis with electric shock.
(I) Animals were tested for avoidance of 1X OCT either naïve (open bars), after 4 minute 1X OCT pre-exposure (dark gray bars), 1X OCT pre-exposure followed by a single 45V electric shock 30 seconds prior to testing (hatched gray bars). Light gray bars indicate the effect of the 45V shock on naïve flies on subsequent OCT avoidance. ANOVA ($F_{(7,65)}$=59.00 $p<0.0001$ SD). Planned comparisons indicated that the performance differences between pre-exposed animals (OCT), and pre-exposed shocked animals (OCT+45V) were significant ($p<0.0001$). However, the performances of naïve, naïve+45V shock and pre-exposed shocked flies (OCT+45V) were not significantly different, indicating that a single 45-volt shock restored normal OCT avoidance after 4 min of pre-exposure ($n\geq7$ for all measurements).
(II) A 45V shock was delivered either 30 seconds prior to, during, or 30 seconds after OCT pre-exposure (line indicates duration of odor exposure) and subsequent OCT avoidance was tested. ANOVA ($F_{(7,64)}$ = 37.59 $p<0.0001$ SD). Subsequent planned comparisons revealed significant differences ($p<0.0001$) in OCT avoidance between animals that received the shock midway, or at the end of pre-exposure, and those that received it prior to or at the onset of the pre-exposure ($n\geq7$ for all measurements).

parameters. A 3-4 minute post pre-exposure rest prior to testing yielded responses not different than those of naïve animals (Figure 27A.I and 27A.II), indicating a time-dependent spontaneous recovery of osmotactic behaviors as predicted for habituation (Thomson and Spencer, 1966). Similar results were obtained for BNZ and butanedione (not shown). Since identical results were obtained for all aversive and attractive odors tested for this and the remaining experimental sets, only data collected with OCT will be presented henceforth for simplicity.

To investigate whether the decrement in osmotactic response depended on stimulus strength, we pre-exposed to 10-fold less octanol (0.1X OCT), which precipitated a smaller decline in subsequent avoidance (18%) than the 60% decline after pre-exposure to 1X OCT (Figure 27B.I). However, naïve avoidance of the reduced odors was robust (Table 15). The reduced habituation elicited by pre-exposure to stimuli weaker than the test stimulus suggests inefficient habituation when the two stimuli are not equivalent, but a degree of OCT avoidance irrespective of stimulus strength was elicited nevertheless. Conversely, increasing the effective amount of OCT by increasing the air flow over the odorant resulted in increased avoidance by naïve animals. However, a modest decrement in avoidance was apparent after 8 minutes of pre-exposure but not after 4 minutes (Figure 27B.II). Therefore, the decline in avoidance depended on both the intensity and duration of the pre-exposure stimulus (Figure 27B.I, II) and the refractory period increased with stronger stimulation consistent with the predictions for habituation of Thomson and Spencer (Thomson and Spencer, 1966).

Finally, if the pre-exposure dependent decline in osmotaxis was olfactory habituation and not sensory desensitization or fatigue, the effect should be eliminated by brief application of an unrelated noxious stimulus (dishabituation) (Thomson and Spencer, 1966). We attempted to eliminate the effects of odor pre-exposure with electric footshock because attempts to dishabituate with visual (strong white light), or strong mechanical stimulation (vortexing) failed (not shown). The strength and number of footshock stimuli required to reverse the osmotactic response decrement with the weakest possible footshock were determined in control experiments (see Materials and Methods). A single 45-Volt shock did not affect subsequent OCT avoidance in naïve flies (Figure 27C.I). However, when delivered after a 4-minute OCT pre-exposure typically precipitating a 60% decrement in avoidance, it resulted in normal odor avoidance indicating that electric shock dishabituated the osmotactic response. If the electric footshock was indeed a dishabituating stimulus, then it should not be effective prior to pre-exposure. In fact, the footshock was effective only if delivered at the end of pre-exposure, or the end of the apparent 120-second refractory period (Figure 27C.II). The latter suggests that the dishabituating stimulus likely interferes with processes necessary for the onset of habituation, effectively re-setting the refractory period. Recovery of normal osmotactic response after footshock strongly suggests that the pre-exposure dependent decline was caused by habituation to the odor and not desensitization or fatigue (Thomson and Spencer, 1966). Qualitatively and quantitatively identical results were obtained with osmotactic responses to BNZ and ETA (not shown).

Collectively, the results suggest that the experience-dependent decrement in osmotactic response conforms fully to habituation parameters. Moreover, the time refractory to obtaining a habituated response will be referred to henceforth as a period that the animals are "protected from premature habituation".

The mushroom bodies are essential for protection from premature habituation

Because the mushroom bodies are central to olfactory information processing and olfactory learning and memory (Zars, 2000; Roman and Davis, 2001; Heisenberg, 2003), we investigated whether these neurons are involved in olfactory habituation. We obtained adult animals with ablated mushroom bodies (Figure 28D-F) by hydroxyurea (HU) treatment of first instar larvae (de Belle and Heisenberg, 1994; Philip et al., 2001) and subjected them to odor pre-exposure and osmotaxis testing (Figure 29A). Lack of mushroom bodies did not affect naïve responses to odors (Figure 29A, 0 time, Table 15 and (de Belle and Heisenberg, 1994)). However, whereas control animals habituated after 3-4 minutes exposure to OCT, mushroom body ablated animals exhibited a dramatic decline in osmotaxis after 10 seconds, the shortest pre-exposure we could deliver reliably (Figure 29A). This drastically reduced refractory period suggested that HU-treated animals lack either all or part of the neuronal circuitry requisite for a normal refractory period and therefore habituated prematurely. Similar results were obtained with pre-exposure to BNZ and ETA for both w^{1118} and ex^{5} mushroom body ablated animals (not shown). Although hydroxyurea ablation did not grossly change the number

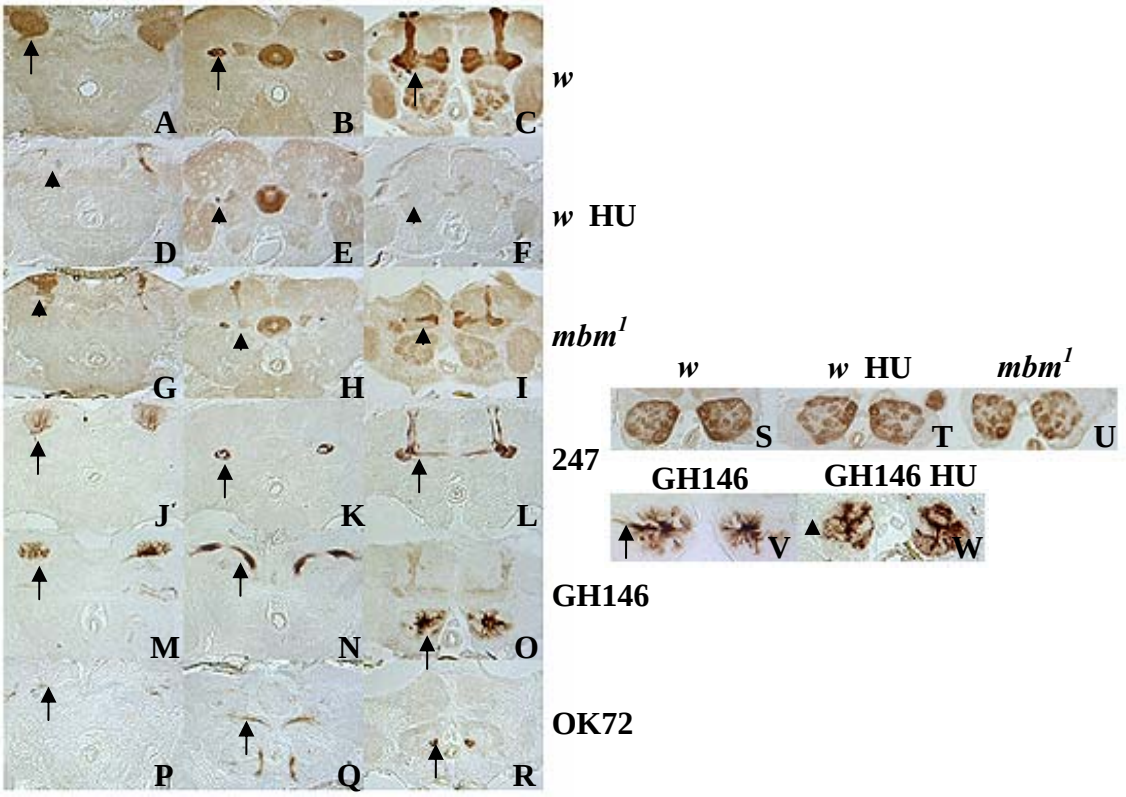

Figure 28. Structural analysis of mushroom body perturbed animals and expression patterns of GAL4 drivers

All histology was performed on frontal, 5μm paraffin sections and shown at 200X except for antennal lobes shown at 400X.

(A-I). Heads stained with α–LEO to reveal the structure of the mushroom bodies (MBs) at the level the calyx (A, D, G), peduncle (B, E, H) and lobes (C, F, I). Arrows point to the MB structures in control animals (*w*) deleted or altered (arrowheads) by hydroxy-urea ablation (HU) and in *mbm*^{1} mutants. Note that HU treatment does not ablate the ellipsoid body (E). (J-R). Sections stained with α–bTAU to reveal the expression patterns of the 247, GH146 and OK72 GAL4 drivers. Sections were taken from the progeny of these GAL4-bearing lines crossed to UAS-*btau*. (J-L). Arrows indicate accumulation in the calyx (J), peduncle (K) and lobes (L) of the MBs under the 247 driver. (M-O). Under GH146, TAU accumulated in the inner antennocerebral tract (iACT) leading into the calyx (M), its projections into the lateral horn (N) and antennal lobe interneurons and relay neurons (O). (P-R). Under OK72, TAU accumulated within the medial antennocerebral tract (mACT) leading to the calyx (P,Q), and antennal lobe glomeruli VM1 (R). (S-U) Antennal lobes of control, ablated and *mbm*^{1} animals stained with the α–SH3PX1 antibody, which appears to decorate a similar number of glomeruli apparently intact and morphologically normal. (V-W) Antennal lobes of GH146/UAS-*btau* stained with α-TAU. Arrow in V indicates the lateral cluster of relay interneurons, absent after HU treatment (arrow head) in W. All other interneurons and relay neurons labeled by GH146 were intact.

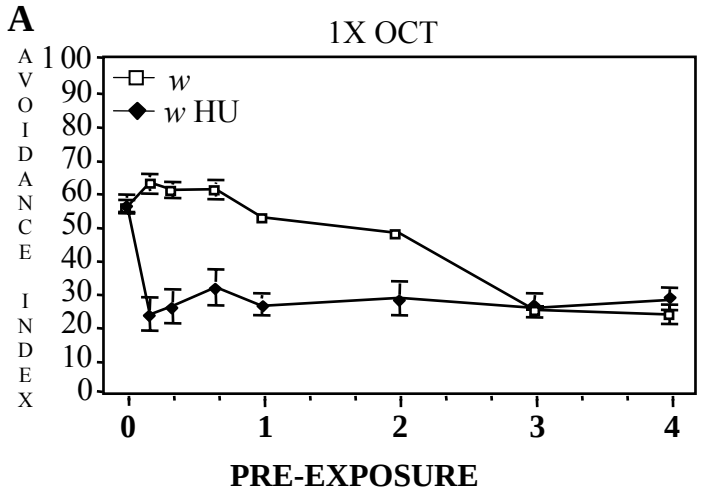

Figure 29. Olfactory habituation in structurally or functionally mushroom body-perturbed flies.

AIs are shown ± SEM. Positive values indicate avoidance and negative values indicate attraction. After pre-exposure for the indicated times avoidance of aversive odors was tested for 90 seconds and attraction for180 seconds. SD: significant differences. NSD: non significant differences.

(A) Time course of habituation onset in mushroom body ablated w^{1118} (*w* HU) compared to controls (*w*). Each minor subdivision in the graph represents 20 seconds. The AI for OCT avoidance after pre-exposure for the indicated times is shown. ANOVA indicated significant effects of pre-exposure times and genotype ($F_{(15,158)}$=69.21 $p<0.0001$). Subsequent ANOVAs for the effect of time revealed significant differences in OCT avoidance of both strains depending on the length of pre-exposure ($F_{(7,82)}$=22.41 $p<0.0001$, SD for *w*, and $F_{(7,76)}$=11.01 $p<0.0001$, SD for *w* HU). Compared to the performance of naïve *w* animals (0 time), significant differences ($p<0.0001$-Dunnett's test) in performance arose after 2 minutes of pre-exposure and remained highly significant at 3 and 4 minutes. In contrast, compared to naïve *w* HU, avoidance declined significantly ($p<0.0001$) after 10 seconds of pre-exposure and remained significantly different for up to 4 minutes of pre-exposure. Cross genotype comparisons demonstrated significant differences ($p<0.0001$) between *w* and *w* HU at 10, 20, 40 seconds, 1 and 2 minutes of pre-exposure, while the differences for longer pre-exposure times where not significant. Ablation of mushroom bodies precipitated premature habituation within 10 seconds of pre-exposure ($n\geq8$ for all measurements).

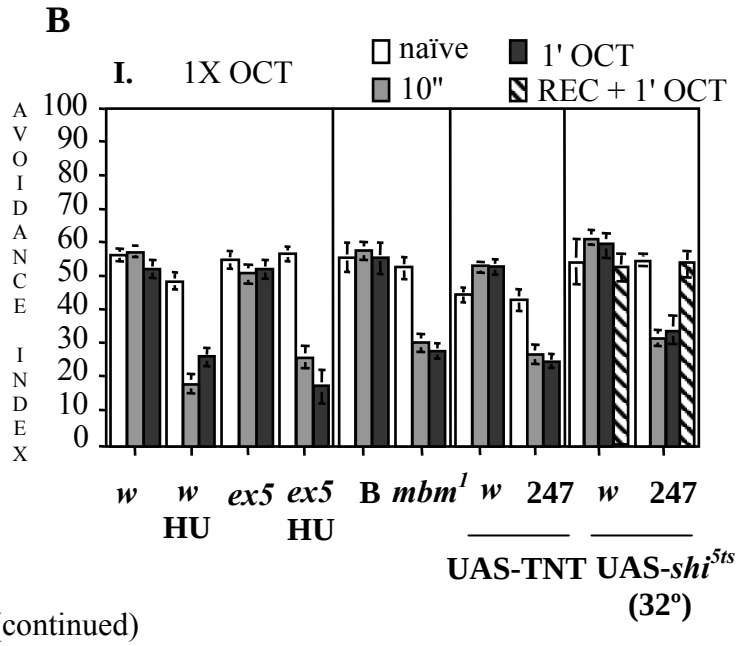

Figure 29. (continued)

(B) Premature habituation upon structural and functional perturbation of the mushroom bodies.

(I) Octanol avoidance following 10 or 60 seconds of octanol pre-exposure is shown for the indicated strains and appropriate controls. All structural or functional perturbations of the MBs did not affect naïve OCT avoidance. ANOVA for all naïve (open bars) genotypes ($F_{(9,89)}$=2.37 p<0.0123, NSD). In contrast, OCT pre-exposure precipitated significant deficits in MB-perturbed animals as indicated below:

Experimental ANOVAs. 10" OCT pre-exposure (light gray bars). Mushroom body ablated group (*w*, *w* HU, *ex5*, *ex5* HU): $F_{(3,37)}$=63.36 p<0.0001, SD. Genetic mushroom body perturbation group (Berlin, mbm^1): $F_{(1,18)}$=94.22 p<0.0001, SD. Permanent functional mushroom body abrogation group (*w*; UAS-TNT/+, *w*; 247/UAS-TNT): $F_{(1,17)}$=113.72 p<0.0001, SD. Conditional functional mushroom body abrogation group (UAS-shi^{5ts}/+, UAS-shi^{5ts}/+; 247/+ -SHI inactivation at 32°C for 15 minutes prior to testing-): $F_{(1,15)}$=55.87 p<0.0001, SD.

1' OCT pre-exposure (dark bars). Mushroom body ablated group (*w*, *w* HU, *ex5*, *ex5* HU): $F_{(3,32)}$=63.50 p<0.0001, SD. Genetic mushroom body perturbation group (Berlin, mbm^1): $F_{(1,16)}$= 72.58 p<0.0001, SD. Permanent functional mushroom body abrogation group (*w*; UAS-TNT/+, *w*; 247/UAS-TNT): $F_{(1,16)}$=55.06 p<0.0001, SD. Conditional functional mushroom body abrogation group (UAS-shi^{5ts}/+, UAS-shi^{5ts}/+; 247/+ -SHI inactivation at 32°C for 15 minutes prior to testing-): $F_{(1,17)}$=69.35 p<0.0001, SD. Subsequent Dunnett's tests among 10 second and 1 minute pre-exposed animals of the same genotype revealed no significant differences in performance. Similar analysis did not reveal significant differences in the performance of HU-treated w^{1188} animals and all other MB-perturbed genotypes after 10 second and 1-minute pre-exposures. For the shi^{ts} recovery group (striped bars-REC+1'OCT) UAS-shi^{5ts}/+, UAS-shi^{5ts}/+; 247/+ animals were subjected to SHI inactivation at 32°C for 15 minutes and then SHI recovery at 25°C for 15 minutes prior to testing. ANOVA for UAS-shi^{5ts}/+, UAS-shi^{5ts}/+; 247/+: $F_{(1,15)}$=0.1988 p<0.6630, NSD. Therefore, 10 seconds or 1 minute pre-exposure to 1X OCT resulted in significant deficits (p<0.0001) in subsequent octanol avoidance for all mushroom body perturbed flies compared to wild type, which is reversible in the case of SHI-mediated inactivation by allowing the protein to recover ($n \geq 8$ for all measurements).

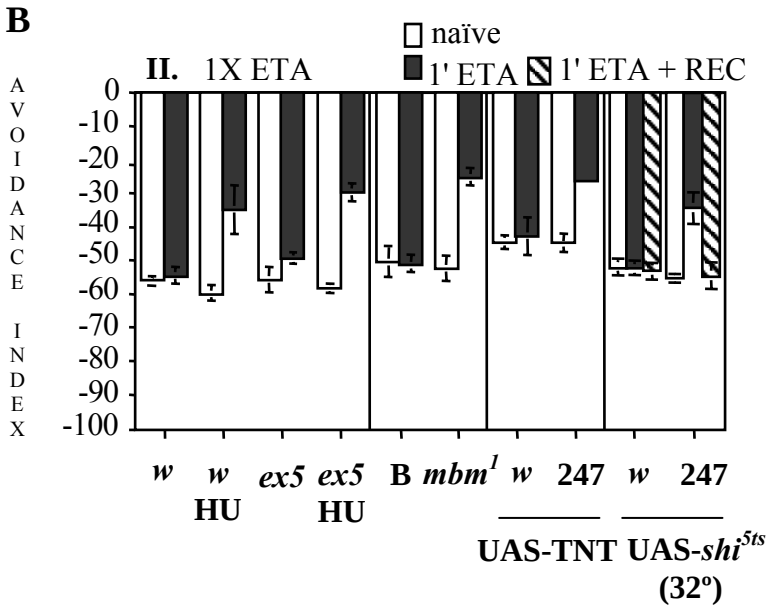

Figure 29. (continued)

(II) The AIs for Ethyl Acetate (ETA) attraction following 1 minute of ETA pre-exposure are shown. All groups and treatments were as described above in II. There were no significant differences in the performance of naïve animals (ANOVA: $F_{(9,87)}$=1.28 p<0.0598, NSD). However, compared to controls, significant differences were uncovered in the performance of mushroom body perturbed animals. Experimental ANOVAs. Mushroom body ablated group (*w*, *w* HU, *ex5*, *ex5* HU): $F_{(3,40)}$=65.84 p<0.0001, SD. Genetic mushroom body perturbation group (Berlin, mbm^1): $F_{(1,16)}$= 82.45 p<0.0001, SD. Permanent functional mushroom body abrogation group (*w*; UAS-TNT/+, *w*; 247/UAS-TNT): $F_{(1,14)}$=81.02 p<0.0001, SD. Conditional functional mushroom body abrogation group (UAS-shi^{5ts}/+, UAS-shi^{5ts}/+; 247/+ -SHI inactivation at 32°C for 15min prior to testing-): $F_{(1,16)}$=40.51 p<0.0001, SD. Recovery group UAS-shi^{5ts}/+, UAS-shi^{5ts}/+; 247/+: $F_{(1,15)}$=0.8574 p<0.3255, NSD. Therefore, as for aversive odors there was a significant decrease in ETA attraction of mushroom body perturbed animals after one minute pre-exposure to this odor (n≥7 for all measurements).

of antennal lobe glomeruli (Figure 28T and Figure 28U), it eliminated a number of antennal lobe inter-neurons and projection neurons (Figure 28V and (Stocker et al., 1997)). Thus, this method disrupts tissues in addition to the MBs that could be involved in olfactory habituation. Alternatively, the observed phenotype could be precipitated entirely by these missing antennal lobe neurons.

To differentiate between these two hypotheses and define the role of the MBs in olfactory habituation more precisely, we used two different methods to specifically disrupt them structurally and functionally. First we used a mutant, *mushroom body miniature* (*mbm*^{1}), with severely perturbed but not totally absent MBs (Heisenberg et al., 1985b; de Belle and Heisenberg, 1996) (Figure 28G-I), which does not appear to affect the antennal lobe structurally (Figure 28U and (de Belle and Heisenberg, 1996)). Second, we used the MB-specific GAL4 driver line 247 (Figure 28J-L) to drive expression of transgenes that mediate constitutive (Tetanus Light Chain-UASTNT), or conditional (*shibire*^{ts}- UAS-shi^{5ts} and UAS-shi^{10ts}- (Kitamoto, 2001)) neurotransmission blockade (see Materials and Methods), leaving these neurons intact but functionally compromised. *mbm*^{1}, *w*; 247/UAS-TNT, UAS-shi^{5ts}/+; 247/+ and 247/+; UAS-shi^{10ts}/+, were fully viable and fertile and did not exhibit gross morphological, neuroanatomical or behavioral aberrations. Furthermore these animals did not appear different from controls in osmotaxis and reactivity to footshock (Table 15, Figure 29B-naïve, Figure 32-naïve). Although the performance of animals bearing the single UAS-shi^{5ts} transgene, is shown in all subsequent figures, identical results were obtained with the two-insert line UAS-shi^{10ts} for all experiments, but not shown for simplicity.

Remarkably, a 10 second OCT pre-exposure was sufficient to precipitate significant habituation in all MB-perturbed genotypes, which was similar to that obtained with hydroxyurea treated animals (Figure 29B.I). Identical results were obtained with pre-exposure to the attractive odor ETA (Figure 29B.II). Normal osmotaxis towards ETA by animals with compromised MBs is in contrast to a recently published report claiming impairment in attraction in such animals (Wang et al., 2003). This difference may be because higher concentrations of odors were used in our experiments and the apparatus to deliver them to the animals was significantly different. Since 60-second and 10-second pre-exposure precipitated similar degrees of habituation (Figure 29B.I), we used the former in all subsequent experiments because of result consistency and ease of manipulations. Functional recovery of the temperature sensitive transgenic dynamin prior to pre-exposure and testing (REC+OCT) resulted in normal responses (Figure 29B.I and B.II, hatched bars), indicating that neither the heat treatment, nor mere expression of the transgene affected habituation. Moreover, animals harboring recovered dynamin habituated identically to controls (not shown), suggesting that the heat treatment or prior inactivation of the transgenic dynamin itself did not disrupt the process. These results indicated that the deficits observed in shi^{ts} animals under non-permissive conditions were indeed caused by the neurotransmission blockade in the MBs and not by other structural or functional alterations in these neurons.

If indeed the mushroom bodies are necessary for evaluation of experience dependent olfactory information and protection from premature habituation, then blocking the flow of such information to these neurons should precipitate deficits in

habituation similar to functional perturbation of the MBs. To test this we blocked neurotransmission from the medial (mACT) and inner (iACT) antenocerebral tracks. An additional reason to investigate the contribution of the GH146-marked iACT neurons is that the driver directs expression in a subset of antennal lobe interneurons and projection neurons ablated by hydroxyurea treatment (Figure 28W). Driver OK72 directs expression in the mACT (Figure 28P and Figure 28Q and antennal lobe glomeruli VM1 (Figure 28R), VM4 and DL1, (Devaud et al., 2003), which do not appear to be involved in perception of OCT, ETA or modest concentrations of BNZ (Devaud et al., 2003).

Inhibition of neurotransmission via the iACT and the mACT using the *UAS-TNT* and *UAS-shi^{ts}* transgenes precipitated deficits in OCT avoidance following either a 10 or 60 second pre-exposure to the same odor, similar to that obtained with MB perturbation (Figure 30A). Expression of the UAS-shi^{ts}, or exposure of control flies to 32^{o}C alone had no effect because recovery of the temperature sensitive dynamin prior to the pre-exposure and testing phases resulted in performance indistinguishable from that of controls (Figure 30A, REC+OCT). Thus, the deficit was the result of inhibiting neurotransmission via the mACT and iACT. Since silencing mACT and iACT synapses allows normal naïve responses, these defects are not the result of the flies becoming anosmic (Figure 31) or unable to engage the appropriate behavioral response (avoidance or attraction) to odors. Rather, the phenotypes of animals with disrupted iACT and mACT neurotransmission suggest that processes necessary for evaluating experience dependent olfactory information and mediating proper behavioral responses to such stimuli occur in their postsynaptic, MB and LH neurons and their disruption is likely

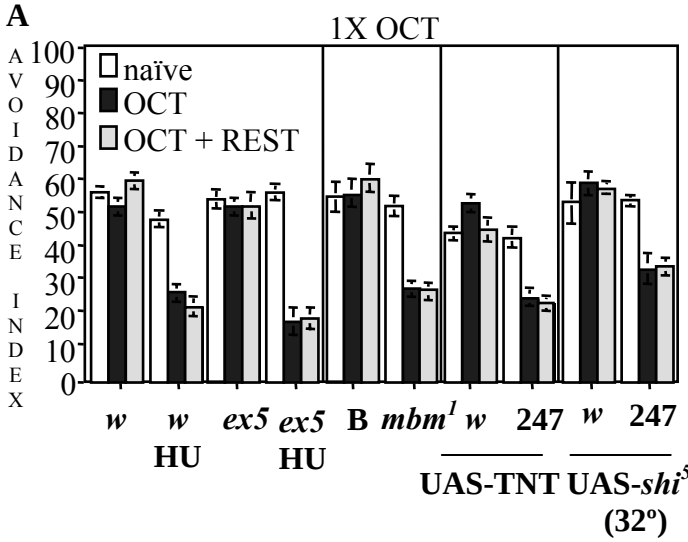

Figure 30. Spontaneous recovery from olfactory habituation and dishabituation requires functional mushroom bodies

SD: significant differences. NSD: Non significant differences.
(A) AIs for OCT avoidance ± SEM are shown for naïve flies (open bars), following pre-exposure for 1 minute to OCT (dark bars), or after 1 minute pre-exposure to OCT followed by 6 minutes of rest (light gray bars). No significant differences were uncovered for naïve flies irrespective of genotype (ANOVA: $F_{(9,89)}$= 2.37 $p<0.0123$, NSD).
Experimental ANOVAs. Mushroom body ablated group (*w*, *w* HU, *ex5*, *ex5* HU): $F_{(11,95)}$=23.85 $p<0.0001$, SD. Subsequent Dunnett's tests revealed significant differences between naïve and pre-exposed ($p<0.0001$) HU-treated animals, but not for controls irrespective of treatment. The performances of HU-treated animals tested immediately after pre-exposure (OCT), or 6 minutes later (OCT + REST) were not significantly different indicating no spontaneous recovery. Genetic mushroom body perturbation group (Berlin, mbm^1): $F_{(5,47)}$=35.84 $p<0.0001$, SD. The differences between naïve and pre-exposed mbm^1 were significant, but pre-exposed mbm^1 (OCT) performed identically with (OCT +REST) indicating no recovery. Permanent functional mushroom body abrogation group (*w*; UAS-TNT/+, *w*; 247/UAS-TNT): $F_{(5,48)}$=38.12 $p<0.0001$, SD. The significant difference was attributed to the depressed performance of pre-exposed *w*; 247/UAS-TNT, compared to *w*; UAS-TNT/+ controls, but there were no differences in performance of *w*; 247/UAS-TNT (OCT) compared to *w*; 247/UAS-TNT (OCT+REST). Conditional functional mushroom body abrogation group (UAS-shi^{5ts}/+, UAS-shi^{5ts}/+; 247/+ -SHI inactivation at 32°C for 15 minutes prior to testing-): $F_{(5,50)}$=25.11 $p<0.0001$, SD, because of the difference between pre-exposed UAS-shi^{5ts}/+; 247/+ and UAS-shi^{5ts}/+, but again the performance of UAS-shi^{5ts}/+; 247/+(OCT) was not different from UAS-shi^{5ts}/+; 247/+(OCT+REST). Similar results were obtained with UAS-shi^{10ts} transgenic animals (not shown). Structural or functional perturbations of the mushroom bodies did not allow spontaneous recovery ($n\geq7$ for all measurements).

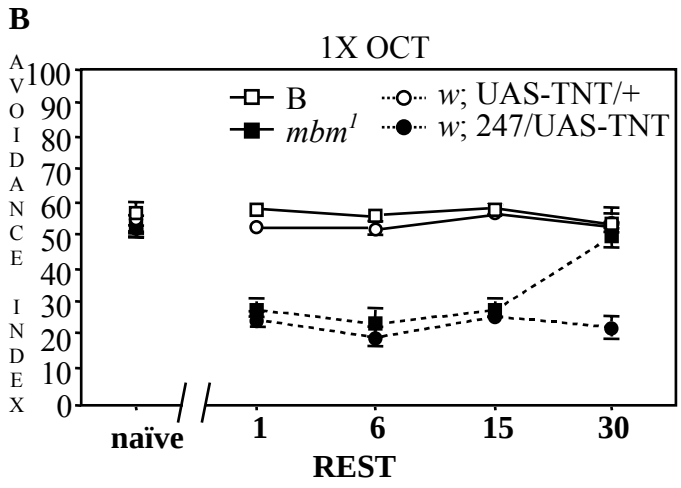

Figure 30. (continued)

(B) Spontaneous recovery in MB-perturbed animals. AIs for OCT avoidance ± SEM are shown after 1 minute pre-exposure to OCT followed by different intervals of rest. No significant differences were uncovered for naïve flies irrespective of genotype (ANOVA: $F_{(3,29)}$= 0.3176 p<0.8125, NSD). However, ANOVA indicated significant differences ($F_{(7,62)}$=38.75 p<0.0001, SD) in the performance of animals in the "genetic mushroom body perturbation group" (Berlin, *mbm*^{1}). Subsequent Dunnett's tests between *B* and *mbm*^{1} demonstrated significant reduction in OCT avoidance (p<0.0001) at the 1, 6 or 15-minute rest intervals, but no significant difference after a 30 minute rest interval between training and testing. Similarly for the "permanent functional mushroom body abrogation" group (*w*; UAS-TNT/+, *w*; 247/UAS-TNT) ANOVA indicated significant differences ($F_{(7,61)}$=48.67 p<0.0001, SD) among the AIs. Subsequent planned comparisons between *w*; UAS-TNT/+ and *w*; 247/UAS-TNT demonstrated significant reduction in OCT avoidance (p<0.0001) at all rest intervals including 30 minutes of rest in contrast with the performance of *mbm*^{1}animals after this rest interval (n≥7 for all measurements).

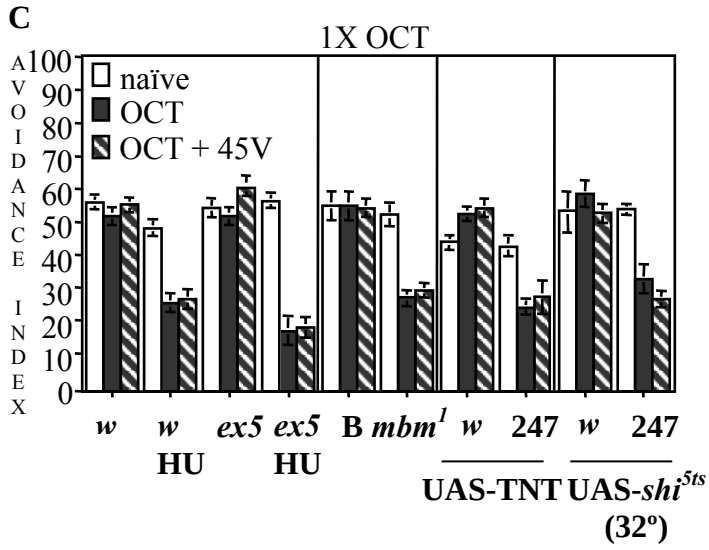

Figure 30. (continued)

(C) Dishabituation in MB-perturbed animals. AIs for OCT avoidance are shown ± SEM for naïve flies (open bars), following pre-exposure for 1 minute to OCT (dark bars), or after 1 minute pre-exposure to octanol followed by a single 45V electric shock (thickly hatched bars). ANOVA for naïve flies of all genotypes, $F_{(9,89)}= 2.37$ $p<0.0123$, NSD. Experimental ANOVAs. Mushroom body ablated group (*w*, *w* HU, *ex5*, *ex5* HU): $F_{(11,95)}=12.25$ $p<0.0001$, SD. Genetic mushroom body perturbation group (Berlin, mbm^{1}): $F_{(5,47)}=15.24$ $p<0.0001$, SD. Permanent functional mushroom body abrogation group (*w*; UAS-TNT/+, *w*; 247/UAS-TNT): $F_{(5,48)}=19.25$ $p<0.0001$, SD. Conditional functional mushroom body abrogation group (UAS-shi^{5ts}/+, UAS-shi^{5ts}/+; 247/+ -SHI inactivation at 32°C for 15min prior to testing-): $F_{(5,50)}=12.22$ $p<0.0001$, SD. Subsequent Dunnett's tests within each group revealed that the 45V shock (OCT+45V) did not precipitate significant differences in the performance of all MB perturbed animals compared to pre-exposed animals (OCT) of the same genotype indicating lack of dishabituation. ($n \geq 7$ for all measurements).

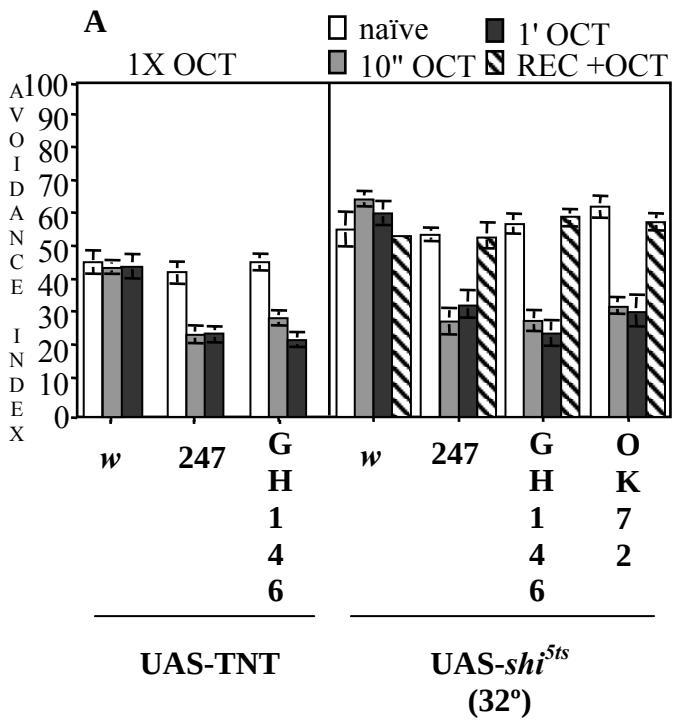

Figure 31. Premature olfactory habituation upon inhibition of neurotransmission in the iACT and mACT

AIs ± SEM are shown for OCT avoidance following OCT pre-exposure. SD: significant differences. NSD: no significant differences. Naïve: open bars. 10" OCT: light gray bars. 1' OCT: dark bars.
(I) Experimental ANOVAs. Permanent functional mushroom body abrogation group (*w*; UAS-TNT/+, *w*; 247/UAS-TNT): Naïve: $F_{(2,26)}$=2.05 p<0.0165, NSD. 10" OCT: $F_{(2,22)}$=22.67 p<0.0001, SD. Dunnett's tests revealed significant differences (p< 0.0001) among *w*; 247/UAS-TNT and *w*; UAS-TNT / GH146 and *w*; UAS-TNT/+ controls. 1' OCT (dark bars): $F_{(1,25)}$=56.99 p<0.0001, SD. The differences among experimental and control groups were significant (p< 0.0001- Dunnett's tests). The OK72/UAS-TNT animals were not viable.
Conditional functional mushroom body abrogation group (UAS-shi^{5ts}/+, UAS-shi^{5ts}/+; 247/+ -SHI inactivation at 32°C for 15min prior to testing-): Naïve: $F_{(3,33)}$= 4.41 p<0.0078, NSD. 10" OCT: $F_{(3,34)}$=43.23 p<0.0001, SD. Dunnett's tests revealed significant differences (p< 0.0001) among UAS-shi^{5ts}/+ and UAS-shi^{5ts}/+; 247/+, UAS-shi^{5ts}/+; GH146/+, UAS-shi^{5ts}/+; OK72/+ animals. 1' OCT: $F_{(3,32)}$=32.64 p<0.0001, SD. The differences among experimental and control groups were significant (p< 0.0001- Dunnett's). Recovery group (REC+OCT-stripped bars): $F_{(3,33)}$=2.41 p<0.1427, NSD indicating full performance recovery of the experimental groups upon recovery of the SHI^{ts} protein. Pre-exposure to OCT either for 10 or 60 seconds resulted in osmotactic habituation upon inhibition of neurotransmission via the iACT, or the mACT. (n≥7 for all measurements).

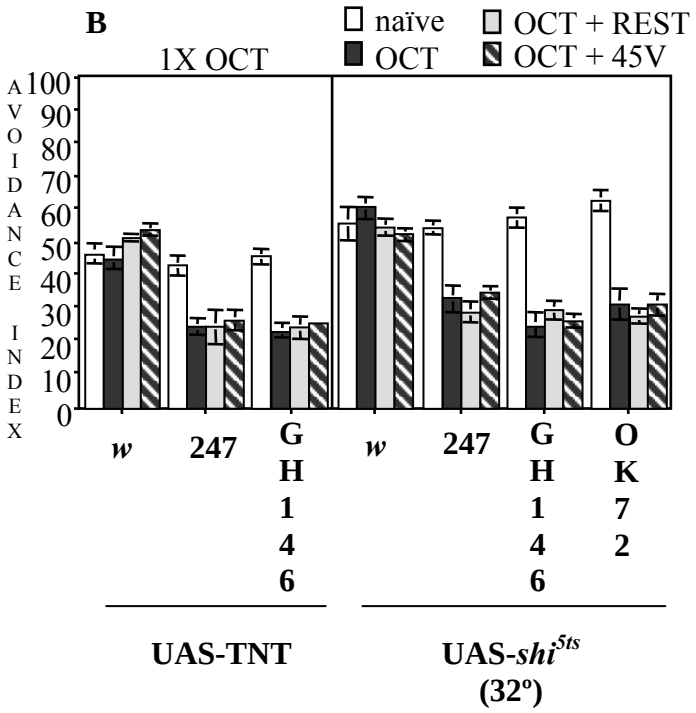

Figure 31. (continued)

(II) iACT and mACT neurotransmission are required for spontaneous recovery and dishabituation of osmotactic habituation. Spontaneous recovery (REST, light gray bars) and dishabituation (OCT+45V-thickly striped bars) by a single 45V electric shock following 60 second pre-exposure to OCT are shown.
Experimental ANOVAs. Permanent functional abrogation group (*w*; UAS-TNT/+, *w*; 247/UAS-TNT and *w*; UAS-TNT / GH146): Naïve $F_{(2,26)}=2.05$ $p<0.0165$, NSD. Group: $F_{(11,62)}=13.89$ $p<0.0001$ SD. Subsequent Dunnett's tests revealed that there were significant differences from the performance of naïve animals of each experimental genotype, but no significant differences in the performance of *w*; 247/UAS-TNT and *w*; UAS-TNT / GH146 animals after OCT pre-exposure irrespective of whether they were allowed to recover spontaneously (OCT+REST) or treated with a 45V electric shock (OCT+45V). The OK72/UAS-TNT animals were not viable.
Conditional functional abrogation group (UAS-shi^{5ts}/+, UAS-shi^{5ts}/+; 247/+, UAS-shi^{5ts}/+; GH146/+, UAS-shi^{5ts}/+; OK72/+-SHI inactivation at 32°C for 15min prior to testing-): Naïve: $F_{(3,33)}= 4.41$ $p<0.0078$, NSD. Group: $F_{(11,88)}=24.66$ $p<0.0001$, SD. Subsequent Dunnett's tests revealed that there were significant differences from the performance of naïve animals of each experimental genotype, but no significant differences in the performance of UAS-shi^{5ts}/+; 247/+, UAS-shi^{5ts}/+; GH146/+, UAS-shi^{5ts}/+; OK72/+ animals after OCT pre-exposure irrespective of whether they were allowed to recover spontaneously (OCT+REST) or treated with a 45V electric shock (OCT+45V). (n>7 for all measurements).

causal of the observed premature habituation phenotype. A role for the LH as a spatial map of olfactory information and odor recognition mediating non-associative, direct responses to odors has been proposed (Marin et al., 2002; Tanaka et al., 2004) and these responses may be modified by the MBs in an experience-dependent manner. Therefore, the premature habituation observed when silencing mACT and iACT synapses is likely the consequence of preventing information flow to the MBs and LH and not because neurons in these tracks are themselves essential for the process.

Spontaneous recovery and dishabituation require MB function

We tested the MB-perturbed animals for spontaneous recovery of their osmotactic response by allowing 6 minutes of rest after 1-minute pre-exposure to OCT, a time adequate for control strains to recover after a more strenuous 4-minute pre-exposure (Figure 27.I and II). All genotypes with perturbed MBs failed to recover within the allotted 6-minute period (Figure 30.I). Similar results were obtained for 10-second pre-exposure to OCT and ETA (not shown). Recovery to naïve levels of osmotaxis was apparent 30 minutes post pre-exposure, only for *mbm*^{1} animals and not for animals with TNT-mediated constitutive neurotransmission blockade (Figure 30B), or HU-ablated MBs (not shown). The results indicate that functional mushroom bodies, or functional MB/LH communication are required for spontaneous recovery. Consistent with this interpretation, presence of even vestigial MBs (and the consequent reduced number of MB/LH synapses) in *mbm*^{1} animals allowed recovery, albeit 10 times slower than in controls, suggesting that the long delay may be a consequence of the drastic

reduction in MB neurons. In addition, MB-perturbed animals could not be dishabituated with a single 45-Volt footshock (Figure 30.II), multiple 45-Volt or higher voltage footshocks (not shown). However, naïve avoidance of the stimuli appeared normal in all MB-perturbed animals (Table 15). Therefore, structurally and functionally intact MBs were required for dishabituation. Moreover, silencing MB synapses did not allow either spontaneous recovery or dishabituation, suggesting that both processes must engage MB afferent neurons.

In addition, preventing olfactory information flow to the MBs by silencing iACT and mACT neurotransmission did not allow spontaneous recovery within the 6-minute period adequate for controls (Figure 31B and Figure 27A.I and 28A.II). In addition, these animals were not dishabituated with a 45-Volt footshock (Figure 31B) despite their normal naïve response to the latter (Table 15). Similar results were obtained with BNZ and ETA pre-exposure (not shown). This is consistent with the hypothesis that the iACT and mACT are necessary for protection from premature habituation spontaneous recovery and dishabituation because they provide the MBs with olfactory information where the stimuli are evaluated. It appears then, that MB neurons are either central, or an essential part of a network evaluating experience-dependent olfactory stimuli and mediating appropriate responses to them.

Protection from premature habituation to footshock requires the mushroom bodies

We chose to investigate whether *Drosophila* could habituate to electric footshocks because the number and strength of stimuli could be easily and reliably adjusted, a new apparatus was not necessary since the assay could be conducted in a

standard T-maze, and we had extensive experience with this system. There were three compelling reasons to establish a habituation assay utilizing a sensory modality other than olfaction. First, to investigate whether MB perturbed animals exhibit deficient protection from habituation to non-olfactory stimuli. Second, to investigate the involvement of the iACT and mACT in protecting from habituation to non-olfactory stimuli. Third, if footshock is sensed as a mechanosensory stimulus and as suggested by Ito *et al.* (Ito et al., 1998), mechanosensory information is transmitted to the MBs via the LH, this paradigm would employ a different route to test MB involvement in pre-experienced stimulus evaluation and response.

To avoid the potential complexity of hydroxyurea ablations of the MBs, we elected to investigate habituation to footshock using the genetic mutant mbm^{1}, and constitutive inhibition of neurotransmission using *w*; 247/UAS-TNT animals. Naïve control animals exhibited robust avoidance of 15, 45-Volt footshocks delivered during the 90-second testing period (Figure 32A.I and Table 15). Pre-exposure to 1 or 4 footshocks prior to testing did not have any apparent effect, but avoidance declined significantly after pre-exposure to 8 and 11 45-Volt shocks (Figure 32A.I). Therefore, as for olfactory habituation, avoidance of repetitive footshocks declined after pre-exposure to multiple stimuli, suggesting that the animals were protected from premature habituation. The 44% decline in footshock avoidance following pre-exposure to 11, 45V shocks was not the result of stimulus induced fatigue or paralysis for the following reasons. First, pre-exposed animals distributed equally in the arms of the maze and did not congregate in the center of the maze in absence of test footshocks. Second,

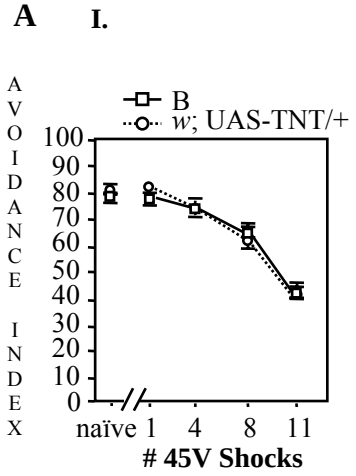

Figure 32. Functional mushroom bodies are necessary for normal habituation to electric footshock

AIs ± SEM are shown for electric footshock avoidance (15 shocks during the 90 second choice period) for naïve and flies pre-exposed to shock as indicated. SD: significant differences. NSD: no significant differences.
(A) Habituation to 45V electric shock
(I) Avoidance of 45V electric shocks in naïve flies was not significantly different between the two different control strains, B and *w*; UAS-TNT/+ (ANOVA (naïve): $F_{(1,16)}=2.06$ $p<0.1336$, NSD). Pre-exposure to 45V shock had significant effects on subsequent shock avoidance dependent on the number of shocks. ANOVA ($F_{(7,64)}=42.68$ $p<0.0001$, SD). Subsequent planned comparisons between naïve and pre-exposed flies revealed significant reduction in 45V avoidance ($p<0.0001$) after pre-exposure to 8 or 11 shocks, but no significant differences after 1 or 4, 45V shocks ($n\geq 8$ for all measurements)

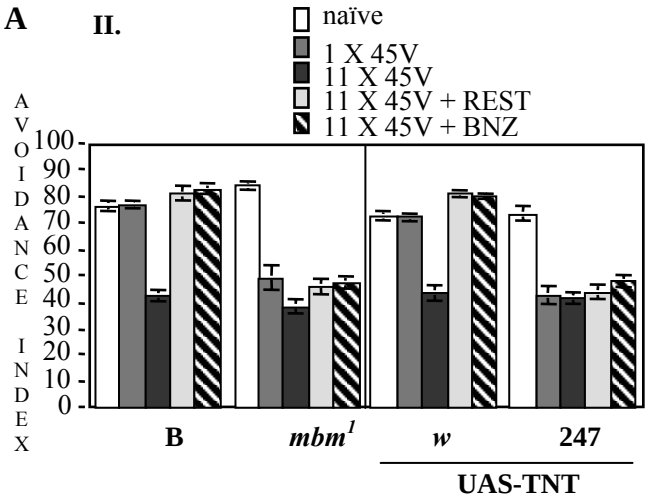

Figure 32. (continued)

(II) Habituation to 45V electric shock in control and mushroom body perturbed animals. Avoidance of 15, 45V electric shocks in naïve flies (open bars) was not significantly different from that of naïve structurally (*mbm*^{1}) and functionally (247/UAS-TNT) perturbed mushroom body animals. ANOVA (naïve): $F_{(3,31)}$=3.86 p<0.2234, NSD. In contrast, exposure to 1X45V electric shock (light gray bars) had significant effects in the MB-perturbed animals compared to controls. ANOVA: Genetic mushroom body perturbation group (Berlin, *mbm*^{1}): $F_{(1,16)}$=78.65 p<0.0001, SD. Permanent functional mushroom body abrogation group (*w*; UAS-TNT/+, *w*; 247/UAS-TNT): $F_{(1,18)}$=75.44 p<0.0001, SD. Subsequent Dunnett's tests revealed a significant decrease (p<0.0001) in the performance of *mbm*^{1} and *w*; 247/UAS-TNT compared to their respective controls (n≥7 for all measurements). Exposure to 11 X 45V (dark gray bars) electric shocks. ANOVA: Genetic mushroom body perturbation group (Berlin, *mbm*^{1}): $F_{(1,17)}$=0.75 p<0.5438, NSD and permanent functional mushroom body abrogation group (*w*; UAS-TNT/+, *w*; 247/UAS-TNT): $F_{(1,18)}$=1.88 p<0.0971 SD, indicating that 11 45V electric shocks resulted in similar reductions in footshock avoidance irrespective of genotype(n≥7 for all measurements).
Spontaneous recovery (11 X 45V + REST-light gray bars). ANOVA: Genetic mushroom body perturbation group (Berlin, *mbm*^{1}): $F_{(1,15)}$=116.49 p<0.0001, SD. Permanent functional mushroom body abrogation group (*w*; UAS-TNT/+, *w*; 247/UAS-TNT): $F_{(1,16)}$=72.73 p<0.0001, SD. Dunnett's tests demonstrated significant differences in recovery between MB-perturbed strains and their respective controls (p<0.0001 for both comparisons), indicating lack of recovery (n≥7 for all measurements).
Dishabituation (11 X 45V + BNZ-thickly hatched bars). ANOVA: Genetic mushroom body perturbation group (Berlin, *mbm*^{1}): $F_{(1,16)}$ =62.31 p<0.0001, SD. Permanent functional mushroom body abrogation group (*w*; UAS-TNT/+, *w*; 247/UAS-TNT): $F_{(1,16)}$=65.25 p<0.0001, SD. The significant differences were attributable to lack of dishabituation in the MB-perturbed strains compared to their respective controls. Dunnett's tests revealed that there was no significant difference in the performance of *mbm*^{1} and *w*; 247/UAS-TNT animals after 1 and 11 shocks or after spontaneous recovery and dishabituation. (n≥7 for all measurements).

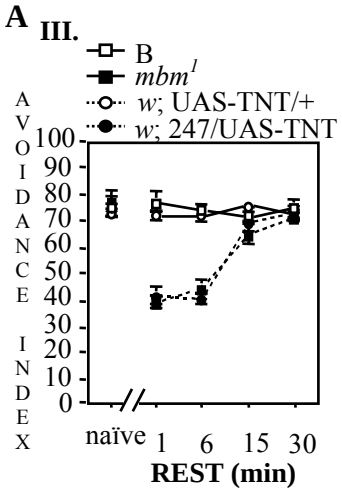

Figure 32. (continued)

(III) Recovery of habituation to 45V electric shock in control and mushroom body perturbed animals. Avoidance of 15, 45V electric shocks in naïve flies was not significantly different from that of structurally (*mbm*^{1}) and functionally (247/UAS-TNT) perturbed mushroom body animals. ANOVA (naïve): $F_{(3,31)}$=0.5567 p<0.6480, NSD. In contrast, exposure to a single 45V had significant effects on the genetic mushroom body perturbation group depending on rest interval between training and testing as indicated by ANOVA ($F_{(7,63)}$=31.73 p<0.0001, SD). Subsequent planned comparisons between *B* and *mbm*^{1} demonstrated significant reduction in 45V avoidance (p<0.0001) at the 1 and 6-minute rest intervals, but no significant avoidance differences after a 15 or 30 minute rest interval between training and testing. Permanent functional mushroom body abrogation group (*w*; UAS-TNT/+, *w*; 247/UAS-TNT): ANOVA indicated significant differences ($F_{(7,61)}$=34.01 p<0.0001, SD) among the AIs. Subsequent planned comparisons between *w*; UAS-TNT/+ and *w*; 247/UAS-TNT demonstrated significant reduction in 45V avoidance (p<0.0001) at the 1 and 6 minute rest intervals, but no significant difference after a 15 or 30 minute rest before testing. This suggested that habituation to electric shock can spontaneously recover even in animals with non-functional mushroom bodies, albeit after a longer rest than controls ($n \geq 7$ for all measurements).

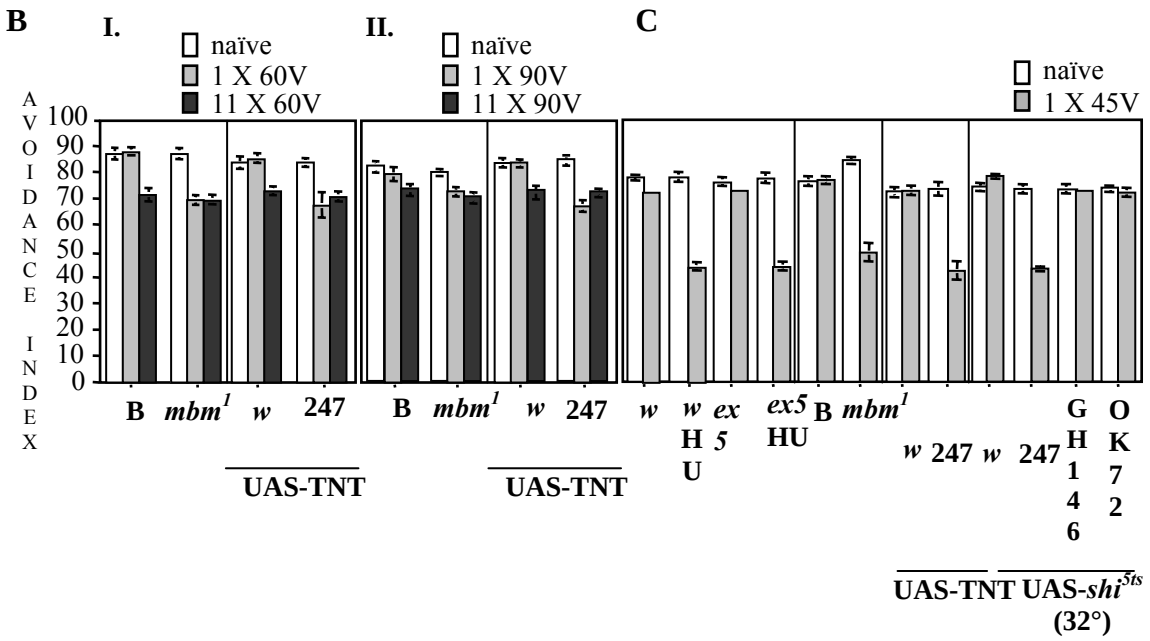

Figure 32. (continued)

(B) Stimulus intensity was inversely proportional to the magnitude of habituation.
(I) 60V. ANOVAs. Naïve: for all genotypes ($F_{(3,34)}$=0.22 p<0.9994, NSD).
1 X 60V. Genetic mushroom body perturbation group (Berlin, *mbm*^{1}): $F_{(1,15)}$=24.28 p<0.0001 SD. Permanent functional mushroom body abrogation group (*w*; UAS-TNT/+, *w*; 247/UAS-TNT): $F_{(1,16)}$=9.32 p<0.0001, SD. The significance stemmed from the avoidance decrement of MB-perturbed animals compared to their respective controls (p<0.0001 for both) (n≥8 for all measurements). 11 X 60V. Genetic mushroom body perturbation group (Berlin, *mbm*^{1}): $F_{(1,17)}$=0.96 P<0.8851, NSD and permanent functional mushroom body abrogation group (*w*; UAS-TNT/+, *w*; 247/UAS-TNT): $F_{(1,18)}$=1.92 p<0.6291, NSD (n≥8 for all measurements).
(II) 90V. ANOVAs. Naïve for all genotypes: $F_{(3,31)}$=0.78 p<0.9987, NSD).
1 X 90V. Genetic mushroom body perturbation group (Berlin, *mbm*^{1}): $F_{(1,16)}$=24.28 p<0.0001, SD. Permanent functional mushroom body abrogation group (*w*; UAS-TNT/+, *w*; 247/UAS-TNT): $F_{(1,16)}$=16.40 P<0.0001, SD. Dunnett's tests indicated significant differences (p<0.0001) in the performance of *mbm*^{1} and /+, *w*; 247/UAS-TNT from their respective controls (n≥7 for all measurements).
11 X 90V. Genetic mushroom body perturbation group (Berlin, *mbm*^{1}): $F_{(1,20)}$=1.22 p<0.8765, NSD. Permanent functional mushroom body abrogation group (*w*; UAS-TNT/+, *w*; 247/UAS-TNT): $F_{(1,17)}$=2.84 p<0.9125 NSD (n≥7 for all measurements).
(C) Functional mushroom bodies, but not the iACT and mACT are required for protection from habituation to footshock. ANOVAs. Naïve for all genotypes: $F_{(11,95)}$= 4.41 p<0.0078, NSD. 1 X 45V. Mushroom body ablated group (w, w HU, ex5, ex5 HU): $F_{(3,30)}$=54.12 p<0.0001, SD. Genetic mushroom body perturbation group (Berlin, mbm^{1}): $F_{(1,16)}$=82.84 p<0.0001, SD. Permanent functional mushroom body abrogation group (w; UAS-TNT/+, w; 247/UAS-TNT): $F_{(1,17)}$=60.25 p<0.0001, SD. Conditional functional abrogation group (UAS-shi^{5ts}/+, UAS-shi^{5ts}/+; 247/+, UAS-shi^{5ts}/+; GH146/+, UAS-shi^{5ts}/+; OK72/+): $F_{(3,30)}$=11.87 p<0.0001, SD. Subsequent Dunnett's tests indicated significant differences between MB-perturbed animals and their respective controls (p<0.0001) for all genotypes except UAS-shi^{5ts}/+; GH146/+, UAS-shi^{5ts}/+; OK72/+ and UAS-shi^{5ts}/+ (n>7 for all measurements).

locomotion away from, or towards aversive and attractive odors was not affected by footshock pre-exposure (not shown).

The pre-exposure-dependent decline in footshock avoidance conformed to habituation parameters as for the olfactory paradigm. First, it spontaneously recovered to naïve levels within 6 minutes (Figure 32A.II). Significantly, it was fully reversible (dishabituated), with a 15-second olfactory stimulus (BNZ) delivered immediately after pre-exposure and prior to testing (Figure 32A.I). Again, attempts to dishabituate with visual (strong white light), or strong mechanical stimulation (vortexing) failed (not shown). Third, the magnitude of habituation declined as the strength of the pre-exposure stimuli increased. The 44% avoidance decline observed with 45V pre-exposure was reduced to 20% and 13% respectively when stimulus intensity was increased to 60-Volt and 90-Volt shocks (Figure 32B.I and B.II). Therefore, control animals habituated to footshocks after repeated stimulation and could be dishabituated with a brief strong odor stimulus. Notably a number of footshocks (5-8) were necessary to obtain a response decrement. This indicates a refractory period to obtaining a habituated response akin to that in the olfactory paradigm. One of the advantages of the footshock paradigm is that the number and strength of stimuli required to obtain habituation can be determined more precisely. Consistent with this, nearly twice as many footshocks were necessary to obtain habituation of similar magnitude with 90-Volt as that with 45-Volt stimuli (not shown).

To investigate the role of the MBs in habituation to footshock we disrupted these neurons structurally and functionally utilizing the methods described above. Naïve

mbm^{1}, *w*; 247/UAS-TNT and controls avoided 45-Volt stimuli equally (Table 15), suggesting that the MBs are not essential for the response to footshock *per se.* However, their avoidance declined by 45-47% following pre-exposure to a single 45-Volt footshock in contrast to control animals that required 11 such footshocks for a similar decrease in avoidance. Therefore, similar to olfactory stimulation, MB-perturbed animals appeared to habituate prematurely to footshock stimuli. In addition, *mbm*^{1} and *w*; 247/UAS-TNT flies habituated after pre-exposure to a single stimulus of increased strength but the magnitude of habituation was decreased (Figure 32B.I and 32B.II). In contrast to controls, MB-perturbed animals were unable to be dishabituated with exposure to BNZ (Figure 32A.II), although avoidance of this odor was normal (Table 15). Unlike control strains, *mbm*^{1} and *w*; 247/UAS-TNT did not spontaneously recover within 6 minutes, but interestingly, both strains recovered shock avoidance to control levels within 15 minutes after pre-exposure (Figure 32A.III). Similar recovery was observed after pre-exposure to olfactory stimuli in *mbm*^{1} animals, but is in contrast to the inability of *w*; 247/UAS-TNT animals to recover from such pre-exposure within the allotted 30 minutes. These results suggest that although structurally and functionally intact MBs are necessary for normal recovery from footshock habituation, additional neurons likely involved in mediating the response to this type of stimulus could mediate recovery, albeit it with lower efficiency.

In addition to *mbm*^{1} and *w*; 247/UAS-TNT, failure to be protected from habituation to 45-Volt footshock was observed with hydroxyurea MB-ablated and UAS-shi^{5ts}/+; 247/+ animals (Figure 32C). This data suggested that functional mushroom

bodies are necessary to protect from habituation to repetitive mild footshock. Importantly, unlike for olfactory habituation, inhibition of neurotransmission in the iACT and mACT did not result in premature habituation (Figure 32C). This is consistent with data suggesting that these ascending tracks transmit solely olfactory stimuli to the MB and LH (Stocker et al., 1997; Marin et al., 2002; Devaud et al., 2003) and thus not expected to be involved in footshock information flow to these brain areas.

Collectively, the data support the hypothesis that as for olfaction the mushroom bodies are essential neural centers mediating responses to pre-experienced footshock stimuli. Furthermore, the data suggest that these areas of the fly brain are essential for stimulus evaluation likely to underlie the refractory period when animals are protected from habituation.

DISCUSSION

Two novel habituation paradigms

A number of studies over the last 20 years have established that *Drosophila* habituate to a number of stimuli using various experimental protocols such as habituation of the landing response (Rees and Spatz, 1989; Asztalos et al., 1993), the proboscis extension reflex (Duerr and Quinn, 1982), the cleaning reflex (Corfas and Dudai, 1989), visual startle reflex (Engel and Wu, 1996; Engel et al., 2000) and leg position (Jin et al., 1998). In general, these assays were tedious because restrained or decapitated animals were used. In some preparations the neuronal circuits mediating the behavior were uncertain (Duerr and Quinn, 1982; Rees and Spatz, 1989; Asztalos et al.,

1993), while paradigms engaging defined neuronal circuits focused primarily on proprioceptive reflexes of thoracic sensory neurons, coupling behavioral manipulation and electrophysiology (Corfas and Dudai, 1989; Engel and Wu, 1996; Jin et al., 1998; Engel et al., 2000). We have established two simple paradigms of habituation to olfactory and electric footshock stimuli. The simplicity of both paradigms makes them suitable to conduct genetic screens aiming to elucidate the molecular basis of habituation. In contrast to previous assays, these paradigms utilize populations of freely moving flies thus eliminating animal manipulations and the behavioral constraints of tethered or decapitated animals. Although in both cases locomotor responses were engaged, the choice of how to respond to a previously experienced stimulus involved specific neurons of the CNS, the MBs and LH.

The pre-exposure dependent decline in osmotactic responses and the pre-exposure dependent decline in footshock avoidance fit the parametric characteristics of habituation described by Thomson and Spencer (Thomson and Spencer, 1966) and not those of desensitization or fatigue. In both paradigms there was a decrease in response after repeated or prolonged application of the stimulus, the decrement returned to naïve levels if the stimuli were withheld (spontaneous recovery), the degree of performance decline appeared to be inversely proportional to stimulus strength and be readily reversed by an unrelated noxious stimulus (dishabituation). Taken together our results do not definitively exclude the possibility that some sensory fatigue, or desensitization may occur, especially upon continuous odor presentation. However, the complete reversal of the decrement upon dishabituation suggests that if any, the contribution of

these processes in the observed behavioral response are likely to be minor. Moreover, *bona fide* habituation to prolonged or repeated presentation of odors is well documented in mammals and humans (Poellinger et al., 2001; Deshmukh and Bhalla, 2003).

The role of mushroom bodies in protection from premature habituation

In agreement with previous reports (Thomson and Spencer, 1966; Corfas and Dudai, 1989; Boynton and Tully, 1992; Beck and Rankin, 1995; Engel and Wu, 1996; Rose and Rankin, 2001), the response decrement characteristic of habituation was apparent after a distinct period of continuous stimulus exposure or after experiencing a number of shock stimuli (Figure 26, Figure 32A.I). We termed the period prior to emergence of habituation "the refractory period", since animals responded to pre-experienced stimuli as if they were naïve. The presence of a refractory period suggests that at this time processes which either prevent premature habituation must be inactivated, ones that mediate habituation must be activated or both. In either case, the refractory period may reflect the time necessary to evaluate a stimulus with respect to its saliency, novelty and potential association with other stimuli prior to decreasing responsiveness towards it. If so, shortening or eliminating the refractory period would precipitate premature habituation and would not allow effective evaluation of stimulus attributes such that inappropriate responses may be elicited.

Collectively the results strongly indicate that the MBs are essential in inhibition of premature habituation to olfactory and footshock stimuli because their structural or functional perturbation precipitated premature habituation with minimal stimulation.

However, it is unlikely that the MBs are the locus where habituation to these stimuli occurs because then their structural or functional ablation would result in failure to habituate, not premature habituation. Rather, it appears that the MBs themselves or in concert with other brain areas delay, prevent or modify the default response to pre-experienced repetitive stimuli, habituation. Our data are consistent with two models regarding the role of the MBs in protection from pre-mature habituation.

First, the MBs themselves inhibit premature habituation to pre-experienced olfactory and footshock stimuli probably during the refractory period. This permits evaluation of these stimuli relative to other environmental cues and mediation of the appropriate response, a property essential for associative learning. This central role for the MBs is consistent with the effects of inhibiting neurotransmission to, or from these neurons. Silencing mACT and iACT synapses essentially had the same effect as abrogating MB function because olfactory stimuli did not arrive in the latter for evaluation. The response to footshock could not be prevented from habituation since these neurons were structurally or functionally absent. In this model, the LH and possibly other brain areas are the likely mediators of the default avoidance response as proposed (Marin et al., 2002; Tanaka et al., 2004).

Alternatively, the MBs are not central, but rather one part of a minimally bipartite system mediating protection from premature habituation. The other main part of this network is the lateral horn because the main synaptic outputs from the mACT and iACT are in this neuropil (Stocker et al., 1997; Heimbeck et al., 2001; Marin et al., 2002; Tanaka et al., 2004), and footshock stimuli may arrive at the MBs via the LH (Ito et al.,

1998). Since silencing MB, or mACT and iACT synaptic output results in premature habituation, bi-directional synaptic output between the two centers likely during the refractory period would be essential for protection from habituation. Consistent with this, extrinsic neurons connecting the MBs and LH have been described (Ito et al., 1998). In both models, the proposed role for the MBs is consistent with their role in context generalization of learned visual information (Liu et al., 1999; Zars, 2000). As for protection from habituation, context generalization also involves deriving and maintaining relationships between stimuli irrespective of the environment they were formed in and requires anticipating future events based on a past experience (Heisenberg, 2003). Moreover, the proposed inhibitory role of the MBs is consistent with their suppression of general locomotor activity and generation, regulation and coordination of motor programs (Martin et al., 1998).

It is difficult to differentiate between the two models with our data at the moment. Functional perturbation of the LH is not possible to date because it appears that appropriate LH GAL4 driver lines are not available. Determination of whether protection from premature habituation is mediated entirely by the MBs or both the MBs and the LH or additional areas would have to await isolation of a mutant in the process. Then, rescue of the mutant phenotype with MB-specific, versus pan-neural GAL4 drivers is likely to distinguish between the two possibilities and these experiments are in progress.

The inability to dishabituate olfactory stimuli with footshock and *vice versa* upon abrogation of MB function is in agreement with the role of the system in stimulus

evaluation and response modification. It has been proposed that olfactory and footshock stimuli must converge in the MBs (Roman and Davis, 2001; Heisenberg, 2003), a condition necessary for associative olfactory learning. Convergence of the stimuli in the MBs appears to be essential for dishabituation for two reasons. First, blocking stimulus convergence by structural or functional ablation of these neurons did not support dishabituation to either olfactory or footshock stimuli. Second, inhibition of neurotransmission in iACT and mACT, in effect blocking olfactory stimuli conveyed to the MBs and thus stimulus convergence by did not allow dishabituation. Moreover, neurotransmission from the MBs was necessary for dishabituation, consistent with the notion that the MBs/LH play a role in modification of the behavioral response to pre-experienced stimuli akin to the requirement for neurotransmission from MB neurons in memory retrieval (Dubnau et al., 2001; McGuire et al., 2001).

If habituation requires inactivation of inhibitory processes that prevent its premature onset, then spontaneous recovery may reflect reactivation of the inhibition dependent on the time the stimulus habituated to, is absent (Rankin and Broster, 1992). Failure, or inefficient establishment of such inhibitory mechanisms would be manifested as prolonged habituation such as that exhibited by animals with perturbed MB function. Slower spontaneous recovery is likely to occur if additional stimuli are given after the response has habituated (over-habituation) (Thomson and Spencer, 1966), as observed in animals with compromised MBs. Delayed spontaneous recovery to both olfactory and footshock stimulation occurred in *mbm*^{1} that retain vestigial MBs. In *w*; 247/UAS-TNT animals recovery was apparent after habituation to the mild single footshock, but not

after the more strenuous one-minute odor pre-exposure. Therefore, as predicted from their proposed role in protection from premature habituation, normal MB function is requisite for spontaneous recovery.

Premature habituation and MB-dependent associative learning

In general it is unclear whether associative learning and habituation are dependent or independent processes. In the conditioned avoidance assay, used to study olfactory learning and memory, the conditioned stimulus (odor-CS+) paired to an unconditioned stimulus (footshock-US) elicits a conditioned response to the CS+ but no such response to an unconditioned odor stimulus, the CS- (Tully and Quinn, 1985). During training in this olfactory associative paradigm, premature habituation to the CS+ and/or the US would not permit CS/US association that leads to CS+ vs. CS- discrimination. Given our results and the documented involvement of the MBs in olfactory learning and memory (Roman and Davis, 2001; Waddell and Quinn, 2001; Heisenberg, 2003), it would appear that during training, the MBs/LH protect from premature habituation to the odor and shock stimuli such that associations between them may be formed. Since structural and functional ablation of the MBs precipitated profound premature habituation to odor and footshock stimuli it is unlikely that such associations can be formed. Even if associations could be formed normally, habituation to any of the test odors would not permit conditioned response dependent CS+ vs. CS- discrimination during testing. In agreement with this, MB ablated animals have been reported totally unable to learn in an olfactory associative paradigm (de Belle and

Heisenberg, 1994). Moreover, even if the footshock US acts as a dishabituator to the continuous odor CS+ presentation as previously suggested (Joynes and Grau, 1996), habituation to the CS- could alter the CS+/CS- discrimination during testing.

In summary, our results predict that animals mutant for genes essential for protection from premature habituation would be unable to learn odor/footshock associations. Conversely, mutants specifically compromised in MB-dependent associative learning would be protected from premature habituation. Therefore, experiments to differentiate between the two possibilities would be essential in determining the underlying mechanistic defect in apparent learning mutants.

EXPERIMENTAL PROCEDURES

Drosophila Strains

Drosophila were cultured in standard cornmeal sugar food supplemented with soy flour and $CaCl_2$. The flies were raised at 20-22°C, except UAS-TetLC II (Keller et al., 2002) crosses, which were raised at 18°C until hatching, then placed at 20-22°C for two days prior to testing. Hydroxyurea ablated flies were prepared with the method described previously (de Belle and Heisenberg, 1994), except that 75mg/ml hydroxyurea (HU) was used (Philip et al., 2001). Each batch of HU-treated adults was monitored histologically for the extend of mushroom body ablation.

Three different strains were utilized as wild type controls. First, a w^{1118} -bearing strain backcrossed to Canton S for 10 generations (*w*) and provided by Dr. Tim Tully.

Second, a w^{1118} -bearing strain derived by excision of a transposon on the third chromosome (ex5), which except for the white-eye color is unrelated to the *w* strain described above. Finally, the wild type strain Berlin was utilized as control for *mushroom body miniature* (mbm^{1}) flies since they share a common genetic background. Berlin and *mushroom body miniature* (mbm^{1}) flies have been described previously (Heisenberg et al., 1985a). The GAL4 lines used were P[GAL4] GH146 (GH146)(Stocker et al., 1997), P[GAL4] OK72 (OK72) (Acebes and Ferrus, 2001), P[GAL4] 247 (247) (Zars, 2000). The UAS strains used were UAS-*btau* (Ito et al., 1997), two independent transformant strains of the temperature sensitive *Drosophila* dynamin *shibire* gene, UAS-shi^{5ts} and UAS-shi^{10ts} (Kitamoto, 2001) and the Tetanus Light Chain transgene, UAS-TetLC II (UAS-TNT) (Keller et al., 2002). Tetanus Light Chain prevents neurotransmitter release by cleaving synaptobrevin, a protein required for synaptic vesicle docking on presynaptic neurons (Humeau et al., 2000). In contrast, inactivation of the temperature sensitive dynamin encoded by the $shibire^{ts}$ transgenes is thought to prevent neurotransmitter recycling to the presynaptic neurons, causing their functional depletion (Kitamoto, 2001).

To obtain flies for behavioral analyses, 247, GH146, OK72 homozygotes were crossed *en masse* to UAS-TetLC and UAS-shi^{5ts} and UAS-shi^{10ts} or the parental w^{1118} and the progeny was collected and tested 3-5 days after emergence. Similarly, UAS-TetLC and UAS-shi^{5ts} and UAS-shi^{10ts} homozygotes were crossed *en masse* to w^{1118}, to obtain heterozygous controls.

Histology

Frontal paraffin sections (5μm) of heads were prepared for immunohistochemistry or histology as described previously (Skoulakis and Davis, 1996; Crittenden et al., 1998). The α-LEO antibody (1:4500) was used to identify the mushroom bodies and ellipsoid body (Crittenden et al., 1998). The α–SH3PX1 antibody used (1:1000) to examine the gross morphology of antennal lobe glomeruli was provided by Dr. J. Dixon (Worby et al., 2001). The α–bovine TAU (α-bTAU) monoclonal antibody (Sigma) was used (1:1000) to investigate the GAL4 expression patterns.

Osmotaxis

Behavioral experiments were performed under red light at 23-24ºC and 65% humidity. Odor avoidance and attraction were quantified by exposing ~50 flies at the choice point of a standard T-maze (Tully and Quinn, 1985; Skoulakis, 1993; Skoulakis and Davis, 1996) to an air-stream (500 ml/min) carrying the odor in one arm and fresh air in the other. The flow rate was adjusted to 600 ml/min or higher to increase the effective amount of odor the flies were exposed to when necessary, as indicated. The odors utilized for these experiments were 1000μl (1X) of 3-Octanol (OCT) (Fluka), 110μl (1X) of benzaldehyde (BNZ) (Sigma) and 10μl of a 1/10 dilution in water (1X) of ethyl acetate (ETA) (Sigma). Flies were given 90 seconds to choose between aversive odors and air. Control experiments (not shown) determined that 180 seconds for the choice between attractive odors and air gave the most consistent and reliable indices. At

the end of the choice period, flies in each arm were trapped and counted. The avoidance index (AI) was calculated as the percentage of flies that avoid or are attracted to a particular odor. An AI of 100 indicates that the flies avoid the odor completely (-100 complete attraction), whereas an AI of 0 indicates equal distribution between the maze arms and therefore no avoidance or attraction.

Olfactory habituation

Olfactory habituation experiments were performed under the conditions described above. For the "training phase", approximately 50 flies were exposed to either attractive (ETA, BUT) or aversive odors (OCT, BNZ) for the indicted times in the upper chamber of a standard T-maze. After a 30 second rest period (unless indicated otherwise), the flies were lowered to the center of the maze for the "testing phase". The flies were tested for their avoidance or attraction to odors by a choice of air vs. either the previously experienced or a novel odor. At the end of the choice period (90 seconds for aversive and 180 for attractive odors) the number of flies in each arm were trapped, counted and the avoidance index (AI) calculated as described above. The UAS-shi^{5ts} and UAS-shi^{10ts} harboring strains were placed in a 32°C water bath for 15 minutes prior to the start of the "training phase" to inactivate the SHIBIRE protein. This treatment results in complete inactivation of SHIBIRE, which recovers within 15 minutes after removal from 32°C (Dubnau et al., 2001; Kitamoto, 2001; McGuire et al., 2001). To examine spontaneous recovery, flies were given a rest period for various lengths of time (6 minutes being the experimentally derived standard recovery period) within the upper

arm of the maze after they were given the odor pre-exposure. Subsequently they were tested against the odor they were pre-exposed to versus air and an AI was calculated as described above. To determine the conditions for dishabituation with electric shock, control experiments were performed first to determine the stimulus strength and number of shocks necessary. Dishabituation was attempted at different shock stimulus strengths with the following results: OCT AI for naïve: 59.2 $\pm$ 2.3. Habituated OCT AI: 20.6 $\pm$ 1.7. Dishabituation with 30 V, OCT AI: 54.8$\pm$ 2.1; with 45 V, OCT AI: 58.7 $\pm$ 2.6; with 90V OCT AI: 58.3 $\pm$ 2.2. Since the 90V and 45V dishabituating shocks had equal effects, the milder of the two was selected. Moreover the number of 45V shocks did not have a significant effect on dishabituating osmotaxis (1X 45V shock OCT AI: 58.7$\pm$ 2.3; 2X 45V shock OCT AI: 59.4$\pm$ 2.8). Therefore, dishabituation was attempted with a single 45 volt shock either prior, during, or at the end of pre-exposure and was followed immediately (within 15-20 seconds) by testing as described above.

Electroshock avoidance

Experiments were performed under the conditions described above. Animals were placed in the choice point of T-maze and given a choice of a standard copper grid (Skoulakis and Davis, 1996) electrified 15 times for 1.25 seconds each during the 90 second choice period with 45 Volts (unless indicated otherwise) versus an un-electrified grid. The avoidance index (AI) was calculated as the percent of flies avoiding the electrified grid.

Habituation to electroshock

Habituation to electric shock experiments were performed under the conditions described above. For the "training phase" ~ 50 flies were sequestered in the upper arm of a standard T-maze lined with an electrifiable grid. They were exposed to 1-11, 1.25-second electric shocks at 45V or 60 V or 90V as indicated. After a 30second rest, the flies were transferred to the lower part of the maze and tested by given a choice between an electrified and an inert grid. The electrified grid was held at the same voltage (45, 60 or 90V) as that the particular set of flies was exposed to previously. During the 90-second choice period 15, 1.25 second electric shocks were delivered to the electrified arm of the maze. At the end of the choice period the flies in each arm were trapped, counted and a performance index was calculated as above. Dishabituation was achieved by exposing the flies to benzaldehyde (500µl BNZ carried in an air stream at 500 ml/sec as described above for olfactory habituation) for 15 seconds immediately after the "training phase". For spontaneous recovery, a 6-minute resting period (REST) was allowed in the upper part of the maze between the training and testing phases. The avoidance index (AI) was calculated as the percent of flies avoiding the electrified grid.

Statistical analysis

Untransformed (raw) data were analyzed parametrically with JMP3.1 statistical software package (SAS Institute Inc., Cary, NC). To maintain a constant experiment wise error rate, initial ANOVA and planned multiple comparisons were performed as suggested by Sokal and Rolf (Appendix B).

CHAPTER V

D14-3-3ε MUTANTS ARE NOT PROTECTED FROM PREMATURE HABITUATION IN *DROSOPHILA*

INTRODUCTION

Stereotypical animal responses to environmental stimuli are modified by experience and by extraction of relationships among them. Temporal coincidence of stimuli often leads to associative learning, such that a strong stimulus (unconditioned stimulus-US) is predicted by presentation of a weak one (conditioned stimulus–CS) because they were presented concurrently. Enhancement or decrement of a behavioral response precipitated by pre-experienced or repetitive stimuli are essential in ensuring appropriate attention and reaction to them and constitute forms of non-associative learning. Such processes include habituation, desensitization, sensory fatigue and adaptation.

Desensitization, sensory fatigue and adaptation involve physiological changes that decrease the sensitivity to a repeated or prolonged stimulus. In contrast, habituation is also manifested as a gradual response decrement to a repetitive stimulus, but it does not appear to involve changes in sensitivity as the response will return after the presentation of a (often noxious) novel stimulus (dishabituation) (Thomson, 1966; Groves, 1970; Marcus et al., 1988; Rankin, 1992). Therefore, habituation could act as a gating mechanism mediating decreased responsiveness to repetitive but meaningless

stimuli and consequently is thought to underlie selective attention (Thomson, 1966; Rose and Kemphues, 2001). Defects in the gating and selective attention aspects of habituation are thought to underlie schizophrenia and attention disorders in humans (Freedman et al., 1991; Adler et al., 1999; Meincke et al., 2004; Slaats-Willemse et al., 2003). However, rapid habituation to prolonged or repeated stimuli is unlikely to permit associations with other more discrete stimuli, a condition necessary for associative learning. In congruence, habituation appears to occur after exposure to a number of repetitive or prolonged stimuli (Thomson, 1966; Rose et al., 2001). Therefore, processes protecting from premature habituation must operate within neuronal circuits and in fact I recently demonstrated this phenomenon in *Drosophila* (Acevedo and Skoulakis, submitted). Prominent neuronal circuits known as mushroom bodies, essential for associative olfactory learning and memory (Roman and Davis, 2001; Heisenberg, 2003) appear indispensable for suppressing premature habituation to olfactory and footshock stimuli also.

Although the behavioral characteristics and parameters of habituation have been characterized extensively, little is known about the molecular mechanisms underlying the process. In *Drosophila*, adenylyl cyclase (*rutabaga*) and cAMP-phosphodiesterase (*dunce*) mutants that alter the cAMP signaling and exhibit deficits in associative olfactory learning could habituate and dishabituate in a number of paradigms utilizing simple proprioceptive reflexes within the thoracic sensory neurons of the peripheral nervous system. However, habituation occurred more quickly and was short lived for the *rut* and *dnc* mutants (Corfas and Dudai, 1989; Duerr and Quinn, 1982; Engel and

Wu, 1996). Habituation could be eliminated by targeted expression of calcium independent CaMKII in thoracic sensory neurons (Jin et al., 1998). The fact that these mutants affect both habituation and associative olfactory learning suggests the two might be linked biochemically and/or associated with the same region of the brain.

In this paper I report on the requirement for D14-3-3ε in processes that mediate protection from premature habituation. D14-3-3ε is a member of the highly conserved 14-3-3 family of small dimeric acidic proteins. The seven members of the family in vertebrates comprise two conservation groups the typical (α, η, ζ, γ and τ) and atypical (ε and σ) isotypes (Skoulakis and Davis, 1998) of which 14-3-3ε is likely the ancestral protein since it is the most similar to the ancient plant and yeast 14-3-3 proteins (Wang and Shakes, 1996). Structurally all family members are characterized by the common nine anti-parallel helices formed into U-shaped molecule with a negatively charged interior which binds phosphoproteins that contain the motifs RSxpS/TxP, or RxxxpS/TxP (where x=any amino acid, pS/T=phosphoserine or phosphothreonine). 14-3-3 binding may protect a target protein from dephosphorylation or proteolysis, modulate its activity, and alter its ability to interact with other partners, or modify its cytoplasmic/nuclear partition. Therefore, it is not unusual that 14-3-3 proteins have been implicated in a diverse number of processes and biochemical pathways (Tzivion et al., 2002; Yaffe, 2002; Berg et al., 2003; Dougherty et al., 2004).

Drosophila is a simpler yet representative model with one isotype from each group, 14-3-3ζ-LEONARDO and D14-3-3ε with 88 and 82% identity to their respective mammalian homologs (Skoulakis and Davis, 1998; Philip et al., 2001). In adult flies,

LEO is preferentially distributed in the mushroom bodies (MBs) where it is acutely required for olfactory associative learning and memory (Skoulakis and Davis, 1996; Philip et al., 2001). In addition to behavioral plasticity, while not essential for synaptogenesis and basal synaptic transmission LEO appears essential for physiological plasticity at the larval neuromuscular junction (Broadie et al., 1997). In contrast, as for its vertebrate homolog (Baxter, 2002), *D14-3-3ε* mRNA is found in all stages of development and in all tissues examined and enriched in adult heads (Philip et al., 2001). However, although highly enriched in the vertebrate and the *Drosophila* nervous system other than a role in Drososphila eye development (Chang and Rubin, 1997), little was known regarding the role of this isotype in nervous system function. The results of this study uncover a novel role for the *Drosophila* 14-3-3ε in protection from premature habituation.

RESULTS AND DISCUSSION

Characterization of new *D14-3-3ε* alleles

Because the available mutant alleles at the onset of this work were an apparent hypomorhic P-element insertion and mis-sense mutations with complex phenotypes (Chang and Rubin, 1997), I characterized excision alleles of the transposon aiming to obtain null or strong hypomorphic alleles. Southern and PCR analyses (not shown) established two classes of alleles. Allele $D14\text{-}3\text{-}3\varepsilon^{ex5}$ was classed as a revertant because it did not appear to harbor molecular lesions or transposon remnants, while in allele

D14-3-3ε^{ex4} exon 1 which harbors the transcription and translation start sites and half of intron 1 were deleted suggesting a null allele (Figure 33A). Both *D14-3-3ε*$^{l(3)j2B10}$ and *D14-3-3ε*^{ex4} were semi-lethal, allowing 43% and 75% viability respectively and were not complementary. Homozygotes did not exhibit gross morphological or behavioral abnormalities except their somewhat reduced size and sterility. D14-3-3ε was totally absent in the heads of these animals and this deficit did not appear to affect the accumulation of the only other 14-3-3 protein in *Drosophila*, LEONARDO-14-3-3ζ (Figure 33B).

Distribution of D14-3-3ε in the adult nervous system and structural analysis in the mutants

Immunohistochemical investigation of the distribution pattern of D14-3-3ε in adult brains revealed accumulation of the protein throughout the neuropil of the central brain (Figure 34A.1-4), the optic lobes and thoracic ganglion (not shown). The protein appeared slightly enriched in the medulla (not shown), the fan shaped body (Figure 34A.2) and antennal lobes (Figure 34A.4). This broad distribution is not background staining confirmed by its total absence from mutant homozygote brains on the same slide (Figure 34A.5-8). D14-3-3ε was characteristically absent from the somata as has been described for the vertebrate isoform, which is also distributed throughout the neuropil of the CNS (Baxter et al., 2002). The D14-3-3ε distribution is in contrast with the preferential expression in the mushroom bodies (MBs) of one of the isotypes (LEOII)

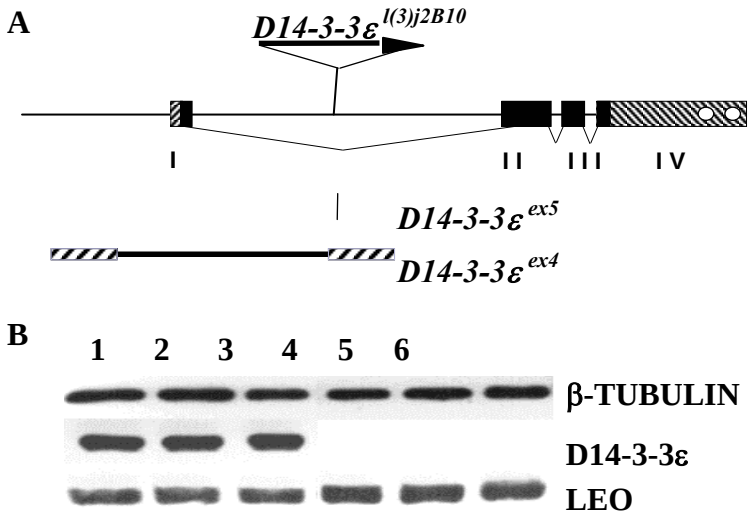

Figure 33. Molecular map and protein expression in D14-3-3ε mutants

(A) The genomic region, structure and mutations of the *D14-3-3ε* gene. Boxes represent exons, whereas lines represent introns and surrounding non-transcribed regions. The stippled boxes indicate untranslated portions of exons. The white circles in exon 4 represent polyadenylation sites. The arrow indicates the location of the P-element insertion in intron 1. The extent of the deficiencies in $D14\text{-}3\text{-}3\varepsilon^{ex4}$ and $D14\text{-}3\text{-}3\varepsilon^{ex24}$ are indicated by the black bars, whereas the region of uncertainty at the ends is indicated by the hatched bars. (Adapted from Chang and Rubin 1997).
(B) A representative blot from adult head lysates used in acquisition of the data on Table 16. Genotypes: (1) $D14\text{-}3\text{-}3\varepsilon^{ex5}$ homozygotes, (2) $D14\text{-}3\text{-}3\varepsilon^{ex5}/\ D14\text{-}3\text{-}3\varepsilon^{l(3)j2B10}$, (3) $D14\text{-}3\text{-}3\varepsilon^{ex5}/\ D14\text{-}3\text{-}3\varepsilon^{ex4}$, (4) $D14\text{-}3\text{-}3\varepsilon^{l(3)j2B10}\ /\ D14\text{-}3\text{-}3\varepsilon^{l(3)j2B10}$, (5) $D14\text{-}3\text{-}3\varepsilon^{l(3)j2B10}/\ D14\text{-}3\text{-}3\varepsilon^{ex4}$, and (6) $D14\text{-}3\text{-}3\varepsilon^{ex4}/\ D14\text{-}3\text{-}3\varepsilon^{ex4}$.

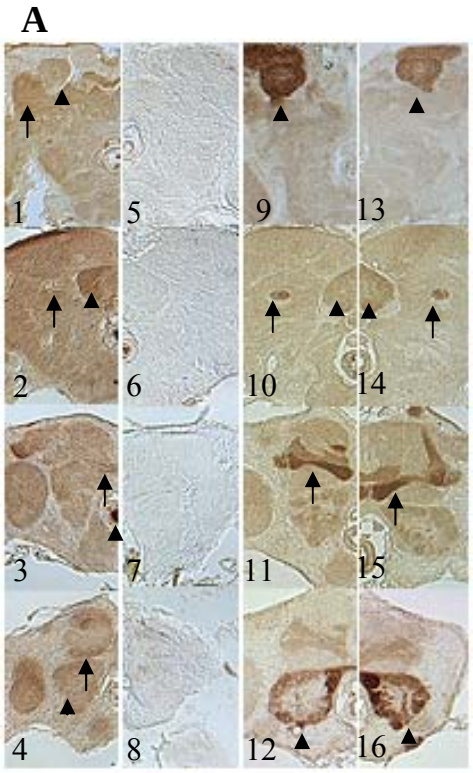

Figure 34. Distribution of D14-3-3ε and structural analysis of *D14-3-3ε* mutant brains

(A) Distribution of D14-3-3ε in *D14-3-3ε*^{ex5} (1-4) and *D14-3-3ε*^{ex4} homozygotes (5-8) indicating ubiquitous distribution of the protein throughout adult brains. 1 and 5: mushroom body calyces (arrowhead) and lateral horn (arrow). 2 and 6: the fan-shaped body (arrowhead) and mushroom body pedunculi (arrow). 3 and 7: the suboesophageal ganglion (arrowhead) and ellipsoid body (arrow). 4 and 8: the mushroom body lobes (arrow) and suboesophageal ganglion (arrowhead).
Structural analysis of brains from *D14-3-3ε* ^{ex4} mutant homozygotes with antigenic markers demonstrating that lack of the D14-3-3ε protein does not precipitate gross neuroanatomical deficits except for a fusion at the tips of the β-lobes of the mushroom bodies (B). (9-12) *D14-3-3ε* ^{ex5} and (13-16) *D14-3-3ε* ^{ex4} homozygotes. 9, 13: mushroom body calyces (arrowheads) stained with anti-LEO. 10, 14: the fan-shaped body (arrowheads) and mushroom body pedunculi (arrows) stained with anti-DRK. 11, 15: the mushroom body lobes (arrows) stained with anti-DRK. 12, 16: the antennal lobes (arrowheads) and stained with anti-JCD5.

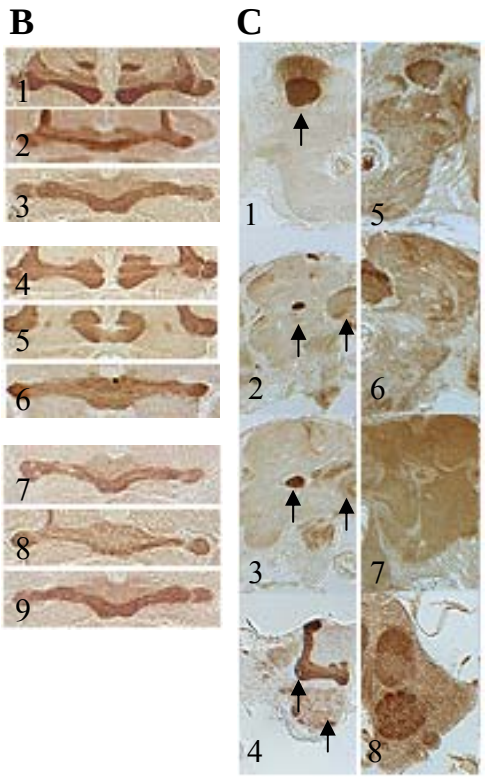

Figure 34. (continued)

(B) Fusion of the tips of the β-lobes of the mushroom bodies in *D14-3-3ε* ^{ex4} homozygotes indicated by anti-DRK (1-3) and anti-LEO (4-6) staining of different mutant animals indicating full penetrance of the phenotype. 1 and 4: mushroom body β-lobes in control animals; 2, 3, 5, 6 β-lobes in *D14-3-3ε*^{ex4} homozygotes. The phenotype was not reversed with *C155-Gal4* (7), *tubulin-Gal4* (8), or *247-Gal4* (9) driven *UAS-mycD14-3-3ε* transgenes.
(C) Accumulation of D14-3-3ε protein in *D14-3-3ε* ^{ex4}homozygotes expressed from *UAS-mycD14-3-3ε* transgenes and detected with the anti-D14-3-3ε antibody under the direction of the *C155-Gal4* driver (1-4) and the *tubulin-Gal4* driver (5-8). Low level ubiquitous accumulation throughout the central nervous system was observed under the *C155-Gal4* driver, but the protein was enriched as indicated by the arrows in the mushroom body calyces (1), mushroom body pedunculi and the fan shaped body (2), mushroom body pedunculi and ellipsoid body (3) and mushroom body lobes and antennal lobe glomeruli (4). In contrast, transgenic D14-3-3ε under the *tubulin-Gal4* driver was found throughout the neuropil of the central nervous system (5-8). All brain structures appear morphologically normal in *D14-3-3ε*^{ex4}homozygotes, except the fused β -lobes of mushroom bodies as described above (B).

of the other 14-3-3 protein in *Drosophila* 14-3-3ζ-LEONARDO, which also accumulates in the MB perikarya. The other LEO isoform appears to be distributed similarly to D14-3-3ε throughout the CNS (Philip et al., 2001; Skoulakis and Davis, 1996).

Because mice deficient in 14-3-3ε exhibit defects in brain development associated with isolated lissencephaly sequence (ILS) and Miller-Dieker syndrome (Toyo-oka et al., 2003), the neuroanatomy of the central brain in *D14-3-3ε* homozygotes was examined using standard hematoxylin-eosin staining (not shown) and staining with MB antigenic markers (Crittenden et al., 1998). The results obtained with the anti-LEO and anti-DRK antibodies are shown in Figures 35A.9-16 and 35B.1-6. Compared to *D14-3-3ε* ^{ex5}controls (Figure 34A.9-12) the brain of *D14-3-3ε*^{ex4} homozygotes appeared normal with respect to structure, expression pattern and level of antigenic markers (Figure 34A.13-16), except for the overall reduced size and fusion of the β lobes of the mushroom bodies (Figure 34B.1-6). The horizontal lobes of the mushroom bodies in a hemisphere are separated from the contra-lateral lobes by the median bundle (Figure 34B.1 and 34B.4). However, in *D14-3-3ε* ^{ex4}homozygotes the median bundle was reduced or missing, the β lobes fused and appeared thickened and somewhat deformed (Figure 34B.2, 3, 5, 6). Similar malformations of the MB β lobes have been reported in flies mutant for the *linotte* Receptor Tyrosine Kinase (Moreau-Fauvarque et al., 1998; Moreau-Fauvarque et al., 2002; Simon et al., 1998). Interestingly, fusion of the lobes was not reversed either by pan-neural expression of *D14-3-3ε* transgenes throughout development of the nervous system (Figure 34B.7-8), conditions that rescue all other mutant phenotypes (see below), or by MB-specific expression (Figure 34B.9). Similar

results were obtained with *D14-3-3ε* $^{l(3)j2B10}$ homozygotes (not shown). These results indicate that fusion of the lobes is not causal of observed behavioral phenotypes.

Experience dependent associative and non-associative deficits in *D14-3-3ε* mutants

Because *leonardo* mutants exhibit deficits in associative learning and memory (Philip et al., 2001; Skoulakis and Davis, 1996), similar effects on the effects on behavioral plasticity precipitated by the total lack of D14-3-3ε were investigated in *D14-3-3ε*^{ex4} and *D14-3-3ε*$^{l(3)j2B10}$ homozygotes. Animals were trained and tested negatively reinforced olfactory classical conditioning paradigm which utilizes odors as conditioning stimuli (CS) and footshock as the unconditioned stimulus (US) (Philip et al., 2001; Tully and Quinn, 1985). *D14-3-3ε*^{ex5}control flies performed identically (not shown) to standard control strains such as outcrossed w^{1118} or *yw* (Philip et al., 2001), in contrast to both *D14-3-3ε* mutants which displayed large (approximately 50% reduction) impairments in immediate memory (Figure 35A). However, both mutants and the *D14-3-3ε*^{ex5}control flies avoided the aversive odors used for training equivalently and furthermore their performance was identical to that of w^{1118} (Table 16A). In addition, all strains were attracted equivalently to appetitive odors in T-maze experiments given the choice of odor and air (Table 16B). In addition, two other members of the lab found that the mutants performed equally with controls in the qualitatively different olfactory trap assays where flies become attracted and navigate towards the source of dilute attractive odors (Table 16B). This indicates that the mutants were able to perceive and respond to the odors properly and locomote towards or away from them. Similarly, the mutants

Table 16. Olfactory avoidance and attraction of *D14-3-3ε* mutants

A			
Genotype	**OCT**	**BNZ**	**ETA**
D14-3-3ε^{ex5}/D14-3-3ε^{ex5}	56.40 ± 2.02	59.00 ± 1.98	-53.48 ± 3.40
D14-3-3ε$^{l(3)j2B10}$/D14-3-3ε$^{l(3)j2B10}$	51.09 ± 2.88	55.47 ± 3.19	-50.30 ± 2.48
D14-3-3ε$^{l(3)j2B10}$/D14-3-3ε^{ex4}	51.73 ± 2.63	56.35 ± 3.39	-50.71 ± 2.11
D14-3-3ε^{ex4}/D14-3-3ε^{ex4}	50.56 ± 1.25	56.28 ± 3.54	-54.70 ± 2.81
w1118	52.50 ± 1.48	53.15 ± 1.59	-53.16 ± 3.64
B			
Genotype	**GER**	**ETA**	**BUT**
D14-3-3ε^{ex5}/D14-3-3ε^{ex5}	78.57 ± 2.42	54.69 ± 3.40	58.21 ± 4.78
D14-3-3ε$^{l(3)j2B10}$/D14-3-3ε$^{l(3)j2B10}$	88.23 ± 3.22	67.78 ± 4.00	62.50 ± 4.52
D14-3-3ε$^{l(3)j2B10}$/D14-3-3ε^{ex4}	84.55 ± 3.63	58.69 ± 3.34	52.01 ± 3.77
D14-3-3ε^{ex4}/D14-3-3ε^{ex4}	77.61 ± 3.42	55.83 ± 3.98	59.17 ± 3.55
w1118	86.55 ± 3.75	58.03 ± 2.81	52.82 ± 3.58
C			
Genotype	**45 Volts**		
D14-3-3ε^{ex5}/D14-3-3ε^{ex5}	34.49 ± 1.18		
D14-3-3ε$^{l(3)j2B10}$/D14-3-3ε$^{l(3)j2B10}$	33.88 ± 2.60		
D14-3-3ε$^{l(3)j2B10}$/D14-3-3ε^{ex4}	33.32 ± 1.56		
D14-3-3ε^{ex4}/D14-3-3ε^{ex4}	29.37 ± 1.37		
w1118	32.04 ± 1.23		

The mean performance indexes (PIs) are shown ± standard error of the mean (± SEM). Positive values indicate avoidance and negative values indicate attraction.

(A) Avoidance or attraction in a standard T-maze. Positive values indicate avoidance and negative values indicate attraction. ANOVA indicated no significant differences among the strains for OCT avoidance ($F_{(4,41)}$=0.98 p<0.4354) or BNZ ($F_{(4,41)}$=1.64 p<0.2014) and ETA attraction ($F_{(4,40)}$=0.99 p<0.4337).

(B) Performance in olfactory traps. Positive values indicate attraction. ANOVA indicated no significant differences among the strains for GER attraction ($F_{(4,77)}$=2.95 p<0.0107), ETA attraction ($F_{(4,74)}$=2.25 p<0.0221) and BUT attraction ($F_{(4,72)}$=2.22 p<0.0593).

(C) Electric footshock avoidance. ANOVA's indicated no significant differences among the strains for ($F_{(4,51)}$=1.62 p<0.1852).

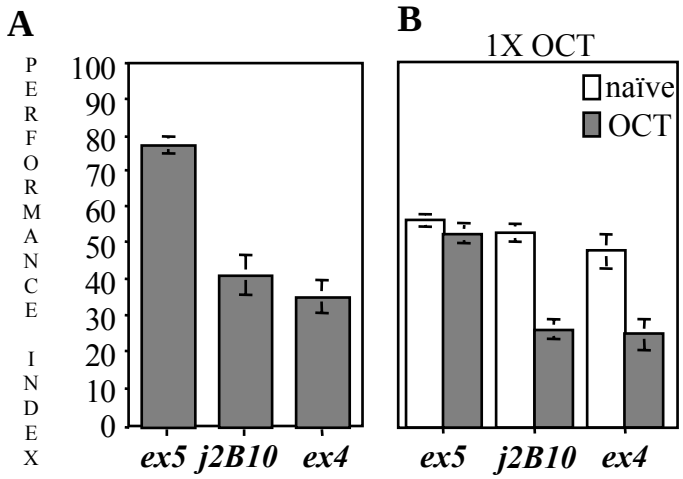

Figure 35. Deficits in olfactory associative learning and osmotactic deficits in *D14-3-3ε* mutant homozygotes

Means + standard error of the mean (SEM) are shown SD: Significant differences, NSD: Non-significant differences. Positive values indicate avoidance and negative values indicate attraction.

(A) Deficient associative learning in *D14-3-3ε* mutants. Performance indices (PIs) for conditioned olfactory discrimination are shown + SEM for control $D14\text{-}3\text{-}3\varepsilon^{ex5}$ (*ex5*) and mutant $D14\text{-}3\text{-}3\varepsilon^{l(3)j2B10}$ (*j2B10*) and $D14\text{-}3\text{-}3\varepsilon^{ex4}$ (*ex4*) homozygotes. ANOVA indicated significant differences in performance ($F_{(2,22)}=41.52$, $p<0.0001$, SD). Subsequent planned comparisons (Dunnett's) between *ex5* and mutant strains revealed highly significant differences ($p<0.0001$) for all comparisons demonstrating a deficit in associative learning in the mutants.

(B) Pre-exposure-dependent decline in Octanol (OCT) avoidance. PIs for Octanol avoidance before (naïve-open bars) and after a 60-second pre-exposure (gray bars) to this odor are shown + SEM. Avoidance without prior exposure to OCT was similar in control and mutant strains (ANOVA: $F_{(2,23)}=3.36$ $p<0.0177$, NSD). However, the performance of mutants after a 60 second pre-exposure was significantly different than that of controls (ANOVA: $F_{(2,28)}=28.39$ $p<0.0001$, SD and subsequent Dunnett's tests highly significant -$p<0.0001$- for all comparisons).

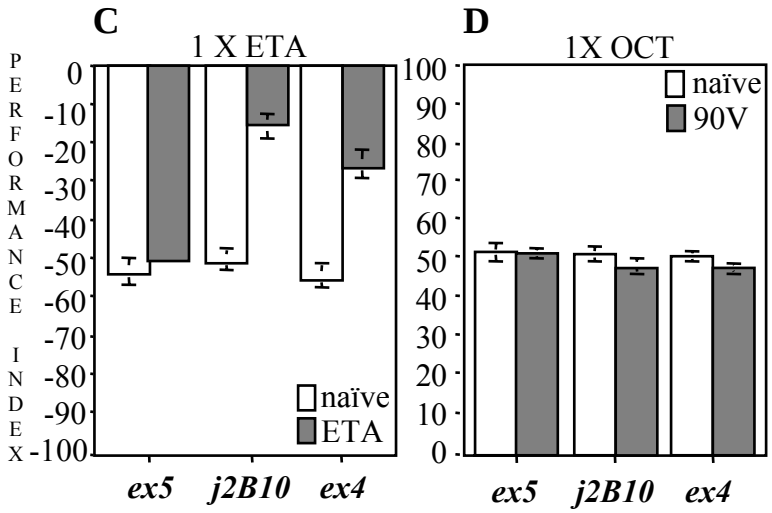

Figure 35. (continued)

(C) Pre-exposure-dependent decline in Ethyl Acetate (ETA) attraction. PIs for ETA attraction following a 60-second ETA pre-exposure is shown for *ex5*, *j2B10* and *ex4* homozygotes (gray bars). Attraction of naïve animals (open bars) was identical between control and mutants (ANOVA: $F_{(2,21)}$=1.24 p<0.3100, NSD). However, a marked decline in attraction to ETA was observed in the mutants, but not the control flies (ANOVA: $F_{(2,24)}$=29.82 p<0.0001, SD; Dunnett's p<0.0001 for all comparisons of mutants to control).

(D) Pre-exposure to shock does not affect responses to an odor. OCT avoidance following pre-exposure to 11 X 90Volt footshocks for control and mutant flies. As in B, there were no significant differences (ANOVA: $F_{(2,23)}$=5.63 p<0.0110, NSD) in OCT avoidance of naïve animals (open bars), or after pre-exposure (gray bars) to footshock ($F_{(2,21)}$=3.27 p<0.0226, NSD).

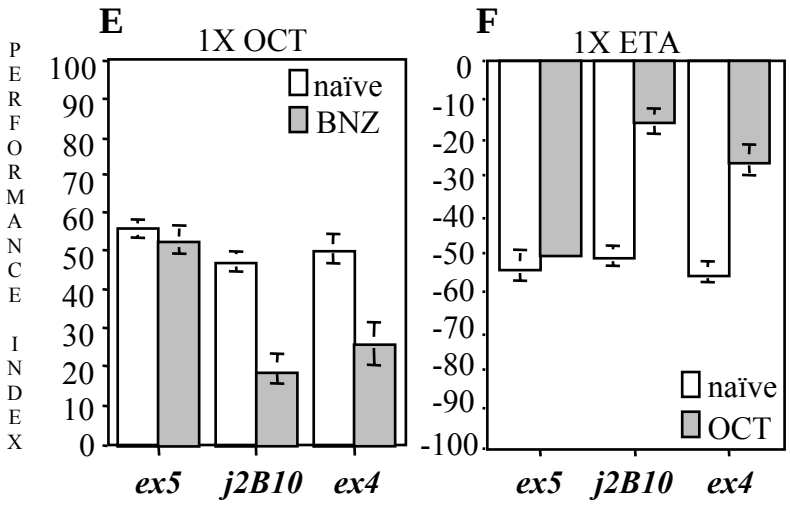

Figure 35. (continued)

(E) Pre-exposure to an aversive odor (benzaldehyde-BNZ) precipitates osmotactic deficits to a novel aversive odor (OCT). Avoidance of OCT after 60 seconds of pre-exposure to BNZ (light gray bars). Avoidance of OCT by naïve animals (open bars) was not significantly different, irrespective of genotype (ANOVA: $F_{(2,27)}=2.38$ $p<0.1133$, NSD). However, OCT avoidance after pre-exposure to BNZ was significantly different in mutant homozygotes from controls (ANOVA: $F_{(2,25}=21.61$ $p<0.0001$, SD and subsequent Dunnett's tests-$p<0.0001$-for all comparisons).

(F) Pre-exposure to an aversive odor (OCT) precipitates osmotactic deficits to a novel attractive odor (ETA). Attraction to ETA after 60 seconds of pre-exposure to OCT (light gray bars). Attraction to ETA by naïve animals (open bars) was not significantly different, irrespective of genotype (ANOVA: $F_{(2,27)}=0.95$ $p<0.7741$, NSD). However, ETA attraction was significantly different in mutant homozygotes and controls after pre-exposure to OCT ($F_{(2,25)}=23.00$ $p<0.0001$, SD and subsequent Dunnett's tests-$p<0.0001$-for all comparisons).

avoid electric footshocks given the choice of an electrified and a non-electrified surface. Therefore, the mutants respond properly given the option between aversive or attractive non-pre-experienced stimuli and a neutral choice (air). This data indicates that differential experience-independent (naive) perception or response to the stimuli cannot account for the observed learning deficits.

Other than differential perception or response to the stimuli, there were two additional experience-dependent reasons that could give rise to the apparent learning deficits exhibited by the mutants. A decrease in perception of the repetitive or prolonged stimuli used during conditioning due to fatigue or desensitization, or a decrease in responsiveness to the stimuli because of premature habituation. Either of these deficits would not allow normal information acquisition from the 11-12 CS/US pairings typically utilized for conditioning, or proper discrimination between the CS+ and CS- during testing. I have shown that premature habituation to odor or footshock stimuli similar to the ones used in conditioning assays occurs within 10 seconds of exposure, or after a single shock if MB function is impaired (Acevedo and Skoulakis, submitted).

Since in the training and testing phases of conditioning experiments, differential responses to pre-experienced stimuli are either established or tested, non-associative experience dependent responses were investigated in the mutants. Initially the effect of pre-experiencing electric footshock on subsequent response to a novel odor stimulus was examined. Footshocks used as US in the conditioning experiments did not affect avoidance of OCT (Figure 35B), BNZ or attraction to ETA (not shown). To investigate

the effect of odor pre-exposure on subsequent olfactory responses, mutants and control animals were exposed to OCT for 60 seconds and their subsequent avoidance of this odor was tested. Compared to their naïve response, mutants displayed a large reduction in OCT avoidance after pre-exposure to this odor. In contrast, avoidance the pre-experienced odor was not different from the naïve response in control animals (Figure 35C). Similar responses were obtained if the animals were pre-exposed to the attractive odor ETA (Figure 35D), or the aversive BNZ (not shown). Furthermore, pre-exposure to one aversive odor (BNZ) affected subsequent avoidance of a novel aversive odor (OCT) (Figure 35E). The same deficit was observed with pre-exposure to an attractive odor decreasing subsequent avoidance of a novel aversive odor (Figure 35F), or pre-exposure to an attractive odor diminishing the response to a novel attractive odor (not shown). Since these odors are perceived by different olfactory receptors and processed in different antennal lobe glomeruli (deBruyne et al., 2001) and naïve avoidance or attraction to the odors was normal, this cross odor experience dependent deficit was likely a centrally mediated phenomenon. Therefore, lack of D14-3-3ε precipitated overt deficits in experience dependent responses to stimuli consistent with desensitization, fatigue and premature habituation.

Physiological neuroplasticity at the larval neuromuscular junction is normal in *D14-3-3ε* mutants

Total lack of 14-3-3ζ-LEO does not affect synaptogenesis or basic synaptic function, but plasticity is compromised at the neuromuscular junction (NMJ) because of

apparent failure in synaptic vesicle mobilization (Broadie et al., 1997). Therefore, to investigate whether loss of D14-3-3ε affects synaptic function and plasticity, which may underlie the observed behavioral deficits, synaptic function was measured at the larval NMJ. Morphologically the NMJ appeared normal in both *D14-3-3ε^{ex4}* and *D14-3-3ε$^{l(3)j2B10}$* homozygous larvae (not shown).

Therefore, our collaborator performed voltage clamp recordings of synaptic currents were performed on muscle 6 of the third abdominal segment (Jan and Jan, 1976; Stimson et al., 1998) and the amplitude of evoked excitatory junctional currents (EJCs) were investigated as an initial measure of normal synaptic function. Amplitudes of a single EJC were measured at two external Ca^{2+} concentrations, 0.5 mM, which results in low probability of release and small EJCs, and 1.5 mM, which produces high probability of release and concomitantly large EJCs. In both conditions, EJC amplitude was indistinguishable between *D14-3-3ε^{ex5}*control larvae and both *D14-3-3ε^{ex4}* and *D14-3-3ε$^{l(3)j2B10}$* mutant homozygotes, whether raw data or normalized to muscle capacitance (because of the slightly smaller size of the mutants) were plotted (Figure 36A). Furthermore, because the relationship between external Ca^{2+} and transmitter release was unaffected in the *D14-3-3ε* mutant larvae, the sensitivity of the Ca^{2+} sensor appeared normal as well.

Although baseline EJC amplitude is normal in *D14-3-3ε* mutants, alterations in neurotransmitter release could be masked by compensatory changes in muscle sensitivity to glutamate (Davis and Goodman, 1998). Such changes are detectable in the amplitude of spontaneous miniature EJCs (mEJCs), which correspond to exocytosis of single

synaptic vesicles. mEJC amplitude was essentially identical among control and mutant larvae (Figure 36B; *D14-3-3ε*^{ex5}: 0.585 ± 0.039; *D14-3-3ε*^{ex4}: 0.583 ± 0.043; *D14-3-3ε*$^{l(3)j2B10}$: 0.592 ± 0.049). Therefore, glutamate receptor sensitivity is normal in the mutants. Furthermore, when the number of these spontaneous events per unit time was measured, vesicles appeared to be fusing with the presynaptic membrane at normal rates (Figure 36C), providing further evidence that presynaptic function is not compromised. Therefore, in *D14-3-3ε* mutants all critical components of basic synaptic function, including excitation, Ca^{2+} influx, vesicle fusion, and glutamate receptor sensitivity and current appeared normal.

Although basic synaptic function appeared intact, defects in synaptic function could be detected under the more strenuous repetitive stimulation potentially approximating the conditions of prolonged or repeated odor or footshock exposure. 10 were compared with that of the first 10 responses. All genotypes showed significant augmentation, with no significant differences between mutants and the control (p=0.36) last EJC in the train was depressed to approximately 40% of initial EJC amplitude in all genotypes (p = 0.81). All genotypes depressed to identical levels. Repetitive stimulation recruits additional pathways, such as those mediating Ca^{2+} sequestration and vesicle recycling. In 0.5 mM Ca^{2+}, the response to a train of stimuli is a mix of facilitation and augmentation, which are distinguished by their time courses (Magleby and Zengel, 1982). Neurons were stimulated with a train of 250 stimuli at 40 Hz in the presence of 0.5 mM $Ca^{2+}$and the average amplitude of the final 10 was compared with that of the first 10 responses. The ratio of the final EJCs to those at the beginning was similar in

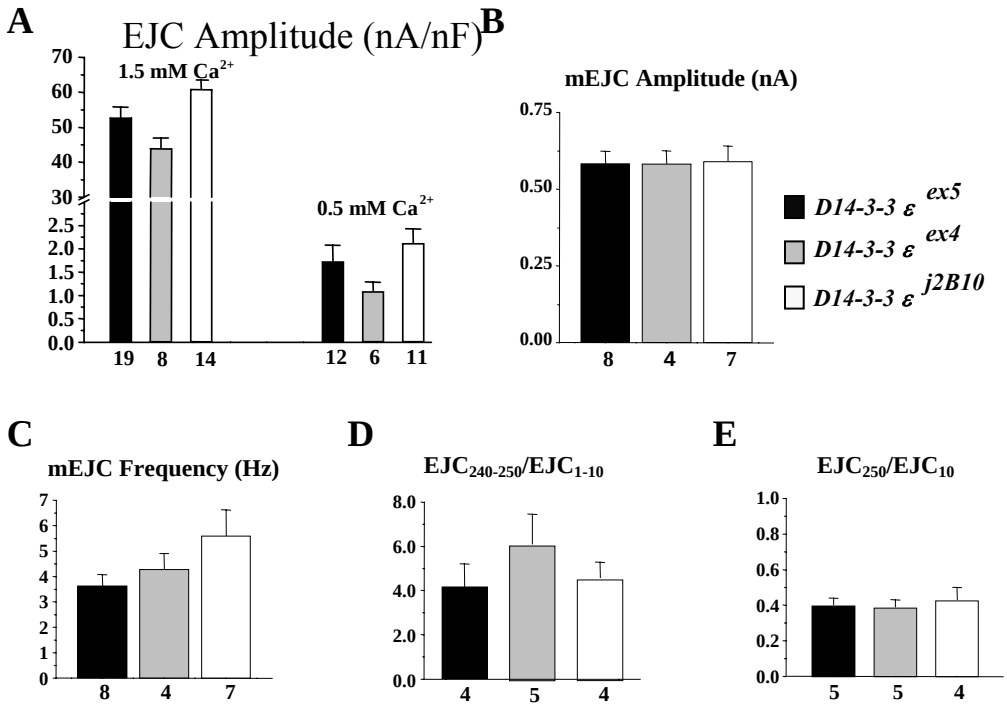

Figure 36. Effect of epsilon mutations on physiology of the larval neuromuscular junction

Means + standard error of the mean (SEM) are shown, with sample sizes below each bar.
(A)Baseline EJC amplitude. Amplitude of the first EJC in a train of stimuli, normalized to muscle capacitance to compensate for possible differences in muscle size. In external Ca^{2+} concentrations of 1.5 mM and 0.5 mM representing conditions of low and high release probability, EJC amplitude is statistically (1.5 mM Ca^{2+} p=0.25, 0.5 mM Ca^{2+} p=0.25, p=0.15) indistinguishable between control (ex5) and epsilon mutants.
(B) Amplitude of spontaneous mEJCs. Each data point represents all mEJCs recorded in a 50 s sample. Amplitudes for controls and mutants were indistinguishable (p=0.62).
(C) Frequency of spontaneous mEJCs. Number of spontaneous events occurring in a 50-second sample, plotted as mEJCs/s (Hz). *D14-3-3*ε^{ex4} and *D14-3-3*ε^{j2b10} exhibited slightly, but not significantly (p=0.13) elevated increases in mEJC frequency.
(D) Augmentation of EJC amplitude. Neurons were stimulated with a train of 250 stimuli at 40 Hz in the presence of 0.5 mM Ca2+, and the average amplitude of the final.
(E) Depression of EJC amplitude. Axons were stimulated with trains of 250 stimuli at 40 Hz, under conditions of high glutamate release (1.5 mM Ca2+). The amplitude of the control and mutant NMJs (Figure 36D) indicating normal synaptic facilitation. At 10 Hz, control and mutant synapses showed more modest levels of facilitation that did not differ from one another (not shown). Furthermore, under conditions of high glutamate release (1.5 mM Ca^{2+}), the neuromuscular synapse undergoes depression when stimulated repeatedly. Axons were stimulated with trains of 250 stimuli at 40 Hz, in 1.5 mM Ca^{2+} and the depression was measured as the ratio of the first EJC to the amplitude of the last current. Under these conditions, all genotypes behaved identically, with synaptic currents becoming depressed to approximately 40% of initial amplitude (Figure 36E).

Therefore, in addition to processes required for basal synaptic function, mechanisms involved in maintained neurotransmitter output, such as Ca^{2+} sequestration and synaptic vesicle recycling which are essential for synaptic modulation appeared unaffected by the loss of D14-3-3ε. This indicates that unlike LEO, D14-3-3 does not appear to play an essential role in synaptogenesis and synaptic function at least at the NMJ. Importantly, these results indicate that *D14-3-3ε* mutants do not suffer from a generalized malfunction of their nervous system likely to underlie the behavioral phenotypes. If synapses of the adult CNS are similarly unaffected by the lack of D14-3-3ε, then the observed normal synaptic transmission under strong stimulation would be inconsistent with premature fatigue or desensitization. These could have been manifested as neurotransmitter depletion resulting in depression instead of facilitation. It is then possible that *D14-3-3ε* mutants may exhibit reduced experience-dependent responses because they habituate to them prematurely.

The behavioral deficits of *D14-3-3* mutants conform to premature habituation

Given that *D14-3-3ε* mutants did not appear to harbor apparent deficits in synaptic physiology and function, I investigated whether the behavioral deficits conform to the classically defined habituation parameters (Thomson and Spencer, 1966). Animals were pre-exposed to an odor for different lengths of time and 30 seconds later their response to this odor given a choice of air was tested. Control animals habituate to an odor after 150-180 seconds of continuous exposure (Acevedo and Skoulakis, submitted). In congruence, 120 seconds of exposure to OCT did not diminish subsequent OCT

avoidance in *D14-3-3ε*^{ex5}control flies. However, OCT avoidance of *D14-3-3ε*^{ex4} and *D14-3-3ε*$^{l(3)j2B10}$ homozygotes declined significantly after 20 seconds of pre-exposure to this odor and was asymptotic after 40 seconds (Figure 37A). Similar results were obtained with pre-exposure to BNZ and ETA (not shown). To investigate whether the pre-exposure dependent response decrement recovered spontaneously, the animals were allowed rest periods prior to testing following 60 seconds of odor exposure. The deficit in OCT avoidance recovered spontaneously to control levels after about 12 minutes of rest (Figure 37B). The rather slow spontaneous recovery is consistent with the predictions for habituation, fatigue and desensitization (Groves and Thomson, 1970; Rose and Rankin, 2001; Thomson and Spencer, 1966).

To differentiate among these possibilities, because fatigue and desensitization would only recover spontaneously given adequate time, I attempted to eliminate the pre-exposure dependent decrement in avoidance acutely, by brief application of an unrelated noxious stimulus (dishabituation) (Groves and Thomson, 1970; Thomson and Spencer, 1966). The nature, strength and number of potentially dishabituating stimuli required were determined previously (Acevedo and Skoulakis submitted). Control and mutant flies were exposed to OCT for 60 seconds as before, but prior to testing a single 45 Volt footshock was administered. Surprisingly, this single footshock was able to fully reverse the osmotactic deficit such that after pre-exposure, the mutants avoided the test odor equally with *D14-3-3ε*^{ex5}controls, or naïve animals (Figure 37C). The result indicated that decreased OCT avoidance was in fact the result of premature habituation.

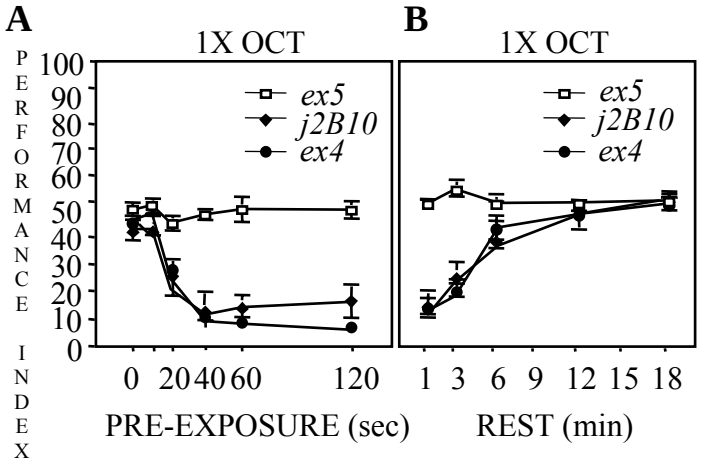

Figure 37. Osmotactic decline onset, spontaneous recovery and reversal in *D14-3-3ε* mutants

Means + standard error of the mean (SEM) are shown SD: Significant differences, NSD: Non-significant differences. Positive values indicate avoidance and negative values indicate attraction.

(A) Time course of osmotactic decline for controls (open symbols) and *j2B10* and *ex4* homozygotes (filled symbols). The PI for OCT avoidance after pre-exposure for the indicated times (0-120 seconds) is shown. ANOVA indicated significant effects of pre-exposure times and genotype ($F_{(17,140)}$=26.03 $p<0.0001$). Compared to naïve (0 time), there was no significant effect of pre-exposure time on subsequent OCT avoidance of *ex5* animals ($F_{(5,46)}$=0.85 $p<0.5219$). However, compared to naïve *j2B10* and *ex4* homozygotes, all avoidances after 20 seconds of pre-exposure remained significantly different ($p<0.0001$). Cross genotype comparisons demonstrated significant differences ($p<0.0001$) between *ex5* and *j2B10* or *ex4* at 20, 40, 60 or 120 seconds of pre-exposure. A pre-exposure dependent decline in osmotaxis in mutant homozygotes occurred between 10 and 20 seconds of pre-exposure to an odor.

(B) Spontaneous recovery of the pre-exposure-dependent osmotactic decline within 9 minutes. Recovery of OCT avoidance to naïve levels by *j2B10* and *ex4* homozygotes (filled symbols) after the indicated rest interval following 60 seconds of OCT pre-exposure. The performance of *ex5* (open symbols) did not change. However, the performance of OCT pre-exposed mutants changed in a rest interval-dependent time (ANOVA: $F_{(14,130)}$=12.65 $p<0.0001$, SD). Planned comparisons indicated that compared to *ex5*, both *j2B10* and *ex4* homozygotes were still deficient in osmotaxis ($p<0.0001$) after 1, 3 and 6 minutes, but not after longer rest times.

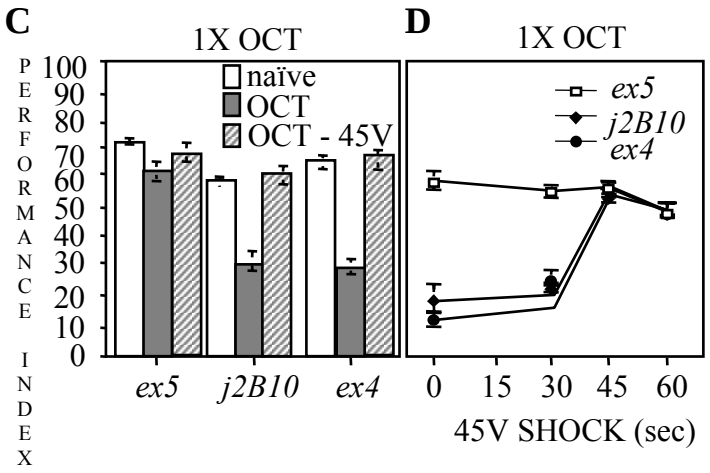

Figure 37. (continued)

(C) Reversal of the pre-exposure dependent osmotactic decline with electric shock. Animals were tested for OCT avoidance either naïve (open bars), after 60 seconds of OCT pre-exposure (gray bars), or after a single 45Volt footshock following 60 seconds of OCT pre-exposure delivered 30 seconds prior to testing (striped bars). OCT avoidance of naïve animals was not significantly different (ANOVA: $F_{(2,24)}$=0.92 p<0.4130, NSD). In contrast, 60 seconds of pre-exposure to OCT precipitated significant differences (ANOVA: $F_{(2,28)}$=43.67 p<0.0001, SD) between *ex5* and *j2B10* and *ex4* (Dunnett's, p<0.0001 for all comparisons). However, the avoidances of naïve and OCT pre-exposed mutants followed by a footshock were not significantly different (ANOVA: $F_{(2,23)}$=1.22 p<0.0.3141, NSD), indicating that a single 45-Volt footshock restored normal OCT avoidance.
(D) Reversal of the osmotactic decline depends on the time of footshock delivery. OCT avoidance after 60 seconds of pre-exposure to this odor. A single 45 Volt footshock was delivered either prior to pre-exposure (0 seconds), during pre-exposure at 30 seconds and 45 seconds, or immediately after (60 seconds). ANOVA indicated significant differences ($F_{(11.96)}$=34.25 p<0.0001, SD). Subsequent planned comparisons indicted significant performance differences (p<0.0001) between controls and mutants when the footshock was delivered in the beginning or 30 seconds after pre-exposure onset., but not when it was delivered at 45 seconds or the end of the 60second pre-exposure.

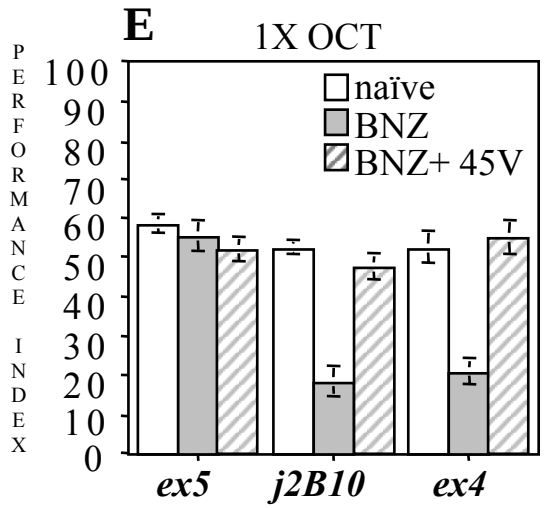

Figure 37. (continued)

(E) Reversal of the pre-exposure dependent osmotactic decline to a novel odor with electric shock. Animals were tested for OCT avoidance either naïve (open bars), after 60 seconds of BNZ pre-exposure (light gray bars), or after a single 45Volt footshock following 60 seconds of BNZ pre-exposure delivered 30 seconds prior to testing (striped gray bars). OCT avoidance of naïve animals was not significantly different (ANOVA: $F_{(2,24)}$=2.38 p<0.1133, NSD). However, compared to controls, avoidance of OCT was significantly decreased in the mutants after BNZ pre-exposure (ANOVA: $F_{(2,25)}$=21.61 p<0.0001, SD and subsequent Dunnett's, p<0.0001 for all comparisons). This pre-exposure dependent difference in avoidance between mutants and controls was eliminated after a single 45 Volt footshock delivered 30 seconds prior to testing (ANOVA: $F_{(2,23)}$=0.01 p<0.9857, NSD).

If the electric footshock was indeed a dishabituating stimulus, then it should not be effective prior to odor pre-exposure which would be characteristic of sensitization. A single 45 Volt footshock was delivered either prior to OCT pre-exposure, in the middle, or at 45 seconds of the 60 second odor exposure. It is apparent from Figure 37D that both mutants dishabituated readily when the footshock was delivered at the end, but not prior to pre-exposure. Interestingly, a footshock delivered after 45 seconds of a 60 second pre-exposure dishabituated the response fully. This indicates that delivery of the footshock 15 seconds prior to termination of odor pre-exposure effectively re-sets the time necessary to obtain a habituated response which is 20-30 seconds (Figure 37A), thus blocking or disallowing habituation. Qualitatively and quantitatively similar results were obtained with animals pre-exposed to BNZ and ETA (not shown).

Finally, a single 45 Volt footshock reversed fully the reduced OCT avoidance after prior exposure to BNZ (Figure 37E). This indicates that the observed cross-odor habituation (Figure 35E, 38F and Figure 37E) is likely generalization of habituation (Groves and Thomson, 1970; Mackintosh, 1974; Thomson and Spencer, 1966) to all odors regardless of their quality as attractive or aversive stimuli. Consistent with this the mutants displayed decreased responses to all aversive and attractive odors tested against but only after pre-exposure to another odor (not shown). Because the odors used in these assays are processed in distinctly different antennal lobe glomeruli (de Bruyne et al., 2001), it seemed likely that lack of D14-3-3ε compromises a general mechanism operating in higher order brain centers and required to prevent premature habituation. This would be consistent with the broad distribution of the protein in adult brains. In

addition lack of apparent synaptic deficits and the acute reversal with a mild footshock strongly indicate that the experience-dependent osmotactic deficits of *D14-3-3ε* mutants are the result of premature habituation to odor stimuli.

Transgenic rescue of the premature olfactory habituation deficits of *D14-3-3ε* mutants

In a recent study, I determined that the MBs are essential in protecting wild-type *Drosophila* from premature habituation to olfactory and footshock stimuli. Moreover, it appeared that neurons in the Lateral Horn (LH) likely play an important role in protection from habituation (Acevedo and Skoulakis, submitted). Because D14-3-3ε is distributed throughout the adult brain including the MBs and LH (Figure 34A), initially I attempted rescue of the behavioral phenotype with *UAS-mycD14-3-3ε* transgenes driven by the *c155-Gal4* (*elav*) and *tub-Gal4* (*β-tubulin*) drivers expressed broadly in the nervous system (Yao and White, 1994).

Both weak ($myc\varepsilon^{L}$) and strong ($myc\varepsilon^{H}$) transgenes directed accumulation of the transgenic protein in heads of animals that contained both the transgene and the driver as expected (Figure 38A). It must be noted that the level of transgenic protein at least from the $myc\varepsilon^{H}$ transgene approached or was greater than that of the native D14-3-3ε as demonstrated in the Western blots on Figure 38. This is particularly important when transgene expression was restricted to a small set of neurons, suggesting that the protein accumulated to very high levels within them. The distribution of the transgenic protein in the brain of $D14\text{-}3\text{-}3\varepsilon^{ex4}$ homozygotes is shown in Figure 34C. Under the *c155-Gal4*

driver low levels of the protein accumulated throughout the neuropil of the adult head and it appeared strikingly enriched throughout the MBs with somewhat lesser amounts in the fan shaped and ellipsoid bodies and the antennal lobe (Figure 34A.1-4). In contrast, under the *tub-Gal4* driver the transgenic protein accumulated nearly evenly throughout the brain neuropil with somewhat elevated accumulation in the calyces of the MBs, fan shaped body and antennal lobes (Figure 34A.5-8).

Upon 60 second pre-exposure to OCT, homozygous mutant animals accumulating the transgenic protein under the *c155-Gal4* driver did not habituate prematurely. However, animals merely carrying either the transgenes or the *Gal4* drivers alone in a homozygous mutant background displayed strong premature habituation (Figure 38A).

The weak ($myc\varepsilon^{L}$) transgene was sufficient to fully rescue the deficit of $D14\text{-}3\text{-}3\varepsilon^{l(3)j2B10}$ homozygotes, whereas for $D14\text{-}3\text{-}3\varepsilon^{ex4}$ homozygotes rescue with this transgene was significant, albeit slightly less than rescue obtained with the $myc\varepsilon^{H}$ transgene (Figure 38A). This is consistent with reports suggesting that $D14\text{-}3\text{-}3\varepsilon^{l(3)j2B10}$ is a hypomorphic allele. Therefore, I focused mostly on rescue of the $D14\text{-}3\text{-}3\varepsilon^{ex4}$ deletion allele. Interestingly, only partial rescue was obtained under the *tub-Gal4* driver despite the nearly equal transgenic protein accumulation (Figure 38A) and broad neuropil distribution in the brain (Figure 34A.5-8). Similar results were obtained with pre-exposure to BNZ and ETA. It appears then that although abundant, D14-3-3ε under the *tub-Gal4* driver was not sufficiently enriched in neurons required to protect from

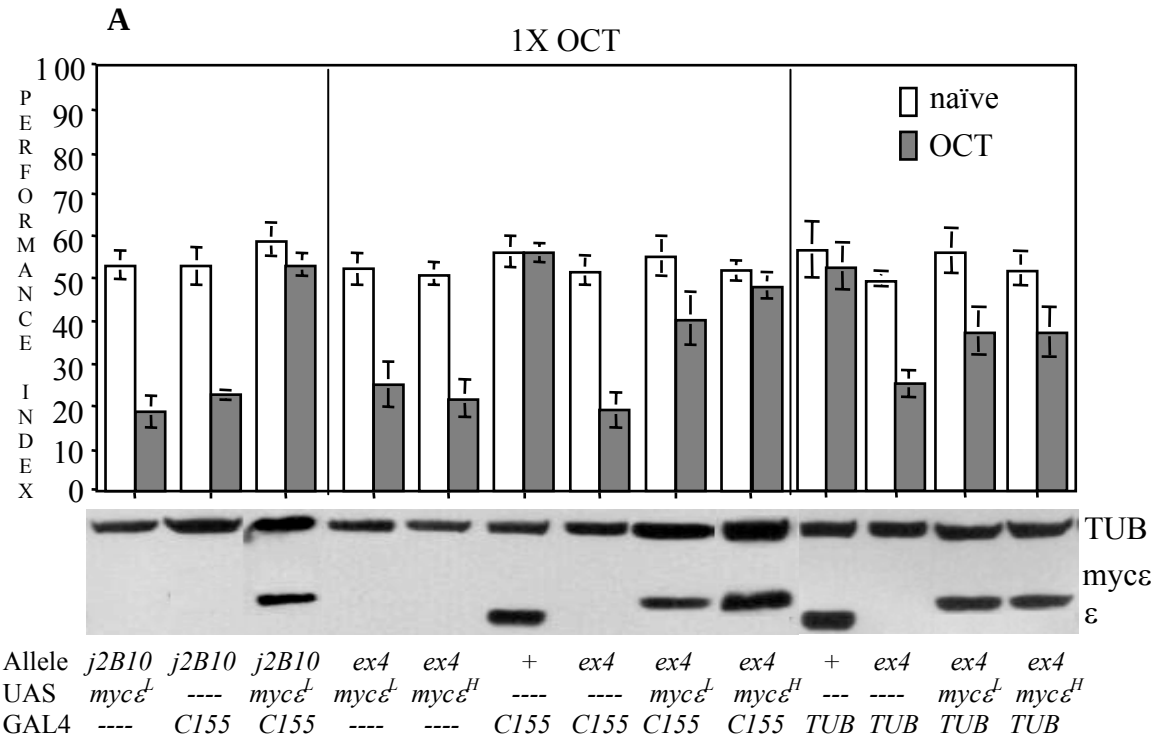

Figure 38. Rescue of olfactory premature habituation in *D14-3-3ε* mutants

Means + standard error of the mean (SEM) are shown SD: Significant differences, NSD: Non-significant differences

(A) Rescue of premature olfactory habituation in $D14\text{-}3\text{-}3\varepsilon^{l(3)j2B10}$ and $D14\text{-}3\text{-}3\varepsilon^{ex4}$ mutant homozygotes by *c155-Gal4* and *tub-Gal4* driven *UAS-mycD14-3-3ε* transgenes. Two independent *D14-3-3ε* transgenic lines were used, which based on protein accumulation levels were classed as high ($myc\varepsilon^{H}$) and low ($myc\varepsilon^{L}$). The level of either the native D14-3-3ε or the slightly larger transgenic mycD14-3-3ε for all genotypes utilized is shown beneath the graphs. The level of the ubiquitous protein β-tubulin is shown as a semi-quantitative control.

Octanol avoidance following 60 seconds of OCT pre-exposure is shown for *j2B10* and *ex4* homozygotes with and without transgenically supplied D14-3-3ε as indicated. Naïve animals (open bars) avoided OCT equally ($F_{(12,104)}$=0.53 p<0.8904, NSD). In contrast, 60 seconds of OCT pre-exposure precipitated significant differences among the genotypes. Group 1- *c155-Gal4* driven transgenes. ANOVA: $F_{(8,65)}$=23.75 p<0.0001, SD. Subsequent planned comparisons revealed significant differences *(*p<0.0001) between *c155-Gal4/+ ;+* and all *j2B10* and *ex4* homozygotes that did not carry both the *UAS-mycD14-3-3ε* transgenes and the *c155-Gal4*driver demonstrating that the premature habituation deficit of *D14-3-3ε* mutants was not reverted by the presence of these transgenes alone. In contrast, there were no significant differences in performance after pre-exposure between *c155-Gal4/+ ;+* and *c155-Gal4/+ ; j2B10,* $myc\varepsilon^{L}$/+, or *c155-Gal4/+ ; ex4,* $myc\varepsilon^{H}$/+ and *c155-Gal4/+ ; ex4,* $myc\varepsilon^{L}$/+, indicating that accumulation of D14-3-3ε specifically in the nervous system can revert the premature habituation deficit. Group 2- *tub-Gal4* driven transgenes. ANOVA: $F_{(3,31)}$=9.86 p<0.0001, SD. Planned comparisons indicated significant differences between controls (*tub-Gal4/+*) and *ex4/ex4,tub-Gal4*, but also with *ex4,* $mycD14\text{-}3\text{-}3\varepsilon^{H}$*/ex4, tub-Gal4* and *ex4,* $mycD14\text{-}3\text{-}3^{L}$*/ex4, tub-Gal4* (p<0.0001). Because the latter were also significantly different from the mutant (*ex4/ex4,tub-Gal4*), the results suggest partial rescue of the phenotype with this driver.

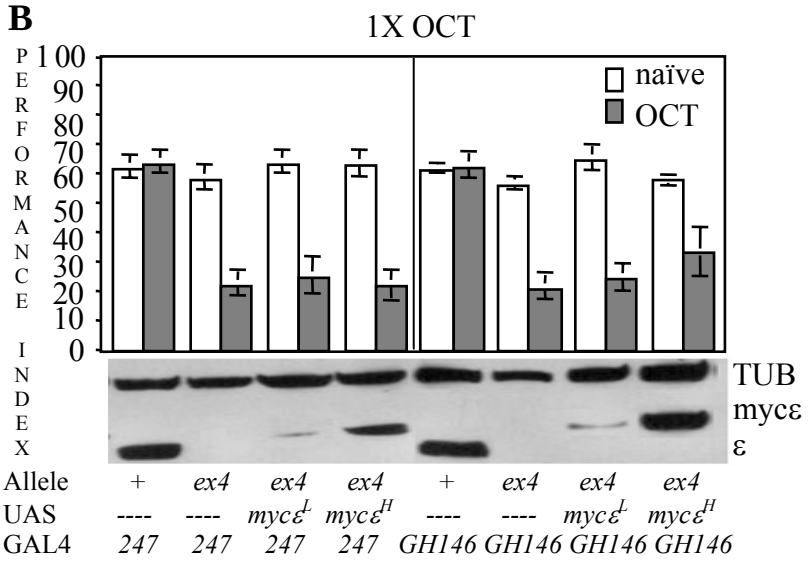

Figure 38. (continued)

(B) Restricted expression of the *UAS-mycD14-3-3ε* transgenes in the mushroom bodies and iACT does not rescue the premature habituation deficit of *D14-3-3ε* mutants. Mushroom body specific expression was achieved with the *247-Gal4* driver, while iACT specific expression was directed by the *GH146-Gal4* driver. Naïve avoidance of OCT was not significantly different among along genotypes tested (ANOVA: $F_{(7,61)}=0.79$ $p<0.5969$, NSD). In contrast, 60 seconds of OCT pre-exposure precipitated significant differences. Group 1-*247-Gal4* driven transgenes: ANOVA: $F_{(3,30)}=17.81$ $p<0.0001$, SD. Subsequent Dunnett's tests revealed that the performance of mutants with or without transgene expression were significantly different from controls ($p<0.0001$) and not different from each other indicating lack of rescue. Group2- *GH146-Gal4* driven transgenes: ANOVA: $F_{(3,32)}=11.74$ $p<0.0001$, SD. Again, subsequent Dunnett's tests revealed that the differences were wholly attributable to differences of all genotypes with the control, indicating lack of rescue.

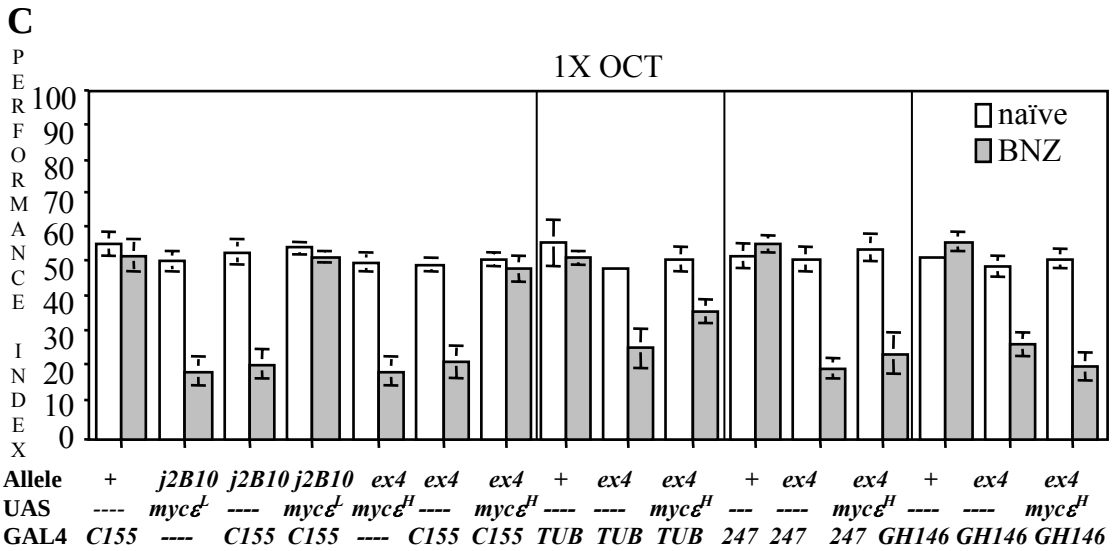

Figure 38. (continued)

(C) Rescue of odor generalization in premature habituation in *D14-3-3ε*$^{l(3)j2B10}$ and *D14-3-3ε*^{ex4} mutant homozygotes by *c155-Gal4* and *tub-Gal4* and tissue restricted *UAS-mycD14-3-3ε* transgenes. Octanol avoidance following 60 seconds of benzaldehyde pre-exposure is shown for *j2B10* and *ex4* homozygotes mutants with and without *mycε*^{H} and *mycε*^{L} transgenes. There were no significant differences in OCT avoidance for all naïve (open bars) genotypes (ANOVA: $F_{(15.133)}$=0.49 p<0.9311, NSD). In contrast, BNZ pre-exposure precipitated significant differences. Group 1- *c155-Gal4* driven transgenes. ANOVA: $F_{(2,23)}$=17.64 p<0.0001, SD. Subsequent Dunnett's tests revealed that the differences (p<0.0001) arose only between control (*c155-Gal4/+*) and mutants without transgenically supplied mycD14-3-3ε indicating complete rescue of the phenotype. Group 2- *tub-Gal4* driven transgenes. ANOVA: $F_{(2.22)}$=11.70 p<0.0001, SD. Dunnett's tests revealed that transgene expression restored the phenotype partially since both mutants and mutants expressing the transgene were significantly different (p<0.0001) than control. Group 3-*247-Gal4* driven transgenes. ANOVA: $F_{(2,23)}$=24.98 p<0.0001, SD. The difference arose because mutants either expressing the transgene or not were significantly (p<0.0001) different from controls indicating lack of rescue. Group 4-*GH146-Gal4* driven transgenes. ANOVA: $F_{(2,23)}$=31.80 p<0.0001, SD. Again, the differences arose between control and mutants either expressing or not expressing the transgene indicating lack of rescue.

habituation (MBs for instance) resulting in significant but nor complete rescue of the phenotype.

I attempted rescue of the behavioral phenotype of the *D14-3-3ε^{ex4}* deletion allele with restricted transgenic protein accumulation in the MBs for two reasons. First, because the transgenic protein appears to accumulate preferentially in the MBs under the *c155-Gal4* driver and rescue completely the premature habituation phenotype; and second because of previous work implicating the MBs in protection from habituation (Acevedo and Skoulakis, submitted). Given that transgene expression is restricted to a comparatively small number of cells in the *Drosophila* brain under the *247*-Gal4 driver, significant amounts accumulated at least from the *mycε^{H}* transgene (Figure 38B). However, the premature habituation phenotype was not rescued or even slightly improved in animals expressing the transgene in their MBs. These results strongly suggest that with respect to D14-3-3ε, accumulation in the mushroom bodies is not sufficient for protection from habituation and the protein is apparently required in additional neurons to mediate this effect.

Because the olfactory information is transmitted to the MBs and the LH primarily via the iACT (Marin et al., 2002; Stocker et al., 1997; Tanaka et al., 2004), and D14-3-3 accumulates in these neurons, I investigated whether restoring the protein in these cells was sufficient to recover protection from premature habituation. However, animals expressing the transgene in iACT neurons under the *GH146*-Gal4 driver habituated prematurely despite high accumulation of the transgenic protein (Figure 38B).

Therefore, D14-3-3ε activity in iACT neurons is not sufficient to mediate protection from habituation.

Finally to investigate whether loss of D14-3-3ε is actually required for the observed generalization of premature habituation across odors, the transgenic animals and control strains described above were pre-exposed for 60 seconds to BNZ and subsequently were tested for OCT avoidance. All naïve transgenic and control strains avoided BNZ equally (Table 17). The results (Figure 38C) were identical to the ones described above. The premature habituation was fully eliminated with transgenic protein accumulation under the *c155-Gal4* driver, partial rescue was obtained under the *tub-Gal4* driver and the deficit remained when the transgenic protein accumulated only in the MBs or the iACT neurons.

Collectively, the data indicate that D14-3-3ε is essential for processes that protect animals from premature habituation to prolonged or repetitive olfactory stimuli. Although present in the MBs and the iACT, restricted activity of the protein in these neurons is not sufficient to protect from premature habituation to olfactory stimuli. Finally, transgene-mediated restoration of normal protection from habituation in *D14-3-3ε* null mutants demonstrates that the behavioral deficit is the result of the genetic lesions in this locus. Interestingly, the fused MB β-lobe phenotype of mutant homozygotes was still observed in transgenic animals with complete recovery of the premature habituation phenotype (*c155-Gal4/+ ; ex4, mycε^{H}/ ex4*, Figure 34B.6), partial

Table 17. Olfactory avoidance in rescued *D14-3-3ε* mutants

D14-3-3ε Allele	*UAS*	*GAL4*	BNZ
$D14\text{-}3\text{-}3\varepsilon^{l(3)j2B10}$	*UAS mycD14-3-3ε*^{L}	+	52.70 ± 2.20
$D14\text{-}3\text{-}3\varepsilon^{l(3)j2B10}$	+	*C155*	54.23 ± 1.35
$D14\text{-}3\text{-}3\varepsilon^{l(3)j2B10}$	*UAS mycD14-3-3ε*^{L}	*C155*	55.60 ± 1.43
$D14\text{-}3\text{-}3\varepsilon^{ex4}$	*UAS mycD14-3-3ε*^{H}	+	54.46 ± 2.32
+	+	*C155*	53.47 ± 1.32
$D14\text{-}3\text{-}3\varepsilon^{ex4}$	+	*C155*	54.01 ± 1.96
$D14\text{-}3\text{-}3\varepsilon^{ex4}$	*UAS mycD14-3-3ε*^{H}	*C155*	52.12 ± 1.54
+	+	*TUB*	54.84 ± 2.23
$D14\text{-}3\text{-}3\varepsilon^{ex4}$	+	*TUB*	51.60 ± 2.19
$D14\text{-}3\text{-}3\varepsilon^{ex4}$	*UAS mycD14-3-3ε*^{H}	*TUB*	56.40 ± 2.28
+	+	*247*	49.74 ± 1.84
$D14\text{-}3\text{-}3\varepsilon^{ex4}$	+	*247*	50.52 ± 2.85
$D14\text{-}3\text{-}3\varepsilon^{ex4}$	*UAS mycD14-3-3ε*^{H}	*247*	54.81 ± 2.60
+	+	*GH146*	52.18 ± 1.37
$D14\text{-}3\text{-}3\varepsilon^{ex4}$	+	*GH146*	53.77 ± 2.70
$D14\text{-}3\text{-}3\varepsilon^{ex4}$	*UAS mycD14-3-3ε*^{H}	*GH146*	58.14 ± 2.82

The mean performance index (PI) for olfactory acuity are shown ± standard error of the mean (± SEM). ANOVA's for olfactory acuity indicated no significant differences among the strains for BNZ avoidance ($F_{(15,130)}$=1.08 P<0.3839) indicate not significant difference in olfactory avoidance.

rescue (*mycD14-3-3ε^{H}/ex4, tub-Gal4* Figure 34B.8), or no rescue (*247-Gal4/+ ; ex4, mycε^{H}/ ex4*, Figure 34B.9). This indicates that the structural deficit is not causal of the premature habituation. Moreover, since *D14-3-3ε* transgenes under the *c155-Gal4*driver were expressed throughout nervous system development, it is unlikely that the deficit is actually caused by the lack of D14-3-3ε.

Defective protection from premature habituation to footshock in *D14-3-3ε* mutants

To determine whether *D14-3-3ε* mutants are generally deficient in protection from habituation or specifically in protection from habituation to olfactory stimuli, I employed a second habituation paradigm I developed recently, habituation to electric footshock stimuli (Acevedo and Skoulakis, submitted). Control animals habituate to and decrease their avoidance of 45-Volt footshocks after pre-exposure to 8 and 11 such stimuli, but animals with compromised MB function habituate prematurely after a single footshock (Acevedo and Skoulakis, submitted). Similarly, *D14-3-3ε* mutants exhibited approximately a 45% decline in 45Volt footshock avoidance after pre-exposure to a single stimulus (Figure 39A). However, naïve mutant animals avoided the stimuli indistinguishably from controls (Table 16 and Figure 39A). Similar to the olfactory paradigm, the pre-exposure-dependent decline in footshock avoidance conforms to habituation parameters by spontaneously recovering to naïve levels within 10 minutes (not shown) and a full reversal of the deficit (dishabituated) with a 15-second exposure to BNZ delivered immediately after pre-exposure and prior to testing (Figure 39A).

To investigate whether lack of D14-3-3ε precipitated the premature habituation to footshock, transgenic rescue of the deficit was attempted. The nervous system specific *c155-Gal4* driver, the ubiquitous *tub-Gal4* driver and since the mushroom bodies are essential for protection from footshock habituation (Acevedo and Skoulakis, submitted), the MB-specific *247-Gal4* driver were utilized. The premature habituation phenotype was fully reversed with *D14-3-3ε* transgene expression under the *c155-Gal4* driver and nearly completely rescued with the *tub-Gal4* driver. As with osmotactic habituation, rescue was not observed with the MB-specific driver (Figure 39B). Therefore in addition to olfactory stimuli, *D14-3-3ε* mutants are not protected from premature habituation to footshocks as well and since the deficit is reversed with *D14-3-3ε* transgene expression, the deficit maps to this locus. Furthermore, as for olfactory stimuli, D14-3-3ε accumulation in the MBs is not sufficient to protect the mutants from premature habituation.

Collectively the results indicate that *D14-3-3ε* mutants habituate prematurely to two different types of stimuli, olfactory and footshock. Thus, it is likely that they harbor a general defect and habituate prematurely to many sensory stimuli. If so, *D14-3-3ε*

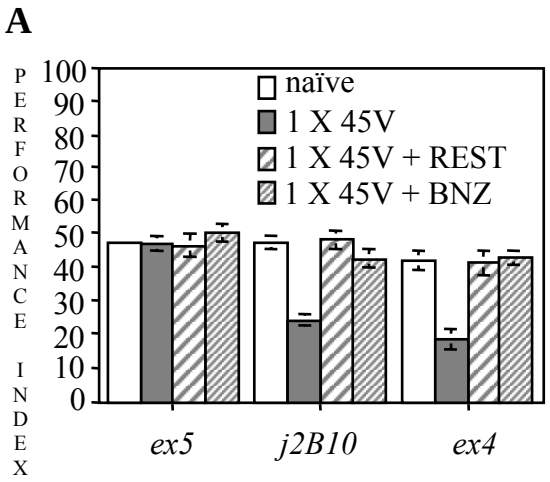

Figure 39. Premature habituation to footshock of *D14-3-3ε* mutants and transgenic rescue

Means + standard error of the mean (SEM) are shown SD: Significant differences, NSD: Non-significant differences

(A) Habituation to 45Volt footshock in *D14-3-3ε* mutants. Avoidance of 4, 45Volt electric footshocks in naïve flies (open bars) was not significantly different among genotypes (ANOVA: $F_{(2,25)}$=2.06 p<0.1496, NSD). In contrast, pre-exposure to a single 45 Volt footshock (dark gray bars) decreased subsequent avoidance 4, 45Volt footshocks significantly (ANOVA: $F_{(2,23)}$=40.08 p<0.0001, SD). Subsequent Dunnett's tests revealed a significant decrease (p<0.0001) in the avoidance of *j2B10* and *ex4* compared to controls (*ex5*). Allowing 6 minutes of rest (thickly hatched bars) between pre-exposure and testing did not result in significant differences in 4, 45Volt footshock avoidance (ANOVA: $F_{(2,23)}$= 1.16 p<0.3300, NSD) indicating full recovery of the effect within 6 minutes. Similarly, the response was fully dishabituated to naïve or control levels (light gray bars) with brief exposure to an odor after shock pre-exposure, but prior to testing (ANOVA: $F_{(2,23)}$=3.26 p<0.0586, NSD).

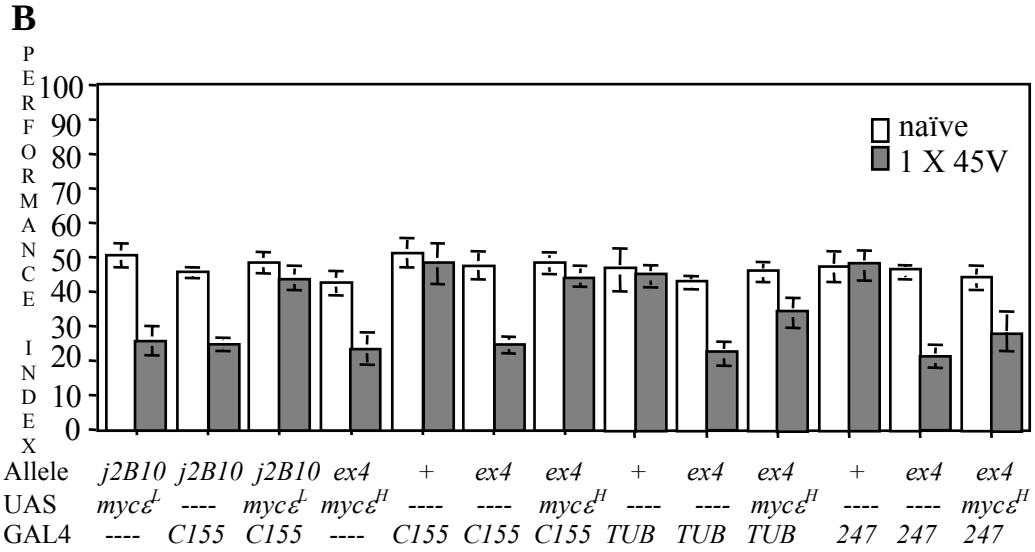

Figure 39. (continued)

(B) Transgenic rescue of premature habituation to footshock in *j2B10* and *ex4* mutants with the indicated *Gal4* drivers crossed to UAS-*mycD14-3-3ε* transgenes. 45volt (45V) shock avoidance following pre-exposure to a single 45Volt footshock is shown for *j2B10* and *ex4* homozygotes mutants with and without transgenically supplied D14-3-3ε. All naïve flies (open bars) performed similarly (ANOVA: $F_{(12.101)}$=0.53 p<0.8869, NSD). In contrast, a single 45Volt pre-exposure (gray bars) precipitated significant differences ($F_{(12,102)}$=8.20 p<0.0001, SD). Subsequent planned comparisons revealed significant differences (p<0.0001) between *c155-Gal4/+ ; ex4* and *c155-Gal4/+ ; j2B10, mycD14-3-3ε^L/+*, or *c155-Gal4/+ ; ex4, mycD14-3-3ε^H/+*, but not between *c155-Gal4/+ ;+* and *c155-Gal4/+ ; j2B10, mycD14-3-3ε^L/+*, or *c155-Gal4/+ ; ex4, mycD14-3-3ε^H/+*, suggesting transgenic rescue of the deficit. Furthermore, the difference between *ex4/ex4,tub-Gal4* and *ex4, mycD14-3-3ε^H/ ex4,tub-Gal4* was significantly different, but is was also different from controls (+/,*tub-Gal4*) indicating partial rescue of the phenotype. In contrast, the performance of 247/+ ; *ex4, mycD14-3-3ε^H/ex4* was not significantly different than that of 247/+ ; *ex4/ex4* and was significantly different that that of controls (247/+) suggesting lack of rescue.

mutants comprise a novel class of behavioral mutants in *Drosophila*. Moreover, the results from the transgenic rescue experiments and the broad distribution of the protein in the adult brain indicate that D14-3-3ε function is required in more than one particular class of neurons and neuronal networks to mediate protection from premature habituation in the adult CNS. Previous work identified the MBs as essential for protection from premature habituation based on structural and functional ablation studies (Acevedo and Skoulakis, submitted). Interestingly, elevated accumulation in the MBs was observed under the *c155-Gal4* driver, which mediated complete rescue of the mutant phenotype. In contrast, MB-restricted D14-3-3ε accumulation was not sufficient to protect from premature habituation. These results refine the proposed model and strongly suggest that although the MBs are essential, they are not sufficient for protection from premature habituation. However, because of the broad distribution of the protein it is not possible to define with precision additional parts of the adult brain involved in the process. The lateral horn has been proposed to be involved in the protection from premature habituation (Acevedo and Skoulakis, submitted) and in fact D14-3-3ε is found in this brain region in normal animals (Figure 34A) and accumulates there albeit at low levels under the *c155-Gal4* driver. Additional areas of the brain likely involved in protection from premature habituation are neurons with prominent D14-3-3ε accumulation under the *c155-Gal4* driver such as the fan shaped and ellipsoid bodies, which will constitute the focus of future work.

Transgenic rescue of the associative learning deficit of *D14-3-3ε* mutants

Given the behavioral rescue of *D14-3-3ε* mutants, I wondered whether animals rescued from premature habituation would also be rescued from the initially observed learning deficit. Habituation has been proposed to constitute the basis for selective attention (Mackintosh, 1974; Rose and Rankin, 2001) and it is likely that premature habituation to a stimulus would not permit formation of the proper CS/US association and lead to deficient, or little associative learning. Furthermore, premature habituation may underlie human learning disabilities linked to Attention Deficit Hyperexcitability Disorder (Gillberg, 2003; Slaats-Willemse et al., 2003).

Therefore, to test the hypothesis that the defective protection from habituation to the odor and shock stimuli was the underlying cause of the learning deficit observed initially in *D14-3-3ε* mutants I investigated associative learning in animals fully and partially rescued from the deficit by *D14-3-3ε* transgene expression. In accord with the hypothesis, animals fully rescued from premature habituation appeared to learn normally an associative olfactory task (Figure 40). Conversely, *D14-3-3ε* mutants partially rescued from premature habituation with the *tub-Gal4* driver displayed a proportionally small but significant improvement in olfactory learning (Figure 40). In contrast directed expression of same strongly expressing *D14-3-3ε* transgenes in the mushroom bodies did not yield any significant improvement in learning over the performance of mutant homozygotes (Figure 40). Since the MBs are unequivocally essential for olfactory learning and memory (Heisenberg, 2003; Roman and Davis, 2001), the results suggest that protection from premature habituation, which requires at least in part these neurons,

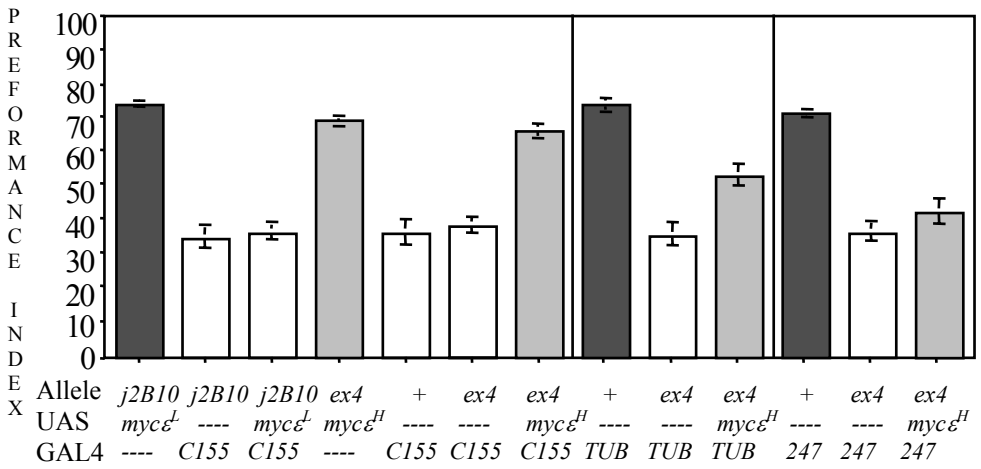

Figure 40. Transgenic rescue of associative olfactory learning in *D14-3-3ε* mutants

Means + standard error of the mean (SEM) are shown SD: Significant differences, NSD: Non-significant differences.

Performance after associative olfactory learning is shown for controls and *j2B10* and *ex4* homozygous mutants with and without transgenically supplied D14-3-3ε *mycε* (*mycε*^{H} and *mycε*^{L}). Significant differences in performance following associative olfactory learning were uncovered ($F_{(12,99)}$=52.00 p<0.0001, SD). Subsequent planned comparisons revealed significant differences (p<0.0001) between the performance of the control *c155-Gal4/+* strain (dark gray bar) and all *j2B10* and *ex4* homozygotes that do not express transgenically supplied protein (white bars) indicating learning deficits in strains not expressing the transgene. In contrast, the performance of *j2B10* or *ex4* homozygous mutant strains expressing the transgene (light gray bars) was not significantly different than that of controls suggesting complete reversal of the olfactory learning deficit. However, although significantly higher than that of *ex4, tub-Gal4/ex4,* the performance of *ex4, tub-Gal4/ ex4, mycD14-3-3ε*^{H} remained significantly lower (p<0.0001) than that of the respective control *+/ ex4, tub-Gal4* indicating partial rescue of the deficit with this *Gal4* driver. In contrast, the performance of *247/+; ex4,mycD14-3-3ε*^{H}*/ex4* remained at the level of *247/+; ex4/ex4* indicating that accumulation of the transgenic protein only in the mushroom bodies was not sufficient to support normal olfactory learning.

is essential for normal learning and memory. Our experiments suggest that premature habituation to odor and footshock stimuli is unlikely to permit CS+/US associations can be formed. However, currently I cannot distinguish that from habituation to the test odors, which would not permit conditioned response dependent CS+ vs. CS- discrimination during testing.

Importantly, *leo* mutants which exhibit a robust learning and memory deficit (Philip et al., 2001; Skoulakis and Davis, 1996) are not deficient in protection from premature habituation (not shown and Philip et al., 2001). Since D14-3-3ε function is ostensibly required at least in part within the MBs to protect from premature habituation and LEO is preferentially distributed within these same neurons, it is interesting that the two *Drosophila* 14-3-3 proteins co-localize but apparently function in distinctly different processes. The biochemical processes that engage the D14-3-3ε to mediate protection from premature habituation such that olfactory learning and memory can occur are currently unknown but of much interest. The identification and characterization of *D14-3-3ε* as the first mutant in this process provides a new avenue for investigating the signaling mechanisms and molecules that serve protection from premature habituation to stimuli. The availability of the two recently developed simple and efficient habituation paradigms are expected to facilitate the identification of novel mutants in the process.

EXPERIMENTAL PROCEDURES

Drosophila strains

Drosophila were cultured in standard cornmeal sugar food supplemented with soy flour and $CaCl_2$. The genetic background of all *D14-3-3ε* alleles was normalized to that of Cantonized w^{1118} (w^{1118} backcrossed to Canton S for 10 generations). The control strain utilized in all experiments was a w^{1118} -bearing strain derived by excision of the *l(3)j2B10* transposon (*ex5*). The performance of *ex5* homozygotes was identical to that of Cantonized w^{1118} in all behavioral assays tested (Acevedo and Skoulakis submitted). The $D14\text{-}3\text{-}3\varepsilon^{l(3)j2B10}$ mutant allele has been described previously (Chang and Rubin, 1997). Alleles $D14\text{-}3\text{-}3\varepsilon^{ex5}$ and $D14\text{-}3\text{-}3\varepsilon^{ex4}$ generated by mobilization of the transposon in $D14\text{-}3\text{-}3\varepsilon^{l(3)j2B10}$ were a gift of Dr. Henry Chang. The Gal4 "driver" strains containing the transgenes *tubP-Gal4* (BL#5138) and *C155-Gal4* (BL#458) were provided by the Bloomington Stock Center. The inner Anteno-Cerebral Tract and Mushroom body specific GAL4 lines *GH146-Gal4* and *247-Gal4* were described previously (Stocker, 1997; Zars, 2000). Animals carrying the *UAS-mycD14-3-3ε* transgene in a Cantonized w^{1118} genetic background were generated by standard methods. Of the six independent transformants, one with strong expression and one with weak expression were selected for further analyses based on eye color and verified by crossing to *tubP-Gal4* and performing Western blot analyses. To facilitate ease of genetics and husbandry the transgenes were recombined into the $D14\text{-}3\text{-}3\varepsilon^{ex4}$ carrying chromosome. Since it is

inserted on the third chromosome, the *tubP-Gal4* driver was also recombined onto the *D14-3-3ε*^{ex4} carrying chromosome.

Larvae for electrophysiology were reared on standard cornmeal molasses medium in 50 ml vials at low density. Female wandering third instar larvae were used for all experiments. Consistent staging of early wandering larvae was facilitated by the use of 0.05% bromophenol blue in the food (Maroney, 1983).

D14-3-3ε transgenic strains were generated by injecting wild type *D14-3-3ε*, and myc-tagged *D14-3-3ε* cDNAs sub-cloned pUAST (Brand and Perrimon, 1993) into *w*^{1118} embryos. Multiple independent transformant lines were obtained and the ones with the darkest or lightest w^+ eye color were used for this analysis.

Generation of anti-D14-3-3ε antibodies

The *D14-3-3ε* -pRSET expression vector was a kind gift of Dr. Chien (Tien et al., 1999). Recombinant D14-3-3 protein was purified from bacterial cultures by virtue of the hexahistidine tag and injected into hens (Charles River laboratories). IgY was purified from eggs using standard protocols (Charles River laboratories). The specificity of the anti-D14-3-3ε antibodies was tested with recombinant D14-3-3ε and LEO proteins and fly head lysates by western blots (see below).

Western blot analysis

Fly heads from control and mutant animals were homogenized in 10 μl of modified radioimmunoprecipitation assay (RIPA) buffer as previously described (Philip

et al., 2001). Extracts equivalent of three heads per lane were run on 18% acrylamide gels. Blots were probed at room temperature with rabbit anti-LEO (1:40,000), or chicken anti-D14-3-3ε (1:5000). Anti-β-tubulin (Developmental Hybridoma Studies Bank, University of Iowa, Iowa City, IA) at 1:500 dilution was used to control the blots quantitatively. Secondary antibodies were used at 1:15,000 for anti-rabbit, 1:5,000 for anti-chicken and 1:4000 for anti-mouse and the results were visualized with enhanced chemiluminescense (Pierce).

Histology

Frontal paraffin sections (5nm) of heads were prepared for immunohistochemistry or histology as described previously (Crittenden et al., 1998; Skoulakis and Davis, 1996). Anti-D14-3-3ε (1:300) was used to reveal the distribution of D14-3-3ε. The anti-LEO antibody (1:4500) was used to investigate the structure of mushroom bodies and ellipsoid body and the anti-DRK (1:2000) to specifically focus on the structure of the horizontal lobes (Crittenden et al., 1998; Mershin et al., 2004; Skoulakis and Davis, 1996). The anti-SH3PX1 antibody that identifies antennal lobe glomeruli was provided by Dr. J. Dixon and used at 1:1000 dilution (Worby et al., 2001).

Electrophysiology

Dissections and recordings were carried out in HL3 saline (in mM 70 NaCl, 5 KCl,, 20 MgCl2, 10 NaHCO3, 5 trehalose, 115 sucrose, 5 HEPES; pH 7.2; (Stewart et

al., 1994)). To reduce movement during dissections, chilled Ca^{2+}-free HL3 saline with 0.5 mM EGTA was used. When Ca^{2+} was varied, no alterations were made to offset the small changes in divalent ion concentration. Each preparation was tested in a single concentration of Ca^{2+}. Stimuli and solution changes were controlled and data were acquired using pClamp 8.1 (Axon Instruments). All recordings were performed at approximately 23ºC.

Voltage clamp recordings of synaptic currents were performed on muscle 6 of the third abdominal segment as previously described (Jan and Jan, 1976; Stimson et al., 1998). Synaptic currents were monitored using 2-electrode voltage clamp (Axoclamp 2B, Axon Instruments), held at –70 mV. To avoid the potential contribution of stimulation to the frequency of spontaneous mEJCs, these were recorded in separate experiments. mEJC frequency was calculated from the same 50 second sample. EJCs were evoked by stimulation of the cut end of the segmental nerve (SN) via a glass-tipped suction electrode. Each sample consisted of 50 seconds of data. For each preparation, amplitude data were plotted as a frequency histogram and a gaussian mean was calculated (Robinson, 1976). Responses to stimulus trains were calculated as the ratio of the average of the last 10 stimuli of a train to that of the first 10.

Olfactory trap assays

Olfactory traps were made from 1.5 ml and 0.5 ml Eppendorf tubes cut at the tips. The cut end of the 0.5 ml tube was inserted tightly into the cut end of the larger tube. 200µl of a 1% agarose solution containing either 0.05% geraniol (GER-Sigma), 0.1% ethyl acetate (ETA-Sigma) or 0.5% butanedione (BUT-Acros) was placed in the

cavity of the inner part of the lid of the 1.5 ml tube, allowed to solidify and the tube was closed. Eight male flies were placed into a 100 X 15mm petri dish with a damp piece of filter paper and the olfactory trap. All experiments were performed at 23-24ºC in the dark for 48 hours. An Attraction Index was calculated as the fraction of flies inside the trap.

Osmotaxis

Behavioral experiments were performed under red light at 23-24ºC and 65% humidity. All animals used in behavioral assays were 2-6 days old, collected the day before the day prior to testing nd kept in food vials in groups of 50-60 at room temperature. Odor avoidance and attraction were quantified by exposing ~50 flies at the choice point of a standard T-maze (Philip et al., 2001; Tully and Quinn, 1985) to an air-stream (500 ml/min) carrying the odor in one arm and fresh air in the other. The odors utilized for these experiments were 1000µl (1X) of undiluted 3-Octanol (OCT) (Fluka), 110µl (1X) of undiluted benzaldehyde (BNZ) (Sigma) and 10µl of a 1/10 dilution in water (1X) of ethyl acetate (ETA) (Sigma). The amounts of odors used were adjusted to yield similar osmotactic responses. Flies were given 90 seconds to choose between aversive odors and air, but 180 seconds for the choice between attractive odors and air (determined in control experiments, Acevedo and Skoulakis, submitted). At the end of the choice period flies in each arm were trapped and counted. The Performance Index (PI) was calculated as the fraction of flies that avoid or are attracted to an odor minus the fraction of flies that do not. A PI of 100 indicates that the flies avoid the odor

completely (or -100 complete attraction), whereas a PI of 0 indicates equal distribution between the arms of the maze and therefore no avoidance or attraction.

Osmotactic habituation

Osmotactic habituation experiments were performed under the conditions described above. For the "training phase", approximately 50 flies were exposed to either attractive (ETA) or aversive odors (OCT, BNZ) for 60 seconds unless otherwise indicated, in the upper chamber of a standard T-maze. After a 30 second rest period (unless indicated otherwise), the flies were lowered to the center of the maze for the "testing phase". The flies were tested for their avoidance or attraction to odors by a choice of Air *versus* either the previously experienced, or a novel odor. At the end of the choice period (90 seconds for aversive and 180 for attractive odors) the number of flies in each arm were trapped, counted and the performance index (PI) calculated as described above. To examine spontaneous recovery, flies were given a rest period for various lengths of time (6 minutes being the experimentally derived standard recovery period) in the upper arm of the maze after they were given the odor pre-exposure. Subsequently they were tested against the odor they were pre-exposed to versus air and a PI was calculated as described above. To determine the conditions for dishabituation with electric shock, control experiments were performed first to determine the stimulus strength and test number required.

Dishabituation of the control strain *D14-3-3ε* ^{ex5} was attempted at different footshock stimulus strengths. OCT PI for naïve *D14-3-3ε* ^{ex5}: 59.2 $\pm$ 2.3. Dishabituation

with 30 V, OCT PI: 54.8± 2.1; with 45 V, OCT PI: 58.7 ± 2.6; with 90V OCT PI: 58.3 ± 2.2. Since the 90V and 45V dishabituating shocks had equal effects, the milder of the two was selected. Moreover the number of 45V shocks did not have a significant effect on dishabituating osmotaxis (1X 45V shock OCT PI: 58.7± 2.3; 2X 45V shock OCT PI: 59.4± 2.8). Therefore, dishabituation was attempted with a single 45 volt shock either prior, during, or at the end of pre-exposure and was followed immediately (within 15-20 seconds) by testing as described above.

Habituation to footshock

Footshock avoidance was assessed as described previously (Philip et al., 2001; Skoulakis and Davis, 1996; Skoulakis, 1993). Footshock habituation conditions were modified from those used previously with both Cantonized w^{1118} and *ex5* (Acevedo and Skoulakis submitted). Briefly, for control strains 11, 1.25-second electric shocks at 45Volts were required for their footshock avoidance response to become habituated. After a 30-second rest, the flies were transferred to the lower part of the maze and tested by a choice between an electrified (45 Volts) and an inert grid. During the 90-second choice period 15, 1.25 second electric shocks were delivered to the electrified arm of the maze. However, these conditions were modified because in preliminary experiments, *D14-3-3ε* mutant animals appeared to habituate maximally after the first footshock. Therefore, for the "training phase" of habituation to electric footshock ~ 50 flies were sequestered in the upper arm of a standard T-maze lined with an electrifiable grid. They were exposed to 1, 1.25-second footshock at 45V. After a 30-second rest, the flies were

transferred to the lower part of the maze and tested with a choice between an electrified and an inert grid. During the 90-second choice period 4, 1.25 second electric shocks were delivered to the electrified arm. At the end of the choice period the flies in each arm were trapped, counted and a performance index was calculated as above. Dishabituation was achieved by exposing the flies to benzaldehyde (500µl BNZ carried in an air stream at 500 ml/sec as described above for olfactory habituation) for 15 seconds immediately after the "training phase". For spontaneous recovery, a 6-minute resting period (REST) was allowed in the upper part of the maze between the training and testing phases.

Olfactory associative learning

The olfactory associative learning paradigm originally described by Tully and Quinn, (Tully and Quinn, 1985) which couples aversive olfactory cues (conditioned stimulus) with electric shock (unconditioned stimulus) with the modifications described previously (Mershin et al., 2004; Philip et al., 2001)were used to assess learning. Because the earliest possible time that I can test the animals past the CS+ and US presentation is 180-200 seconds, our measurements cannot differentiate between "acquisition" and "3-minute memory". This earliest performance assessment will be referred to as "learning". Performance was measured by calculating a Performance Index (PI), which is the average of the half-learning indexes for each of two groups of animals trained to complementary conditioning stimuli as previously described (Philip et al., 2001).

Statistical analysis

Untransformed (raw) data were analyzed parametrically with JMP3.1 statistical software package (SAS Institute Inc., Cary, NC). For electrophysiological data values presented are means $\pm$ SEM. Differences between means were compared with one way ANOVA. For behavioral data, to maintain a constant experiment wise error rate, initial ANOVA and planned multiple comparisons (Dunnett's tests) were performed as suggested by Sokal and Rolf (Appendix B) (Sokal and Rohlf, 1981).

CHAPTER VI

CONCLUSION

Previous work with 14-3-3 proteins led to the suggestion that all isoforms or isotypes of this protein family are equivalent (Rosenquist et al., 2000). My hypothesis is that both isoform-specific and overlapping functions mediated through tissue specific expression, co-localization and dimerization of 14-3-3 proteins occur in vivo. It is a requirement of this hypothesis that 14-3-3 isotypes or isoforms are dynamically expressed through development and within different tissues. Another requirement is homo and heterodimer formation, or even selective heterodimerization when isotypes co-localize in the same cells.

Previous experiments determined a role for *14-3-3ζ*, in *Drosophila* development (Kockel et al., 1997, Li et al., 1997) and associative learning and memory (Skoulakis and Davis, 1996; Philip et al., 2001). Therefore, the primary focus of this research was on the other *Drosophila* 14-3-3, D14-3-3ε. To examine the functional equivalence of 14-3-3s in *Drosophila*, first I determined the temporal and spatial expression of each isotype and described the phenotypes of mutations in *D14-3-3ε* and compared them with those in *14-3-3ζ* (*leo*). This led to the discovery of two unique D14-3-3ε phenotypes. Then using a largely genetic approach the functional equivalence of LEOI and LEOII with D14-3-3ε was examined.

D14-3-3ζ

Temporal and spatial expression of D14-3-3ζ (leonardo, leo)

In *Drosophila*, the two LEO proteins are essential for embryonic, eye and oocyte development as well as synaptic activity, and learning and memory (Skoulakis and Davis, 1998, Kockel et al., 1997, Broadie et al., 1997). Using RT-PCR the temporal and spatial patterns of the RNAs that encode them was determined. *leoI* RNA was found to be expressed in early embryos (0-3 hour), late embryos (20-22 hour), all larval stages, and in adult heads. In 12-14 hour embryos when the nervous system is developing, *leoI* is absent. *leoI* appears to be present throughout the head and enriched in ellipsoid body (Philip et al., 2001). In contrast, *leoII* appears to be adult mushroom body specific and found in all embryonic stages including 12-14 hour embryos, larval stages, thorax, abdomen, and adults heads (Philip et al, 2001). In larval brains both *leoI* and *leoII* are present. One larval tissue where *leoII* is absent is the larval wing disc. This evidence suggests that there is differential expression of *leoI* and *leoII* throughout development.

LEOI versus LEOII in vital embryonic functions.

leonardo is an essential gene, therefore homozygous null alleles are lethal. The equivalence of the two LEO isoforms in vital functions was examined by transgenic rescue. To determine whether indeed LEOI and LEOII are equivalent in rescuing vital functions, the LEOI and LEOII transgenics were crossed into the homozygous lethal leo^{12X}, a deletion mutant, into leo^{P1188} a strong P-element mutant, and leo^{P1375}, a weaker allele. Both LEOI and LEOII were able to rescue the weaker leo^{P1375} allele, which still

has low levels of endogenous LEO transcription. In contrast, only LEOI transgenes were able to rescue the strong *leo*^{P1188} insertion and *leo*^{12X} deletion that lack LEO protein (Broadie et al 1997). This result leads to the conclusion that LEOI and LEOII are not equivalent in their ability to support embryonic development, although they only differ by five amino acids. The differences occur within the target-binding domain, which likely mediates the protein interactions necessary for survival. This is consistent with our hypothesis that the two LEO isoforms are functionally distinct, perhaps in compensation of LEOs apparent inability to become phosphorylated like the ζ/δ pair in vertebrates.

Novel role for 14-3-3s in pole cell development

At first look LEO and 14-3-3ε appear to function redundantly with respect to sterility, but on further examination, I found that they affect pole cell development differently. The rare escapers homozygous or heteroallelic with the weak *leo*^{P1375} allele and *leo*^{P1188} homozygotes or *leo*^{P1375}/*leo*^{12X} heteroallelics rescued from lethality by maternal *leoI* transgene expression were sterile. Partial sterility was observed with rescued *leo*^{P1375} homozygotes that retain low levels of LEO throughout development. These mutant animals were observed mating and devoid of gross morphological aberrations of their genitalia. The lack of LEO appears to affect both the germ-line and somatic gonadal development.

To examine the cause of sterility, sections of adult *leo*^{P1188} homozygous females rescued from lethality by induction of the *hsleoI* transgene were examined. The number

of ovarioles was severely reduced with few cell cysts per ovariole compared to controls. Initial division of pole cells (stage 5) in *leo* mutant homozygous embryos appeared normal likely due to perdurance of maternal LEO, but their numbers declined through stage 8 and 11 to 22-23 cells. These results suggested that pole cell survival declined concomitantly with the level of LEO protein in mutant homozygotes. The *hsleoII* (*LII*) transgenic lines were excluded from this analysis though tested in preliminary tests, because they did not rescue lethality. Therefore, the functional equivalence between LEOI and LEOII with respect to germ-line development is currently unknown.

Homozygous *D14-3-3ε* mutants are completely sterile. *D14-3-3ε^{ex4}* and D14-3-3ε$^{l(3)j2B10}$ females did not appear to have ovaries. Histological sections of *D14-3-3ε^{ex4}* homozygotes revealed disorganized internal reproductive structures and decreased egg and sperm cells. Consistent with this in *D14-3-3ε^{ex4}* and *D14-3-3ε$^{l(3)j2B10}$* homozygous mutant embryos, 8 to 10 pole cells differentiated in the pole plasm at the posterior tip of the embryo (Williamson and Lehman,1996) and after apparently reduced divisions, many pole cells failed to migrate properly and were lost, leading to a reduction in oocyte and sperm production.

Complete rescue was obtained with UAS-*D14-3-3ε* transgenes driven with GAL4 (Brand and Perrimon 1993) under the direction of the beta tubulin promoter (*tub-GAL4)*, but not the cytoplasmic actin 5C promoter (*act5C-GAL4*). Although *tub-GAL4* and *act5C* GAL4 drivers apparently are equivalently strong, only *tub-GAL4*, which directs expression in the germ-line was able to rescue sterility. In addition, the data demonstrate that the observed homozygous mutant sterility was indeed precipitated by

the lack of D14-3-3ε in the germ-line cells. In contrast, similarly expressed *hsleo* transgenes could not rescue the sterility deficit in *D14-3-3ε* mutant homozygotes, suggesting that with respect to germ-line development LEO is not equivalent to D14-3-3ε.

Germ-line cells, named pole cells in *Drosophila* or promodial germ cells (PGCs) in mice, express unique genes and undergo a differentiation program unlike any other type of cells (Wei and Mahowald, 1994). Currently a limited number of mutants have been described that effect germ-line migration (Starz-Gaiano and Lehman, 2001). These mutants completely halt migration at specific stages, do not allow mesoderm migration, attachment or alignment (Starz-Gaiano and Lehman, 2001; Ribero et al., 2003), in all cases, inhibiting final gonadal coalescence. Therefore, the *leo* and *D14-3-3ε* mutants are part of a novel class of mutants that effect germ-line migration of pole cells, but allow mesoderm migration, attachment and alignment and normal gonad coalescence. Therefore, it is unknown why some pole cells in LEO and D14-3-3ε migrate normally while others do not. Most of the known *Drosophila* migration mutants inhibit or alter the formation of attractant or repellent guidance cues similar to that of zebrafish or mice (Starz-Gaiano and Lehman, 2001). This may also be true for *leo* and *D14-3-3ε* mutants, although the role of 14-3-3s may be specific to *Drosophila* suggested by the fact that mouse PGCs differ from *Drosophila* pole cells in what attracts them to their target (Wei and Mahowald, 1994). Regardless, further work is needed to understand the role of 14-3-3s in germ-line development.

D14-3-3ε

Temporal and spatial expression of D14-3-3ε

D14-3-3ε is ubiquitously expressed in all tissues, stages of development, and cells examined (Philip et al., 2001). This expression is suggestive of the importance of the protein for basic cellular functions. Head sections of wild type *Drosophila* indicate D14-3-3ε accumulation throughout the head similar to the pattern of expression seen in murine brains (Baxter et al., 2002). There is also co-localization with LEO in the mushroom bodies, the centers for learning and memory and in various other tissues.

Role of D14-3-3ε in embryonic development

To investigate the D14-3-3ε loss of function phenotypes, novel deficiency alleles of the gene were characterized. Given that the pattern of expression is established, I investigated the phenotypes associated with D14-3-3ε mutants and determined whether they are the same as in LEO mutants. Genetic complementation was used to determine that null mutations in D14-3-3ε are semi-lethal. Dissection and staining of embryos indicates that death occurs because embryos are unable to hatch similar to leo^{P1188} mutants. leo^{P1188} mutants have deficits in neurotransmission at the larval Neuromuscular Junction (NMJ) (Broadie et al., 1997). However, physiological recordings at the NMJ of D14-3-3ε homozygous mutant larvae did not reveal deficits in synaptic transmission as seen in *leo* mutants (Broadie et al., 1997). This suggests that in the larva, although D14-3-3ε is present it is not required for neurotransmission. Alternatively, since these

recordings were performed in larvae that were able to hatch as embryos it is formally possible that a compensatory mechanism was activated which allowed them to hatch and survive and exhibit normal NMJ function without D14-3-3ε. However, full rescue of this lethality was achieved with the nervous system specific GAL 4 driver (elav-GAL4, C155), suggesting a role for D14-3-3ε in the embryonic nervous system, possibly required as a heterodimer with LEO for neurotransmission in embryonic development necessary for hatching. Thus supporting the hypothesis that in different life stages there are isoform-specific and overlapping functions among the 14-3-3s.

Functional complementation of the vital functions of D14-3-3ε in embryos with LEOI and LEOII

In homozygous *D14-3-3ε* null embryos, there was a highly significant increase in the amount of LEO compared to that in heterozygotes, or control animals. This appears to be due to a significant increase specifically in accumulation of *leoII* transcripts. This suggests that with respect to developmental processes it is LEOII that is at least partially redundant with D14-3-3ε as previously proposed (Chang and Rubin, 1997). However, high levels of LEOII are necessary to compensate for the loss of D14-3-3ε. It is possible that large abundance of LEOII homodimers functionally compensates for LEOII/D14-3-3ε potential heterodimers, or even for D14-3-3ε homodimers for processes essential for embryonic development. The fact that both are capable of binding signaling molecules such as Raf and are both expressed in embryos suggest that LEO and D14-3-3ε may work together as heterodimers to regulate signaling in these tissues. This is consistent

with the removal of a single copy of *leo* completely abolishing recovery of either *D14-3-3ε*^{ex4} or *D14-3-3ε*$^{l(3)j2B10}$ homozygous adults (Chang and Rubin, 1997). This interpretation is further supported by the fact that transgenically supplied LEOII can completely rescue the *D14-3-3ε* homozygous lethality, whereas high LEOI expression could only do so partially.

The mechanism of over-accumulation of LEO in *D14-3-3ε* null embryos is unknown. I propose that this may be a manifestation of the known function of 14-3-3s in nuclear/cytoplasmic partition of transcription factors (Muslin and Xing, 2000; Rittinger et al., 1999; Tzivion and Avruch, 2002). In this model, wild type D14-3-3ε modulates the level of *leoII* mRNA either by exclusion of transcription factors from the nucleus, or by keeping factors necessary for its transcription in an inactive conformation. The up-regulation of *leoII* compared to *leoI* may be due to the fact that one of the *leoII* transcripts has a unique promoter (Kockel et al., 1997). In either case, loss of D14-3-3ε in null embryos allows elevated transcription of *leoII* specifically. This is consistent with the hypothesis of isoform-specific functions, although additional work is necessary to understand why there is isoform-specific up-regulation and if normal embryonic development requires co-localization and dimerization of LEO and D14-3-3ε.

Novel role for D14-3-3ε in wing cross-vein development

D14-3-3ε exhibit a unique wing phenotype that varies based on the strength of mutant allele. The ex4, j2B10, and ex24 mutant homozygotes and transheterozygotes (except when crossed to ex5 revertants) had partial posterior cross-veins. Examination

of third instar larval wing disk, suggested that D14-3-3ε accumulates in folds of the wing disk which appeared to have organizational defects in homozygous *D14-3-3ε*^{ex4} mutants. Although LEOI is expressed and co-localizes with D14-3-3ε, *leo* null mutants did not display any wing disk or wing vein defects. However, *leoI* transgenes were able to rescue the anterior cross-vein malformation, but neither *leoI* nor *leoII* transgenes can rescue posterior cross-vein malformation, suggesting that LEO is not fully functionally equivalent with respect to wing cross-vein development. It is not clear whether LEO normally participates in wing vein formation altogether, but as for embryonic development, when the proper isoform is over-expressed it appears to function at least partially like D14-3-3ε.

D14-3-3ε mutants which were first isolated as dominant suppressors of activated Ras (Karim et al., 1996) are known to regulate Ras signaling through their interactions with Raf (Morrison, 1994; Michaud et al. 1995; Morrison and Cutler, 1997). Constitutive activated Ras1 expressed in developing wing disk using *dpp*-GAL4 (Prober and Edgar, 2000), affects anterior cross-vein formation producing similar aberrations to that seen in *D14-3-3ε* mutants. The aberrations of *D14-3-3ε* mutants can be completely rescued by expressing UAS-*mycD14-3-3ε* transgenes with the *dpp*-GAL4 driver. This suggests that the loss of D14-3-3ε in the wing disk where *dpp* is expressed may lead to over-activation of the RAS-RAF pathway, which may cause aberrant anterior cross-veins as suggested by the Ras1-dpp experiments. The mechanism of posterior cross-vein formation is currently unknown, primarily due to the fact there are no known mutants with similar aberrations.

Novel behavioral deficit associated with lack of D14-3-3ε

Viable *leonardo* mutants that lack LEO in the mushroom bodies appear to have a deficit in associative olfactory learning and memory (Philip et al., 2001). Similarly, *D14-3-3ε* mutants have a deficit in associative olfactory learning, which in fact is more severe than that in leo mutants. Behavioral experiments demonstrated that all *D14-3-3ε* mutants were capable of proper responses to aversive and attractive odors equally with controls (ex5). However, they exhibited a strong deficit in responding properly to an odor after they had been pre-exposed to it or another odor. In fact, the mutants have a general pre-exposure defect, not only toward an aversive second odor, but toward attractive odors as well. This deficit is not apparent if flies are pre-exposed to shock prior to testing odor responses suggesting that the deficit is stimulus specific. Behavioral investigation of the deficit indicated that: a minimum of twenty seconds pre-exposure was necessary to cause the deficit, suggesting desensitization, fatigue or habituation during pre-exposure, which renders mutants incapable of responding to subsequent olfactory stimuli. The non-associative pre-exposure phenotype is independent of odor quality, but depends on the strength of the stimulus and is spontaneously recoverable. Using presentation of a novel stimulus, in this case footshock, resulted in recovery of the response. The fact the deficit could be dishabituated, suggested the mechanism was not desensitization or fatigue, but premature habituation.

In addition, *D14-3-3ε* null mutants exhibit a deficit in response to repetitive footshock stimulation after pre-exposure. This deficit appears to be stimulus specific and can recover spontaneously and a pulse of strong odor can dishabituate the deficit. This suggests that the flies are not paralyzed and can feel the footshock, but simply habituated with increased numbers of repetitive presentations. This rapid habituation is consistent with the olfactory deficit, suggesting that habitation to footshock and odor may involve the same neurons.

Therefore, *D14-3-3ε* mutants suffer from a distinctly rapid habituation to odor or footshock. This effect is not observed in LEO mutants or any other mutants previously tested (data not shown). Therefore, the *D14-3-3ε* mutants define a new and uncharacterized class of behavioral mutants. This deficit in the ability to be "protected from premature habituation", may account for olfactory conditioning deficit of D14-3-3ε mutants. It is likely that the mutants are unable to establish the CS+/US (CS+: odor and US: shock) relationship because of rapid habituation.

In wild type animals, olfactory habituation occurred after 3 minutes of pre-exposure to aversive or attractive odor. However, odor avoidance did not change if the animals were pre-exposed to different equally aversive odor, indicating odor specificity in the pre-exposure dependent osmotactic decrement and argues against generalized olfactory fatigue or sensory adaptation both predicted to have poor odor specificity. Interestingly, in all experiments I observed a 3-minute refractory period when animals appeared to respond to the pre-exposed odor as if they were naïve we term a period when they are “protected from premature habituation”. This pre-exposure dependent

decline in osmotaxis was olfactory habituation and not sensory desensitization or fatigue because the effect was eliminated (dishabituation) by brief application of an unrelated noxious stimulus, footshock

Structural and functional ablation analysis was applied to define brain areas involved in protection from premature habituation. Mushroom body ablated animals exhibited a dramatic decline in osmotaxis after 10 seconds, the shortest pre-exposure we could deliver reliably. This drastically reduced refractory period suggested that HU-treated animals lack either all or part of the neuronal circuitry requisite for a normal refractory period and therefore habituated prematurely. The same phenotypes were exhibited by *mushroom body miniature* (*mbm*^{1}) mutants with severely perturbed but not totally absent MBs, and constitutive (Tetanus Light Chain-UASTNT), or conditional (*shibire*^{ts}- UAS-shi^{5ts}) neurotransmission blockade of the mushroom bodies with the MB-specific GAL4 driver line 247. These data confirm that the mushroom bodies are necessary for evaluation of experience dependent olfactory information and protection from premature habituation.

Similar to that exhibited by MB manipulated flies, inhibition of neurotransmission via the iACT and the mACT using the *UAS-TNT* and *UAS-shi*^{ts} transgenes precipitated deficits in osmotactic response following a minimum of 10 seconds pre-exposure to an odor. The deficit was likely the result of inhibiting neurotransmission and therefore information flow to the MBs and LH via the mACT and iACT and not because these tracks are themselves essential for the process.

The mushroom bodies are essential for protection from premature habituation to electric footshocks, the non-olfactory stimulus that also caused *D14-3-3* mutants to habituate prematurely. As for olfactory habituation, avoidance of repetitive footshocks declined after pre-exposure to multiple stimuli and conformed to habituation parameters, suggesting that the animals were protected from premature habituation. Functional mushroom bodies are necessary to protect from habituation to repetitive mild footshock. Importantly, unlike for olfactory habituation, inhibition of neurotransmission in the iACT and mACT did not result in premature habituation. This supports the hypothesis that as for olfaction the mushroom bodies are essential neural centers mediating responses to pre-experienced footshock stimuli. Furthermore, the data suggest that these areas of the fly brain are essential for stimulus evaluation likely to underlie the refractory period when animals are protected from habituation.

Based on the results of the mapping experiments, UAS rescue constructs were used to restore D14-3-3ε in the mutants to investigate whether replacement allowed rescue of the premature habituation and therefore the olfactory learning deficit. Because protection from habituation requires the mushroom bodies, iACT and mACT, and probably the LH it was not surprising that restricted expression in any one of these tissues was unsuccessful. Complete rescue of olfactory habituation and the olfactory learning deficit was only possible using general expression in the nervous system. This supports the notion that D14-3-3ε is minimally required in the MBs, iACT, mACT and probably the LH for normal protection from premature habituation. If D14-3-3ε is not present, the flies habituate rapidly, are unable to form the appropriate CS+/US

relationships and thus learning deficient. The inability of D14-3-3ε mutants to protect from premature habituation is likely the cause of the deficit seen in the associative olfactory learning paradigm. *leo* mutants are deficient in olfactory learning, but do not suffer from rapid habituation. Thus LEO is not functionally redundant with D14-3-3ε in respect to nervous system functions.

A number of studies over the last 20 years have established that *Drosophila* habituate to a number of stimuli using various experimental protocols such as habituation of the landing response (Rees and Spatz, 1989; Asztalos et al., 1993), the proboscis extension reflex (Duerr and Quinn, 1982), the cleaning reflex (Corfas and Dudai, 1989), visual startle reflex (Engel and Wu, 1996; Engel et al., 2000) and leg position (Jin et al., 1998). I have established two simple paradigms of habituation to olfactory and electric footshock stimuli, which appear to involve the mushroom bodies of the adult brain. The simplicity of both paradigms makes them suitable to conduct genetic screens aiming to elucidate the molecular basis of habituation. Within the *Drosophila* CNS it is unclear what may interact with D14-3-3ε to regulate habituation, however there is evidence that the *Drosophila* 14-3-3s complex with the calcium dependent potassium channel Slowpoke via Slowpoke binding protein (Slob), which is expressed in the adult central nervous system in *Drosophila* (Zhou et al., 1999; Zhou et al., 2001). Therefore, one possibility is that habituation may involve D14-3-3ε regulation of channel activity by mediating phosphorylation of the receptor/channel or coupling them with other proteins or signaling complexes (Sugita et al., 2001; Zhou et al., 1999; Zhou et al., 2003).

It is also unclear whether associative learning and habituation are dependent or independent processes. In the conditioned avoidance assay, used to study olfactory learning and memory, the conditioned stimulus (odor-CS+) paired to an unconditioned stimulus (footshock-US) elicits a conditioned response to the CS+, but no such response to an unconditioned odor stimulus, the CS- (Tully and Quinn, 1985). During training in this olfactory associative paradigm, premature habituation to the CS+ and/or the US would not permit CS/US association that leads to CS+ vs. CS- discrimination. Given my results and the documented involvement of the MBs in olfactory learning and memory (Roman and Davis, 2001; Waddell and Quinn, 2001; Heisenberg, 2003), it would appear that during training, the MBs/LH protect from premature habituation to the odor and footshock stimuli such that associations between them may be formed. Since structural and functional ablation of the MBs precipitated profound premature habituation to odor and footshock stimuli it is unlikely that such associations can be formed. Therefore, mutants that habituate prematurely should not be labeled as defective in associative olfactory learning. Therefore, the habituation assay is necessary as a control to separate mutants that have deficit in forming the CS+/US association or "true learning mutants" from those with non-associative learning deficits. Because this assay has not been included in previous publications of reported associative olfactory learning and memory mutants, only those of which were screened by other members of the lab (*drk, leo, rutabaga* and *dunce*) which do not appear to prematurely habituate should be classified as "true learning mutants".

ARE THE *DROSOPHILA* 14-3-3'S FUNCTIONALLY REDUNDANT?

Although there is 66% sequence identity among LEO and D14-3-3ε isotypes (Table 4) and only a five amino acid difference between LEOI and LEOII, this work uncovered functional difference among isotypes in *Drosophila* development and nervous system functions. Overall, despite the high homology among the 14-3-3 isotypes in *Drosophila* the data suggests that the isoforms/isotypes are not functionally redundant in most biological processes examined. This appears to be contrary to what previous studies suggested. This is particularly evident in the adult central nervous system where, although LEO and D14-3-3ε co-localize in the MBs the two proteins appear to be involved in distinctly different processes.

With respect to functional redundancy I found that:

1. LEOI can rescue lethality in *leonardo* mutants, therefore LEOI is not redundant with LEOII in processes that support embryonic development.

2. Both LEOI and LEOII can rescue the homozygous lethality of *D14-3-3ε* mutants with LEOII more efficient at rescue, therefore LEOII is redundant with D14-3-3ε and LEOI partially so, in processes that support embryonic development.

3. Both LEOI and LEOII cannot rescue posterior wing cross-vein deficits in *D14-3-3ε* mutants, therefore LEO is not redundant with D14-3-3ε in processes that support posterior wing cross-vein development.

4. LEOI can completely rescue anterior cross-vein malformations, therefore LEOI is redundant with D14-3-3ε in processes that support anterior wing cross-vein development. The potential contribution of LEOII is yet unknown.

5. Both LEOI and LEOII cannot rescue the germ cell deficit of *D14-3-3ε* mutants, therefore LEO is not redundant with D14-3-3ε in processes that support germ cell development.

6. D14-3-3ε and LEO appear to have functionally distinct roles within the mushroom bodies.

REFERENCES

Abel, T., and Kandel, E. (1998). Positive and negative regulatory mechanisms that mediate long-term memory storage. Brain Res. Brain Res. Rev. 26, 360-378.

Abrams, J.M., White, K., Fessler L.I., and Steller, H. (1993). Programmed cell death during *Drosophila* embryogenesis. Development 117, 29-43.

Acebes, A., and Ferrus, A. (2001). Increasing the number of synapses modifies olfactory preception in *Drosophila*. J. Neurosci. 21, 6264-6273.

Adachi, M., Zhang, Y.-B., and Imai, K. (2003). Mutation of BAD within the BH3 domain impairs its phosphorylation-mediated regulation. FEBS Lett. 551, 147-152.

Adachi-Yamada, T., Nakamura, M., Irie, K., Tomoyasu, Y., Sano Mori, E., Goto, S., Ueno, N., Nishida, Y., and Matsumoto, K. (1999). p38 Mitogen-Activated Protein Kinase can be involved in transforming growth factor β superfamily signal transduction in *Drosophila* wing morphogenesis. Mol. Cell. Biol. 19, 2322-2329.

Adler, L.E., Freedman, R., Ross, R.G., Olincy, A., and Waldo, M. (1999). Elementary phenotypes in the neurobiological and genetic study of Schizophrenia. Biol. Psychiatry 46, 8-18.

Aitken, A. (1995). 14-3-3 proteins on the MAP. Trends Biochem. Sci. 20, 95-97.

Aitken, A., Baxter, H., Dubios, T., Clokie, S., Mackie, S., Mitchell, K., Peden, A., and Zemlickova, E. (2002). 14-3-3 proteins in cell regulation. Biochem. Soc. Trans. 30, 351-360.

Aitken, A., Collinge, D.B., Van Heusden, B.P.H., Isobe, T., Roseboom, P.H., Rosenfeld, G., and Soll, J. (1992). 14-3-3 proteins: A highly conserved, widespread family of eukaryotic proteins. Trends Biochem. Sci. 17, 498-501.

Andrews, R.K., Harris, S.J., McNally, T., and Berndt, M.C. (1998). Binding of purified 14-3-3ζ signaling protein to discrete amino acid sequence within the cytoplasmic domain of the platelet membrane glycoprotein Ib-IX-V complex. Biochemistry 37, 638-647.

Armstrong, J.D., de Belle, J.S., Wang, Z., and Kaiser, K. (1998). Metamorphosis of the mushroom bodies; large scale rearrangement of the neural substrates for associative learning and memory in *Drosophila*. Learn. Mem. 5, 102-114.

Asaoka, Y., Nakamura, S., Yoshida, K., and Nishizuka, Y. (1992). Protein kinase C, calcium and phospholipid degradation. TIBS 17, 414-417.

Ashburner, M. (1989). *Drosophila* A Laboratory Handbook. (New York, Cold Springs Harbor Laboratory Press).

Asztalos, Z., von Wegerer, J., Wustmann, G., Dombradi, V., Gausz, J., Spatz, H.-C., and Friedrich, P. (1993). Protein phosphatase 1-deficient mutant *Drosophila* is affected in habituation and associative learning. J. Neurosci. 13, 924-930.

Ayer, R.K., and Carlson, J. (1992). Olfactory physiology in the *Drosophila* antennand maxillary palp: acj6 distinguishes two classes of odorants. J. Neurobiol. 8, 965-968.

Bailey, C.H., Bartsch, D., and Kandel, E.R. (1996). Toward a molecular definition of long term-memory storage. Proc. Natl. Acad. Sci. USA 93, 13445-13452.

Bailey, C.H., Kaang, B-K., Chen, M., Martin, K.C., Lim, C-S., Casadio, A., and Kandel, E.R. (1997). Mutation in the phosphorylation sites of MAP kinase blocks learning-related internalization of apCAM in Aplysia sersory neurons. Neuron 18, 913-924.

Banik, U., Wang, G.-A., Wagner, P.D., and Kaufman, S. (1997). Interaction of phosphorylated Tryptophan hydroxylase with 14-3-3 proteins. J. Biol. Chem. 272, 26219-26225.

Bartsch, D., Ghirardi, M., Skehel, P.A., Karl, K.A., Herder, S.P., Chen, M., Bailey, C.H., and Kandel, E.R. (1995). Aplysia, CREB2 represses long term facilitation: relief of repression converts transient facilitation into long-term functional and structural change. Cell 83, 979-992.

Baxter, H.C., Liu, W.-G., Forster, J.L., Aitken, A., and Fraser, J.R. (2002). Immunolocalisation of 14-3-3 isoforms in normal and scrapie-infected murine brain. Neuroscience 109, 5-14.

Beck, C.D.O., and Rankin, C.H. (1995). Long term habituation is produced by distributed training at long ITIs and not by massed training or short ITIs in Caenorabdhitis elegans. Anim. Learn. Behav. 25, 446-457.

Beck, C.D.O., Schroeder, B., and Davis, R.L. (2000). Learning performance of normal and mutant drosophila after repeated conditioning trails with discrete stimuli. J. Neurosci. 20, 2944-2953.

Bellen, H.J., O'Kane, C.J., Wilson, C., Grossniklaus, U., Pearson, R.K., and Gehring, W. (1989). P-element mediated enhancer detection: a versatile method to study development in *Drosophila*. Genes Dev. 3, 1288-1300.

Bellen, H.J. (1998). The fruit fly: a model organism to study the genetics of alcohol abuse and addiction? Cell 93, 997-1007.

Benton, R., Palacios I.M., and St Johnston, D. (2002). *Drosophila* 13-3-3/PAR5 in an essential mediator of PAR-1 function in Axis Formation. Dev. Cell 3, 659-671.

Benton, R., and St Johnston, D. (2003). *Drosophila* PAR-1 and 14-3-3 inhibit Bazooka/PAR-3 to establish complementary cortical domains in polarized cells. Cell 115, 691-704.

Berg, D., Holzmann, C., and Riess, O. (2003). 14-3-3 proteins in the nervous system. Nature 4, 752-762.

Boston, P.F., Jackson, P., Kynoch, P.A.M., and Thomson, R.J. (1982). Purification, properties and immunohistochemical localization of human brain 14-3-3 protein. J. Neurochem. 38, 1466-1474.

Bourtchouladze, R., Frenguelli, B., Blendy, J., Cioffi, D., Schutz, G., and Silva, A.J. (1994). Deficient long-term memory in mice with a targeted mutation of the cAMP-responsive element-binding protein. Cell 79, 59-68.

Bouton, M.E., Nelson, J.B., and Rosas, J.M. (1999). Stimulus generalization, context change, and forgetting. Psychol. Bull. 125, 171-186.

Boynton, S., and Tully, T. (1992). latheo, a new gene involved in associative learning and memory in *Drosophila melanogaster* identified from P element mutagenesis. Genetics 131, 655-672.

Brand, A.H., and Perrimon, N. (1993). Targeted gene expression as a means of altering cell fates and generating dominant phenotypes. Development 118, 401-415.

Brasselman, S., and McCormick, F. (1995). BCR and RAF form a complex in vivo via 14-3-3 proteins. EMBO J. 14, 4839-4848.

Broadie, K., Rushton, E., Skoulakis E.M.C., and Davis, R.L. (1997). Leonardo, a *Drosophila* 14-3-3 protein involved in learning, regulates presynaptic function. Neuron 19, 391-402.

Burgoyne, R.D., and Morgan, A. (1993). Regulated exocytosis. Biochem. J. 293. 305-316.

Byrne, J.H. (1987). Cellular analysis of associative learning. Physiol. Rev. 67, 329-439.

Campbell, J.K., Gurung, R., Romero, S., Speed, C.J., Andrews, R.K., Berndt, M.C., and Mitchell, C.A. (1997). Activation of 43 kDa Inositol polyphosphate 5-Phosphatase by 14-3-3ζ. Biochemistry 36, 15363-15370.

Carew, T.J. (1996). Molecular enhancement of memory formation. Neuron 16, 5-8.

Chamberlain, L.H., Roth, D., and Burgoyne, R.D. (1995). Distinct effects of α-SNAP, 14-3-3 proteins and calmodulin on priming and triggering of regulated exocytosis. J. Cell Biol. 130, 1063-1070.

Chan, T.A., Hermeking, H., Lengauer, C., Kinzler, K.W., and Vogelstein, B. (1999). 14-3-3sigma is required to prevent mitotic catastrophe after DNA damage. Nature 401, 616-620.

Chan, T.A., Hwang, P.M., Hermeking, H., Kinzler, K.W., and Vogelstein, B. (2000). Cooperative effects of genes controlling the G2/M checkpoint. Genes Dev. 14, 1584-1588.

Chang, H.C., and Rubin, G.M. (1997). 14-3-3ε positively regulates Ras mediated signaling in *Drosophila*. Genes Dev. 11, 1132-1139.

Chen, H.-K., Fernandez-Funez, P., Acevedo, S.F., Lam, Y.C., Kaytor, M.D., Fernandez, M.H., Aitken, A., Skoulakis, E.M.C., Orr, H.T., Botas, J., and Zoghbi, H.Y. (2003). Interaction of akt-phosphorylated ataxin-1 with 14-3-3 mediates neurodegeneration in spinocerebellar ataxia type 1. Cell 113, 457-468.

Cheng, Y., Endo, K., Wu, K., Rodan, A.R., Heberlein, U., and Davis, R.L. (2001). *Drosophila* fasciclin is required for the formation of odor memories and for normal sensitivity to alcohol. Cell 105, 757-768.

Choi, K.-W., Smith, R.F., Buratowski, R.M., and Quinn, W.G. (1991). Deficient protein kinase C activity in turnip a *Drosophila* learning mutant. J. Biol. Chem. 266, 15999-16006.

Chong, H., Vikis, H.G., and Guan, K. (2003). Mechanism of regulating the Raf kinase family. Cell Signal. 15, 463-469.

Coffman, C.R., Strohm, R.C., Oakley, F.D., Yamada, Y., Przychodzin, D., and Boswell, R.E. (2002). Identification of X-linked Genes required for migration and programmed cell death of *Drosophila melanogaster* germ cells. Genetics 162, 273-284.

Cohan, F.M., and Graf, J.-D. (1985). Latitudinal cline in *Drosophila melanogaster* for knockdown resistance to ethanol fumes and for rate of response to selection for further resistance. Evolution 39, 278-293.

Connolly, K., and Cook, R. (1973). Rejection response by female *Drosophila melanogaster*: Their ontogeny, causality, and effects upon the behavior of the courting male. Behavior 52, 155-171.

Connoly, J.B., Roberts, I.J.H., Armstrong, J.D., Kaise, K., Forte, M., Tully, T., and O'Kane, C.J. (1996). Associative learning disrupted by impaired Gs signaling in *Drosophila* mushroom bodies. Science 274, 2104-2107.

Corfas, G., and Dudai, Y. (1989). Habituation and dishabituation of a cleaning reflex in normal and mutant drosophila. J. Neurosci. 9, 56-62.

Corfas, G., and Dudal, Y. (1990). Adaptation and fatigue of a mechanosensory neuron in wild-type *Drosophila* and in memory mutants. J. Neurosci. 10, 491-499.

Couve, A., Kittler, J.T., Uren, J.M., Calver, A.R., Pangalos, M.N., Welsh, F.S., and Moss, S. J. (2001). Association of GABAβ receptors and members of the 14-3-3 family of signaling proteins. Mol. Cell Neurosci. 17, 317-328.

Craparo, A., Freund, R., and Gustafson, T.A. (1997). 14-3-3 ε interacts with the insulin-like Growth factor I receptor and insulin receptor substrate I in a phosphoserine-dependent manner. J. Biol. Chem. 272, 11663-11669.

Creutzfeldt, H.G. (1920). Uber eine egenartige herdformige erkrankung des zentralnervensystems. Neurol. Psychiat. 57, 1-18.

Crittenden, J. R., Skoulakis, E.M.C., Han, K.-A., Kalderon, D., and Davis, R.L. (1998). Tripartite mushroom body architecture revealed by antigenic markers. Learn. Mem. 5, 38-51.

Dai, J., and Murakami, K. (2003). Constitutively and autonomously active protein kinase C associated with 14-3-3 ζ in the rodent brain. J. Neurochem. 84, 23-34.

Dalton, P. (2000). Psychophysical and behavioral characteristics of olfactory adaptation. Chem. Senses 25, 487-492.

Datta, S.R., Katsov, A., Hu, L., Petros, A., Fesik, S.W., Yaffe, M.B., and Greenberg, M.E. (2000). 14-3-3 proteins and survival kinases cooperate to inactivate BAD by BH3 domain phosphorylation. Mol. Cell 6, 41-51.

Davis, G.W., and Goodman, C.S. (1998). Synapse-specific control of synaptic efficacy at the terminals of a single neuron. Nature 392, 82-85.

Davis, R. (1996). Physiology and biochemistry of *Drosophila* Learning Mutants. Physio. Rev. 76, 299-315.

Davis, R.L. (2001). Mushroom bodies, Ca^{2+} oscillations and the memory gene amnesiac. Neuron 30, 653-656.

Davis, R. L., and Davidson, N. (1986). The memory gene dunce+ encodes a remarkable set of RNAs with internal heterogeneity. Mol. Cell Biol. 6, 1464-1470.

Davis, R. L., and Han, K.-A. (1996). Mushrooming mushroom bodies. Curr. Biol. 6, 146-148.

de Belle, J.S., and Heisenberg, M. (1996). Expression of *Drosophila* mushroom body mutations in alternative genetic backgrounds: a case study of the mushroom body miniature gene (mbm). Proc. Natl. Acad. Sci. USA 93, 9875-9880.

de Belle, S. J., and Heisenberg, M. (1994). Associative odor learning in *Drosophila* is abolished by chemical ablation of mushroom bodies. Science 263, 692-695.

de Bruyne, M., Foster, K., and Carlson, J.R. (2001). Odor coding in the drosophila antenna. Neuron 30, 537-552.

Delgado, R., Hidalgo, P., Diaz, F., Latorre, R., and Labarca, P. (1991). A cyclic AMP-activated K^+ channel in *Drosophila* larval muscle is presisently activated in dunce. Proc. Natl. Acad. Sci. USA 88, 557-569.

Dent, P., Jelinek, T., Morrison, D.K., Weber, M.J., and Sturgill, T.W. (1995). Reversal of Raf-1 activation by purified and membrane-associated protein phosphatases. Science 268, 1902-1906.

Deshmukh, S.S., Bhalla, U.S. (2003). Representation of odor habituation and timing in the Hippocampus. J. Neurosci. 23, 1903-1915.

Deshpande, G., Calhoun, G., Yanowitz, J.L. and Schedi, P.D. (1999). Novel functions of nanos in downregulating mitosis and transcription during development of the drosophila germline. Cell 99, 271-281.

Devaud, J-M. (2003). Experimental studies of adult drosophila chemosensory behavior. Behav. Processes 64, 177-196.

Devaud, J.-M., Acebes, A., and Ferrus, A. (2001). Odor exposure causes central adaptation and morphological changes in selected olfactory glomeruli in *Drosophila*. J. Neurosci., 21, 6274-6282.

Devaud, J.-M., Keane, J., and Ferrus, A. (2003). Blocking sensory inputs to identified antennal glomeruli selectively modifies odorant perception in *Drosophila*. J. Neurobiol. 56, 1-12.

DeZazzo, J., and Tully, T. (1995). Dissection of memory formation: from behavioral pharmacology to molecular genetics. Trends Neurosci. 18, 212-218.

DeZazzo, J., Xia, S., Christensen, J., Velizon, K., and Tully, T. (1999). Development expression of an amn(+) transgene rescues the mutant memory defect of amnesiac adults. J. Neurosci. 19, 8740-8746.

DeZazzo, J., Sandstrom, D., de Belle, S., Velinzon, K., Smith, P., Grady, L., DelVecchio, M., Ramaswami, M., and Tully, T. (2000). nalyot, a mutation of the *Drosophila* Myb-related Adt1 transcription factor, disrupts synapse formation an olfactory memory. Neuron 27, 145-158.

Dhillion, A.S., and Kolch, W. (2002). Untying the regulation of the Raf-1 kinase. Arc. Biochem. Biophy. 404, 3-9.

Diamond, I., and Gordon, A.S. (1997). Cellular and molecular neuroscience of alcoholism. Physio. Rev. 77, 1-20.

Dickson, B.J., van der Straten, A., Dominguez, M., and Hafen, E. (1996). Mutations modulating Raf signaling in *Drosophila* eye development. Genetics 142, 163-171.

Donzelli, M., and Draetta, G.F. (2003). Regulating mammalian checkpoints through Cdc25 inactivation. EMBO Reports 4, 671-677.

Dougherty, M.K., and Morrison, D.K. (2004). Unlocking the code of 14-3-3. J. Cell Sci. 117, 1875-1884.

Drain, P., Folkers, E., and Quinn, W. G. (1991). cAMP-dependent protein kinase and the disruption of learning in transgenic flies. Neuron, 6, 71-82.

Drier, E.A., Tello, M.K., Cowan, M., Wu, P., Blace, N., Sacktor, T.C., and Yin, J.C. (2002). Memory enhancement and formation by atypical PKM activity in *Drosophila melanogaster*. Nat. Neurosci. 5, 316-324.

Dubnau, J., and Tully, T. (2001). Functional anatomy: from molecule to memory. Curr. Bio. 11, R240-R243.

Dubnau, J., Grady, L., Kitamoto, T., and Tully, T. (2001). Disruption of neurotransmission in *Drosophila* mushroom body blocks retrieval, but not acquisition of memory. Nature 411, 476-480.

Dubois, T., Rommel, C., Howell, S., Steinhussen, U., Soneji, Y., Morrice, N., Moelling, K., and Aitken, A. (1997). 14-3-3 is phosphorylated by Casein Kinase I on Residue 233; phosphorylation at this site in vivo regulates Raf/14-3-3 interaction. J. Biol. Chem. 272, 28882-28888.

Dudai, Y. (1988). Neurogenetic Dissection of Learning and Short-Term Memory in *Drosophila*. Ann. Rev. Neurosci. 11, 537-563.

Dudai, Y., Jan, Y.-N., Byers, D., Quinn, W.G., and Benzer, S. (1976). dunce, a mutant of *Drosophila* deficient in learning. Proc. Natl. Acad. Sci. USA 73, 1684-1688.

Duerr, J.S., and Quinn, W.G. (1982). Three *Drosophila* mutations that block associative learning also affect habituation and sensitization. Proc. Natl. Acad. Sci. USA 79, 3646-3650.

Dujardin, F. (1850). Memoire sur le systeme nerveux des insectes. Ann. Sci. Nat. Zool. 14, 95-206.

Edgar, B.A., and Lehner, C.F. (1996). Developmental control of cell cycle regulators: A fly's perspective. Science 274, 1646-1455.

Edgar, B.A., Sprenger, F., Duronio, R.J., Leopold, P., and O'Farrell, P.H. (1994). Distinct molecular mechanisms regulate cell cycle timing at successive stages of *Drosophila* embryogenesis. Genes Dev. 8, 440-452.

Engel, J.E., and Wu, C. (1996). Altered habituation of and identified escape circuit in drosophila memory mutants. J. Neurosci. 16, 3486-3499.

Engel, J.E., and Wu, C. (1998). Genetic dissection of functional contributions of specific potassium channel subunits in habituation of an escape circuit in drosophila. J. Neurosci. 18, 2254-2267.

Engel, J.E., Xie, X., Sokolowski, M., and Wu, C.-F. (2000). A cGMP-dependent protein kinase gene, foraging, modifies habituation-like response decrement of the giant fiber escape circuit in drosophila. Learn. Mem. 7, 341-352.

Fanger, G.R., Gerwin, P., Widmann, C., Jarpe, M.B., and Johnson, G.L. (1997). MEKKs, GCKs, MLKs, PAKs, TAKs, and Tpls: upstream regulators of the c-Jun amino-terminal kinases? Curr. Biol. 7, 67-74.

Fanger, G.R., Widmann, C., Porter, A.C., Sather, S., Johnson, G.L., and Vaillancourt, R.R. (1998). 14-3-3 proteins interact with specific MEK kinase. J. Biol. Chem. 273, 3476-3483.

Feany, M.B., and Quinn, W.G. (1995). A neuropeptide gene defined by the *Drosophila* memory mutant amnesiac. Science 268, 825-826.

Featherstone, D.E., and Broadie, K. (2000). Surprise from *Drosophila*: genetic mechanism of synaptic development and plasticity. Brain Res. Bull. 53, 501-511.

Freedman, R., Waldo, M., Bickford-Wimer, P., and Nagamoto, H. (1991). Elementary neuronal dysfunctions in schizophrenia. Schizo. Res. 4, 233-243.

Ferguson, A.T., Evron, E., Umbricht, C.B., Pandita, T.K., Chan, T.A., Hermeking, H., Marks, J.R., Lambers, A.R., Futreal, P.A., Stampfer, M.R., and Sukumar, S. (2000). High frequency of hypermethylation at the 14-3-3 sigma locus leads to gene silencing in breast cancer. Proc. Natl. Acad. Sci. USA 97, 6049-6054.

Ferl, R.J., Manak, M.S., and Reyes, M.F. (2002). The 14-3-3s. Genome Biol. 3, 3010.3011-3010.3017.

Ferveur, J.-F. (1997). The pheromonal role of cuticular hydrocarbons in *Drosophila melanogaster*. BioEssays 19, 353-358.

Folkers, E., Drain, P., and Quinn, W.G. (1993). radish, a *Drosophila* mutant deficient in consolidated memory. Proc. Natl. Acad. Sci. USA 90, 8123-8127.

Forrest, A., and Gabrielli, B. (2001). Cdc25B activity is regulated by 14-3-3. Oncogene 20, 4393-4401.

Fountoulakis, M., Cairns, N., and Lubec, G. (1999). Increased levels of 14-3-3 gamma and epsilon proteins in brain of patients with Alzheimer's disease and Down syndrome. J Neural Transm. Suppl. 57, 323-335.

Freed, E., Symons, M., Macdonald, S.G., McCormick, F., and Ruggieri, R. (1994). Binding of 14-3-3 proteins to the protein kinase Raf and effects on its activation. Science 265, 1713-1716.

Frye, M.A., and Dickinson, M.H. (2003). A signature of salience in the *Drosophila* brain. Nat. Neurosci. 6, 544-546.

Fu, H., Coburn, J., and Collier, R.J. (1993). The eukaryotic host factor that activates exoenzyme S of Pseudomonas aeruginosa is a member of the 14-3-3 protein family. Proc. Natl. Acad. Sci. USA 90, 2320-2324.

Fu, H., Subramanian, R.R., and Masters, S.C. (2000) 14-3-3 proteins: Structure, Function and Regulation. Annu. Rev. Pharmacol. Toxicol 40, 617-647.

Fu, H., Xia, K., Pallas, D.C., Cui, C., Conroy, K., Narsimhan, R.P., Mamon, H., Collier, R.J., and Roberts, T.M. (1994). Interaction of the protein kinase Raf-1 with 14-3-3 proteins. Science 266, 126-129.

Gabrielli, B., De Souza, C.P.C., Tonka, I.D., Clark, J.M., Hayward, N.K., and Ellem, K.A.O. (1996). Cytoplasmic accumulation of cdc25B phosphatase in mitosis triggers centrosomal microtuble nucleation in HeLa cells. J. Cell Sci. 109, 1081-1093.

Ganguly, S., Gastel, J.A., Weller, J.L., Schwartz, C., Jeffe, H., Namboodiri, M.A.A., Coon, S.L., Hickman, A.B., Rollage, M., Obsil, T., Beauverger, P., Ferry, G., Boutin, J.A., Klein, D.C. (2001). Role of a pineal cAMP-operated arylalkyamine N-acetyltransferase/ 14-3-3 binding switch in melatonin synthesis. Proc. Natl. Acad. Sci. USA 98, 8083-8088.

Gannon-Murakami, L., and Murakami, K. (2002). Selective association of protein kinase C with 14-3-3ζ in neuronally differentiated PC12 cells. J. Biol. Chem. 277, 23116-23122.

Gillberg, C. (2003). Deficits in attention, motor control and perception: A brief review. Arch. Dis. Child 88, 904-910.

Giraud, P., Biacabe, A.-G., Chazot, G., Later, R., Joyeux, O., Moene, Y., and Perret-Liaudet, A. (2002). Increased detection of 14-3-3 protein in cerebrospinal fluid in sporadic Creutzfeldt-Jakob disease during the disease course. Eur. Neurol. 48, 218-221.

Goelet, P., Castellucci, V. F., Schacher, S., and Kandel, E. R. (1986). The long and the short of long-term memory- a molecular framework. Nature 322, 419-422.

Graves, P.R., Louly, C.M., Uy, G.L., and Piwnic-Worms, H. (2001). Localization of human Cdc25 is regulated both by nuclear export and 14-3-3 protein binding. Oncogene 20, 1839-1851.

Greenberg, S.M., Castellucci, V. F., Bayley, H., and Schwartz, J. H. (1987). A molecular mechanism for long-term sensitization in Aplysia. Nature 329, 62-65.

Greenspan, R.J. (1995). Flies, Genes, Learning and Memory. Neuron, 15, 747-750.

Grotewiel, M.S., Beck, C.D., Wu, K.H., Zhu, X.-R., and Davis, R.L. (1998). Integrin-mediated short-term memory in *Drosophila*. Nature 391, 455-460.

Groves, P.M., and Thomson, R.F. (1970). Habituation: A dual-process theory. Phychol. Rev. 77, 419-450.

Guarnieri, D.J., and Heberlein, U. (2003). *Drosophila melanogaster*, a genetic model system for alcohol research. Int. Rev. Neurobiol. 54, 199-228.

Guo, A., and Gotz, K.G. (1997). Association of visual objects and olfactory cues in *Drosophila*. Learn. Mem. 4, 192-204.

Hall, J. C. (1985). Comprehensive Insect Physiology, Biochemistry and Pharmacology. (Oxford: Pergamon Press), pp. 287-383.

Hall, J.C. (1994). The mating of a fly. Science 264, 1702-1714.

Han, P.-L., Levin, L.R., Reed, R.R., and Davis, R.L. (1992). Preferential expression of the *Drosophila* rutabaga gene in mushroom bodies, neural centers for learning in insects. Neuron 9, 619-627.

Han, P.-L., Meller, V., and L., D.R. (1996). The *Drosophila* brain revisited by enhancer detection. J. Neurobiol. 31, 88-102.

Hashiguchi, M., Sobue, K., and Paudel, H.K. (2000). 14-3-3 ζ is an effector of tau protein phosphorylation. J. Biol. Chem. 275, 25247-25245.

Hausser, A., Storz, P., Link, G., Stoll, H., Liu, Y.-C., Altman, A., Pfizenmeier, K., and Johannes, F.J. (1999). Protein kinase C μ is negatively regulated by 14-3-3 signal transduction proteins. J. Biol. Chem. 274, 9258-9264.

Hawkins, R.D. (1988). Neural models of plasticity (San Diego: Academic Press), pp. 73-93.

Hay, B., Ackerman, L., Barbel, S., Jan, L.-Y., and Jan, Y.-N. (1988). Identification of a component of *Drosophila* polar granules. Development 103, 625-640.

Hay, B., Jan, L.-Y., and Jan, Y.-N. (1988). A protein component of *Drosophila* polar granules is encoded by vasa and has extensive sequence similarity to ATP-dependent helicases. Cell 55, 577-587.

Heberlein, U. (2000). Genetics of alcohol-induced behaviors in Drosophlia. Alcohol Res. Health 24, 185-188.

Heimbeck, G., Bugnon, V., Gendre, N., Keller, A., and Stocker, R.F. (2001). A central neural circuit for experience-independent olfactory and courtship behavior in *Drosophila melanogaster*. Proc. Natl. Acad. Sci. USA 93, 15336-15341.

Heisenberg, M. (1980). Development and Biology of *Drosophila*. (New York: Plenum Press), pp. 373-390.

Heisenberg, M. (1989). Fundamentals of Memory Formation: Neuronal Plasticity and Brain Function. (New York: Gustav Fischer Verlag), pp. 3-45.

Heisenberg, M. (1998). What do the mushroom bodies do for the insect brain? Learn. Mem. 5, 1-10.

Heisenberg, M. (2003). Mushroom body memoir: from maps to models. Nat. Rev. Neurosci. 4, 266-275.

Heisenberg, M., Borst, A., Wagner, S., and Byers, D. (1985a). *Drosophila* mushroom body mutants are deficient in olfactory learning. J. Neurogenet. 2, 1-30.

Heisenberg, M., Borst, A., Wagner, S., and Byers, D. (1985b). *Drosophila* mushroom body mutants are deficient in olfactory learning. J. Neurogenet. 2, 1-30.

Helfrich-Forster, C., Wulf, J., and de Belle, J.S. (2002). Mushroom body influence on locomotor activity and circadian rhythms in *Drosophila melanogaster*. J. Neurogenet. 16, 73-109.

Hermeking, H., Lengauer, C., Polyak, K., He, T., Zhang, L., Thiagalingam, S., Kinzler, K. W., and Vogelstein, B. (1997). 14-3-3s is a p53-regulated inhibitor of G2/M progression. Mol. Cell 1, 3-11.

Huang, N., Marie, S. K., Livramento, J. A., Chammas, R., and Nitrini, R. (2003). 14-3-3 protein in the CSF of patients with rapidly progressive dementia. Neurology 61, 354-357.

Humeau, Y., Doussau, F., Grant, N.J., and Poulain, B. (2000). How botulinum and tetanus neurotoxins block neurotransmitter release. Biochimie. 82, 427-446.

Ichimura, T., Isobe, T., Okuyama, T., Takahashi, N., Araki, K., Kuwano, R., and Takahashi, Y. (1988). Molecular cloning of cDNAs coding for brain specific14-3-3 protein, a protein kinase dependent activator of tyrosine and tryptophan hydroxylases. Proc. Natl. Acad. Sci. USA 85, 7084-7088.

Ichimura, T., Isobe, T., Okuyama, T., Yamauchi, T., and Fujisawa, H. (1987). Brain 14-3-3 protein is an activator protein that activates tryptophan 5- monooxygenase and tyrosine 3-monooxygenase in the presence of Ca^{2+}, calmodulin-dependent protein kinase II. FEBS Lett. 219, 79-82.

Ichimura, T., Sugano, H., Kuwano, R., Sunaya, T., Okuyama, T., and Isobe, T. (1991). Widespread distribution of the 14-3-3 protein in verterbrate brains and bovine tissues:

Correlation with the distributions of calcium-dependent protein kinases. J. Neurochem. 56, 1449-1451.

Isobe, T., Hiyane, Y., Ichimura, T., Okuyama, T., Takahashi, N., Nakajo, S., and Nakaya, K. (1992). Activation of protein kinase C by the 14-3-3 proteins homologous with Exo1 protein that stimulates calcium-dependent exocytosis. FEBS Lett. 308, 121-124.

Isobe, T., Ichimura, T., Sunaya, T., Okuyama, T., Takahashi, N., Kuwano, R., and Takahashi, Y. (1991). Distinct forms of the protein kinase-dependent activator of tyrosine and tryptophan hydroxylases. J. Mol. Biol. 217, 125-132.

Ito, K., and Hotta, Y. (1992). Proliferation pattern of postembryonic neuroblasts in the brain of *Drosophila melanogaster*. Dev. Biol. 149, 134-148.

Ito, K., Sass, H., Urban, J., Hofbauer, A., and Schneuwly, S. (1997). GAL4-responsive UAS-tau as a tool for studying the anatomy and development of the *Drosophila* central nervous system. Cell Tissue Res. 90, 1-10.

Ito, K., Suzuki, K., Estes, P., Ramaswami, M., Yamamoto, D., and Strausfeld, N. J. (1998). The organization of extrinsic neurons and their implications in the functional roles of the mushroom bodies in *Drosophila melanogaster*. Learn. Mem. 5, 52-77.

Ito, Y., Miyoshi, E., Uda, E., Yoshida, H., Uruno, T., Takamura, Y., Miya, A., Kobayashi, K., Matsuzuka, F., Matsuura, N., Kakudo, K., Kuma, K., Miyauchi, A. (2003). 14-3-3s possibly plays a constitutive role in papillary carcinoma but not in follicular tumor of the thyroid. Cancer Lett. 200, 161-166.

Jakob, A. (1921). Uber eigenartige erkrankungen des zentralnervensystems mit bemerkenswertem anatmishcen befunde. Neurol. Psychiat. 64, 147-228.

Jan, L.Y., and Jan Y.N. (1976). L-glutamate as an excitatory transmitter at the *Drosophila* larval neuromuscular junction. J. Physiol. 262, 215-236.

Jaumot, M., and Hancock, J.F. (2001). Protein phosphatases 1 and 2A promote Raf-1 activation by regulating 14-3-3 interaction. Oncogene 20, 3949-3958.

Jin, P., Griffith, L.C., and Murphey, R.K. (1998). Presynaptic calcium/calmodulin-dependent protein kinase II regulates habituation of a simple reflex in adult *Drosophila*. J. Neurosci. 18, 8955-8964.

Johnson, N.L., Gardner, A.M., Diener, K.M., Lange-Carter, C. A., Gleavy, J., Jarpe, M. B., Minden, A., Karin, M., Zon, L.I., and Johnson, G.L. (1996). Signal transduction

pathways regulated by mitogen-activated/extracellular response kinase kinase kinase induce cell death. J. Biol. Chem. 271, 3229-3237.

Joiner, M.A., and Griffith, L.C. (1999). Mapping of the anatomical circuit of CaM kinase-dependent courtship conditioning in drosophiola. Learn. Mem. 6, 177-192.

Jones, D.H., Ley, S., and Aitken, A. (1995a). Isoforms of 14-3-3 protein can form homo- and heterodimers in vivo and in vitro: implications for function as adapter proteins. FEBS Lett. 368, 55-58.

Jones, D. H. A., Martin, H., Madrazo, J., Robinson, K.A., Neilsen, P., Roseboom, P.H., Patel, Y., Howell, S.A., and Aitken, A. (1995b). Expression and structural analysis of 14-3-3 proteins. J. Mol. Biol. 245, 375-384.

Joynes, R.L., and Grau, J.W. (1996). Mechanisms of pavlovian conditioning: role of protection from habituation in spinal conditioning. Behav. Neurosci. 110, 1375-1387.

Kagan, A., Melman, Y.F., Krumerman, A., and McDonald, T.V. (2002). 14-3-3 amplifies and prolongs adrenergic stimulation of HERG K+ channel activity. EMBO J. 21, 1889-1898.

Kaiser, K., and Goodwin, S.F. (1990). "Site selected" transposon mutagenesis of *Drosophila*. Proc. Natl. Acad. Sci. 87, 1686-1690.

Kalderon, D., and Rubin, G. M. (1988). Isolation and characterization of *Drosophila* cAMP-dependent protein kinase genes. Genes Dev. 2, 1539-1556.

Kamyshev, N.G., IIiadi, K.G., and Bragina, J.V. (1999). *Drosophila* conditioned courtship: Two ways to testing memory. Learn. Mem. 6, 1-20.

Kandel, E.R., Abrams, T., Bernier, L., Carew, T.J., Hawkins, R.D., and Schwartz, J.H. (1983). Classical conditioning and sensitization share aspects of the same molecular cascade in Aplysia. Cold Spring Harbor Symp. Quant. Biol. 48, 821-830.

Kane, N.S., Robichon, A., Dickinson, J.A., and Greenspan, R.J. (1997). Learning without performance in PKC-deficient *Drosophila*. Neuron 18, 307-314.

Karim, F.D., Chang, H.C., Therrien, M., Wassarman, D.A., Laverty, T., and Rubin, G.M. (1996). A screen for genes that function downstream of Ras1 during *Drosophila* eye development. Genetics 143, 315-329.

Kawamoto, Y., Akiguchi, I., Nakamura, S., Honjyo, Y., Shibasaki, H., and Budka, H. (2002). 14-3-3 proteins in Lewy bodies in Parkinson disease and diffuse Lewy body disease brains. J Neuropathol. Exp. Neurol. 61, 245-253.

Keller, A., Sweeney, S.T., Zars, T., O'Kane, C. J., and Heisenberg, M. (2002). Targeted expression of tetanus neurotoxin interferes with behavioral responses to sensory input in *Drosophila*. J. Neurobiol. 50, 221-233.

Kiryu, S., Morita, N., Ohno, K., Maeno, H., and Kiyama, H. (1995a). Regulation of mRNA expression involved in Ras and PKA signal pathway during rat hypoglossal nerve regeneration. Mol. Brain Res. 29, 147-156.

Kiryu, S., Morita, N., Ohno, K., Maeno, H., and Kiyama, H. (1995b). Regulation of mRNA expression involved in Ras and PKA signal pathways during rat hypoglossal nerve regeneration. Brain Res. Mol. Brain Res. 29, 147-156.

Kitamoto, T. (2001). Conditional modification of behavior in drosophila by targeted expression of a temperature-sensitive shibire allele in defined neurons. J. Neurobiol. 47, 81-92.

Klein, D.C., Ganguly, S., Coon, S.L., Shi, Q., Morin, F., Weller, J.L., Obsil, T., Hickman, A., and Dyda, F. (2003). 14-3-3 proteins in pineal photoneuroendocrine transduction: how may roles? J. Neuroendocrin. 15, 370-377.

Kockel, L., Vorbraggen, G., Jackle, H., Mlodzik, M., and Bohnmann, D. (1997). Requirement for *Drosophila* 14-3-3ζ in cell proliferation and Raf-dependent photoreceptor development. Genes Dev. 11, 1140-1147.

Konishi, Y., Lehtinen, M., Donovan, N., and Bonni, A. (2002). Cdc2 phosphorylation of BAD links the cell cycle to the cell death machinery. Mol. Cell 9, 1005-1016.

Kumer, S.C., and Vrana, K.E. (1996). Intricate regulation of tyrosine hydroxylase activity and gene expression. J. Neurochem. 67, 443-462.

Kyriakis, J., and Avruch, J. (2001). Mammalian mitogen-activated protein kinase signal transduction pathways activated by stress and inflammation. Physiological Rev. 81, 808-869.

Laissue, P.P., Reiter, C., Hiesinger, P.R., Halter, S., Fischbach, K.F., and Stocker, R.F. (1999). Three dimensional reconstruction of the antennal lobe in drosophila *melanogaster*. J Compara. Neurobiol. 405, 543-552.

Lane, M.E., and Kalderon, D. (1993). Genetic investigation of cAMP-dependent protein kinase function in *Drosophila* development. Genes Dev. 7, 1229-1243.

Laronga, C., Yang, H.Y., Neal, C., and Lee, M.H. (2000). Association of the cyclin-dependent kinase and 14-3-3σ negatively regulates cell cycle progression. J. Biol. Chem. 275, 23106-23112.

Lasko, P.F., and Ashburner, M. (1990). Posterior localization of vasa protein correlates with, but is not sufficient for, pole cell development. Genes Dev. 4, 905-921.

Laurent, G., Wehr, M., and Davidowita, A. (1996). Temporal representation of odors in olfactory network. J. Neurosci. 16, 3837-3847.

Levine, A.J. (2003). p53, the cellular gatekeeper for growth and division. Cell 88, 323-331.

Levin, L. R., Han, P.-L., Hwang, P. M., Feinstein, P. G., Davis, R. L., and Reed, R. R. (1992). The *Drosophila* learning and memory gene, rutabaga, encodes a Ca^{2+}/calmodulin-responsive adenylyl cyclase. Cell. 68, 479-489.

Li, W., Noll, E., and Perrimon, N. (2000). Identification of autosomal regions involved in *Drosophila* Raf function. Genetics 156, 763-774.

Li, W., Skoulakis, E.M.C., Davis, R.L., and Perrimon, N. (1997). The *Drosophila* 14-3-3 protein Leonardo enhances Torso signaling through D-Raf in a Ras1-dependent manner. Development 124, 4163-4171.

Light, Y., Paterson, H., and Marais, R. (2002). 14-3-3 antagonizes Ras mediated Raf-1 recruitment to the plasma membrane to maintain signaling fidelity. Mol. Cell Biol. 22, 4984-4996.

Lin, S.C., Lin, M.H., Horvath, P., Reddy, K.L., and Storti, R.V. (1997). PDP1, a novel *Drosophila* PAR domain bZIP transcription factor expressed in developing mesoderm, endoderm and ectoderm, is a transcriptional regulator of somatic muscle genes. Development 124, 4685-4696.

Liu, D., Blenkowska, J., Petosa, C., Collier, R.J., Fu, H., and Liddington, R. (1995). Crystal structure of the zeta isoform of the 14-3-3 protein. Nature 376, 191-194.

Liu, L., Wolf, R., Ernst, R., and Heisenberg, M. (1999). Context generalization in *Drosophila* visual learning requires the mushroom bodies. Nature 400, 753-756.

Livingstone, M. S., Sziber, P. P., and Quinn, W. G. (1984). Loss of calcium/calmodulin responsiveness in adenylate cyclase of rutabaga, a *Drosophila* learning mutant. Cell 37, 205-215.

Luo, Z., Zhang, X., Rapp, U., and Avruch, J. (1995). Identification of the 14-3-3ζ domains important for self-association and Raf Binding. J. Biol. Chem. 270, 23681-23687.

Mackintosh, N.J. (1974). The Psychology of Animal Learning. (New York: Academic Press), pp. 485-542.

Magleby K.L., and Zengel J.E. (1982). A quantitative description of stimulation-induced changes in transmitter release at the frog neuromuscular junction. J. Gen. Physiol. 80, 613-638.

Makita, Y., Okuno, S., and Fujisawa, H. (1990). Involvement of activator protein in the activation of tryptophan hydroxylase by cAMP-dependent protein kinase. FEBS Lett. 268, 185-188.

Marcus, E.A., Nolen, T.G., Rankin, C.H., and Carew, T.J. (1988). Behavioral dissociation of dishabituation, sensitization, and inhibition in Aplysia. Science 241, 210-213.

Marin, E.C., Jefferis, G.S.X.E., Komiyama, T., Zhu, H., and Luo, L. (2002). Representation of the glomeruli olfactory map in the *Drosophila* brain. Cell 109, 243-255.

Maroney, G., and Stamey, S.C. (1983). Use of blue food to select synchronous, late third-instar larvae. *Drosophila* Information Service 59, 142-143.

Martin, H., Patel, Y., Jones, D., Howell, S., Robinson, K., and Aitken, A. (1993). Antibodies against the major brain isoforms of 14-3-3 protein. An antibody specific for the N-acetylated amino-terminus of a protein. FEBS Lett. 331, 296-303.

Martin, J., Keller, A., and Sweeney, S.T. (2002). Targeted expression of tetanus toxin: A new tool to study the neurobiology of behavior. Advan. Genetics 47, 1-43.

Martin, J.-R., Ernst, R., and Heisenberg, M. (1998). Mushroom bodies suppress locomotor activity in *Drosophila melanogaster*. Learn. Mem. 5, 179-191.

Martin, K. C., and Kandel, E. R. (1996). Cell adhesion molecules, CREB, and the formation of new synaptic connections during development and learning. Neuron 17, 567-570.

Martin, K. C., Michael, D., Rose, J. C., Barad, M., Casadio, A., Zhu, H., and Kandel, E. R. (1997). MAP kinase translocates into the nucleus of the presynaptic cell and is required for Long-term facilitation in Aplysia. Neuron 18, 899-912.

Martin-Blanco, E. (2000). p38 MAPK signalling cascades: ancient roles and new functions. BioEssays 22, 637-645.

Masters, S.C., Pederson, K.J., Zhang, L., Barbieri, J.T., and Fu, H. (1999). Interaction of 14-3-3 with a nonphosphorylated protein ligand, Exoenzyme S of Pseudomonas aeruginosa. Biochem. 38, 5216-5221.

Matto-Yelin, M., Aitken, A., and Ravid, S. (1997). 14-3-3 inhibits the Dictyostelium myosin II heavy-chain-specific protein kinase C activity by a direct interaction: identification of the 14-3-3 binding domain. Mol. Biol. Cell 8, 1889-1899.

Mayford, M., Bach, M.E., Huang, Y.Y., Wang, L., Hawkins, R.D., and Kandel, E.R. (1996). Control of memory formation through regulated expression of CaMKII transgenes. Science 274, 1678-1683.

McBride, S.M.J., Giuliani, G., Chio, C., Krause, P., Correale, D., Watson, K., Baker, G., and Siwicki, K.K. (1999). Mushroom body ablation impairs short-term memory and long-term memory of courtship conditioning in *Drosophila melanogaster*. Neuron 24, 967-977.

McConnell, J.E., Armstrong, J. F., Hodges, P.E., and Bard, J.B.L. (1995). The mouse 14-3-3ε isoform, a kinase regulator whose expression pattern is modulated in mesenchyme and neuronal differentiation. Dev. Biol. 169, 218-228.

McGonigle, S., Beall, M. J., Feeny, E.L., and Pearce, E.J. (2001). Conserved role for 14-3-3ε downstream of type I TGFβ receptors. FEBS Lett. 490, 65-69.

McGonigle, S., Beall, M.J., and Pearce, E.J. (2002). Eukaryotic initiation factor 2a subunit associates with TGFβ receptors and 14-3-3ε and acts as a modulator of the TGFβ response. Biochemistry 41, 579-587.

McGonrangle, S., Beall, M.J., Ferney, E.L., and Pearce, E.J. (2001). Conserved role for 14-3-3s downstream of type1 TGFβ receptor. FEBS Lett. 490, 65-69.

McGuire, D.E., Le, P.T., and Davis, R.L. (2001). The role of drosophila mushroom body signaling in olfactory memory. Science 293, 1330-1333.

McPherson, R.A., Harding, A., Roy, S., Lane, A., and Hancock, J.F. (1999). Interaction of c-Raf-1 with phosphatidylserine and 14-3-3. Oncogene 18, 3862-3869.

Megidish, T., Cooper, J., Zhang, L., Fu, H., and Hakomori, S. (1998). A novel Sphingosine-dependent protein kinase (SDK1) specifically phosphorylates certain isoforms of 14-3-3 Protein. J. Biol. Chem. 273, 21834-21845.

Meincke, U., Light, G.A., Geyer, M.A., Braff, D.L., and Gouzoulis-Mayfrank, E. (2004). Sensitization and habituation of the acoustic startle reflex in patients with schizophrenia. Psychiatry Res. 12, 51-61.

Meller, N., Liu, Y.-C., Collins, T., Bonnefoy-Berand, N., Baier, G., Isakov, N., and Altman, A. (1996). Direct interaction between protein kinase C theta and 14-3-3 tau in T cells: 14-3-3 overexpression results in inhibition of PKCtheta translocation and function. Mol. Cell Biol. 16, 5782-5791.

Menzel, R., Hammer, M., Braun, G., Mauelshagen, J., and Sugawa, M. (1991). The Behavior and Physiology of Bees. (London: CAB International).

Mershin, A., Pavlopoulos, E., Fitch, O., Braden, B.C., Nanopoulos, D.V., and Skoulakis, E.M.C. (2004). Learning and Memory Deficits upon TAU accumulation in *Drosophila* Mushroom body Neurons. Learn. Mem. 11.

Michaud, N.R., Fabian, J.R., Mathes, K.D., and Morrison, D.K. (1995). 14-3-3 is not essential for Raf-1 function: Identification of Raf-1 proteins that are biologically activated in a 14-3-3 and Ras-independent manner. M C B 15, 3390-3397.

Mihalek, R.M., Jones, C.J., and Tully, T. (1997). The *Drosophila* mutation turnip has pleiotropic behavioral effects and does not specifically affect learning. Learn. Mem. 3, 425-444.

Misonou, H., Ohara-Imaizumi, M., Murakami, T., Kawasaki, M., Ikeda, K., Wakai, T., and Kumakura, K. (1998). Protein kinase C controls the priming step of regulated exocytosis in adrenal chromaffin cells. Cellular Mol. Neurobiol. 18, 379-390.

Mochly-Rosen, D., Khaner, H., Lopez, J., and Smith, B.L. (1991). Intracellular receptors for activated protein kinase C. J. Biol. Chem. 266, 14866-14868.

Moore, B.W., and Perez, V.J. (1967). Physiological and Biochemical Aspects of Nervous Integration. (New York: Prentice-Hall), pp. 343-359.

Moore, M.S., DeZazzo, J., Luk, A.Y., Tully, T., Singh, C.M., and Heberlein, U. (1998). Ethanol intoxication in *Drosophila*: Genetic and pharmacological evidence for regulation by the cAMP signaling pathway. Cell 93, 997-1007.

Moreau-Fauvarque, C., Taillebourg, E., Boissoneau, E., Mesnard, J., and Dura, J.-M. (1998). The receptor tyrosine kinase linotte is required for neuronal pathway selection in the *Drosophila* mushroom bodies. Mech. Dev. 78, 47-61.

Moreau-Fauvarque, C., Taillebourg, E., Preat, T., and Dura, J.-M. (2002). Mutation of linotte causes behavioral defects independently of pigeon in *Drosophila*. NeuroReport 13, 2309-2312.

Morgan, A., and Burgoyne, R.D. (1992a). Interactions between protein kinase C and Exo1 (14-3-3 protein) and its relevance to exocytosis in permeabilized adrenal chromaffin cells. Biochem. J. 286, 807-811.

Morgan, A., and Bygourne, R.D. (1992b). Exo1 and Exo2 proteins stimulate calcium-dependent exocytosis in permeabilized adrenal chromaffin cells. Nature 355, 833-836.

Morrison, D. (1994). 14-3-3: Modulators of signaling proteins? Science 266, 56-57.

Morrison, D.K., and Culter, R.E.J. (1997). The complexity of Raf-1 regulation. Curr Opin. Cell Biol. 9, 174-179.

Morrison, D.K., Heidecker, G., Rapp, U.R., and Copeland, T.D. (1993). Identification of the major phosphorylation sites of the Raf-1 kinase. J. Biol. Chem. 268, 17309-17316.

Muller, J., Ory, S., Copeland, T., Piwnic-Worms, H., and Morrison, D.K. (2001). C-TAK1 regulates Ras signaling by phosphorylating the MAPK scaffold, KSR1. Mol. Cell 8, 983-993.

Muller, U., and Carew, T.J. (1998). Serotonin induces temporally and mechanistically distinct phase of persistent PKA activity in aplysia sensory neurons. Neuron 21, 1423-1434.

Munday, A.D., Berndt, M., and Mitchell, C.A. (2000). Phosphoinositide 3-kinase forms a complex with platelet membrane glycoprotein Ib-IX-V complex and 14-3-3ζ. Blood 96, 577-584.

Muslin, A.J., Tanner, J.W., Allen, P.M., and Shaw, A.S. (1996). Interaction of 14-3-3 with signaling proteins is mediated by the recognition of phosphoserine. Cell 84, 889-897.

Muslin, A. J., and Xing, H. (2000). 14-3-3 proteins: regulation of subcellular localization by molecular interference. Cellular Signal. 12, 703-709.

Nagata, K., Puls, A., Futter, C., Aspenstorm, P., Schaefer, E., Nakata, T., Hirokawa, N., and Hall, A. (1998). The MAP kinase kinase kinase MLK2 co-localizes with activated JNK along microtubules and associates with kinesin superfamily motor KIF3. EMBO J. 17, 149-158.

Namikawa, K., Su, Q., S., K.-S., and Kiyama, H. (1998). Enhanced expression of 14-3-3 family members in injured motorneurons. Mol. Brain Res. 55, 315-320.

Newton, A. C. (2003). Regulation of the ABC kinase by phosphorylation: protein kinase C as a paradigm. Biochem. J. 370, 361-371.

Nighorn, A., Healy, M.J., and Davis, R.L. (1991). The cyclic AMP phosphodiesterase encoded by the *Drosophila* dunce gene is concentrated in the mushroom body neuropil. Neuron 6, 455-467.

Nishizuka, Y. (1988). The molecular heterogeneity of protein kinase C and its implications for cellular regulation. Nature 334, 661-665.

Nusslein-Volhard, C., Frohnhofer, H.G., and Lehman, R. (1987). Determination of anteroposterior polarity in *Drosophila*. Science 238, 1675-1681.

Obsil, T., Ghirlando, R., Klein, D.C., Ganguly, S., and Dyda, F. (2001). Crystal structure of the 14-3-3z: serotonin N-acetyltransferase comples: a role for scaffolding in enzyme regulation. Cell 105, 257-267.

Obsilova, V., Herman, P., Vecer, J., Sulc, M., Tisinger, J., and Obsil, T. (2003). 14-3-3zeta C-terminal stretch changes its conformation upon ligand binding and phosphorylation at Thr232. J. Biol. Chem. 279, 4531-4540.

Ory, S., Zhou, M., Conrads, T.P., Veenstra, T.D., and Morrison, D.K. (2003). Protein phosphatase 2A positively regulates Ras signaling by dephosphorylating KSR1 and Raf-1 on critical 14-3-3 binding sites. Curr. Biol. 13, 1356-1364.

Osada, H., Tatematsu, Y., Yatabe, Y., Nakagawa, T., Konishi, H., Harano, T., Tezel, E., Takada, M., and Takahashi, T. (2002). Frequent and histological type-specific inactivation of 14-3-3σ in human lung cancer. Oncogene 21, 2418-2424.

Pascual, A., and Preat, T. (2001). Localization of long-term memory within the drosophila mushroom bodies. Science 294, 1115-1117.

Pavlov, I. (1927). Conditioned Reflexes (London:Oxford University Press).

Pendergast, A.M., Muller, A.J., Havlik, M.H., Maru, Y., and Witte, O.N. (1991). BCR seqences essential for transformation by the BCR/ABL oncogene bind to the ABL SH2 regulatory domain in a non-phosphotyrosine-dependent manner. Cell 66, 161-171.

Petosa, C., Masters, S.C., Bankston, L.A., Pohl, J., Wang, B., Fu, H., and Lidington, R. C. (1998). 14-3-3ζ binds a phosphorylated Raf peptide and an unphosphorylated peptide via its conserved amphipathic groove. J. Biol. Chem. 273, 16305-16310.

Petronczki, M., and Knoblich, J.A. (2001). DmPAR-6 directs epithelial polarity and asymmetric cell division of neuroblast in *Drosophila*. Nat. Cell Biol. 3, 43-49.

Philip, N., Acevedo, S.F., and Skoulakis, E.M.C. (2001) Conditional rescue of olfactory learning and memory defects in mutants of the 14-3-3ζ gene leonardo. J. Neurosci. 21, 8417-8425.

Poellinger, A., Thomas, R., Lio, P., Lee, A., Makris, N., Rosen, B.R., and Kwong, K.K. (2001). Activation and habituation in Olfaction-An fMRI study. NeuroImage 13, 547-560.

Powell, D.W., Rane, M.J., Chen, Q., Saurabh, S., and McLeish, K.R. (2002). Identification of 14-3-3ζ as a protein kinase B/Akt substrate. J. Biol. Chem. 277, 21639-21642.

Preat, T. (1998). Decreased odor avoidance after electric shock in *Drosophila* mutants Biases Learning and Memory tests. J. Neurosci. 18, 8534-8538.

Prober, D.A., and Edgar, B.A. (2000) Ras1 promotes cellular growth in the *Drosophila* wing. Cell 100, 435-446.

Putz, G., and Heisenberg, M. (2002). Memories in drosophila heat-box learning. Learn. Mem. 9, 349-359.

Qi, W., and Martinez, J.D. (2003). Reduction of 14-3-3 proteins correlates with increased sensitivity killing of human lung cancer cells by ionizing radiation. Rad. Res. 160, 217-223.

Qui, Y., Chan, C.N., Malone, T., Richter, L., Beckendorf, S.K., and Davis, R.L. (1991). Characterization of the memory gene dunce of *Drosophila melanogaster*. J. Mol. Biol. 222, 553-565.

Qui, Y., and Davis, R.L. (1993). Genetic dissection of the learning/memory gene dunce of *Drosophila melanogaster*. Genes Dev. 7, 1447-1458.

Qiu, W., Zhuang, S., von Lintig, F.C., Boss, G.R., and Pilz, R.B. (2000). Cell type-specific regulation of B-Raf kinase by cAMP and 14-3-3 proteins. J. Biol. Chem. 275, 31921-31929.

Raftery, L.A., and Sutherland, D.J. (1999) TGF-β family signal transduction in *Drosophila* development: from Mad to Smads. Dev. Biol. 210, 251-268.

Rankin, C.H. (2000). Context conditioning in habituation in the nematode Caenorabditis elegans. Behav. Neurosci. 114, 496-505.

Rankin, C.H., and Broster, B.S. (1992). Factors affecting habituation and recovery from habituation in the nematode Caenorhabtitis elegans. Behav. Neurosci. 106, 239-249.

Reddy, S., Jin, P., Trimarchi, J., Caruccio, P., Phillis, R., and Murphey, R.K. (1997). Mutant molecular motors disrupt neural circuits in *Drosophila*. J. Neurobiol. 33, 711-723.

Rees, C.T., and Spatz, H-C. (1989). Habituation of the landing response of *Drosophila* wild-type and mutants defective in olfactory learning. J. Neurogenet. 5, 105-118.

Reuther, G.W., Fu, H., Cripe, L.D., Collier, R.J., and Pendergast, A.M. (1994). Association of the protein kinases c-Bcr and Bcr-Abl with proteins of the 14-3-3 family. Science 266, 129-133.

Rittinger, K., Budman, J., Xu, J., Volinia, S., Cantley, L.C., Smerdon, S.J., Gamblin, S.J., and Yaffe, M.B. (1999) Structural analysis of 14-3-3 phosphopeptide complexes identifies a dual role for the nuclear export signal of 14-3-3 in ligand binding. Molecular Cell 4, 153-166.

Robinson, J. (1976). Estimation of parameters for a model of transmitter release at a synapse. Biometrics 32, 61-68.

Roman, G., and Davis, R.L. (2001). Molecular biology and anatomy of drosophila olfactory associative learning. BioEssay 23, 571-581.

Rommel, C., Radziwill, G., Lovric, J., Noeldeke, J., Heinicke, T., Jones, D., Aitken, A., and Moelling, K. (1996). Activated Ras displaces 14-3-3 protein from the amino terminus of c-Raf-1. Oncogene 12, 609-619.

Rommel, C., Radziwill, G., Moelling K, and Hafen, E. (1997). Negative regulation of Raf activity by binding of 14-3-3 to the aminoterminus of Raf in vivo. Mech. Dev. 64, 95-104.

Rose, L.S., and Kemphues, K.J. (1998). Early patterning of the C. elegans embryo. Annu. Rev. Genet. 32, 521-545.

Rose, J.K., and Rankin, C.H. (2001). Analyses of habituation in Caenorhabditis elegans. Learn. Mem. 8, 63-69.

Rosenboom, P., Weller, J., Babila , T., Aitken, A., Sellers, L., Moffet, J., Namboodiri, M.A.A., and Klein, D.C. (1994). Cloning and characterization of the ε and ζ isoforms of the 14-3-3 proteins. DNA Cell Biol. 13, 629-640.

Rosenquist, M., Sehnke, P., Ferl, R.J., Sommarin, M., and Larsson, C. (2000). Evolution of the 14-3-3 protein family: Does the large number of isoforms in multicellular organisms reflect functional specificity. J.Mol. Evol. 51, 446-458.

Roth, D. (1999). Dominant-negative alleles of 14-3-3 proteins cause defects in actin organization and vescile targeting in the yeast Saccharomyces cerevisiae. FEBS Lett. 460, 411-416.

Roth, D., and Burgoyne, R.D. (1995). Stimulation of catecholamine secretion from adrenal chromaffin cells by 14-3-3 proteins is due to reorganization of the cortical actin network. FEBS Lett. 374, 77-81.

Roth, D., Morgan, A., and Burgoyne, R.D. (1993). Identification of a key domain in annexin and 14-3-3 proteins that stimulate calcium- dependent exocytosis in permeabilized adrenal chromaffin cells. FEBS Lett. 320, 207-210.

Roth, D., Morgan, A., Jones, D., Martens, G.J.M., Aitken, A., and Burgoyne, R.D. (1994). Characterization of 14-3-3 proteins in adrenal chromaffin cells and demonstration of isoform-specific phospholipid binding. Biochem. J. 301, 305-310.

Roy, S., McPherson, R.A., Appoloni, A., Yan, J., Lane, A., Clyde-Smith, J., and Hancock, J.F. (1998). 14-3-3 facilitates Ras-Dependent Raf-1 Activation in vitro and in vivo. Mol. Cell Biol. 18, 3947-3955.

Sambrook, J., Fritsch, E. F., and Maniatis, T. (1989). Molecular Cloning: A laboratory manual. (New York: Cold Spring Harbor Laboratory: CSHL Press).

Sanchez-Valle, R., Saiz, A., and Graus, F. (2002). 14-3-3 protein isoforms and atypical patterns of 14-3-3 assay in the diagnosis of Creutzfeldt-Jakob disease. Neurosci. Lett. 320, 69-72.

Satoh, J.-I., Yukitake, M., Kurohara, K., Takashima, H., and Kuroda, Y. (2003). Detection of the 14-3-3 protein in the cerebrospinal fluid of Japanese multiple sclerosis patients presenting with severe myelitis. J. Neurol. Sci. 212, 11-20.

Schaeffer, E., Smith, D., Mardon, G., Quinn, W., and Zuker, C. (1989). Isolation and characterization of two new *Drosophila* protein kinase C genes, including one specifically expressed in photoreceptor cells. Cell 57, 403-412.

Schiavo, G., Benfenati, F., Paulain, B., Rossetto, O., Polverino de Laureto, P., DasGupta, B.R., and Montecucco, C. (1992). Tetanus and botulinum-B neurotoxins block neurotransmitter release by proteolytic cleavage of synaptobrevin. Nature 359, 832-835.

Schiavo, G., Matteoli, M., and Montecucco, C. (2000). Neurotoxins affecting neuroexocytosis. Physiol. Rev. 80, 717-766.

Schildberger, K. (1984). Multimodal interneurons in the cricket brain: properties of identified extrinsic mushroom body cells. J. Comp. Physiol. 154, 71-79.

Schuster, C.M., Davis, G.W., Fetter, R.D., and Goodman, C.S. (1996). Genetic dissection of structural and functional components of synaptic plasticity II. Fasciclin II controls presynaptic structural plasticity. Neuron 17, 655-667.

Schwaerzef, M., Heisenberg, M., and Zars, T. (2002). Extinction antagonize olfactory memory at the subcellular level. Neuron 35, 951-960.

Schwartz, J. H. (1993). Cognitive kinases. Proc. Natl. Acad. Sci. USA 90, 8310-8313.

Shen, Y.H., Godlewski, J., Bronisz, A., Zhu, J., Comb, M.J., Avruch, J., and Tzivion, G. (2003). Significance of 14-3-3 self-dimerization for phosphorylation-dependent target binding. Mol. Biol. Cell 14, 4721-4733.

Shi, L., Nishioka, W.K., Th'ng, J., Bradbury, E.M., Litchfield, D.W., and Greenberg, A.H. (1994). Premature $p34^{cdc2}$ activation required for apoptosis. Science 263, 1143-1145.

Siegel, R. W., and Hall, J. C. (1979). Conditioned response in courtship behavior of normal and mutant *Drosophila*. Proc. Natl. Acad. Sci. USA 76, 3430-3434.

Siegel, R.W., Hall, J.C., Gailey, D.A., and Kyriacou, C.P. (1984). Genetic elements of courtship in *Drosophila*: mosaics and learning mutants. Behav. Genet. 14, 383-410.

Simon, M. A. (1994). Signal transduction during the development of the *Drosophila* R7 photoreceptor. Dev. Biol. 166, 431-442.

Siniatchkin, M., Kropp, P., and Gerber, W-D. (2003). What kind of habituation is impaired in migraine patients? Cephalalgia 23, 511-518.

Siwicki, K.K., and Ladewski, L. (2003). Associative learning and memory in *Drosophila* beyond olfactory conditioning. Behav. Proc. 64, 225-238.

Skoulakis, E.M.C., and Davis, R.L. (1998). 14-3-3 proteins in neuronal development and function. Mol. Neurobiol. 16, 269-284.

Skoulakis, E.M.C., Han, P.-L., and Davis, R.L. (1993a). Learning and Memory in *Drosophila*. (Amsterdam: Elsevier Science Publishers), pp. 99-111.

Skoulakis, E.M.C., Kalderon, D., and Davis, R.L. (1993b). Preferential expression in mushroom bodies of the catalytic subunit of protein kinase A and its role in learning and memory. Neuron 11, 197-208.

Slaats-Willemse, D., Swaab-Barneveld, H., de Sonneville, L., van der Meulen, E., and Buitelaar, J. (2003). Deficient response inhibition as a cognitive endophenotype of ADHD. J. Am. Acad. Child Adolesc. Psychiatry 42, 1242-1248.

Sokal, R.R., and Rohlf, F.J. (1981). Biometry: The Principles and Practice of Statistics in Biological Research. (New York: W. H. Freeman).

Sokolowski, M. (2001). *Drosophila*: genetics meets behavior. Nat. Rev. Neurosci. 2, 879-890.

Sonnenblick, B.P. (1950). Biology of *Drosophila*. (New York: John Wiley and Sons), pp. 62-167.

Springer, J.E., Azbill, R.D., Nottingham, S.A., and Kennedy, S.E. (2000). Calcineurin-mediated BAD dephosphorylation activates the Caspase-3 apoptotic cascade traumatic spinal cord injury. J. Neurosci. 20, 7246-7251.

Starz-Gaiano, M., and Lehmann, R. (2001). Moving towards the next generation. Mech. Dev. 105, 5-18.

Stewart B.A., Atwood H.L., Renger J.J., Wang J., and Wu C-F (1994). Improved stability of *Drosophila* larval neuromuscular preparations in hemolymph-like physiological solutions. J. Comp. Physiol. 175, 179-191.

Stimson, D.T., Estes, P.S., Smith, M., Kelly, L.E., and Ramaswami, M. (1998). A product of the *Drosophila* stoned locus regulates neurotransmitter release. J. Neurosci. 18, 9638-9649.

Stocker, R.F. (1994). The organization of the chemosensory system in drosophila *melanogaster*. Cell Tissue Res. 275, 3-26.

Stocker, R.F. (2001). *Drosophila* as a focus in olfactory research mapping of olfactory sensilla by fine structure, odor specificity, odorant receptor expression, and central connectivity. Microscopy Res. Tech. 55, 284-296.

Stocker, R.F., Lienhard, M.C., Bost, A., and Fischbach, K.-F. (1990). Neuronal architecture of the antennal lobe in *Drosophila melanogaster*. Cell Tissue Res. 262, 9-34.

Stocker, R.F., Heimbeck, G., Gendre, N., and de Belle, J.S. (1997). Neuroblast ablation in *Drosophila* P[GAL4] lines reveals the origin of olfactory interneurons. J Neurobiol. 32, 443-456.

Stortkuhl, K.F., Hovemann, B.T., and Carlson, J.R. (1999). Olfactory adaptation depends on the Trp Ca2+ channel in *Drosophila*. J. Neurosci. 19, 4839-4846.

Strausfeld, N.J. (1976). Atlas of an Insect Brain (New York: Springer-Verlag).

Strausfeld, N.J., Hansen, L., Li, Y., Gomez, R.S., and Ito, K. (1998). Evolution, discovery and interpretations of Arthropod mushroom bodies. Learn. Mem. 5, 11-37.

Strauss, R., Renner, M., and Gotz, K. (2001). Task-specific association of photoreceptor systems and steering parameters in *Drosophila*. J. Comp. Physiol. 187, 617-632.

Styhler, S., Nakamura, A., Swan, A., Suter, B., and Lasko, P. (1998). vasa is required for GURKEN accumulation in the oocyte, and is involved in oocyte differentiation and germ-line cyst development. Development 125, 1569-1578.

Su, T.T., Campbell, S.D., and O'Farrell, P.H. (1998). The Cell cycle program in germ cells of the *Drosophila* embryo. Dev. Biol. 196, 160-170.

Su, T.T., Parry, D.H., Donahoe, B., Chien, C.-T., O'Farrell, P.H., and Purdy, A. (2001). Cell cycle roles for the two 14-3-3 proteins during *Drosophila* development. J. Cell Sci. 114, 3445-3462.

Suginta, W., Karoulias, N., Aitken, A., and Ashley, R.H. (2001). Chloride intracellular channel protein CLIC4 (p64H1) binds directly to brain dynamin I in a complex containing actin, tublin and 14-3-3 isoforms. Biochem. J. 359, 55-64.

Sutherland, C., Alterio, J., Campbell, D.G., LeBourdelles, B., Mallet, J., Haavik, J., and Cohen, P. (1993). Phosphorylation and activation of human tyrosine hydroxylase in vitro by mitogen-activated protein (MAP) kinase and MAP-kinase-activated kinases 1 and 2. Eur. J. Biochem 217, 715-722.

Sweeney, S.T., Broadie, K., Keane, J., Niemann, H., and O'Kane, C.J. (1995). Targeted expression of tetanus toxin light chain in *Drosophila* specifically eliminates synaptic transmission and causes behavioral defects. Neuron 14, 341-351.

Takahashi, H., Toshinari, I., Takahashi, R.H., Sato, Y., Wakabayashi, H., Takashima, M., Hiroshi, K., Nagashima, K., Kenney, K., Gibbs, C.J., and Kurata, T. (1999). Increased levels of ε and γ isoforms of 14-3-3 proteins in cerebrospinal fluid in patients with Creutzfeldt-Jacob disease. Clin. Diag. Lab Immuno. 6, 983-985.

Takahashi, Y. (2003). The 14-3-3 proteins: gene, gene expression, and function. Neurochem. Res. 28, 1265-1273.

Takashima, H., Iwata, T., Kitagawa, Y., Takahashi, R.H., Sato, Y., Wakabayashi, H., Takashima, M., Nagashima, K., Kenney, K., Gibbs, C.J. Jr, and Kurata, T. (1999). Increased levels of ε and γ isoforms of 14-3-3 proteins in Cerebrospinal fluid in patients with Creutzfeldt-Jakob disease. Clin. Diag Lab Immuno. 6, 983-985.

Tanabe, K., Kiryu-Seo, S., Nakamura, T., Mori, N., Tsujino, H., Ochi, T., and Kiyama, H. (1998). Alternative expression of Shc family members in nerve-injured motorneurons. Brain Res. Mol. Brain Res. 53, 291-296.

Tanaka, N.K., Awasaki, T., Shimada, T., and Ito, K. (2004) Integration of chemosensory pathways in the *Drosophila* second-order olfactory centers. Curr. Biol. 14, 449-457.

Tanji, M., Horwitz, R., Rosenfeld, G., and Waymire, J.C. (1994). Activation of protein kinase C by purified bovine brain 14-3-3: comparison with tyrosine hydroxylase activation. J. Neurochem. 63, 1908-1916.

Tempel, B. L., Bonini, N., Dawson, D.R., and Quinn, W.G. (1983). Reward learning in normal and mutant. Proc. Natl. Acad. Sci. USA 80, 1482-1486.

Therrien, M., Morrison, D.K., Wong, A.M., and Rubin, G.M. (2000). A screen for genetic modifiers of a kinase suppressor of Ras-dependent rough eye phenotype in *Drosophila*. Genetics 156, 1231-1242.

Thomson, R.F., and Spencer, W.A. (1966) Habituation: A model phenomenon for the study of neuronal substrates of behavior. Phychol. Rev. 73, 16-43.

Thorndike, E.L. (1911). Animal Intelligence (New York: Macmilliam).

Tien, A.-C., Hsei, H.-Y., and Chien, C.-T. (1999). Dynamic expression and cellular localization of the *Drosophila* 14-3-3ε during embryonic development. Mech. Dev. 81, 209-212.

Toda, T., Cameron, S., Sass, P., Zoller, M., and Wigler, M. (1987). Three different genes in S. cerevisiae encode the catalytic subunits of the cAMP-dependent protein kinase. Cell 50, 277-287.

Toker, A., Sellers, L., Amess, B., Patel, Y., Harris, A., and Aitken, A. (1992). Multiple isoforms of a protein kinase C inhibitor (KCIP/14-3-3) from sheep brain. Amino acid sequence of phosphorylated forms. Eur. J. Biochem. 206, 453-461.

Toyo-oka, K., Shionoya, A., Gambello, M.J., Cardoso, C., Levender, R., Ward, H.L., Ayala, R., Tsai, L.-H., Dobyns, W., Ledbetter, D., Shinji, H., and Wynshaw-Boris, A. (2003). 14-3-3ε is important for neuronal migration by binding to NUDEL: a molecular explanation for Miller-Dieker syndrome. Nat. Genetics 34, 274-285.

Toyooka, K., Muratake, T., Watanabe, H., Hayashi, S., Ichikawa, T., Usui, H., Washiyama, K., Kumanishi, T., and Takahashi, Y. (2002). Isolation and structure of the mouse 14-3-3η mRNA in the mouse brain. Mol. Brain Res. 100, 13-20.

Trimarchi, J.R., and Schneiderman, A.M. (1995). Different neural pathways coordinate *Drosophila* flight initiation evoked by visual and olfactory stimuli. J. Exp. Bio. 198, 1099-1104.

Truong, A.B., Masters, S.C., Yang, H., and Fu, H. (2002). Role of the 14-3-3 C-terminal loop in ligand interaction. Proteins 49, 321-325.

Tschampa, H.J., Neumann, M., Zerr, I., Henkel, K., Schroter, A., Schulz-Schaeffer, W.J., Steinhoff, B.J., Kretzschmar, H.A., and Poser, S. (2001). Patients with Alzheimer's disease and dementia with Lewy bodies mistaken for Creutzfeldt-Jakob disease. J. Neurol. Neurosurg. Psychiatry 71, 33-39.

Tully, T. (1987). *Drosophila* learning and memory revisited. TINS 10, 330-335.

Tully, T., Boynton, S., Brandes, C., Dura, J.M., Mihalek, R., Preat, T., and Villella, A. (1990). Genetic dissection of memory formation in *Drosophila melanogaster*. Cold Spring Harbor Symp. Quant. Biol. 55, 203-211.

Tully, T., Preat, T., Boynton, S.C., and Del Vecchio, M. (1994). Genetic dissection of consolidated memory in *Drosophila*. Cell 79, 35-47.

Tully, T., and Quinn, W. (1985). Classical conditioning and retention in normal and mutant *Drosophila melanogaster*. J. Comp. Physiol. 157, 263-277.

Tzivion, G., and Avruch, J. (2002). 14-3-3 Proteins: Active cofactors in cellular regulation by Serine/Threonine phosphorylation. J. Biol. Chem. 277, 3061-3064.

Tzivion, G., Luo, Z., and Avruch, J. (1998). A dimeric 14-3-3 protein is an essential cofactor for Raf kinase activity. Nature 394, 88-92.

Tzivion, G., Shen, Y.H., and Zuh, J. (2001). 14-3-3 proteins; bringing new definitions to scaffolding. Oncogene 20, 6331-6338.

van der Bliek, A.M., Redelmeier, T.E., Damke, H., Tisdale, E.J., Meyerowitz, E.M., and Schmid, S.L. (1993). Mutations in human dynamin block an intermediate stage in coated vesicle formation. J. Cell Biol. 122, 553-563.

van der Brug, M.P., Goodenough, S., and Wilce, P. (2002). Kainic acid induces 14-3-3 ζ expression in distinct regions of rat brain. Brain Res. 956, 110-115.

Van Der Hoeven, P.C.J., Van Der Wal, J., Ruurs, P., Van Dijk, M.C.M., and Van Blitterswijk, W. (2000). 14-3-3 isotypes facilitate coupling of protein kinase C-z to Raf-1: negative regulation by 14-3-3 phosphorylation. Biochem. J. 345, 297-306.

van Hemert, M.J., Steensma, H.Y., and van Heudsen, G.P.H. (2001). 14-3-3 proteins: key regulators of cell division, signalling and apoptosis. BioEssays 23, 936-946.

Vosshall, L.B. (2000). Olfaction in *Drosophila*. Curr. Opin. Neurobiol. 10, 498-503.

Waddell, S., Armstrong, J.D., Kitamoto, T., Kaiser, K., and Quinn, W.G. (2000). The amnesiac gene product is expressed in two neurons in the Drosophiila brain that are critical for memory. Cell 103, 805-813.

Waddell, S., and Quinn, W.G. (2001a). Flies, genes and learning. Annu. Rev. Neurosci. 24, 1283-1309.

Waddell, S., and Quinn, W.G. (2001b). What can we teach drosophila? What can they teach us? Trends Genet. 17, 719-726.

Wakabayashi, H., Yano, M., Tachikawa, N., Oka, S., Meada, M., and Kido, H. (2001). Increased concentration of 14-3-3ε, γ and ζ isoforms in cerebrospinal fluid of AIDS patients with neuronal destruction. Clin. Chimica. Acta. 312, 97-105.

Wakui, H., Wright, A. P. H., Gustafson, J.-A., and Zilliacus, J. (1997). Interaction of the ligand activated glucocorticoid receptor with the 14-3-3η protein. J. Biol. Chem. 272, 8153-8156.

Wang, W., and Shakes, D. (1996). Molecular evolution of the 14-3-3 family. Mol. Evo. 43, 384-398.

Wang, H., Zhang, L., Liddington, R., and Fu, H. (1998). Mutations in the Hydrophobic surface of an Amphipathic groove of 14-3-3ζ Disrupt its interaction with Raf-1 kinase. J. Biol. Chem. 26, 16297-16304.

Wang, J.Z., Gong, C.X., Zaidi, T., Grundke-Iqbal, I., and Iqbal, K. (1995). Dephosphorylation of Alzheimer paired helical filaments by protein phosphatase-2A and -2B. J. Biol. Chem. 270, 4854-4860.

Wang, Y., Chiang, A.-S., Xia, S., Kitamoto, T., Tully, T., and Zhong, Y. (2003). Blockage of neurotransmission in *Drosophila* mushroom bodies impairs odor attraction, but not repulsion. Curr. Bio. 13, 1900-1904.

Wang, Y., Jacobs, C., Hook, K. E., Duan, H., Booher, R. N., and Sun, Y. (2000). Binding of 14-3-3β to the carboxyl terminus of Wee1 increases Wee1 stability, kinase activity and G_2-M cell population. Cell Growth Diff. 11, 211-219.

Wassarman, D.A., Therrien, M., and Rubin, G.M. (1995). The Ras signaling pathway in *Drosophila*. Curr. Opin. Genet. Dev. 5, 44-50.

Wassarman, D.A., and Therrien, M. (1997). Ras-mediated photoreceptor development in *Drosophila*. Adv. Dev. Biol. 5, 1-41.

Watanabe, M., Isobe, T., Ichimura, T., Kuwano, R., Takahashi, Y., and Kondo, H. (1993). Molecular cloning of rat cDNAs for β and γ subtypes of 14-3-3 protein and developmental changes in expression of their mRNAs in the nervous system. Mol. Brain Res. 17, 135-146.

Watanabe, M., Isobe, T., Ichimura, T., Kuwano, R., Takahashi, Y., Kondo, H., and Inoue, Y. (1994). Molecular cloning of rat cDNAs for the ζ and θ subtypes of 14-3-3 proteins and differential distributions of their mRNAs in the brain. Mol Brain Res 25, 113-121.

Watanabe, M., Isobe, T., Okuyama, T., Ichimura, T., Kuwano, R., Takahashi, Y., and Kondo, H. (1991). Molecular cloning of cDNA to rat 14-3-3η chain polypeptide and the neuronal expression of the mRNA in the central nervous system. Mol. Brain Res. 10, 151-158.

Waterman, M.J.F., Stavridi, E. S., Waterman, J.L.F., and Halazonetis, T.D. (1998). ATM-dependent activation of p53 involves dephosphorylation and association with 14-3-3 proteins. Nat. Genet. 19, 175-178.

Wei, G., and Mahowald, A.P. (1994) The germline: familiar and newly uncovered properties. Annu. Rev. Genet. 28, 309-324.

Widen, C., Zilliacus, J., Gustafsson, J., and Wikstrom, A. (2000). Glucocorticoid receptor interaction with 14-3-3 and Raf-1 a proposed mechanism for cross-talk of two signal transduction pathways. J. Biol. Chem. 275, 39296-39301.

Williamson, A., and Lehman, R. (1996). Germ cell development in *Drosophila*. Annu. Rev. Cell Dev. Biol. 12. 365-391.

Wilson, D.A. (1998). Habituation to odor responses in the rat anterior piriform cortex. J. Neurophysiol. 79, 1425-1440.

Wiltfang, J., Otto, M., Baxter, H.C., Bodemer, M., Steinacker, P., Bahn, E., Zerr, I., Kornhuber, J., Kretzschmar, H.A., Poser, S., Ruther, E., and Aitken, A. (1999). Isoform pattern of 14-3-3 proteins in the cerebrospinal fluid of patients with Creutzfeldt-Jakob disease. J. Neurochem. 73, 2485-2490.

Wolf, R., and Heisenberg, M. (1991). Basic organization of operant behavior as revealed in *Drosophila* flight orientation. J. Comp. Physiol. 169, 373-388.

Wolf, R., Wittig, T., Liu, L., Wustmann, G., Eyding, D., and Heisenberg, M. (1998). *Drosophila* mushroom bodies are dispensible for visual, tactile, and motor learning. Learn. Mem. 5, 166-178.

Woodcock, J., Murphy, J., Stomski, F., Berndt, M., and Lopez, A. (2003). The dimeric versus monomeric status of 14-3-3ζ is controlled by phosphorylation of ser^{58} at the dimer interface. J. Biol. Chem. 278, 36323-36327.

Worby, C.A., Simonson-Leff, N., Clemens, J.C., Kruger, R.P., Muda, M., and Dixon, J.A. (2001). The sorting nexin DSH3PX1, connects the axonal guidance receptor, Dscam to the actin cytoskeleton. J. Biol. Chem. 276, 782-789.

Wu, Y.N., Vu, N.-D., and Wagner, P.D. (1992). Anti-(14-3-3 protein) antibody inhibits stimulation of noradrenaline (norepinephrine) secretion by chromaffin-cell cytosolic proteins. Biochem. J. 285, 697-700.

Xiao, B., Smerdon, S., Jones, D.H., Dodson, G.G., Soneji, Y., Aitken, A., and Gamblin, S. J. (1995). Structure of a 14-3-3 protein and implications for coordination of multiple signaling pathways. Nature 376, 188-191.

Xing, H., Kornfeld, K., and Muslin, A.J. (1997). The protein kinase KSR interacts with 14-3-3 protein and Raf. Curr. Bio. 7, 294-300.

Xing,, H., Zang, S., Weinheimer, C., Kovacs, A., and Muslin, A.J. (2000). 14-3-3 proteins block apoptosis and differentially regulate MAPK cascades. EMBO J. 19, 349-358.

Xu, J., Kao, S.Y., Lee, F.J., Song, W., Jin, L.W., and Yankner, B.A. (2002). Dopamine-dependent neurotoxicity of α-synuclein: a mechanism for selective neurodegeneration in Parkinson disease. Nat. Med. 8, 600-606.

Yaffe, M.B. (2002). How do 14-3-3 protein work? Gatekeeper phosphorylation and the molecular anvil hypothesis. FEBS Lett. 513, 53-57.

Yaffe, M.B., and Elia, A.E.H. (2001). Phosphoserine/threonine-binding domains. Curr Opin. Cell Bio. 13, 131-138.

Yaffe, M.B., Rittinger, K., Volinia, S., Caron, P.R., Aitken, A., Leffers, H., Gamblin, S.J., and Cantley, L.C. (1997). The structural basis for 14-3-3 phosphopeptide binding specificity. Cell 91, 961-971

Yang, H.-Y., Wen, Y.-Y., Chen, C.-H., Lozano, G., and Lee, M.-H. (2003). 14-3-3σ positively regulates p53 and suppresses tumor growth. Mol. Cell Biochem. 23, 7096-7107.

Yin, J. C.P., Del Vecchio, M., and Tully, T. (1995). CREB as a memory modulator: induced expression of a dCREB2 activators isoform enhances long-term memory in *Drosophila*. Cell 81, 107-115.

Yin, J.C.P., Wallach, J.S., Del Vecchio, M., WIlder, E.L., Zhou, H., Quinn, W.G., and Tully, T. (1994). Induction of a dominant negative CREB transgene specifically blocks long-term memory in drosophila. Cell 79, 49-58.

Yoshihara, M., Ensminger, A.W., and Littleton, J.T. (2001). Neurobiology and the *Drosophila* genome. Func. Integr. Genomics 1, 235-240.

Yu, L., Orlandi, L., Wang, P., Orr, M.S., Senderowicz, A.M., Sausville, E.A., Silvestrini, R., Watanabe, N., Piwnica-Worms, H., and O'Connor, P.M., (1998). UNC-01 abrogates G2 arrest through a Cdc2-dependent pathway that is associated with inactivation of the WeeHu kinase and activation of the Cdc25C phosphatase. J. Biol. Chem. 273, 33455-33464.

Zars, T. (2000). Behavioral functions of the insect mushroom bodies. Curr. Opin. Neurobiol. 10, 790-795.

Zars, T., Fischer, M., Schulz, R., and Heisenberg, M. (2000). Localization of short-term memory in *Drosophila*. Science 288, 672-675.

Zerr, I., Bodemer, M., Gefeller, O., Otto, M., Poser, S., Wiltfang, J., Windl, O., Kretzschmar, H.A., and Weber, T. (1998). Detection of 14-3-3 protein in the

cerebrospinal fluid supports the diagnosis of Creutfeldt-Jakob disease. Ann. Neurol. 43, 32-40.

Zerr, I., and Poser, S. (2002). Clinical diagnosis and differential diagnosis of CJD and vCJD. APMIS 110, 88-98.

Zerr, I., Schulz-Schaeffer, W.J., Giese, A., Bodemer, M., Schroter, A., Henkel, K., Tschampa, H.J., Windl, O., Pfahlberg, A., Steinhoff, B.J., Gefeller, O., Kretzschmar, H.A. and Poser, S. (2000). Current clinical diagnosis in Creutzfeldt–Jacob disease: identification of uncommon variants. Ann. Neurol. 48, 323-329.

Zha, J., Harada, H., Yang, E., Jockel, J., and Korsmeyer, S.J. (1996). Serine phosphorylation of death agonist BAD in response to survival factor results in binding to 14-3-3 not BCL-X(L). Cell 87, 589-592.

Zhong, Y. (1995). Mediation of PACAP-like neuropeptide transmissioin by coactivation of Ras/Raf and cAMP signal transduction pathways in *Drosophila*. Nature 375, 88-92.

Zhong, Y., Budnik, V., and Wu, C-F. (1992). Synaptic plasticity in *Drosophila* memory and hyperexcitable mutants: role of cAMP cascade. J. Neurosci. 12, 644-651.

Zhong, Y., and Wu, C.-F. (1991). Altered synaptic plasticity in *Drosophila* memory mutants with a defective cyclic AMP cascade. Science 251, 198-201.

Zhou, Y., Reddy, S., Murrey, H., Fei, H., and Levitan, I.B. (2003). Monomeric 14-3-3 protein is sufficient to modulate the activity of the drosophila slowpoke calcium-dependent potassium channel. J. Biol. Chem. 278, 10073-10080.

Zhou, Y., Schopporle, W.M., Murrey, H., Jaramillo, A., Dagan, D., Griffith, L.C., and Levitan, I.B. (1999). A Dynamically regulated 14-3-3, slob, and slowpoke potassium channel complex in *Drosophila* presynaptic nerve terminals. Neuron 22, 809-818.

Zipursky, S.L., and Rubin, G.M. (1994). Determination of neuronal cell fate: lessons form the R7 neuron of *Drosophila*. Annu. Rev. Neurosci. 17, 373-397.

VITA

SUMMER FONTAINE ACEVEDO

Address:

1604 19th Street
Georgetown, TX 78626

Education

Doctor of Philosophy in Genetics 2004
Texas A & M University

Bachelor of Arts in Chemistry (Biochemistry) 1998
University of Northern Colorado

Publications

Philip, N., Acevedo, S.F., and Skoulakis, E.M.C. (2001) Conditional rescue of olfactory learning and memory defects in mutants of the 14-3-3ζ gene leonardo. J. Neurosci. *21*, 8417-8425.

Chen, H., Fernandez-Funez, P., Acevedo, S.F., Lam , Y. C., Kaytor, M.D., Fernandez, M.H., Aitken, A., Skoulakis, E.M.C., Orr, H.T., Botas, J., and Zoghibi, H.Y. (2003) Interaction of Akt-phosphorylated ataxin-1 with 14-3-3 mediates neurodegeneration in spinocerebellar ataxis type 1. Cell *113*, 457-468.

Sathyanarayana, P., Barthwal, M.K., Lane, M.E., Acevedo, S.F., Skoulakis, E.M.C., Bergmann, A., and Rana, A. (2003) *Drosophila* mixed lineage kinase/slipper, a missing biochemical link in *Drosophila*, Biochimica. Biophyscia. Acta. *1640*, 77-84.